Modelling and Optimisation of a Free Piston Stirling Engine for Micro-CHP Applications

Ayodeji Olubayo Sowale

A thesis submitted in partial fulfilment of the requirements of the University of Northumbria at Newcastle for the award of Doctor of Philosophy

Research undertaken in the Mechanical and Construction Engineering Department of the
Faculty of Engineering and Environment

November 2015

Abstract

This study is carried out to investigate the solar thermal energy conversion for generating power. This form of renewable energy can be utilised for power production deploying the free piston Stirling engines, which convert thermal energy into mechanical energy. Such systems have an advantage of production of work using low and high temperature differences in the cycle which could be created by different sources of heat including solar energy, combustion of a fuel, geothermal energy, nuclear energy or waste heat. The thermodynamic analysis of the free piston Stirling engine have been carried out and implemented in past studies with different methods of approach with various difficulties exhibited. In the present study isothermal, ideal adiabatic and Quasi steady flow models have been produced and used for investigation of the engine performance. The approach in this study deals with simultaneous mathematical modelling of thermodynamic processes and pistons dynamics. The steady state operation of the engine depends on the values of damping coefficients, spring stiffness and pressure drop within the heat exchangers during engine's operation, which is also a result of the energy transfer in each engine's component. In order to design effective high performance engines it is necessary to develop such advanced mathematical models to perform the analysis of the engine's operation and to predict its performance satisfactorily. The aim of this study was to develop several levels of mathematical models of free piston Stirling engines and to evaluate their accuracy using experimental and theoretical results available in published sources. The validation of the developed free piston Stirling engine models demonstrates a good agreement between the numerical results and experimental data.

The validated model then was used for optimisation of the engine, deploying Genetic Algorithm approach with the purpose to determine its optimal design parameters. The

developed optimisation procedure provides a noticeable improvement in the engine's performance in terms of power output and efficiency.

Table of Contents

List of Figures

List of Tables

Nomenclature

A = cross sectional area (m^2)

A_d = Cross sectional area of the piston (m^2)

A_p = Cross sectional area of the displacer (m^2)

C_{ap}= specific heat at constant pressure (J/ kgK)

C_{av}= specific heat at constant volume (J/ kgK)

d = diameter (m)

diss = heat loss due to the flow friction in the regenerator

FPSE = Free piston Stirling engine

k_p = Stiffness of piston spring(N/m)

k_d = Stiffness of displacer spring (N/m)

k = thermal conductivity

l= length

lir = heat loss due to heat transfer due to the heat conduction

m_d = Mass of the displacer (kg)

m_p = Mass of the piston (kg)

Npop = number of chromosome

NTU = number of heat transfer unit

Nu = Nusselt number

N_{sc} = number of survival chromosomes

P_b = Bounce space pressure (Pa)

Pop =chromosomes

P = power (W)

$\bar{P}$ = mean gas pressure in the cycle

Pr = Prandtl number

Q = heat transfer rate (W)

T_k = Temperature of the cooler (K)

T_r = Temperature of the regenerator (K)

T_h = Temperature of the heater (K)

T_{ck} = Temperature of the compression space to cooler (K)

T_{he} = Temperature of the heater to expansion space (K)

T_{rh} = Temperature of the regenerator to heater (K)

T_{kr} = Temperature of the cooler to regenerator (K)

V_b = Bounce space volume(m^3)

V_{sc} = Swept volume of the compression space(m^3)

V_{se} = Swept volume of the expansion space(m^3)

V_r = Volume of the regenerator(m^3)

V_h = Volume of the heater(m^3)

V_k = Volume of the cooler(m^3)

X_{de} = Ratio of heater volume to expansion space swept volume

X_{dc} = Ratio of cooler volume to compression space swept volume

X_r = Ratio of regenerator volume to expansion space swept volume

X_c = Ratio of bounce space volume to expansion space swept volume

X_b = Ratio of bounce space volume to compression space swept volume

Var = variables

V_{clc} = Compression space clearance volume(m^3)

V_{cle} = Expansion space clearance volume(m^3)

V_l = is maximum of the expansion volume. (m^3)

W = work done (J)

x_p = Displacement of piston (m)

$\dot{x}_p$ = Velocity of piston (m/s)

$\ddot{x}_p$ = Acceleration of piston (m/s^2)

x_d = Displacement of displacer (m)

$\dot{x}_d$ = Velocity of displacer (m/s)

$\ddot{x}_d$ = Acceleration of displacer (m/s^2)

R = gas constant value

Re = Reynolds number

S_{rate} = selection rate

$shtl$ = shuttle heat loss from the heat transfer to the cooler from the heater

Δp = pressure drop (Pa)

Subscripts

c = compression space

d = dead volume

e = expansion space

freesurf = free surface area

g = working fluid

h = heater

in = indicated

j = parts of the regenerator matrix

k = cooler

m = regenerator matrix

max = maximum

num= number

r = regenerator

$value$= value of chromosome

Greek Symbols

β = angle in Schmidt analysis

ε = is emissivity

θ = phase angle

α = difference in compression space and expansion space phase

ρ = density (kg/m^3)

μ = dynamic viscosity

δ = pressure coefficient

Declaration

I declare that the work contained is this Thesis has not been submitted for any other award and it is all my own work. I also confirm that this work fully acknowledges the ideas, opinions and contributions from the work of others.

Word count of main body of Thesis: 35,275

Name: Ayodeji Sowale

Signature:

Date: November 2015

Acknowledgement

I wish to express my sincere appreciation to my supervisor Prof. Khamid Mahkamov for his invaluable support and encouragement throughout my study.

I will also like to thank Dr. Kwanchai Kraitong for his assistance. I would also like to thank my friends in Northumbria University for their support.

Finally I will like to give special thanks to my parents Rt. Rev Dr. and Mrs Sowale for their constant care, financial and moral support throughout my study.

Chapter 1 Introduction

Numerous methods have been researched to create an alternative means of energy saving to benefit the environment. These include the combined heat and power generation on micro scale for domestic applications. The financial and environmental benefits of the micro CHP have given it an advantage as an uprising source of energy for use in residence and medium scale commercial environment. The use of micro CHP will decrease the consumption of primary energy, emission of CO2 and the end user's bill. Based on research and investigations results, Stirling engines are considered favourably for micro CHP generation due to their ability to use various fuels, low level of harmful emissions, good performance at partial load, relatively high efficiency and quietness of operation [1]. In the energy market today, there is an increase in demand for systems that can produce savings in terms of fuel and CO2 emissions [2]. This is a major reason for a strong interest in the use of cogeneration technologies. To reduce the negative environmental effect and increase the efficiency of energy conversion, a number of effective decentralized energy systems are being developed [3]. Stirling engines have been tried for use in different applications since its invention by Robert Stirling in 1816 [4]. Prototype Stirling engines have been designed and tested in transport industry (such as buses, trucks and boats) [5]. They have been also used as a propulsion engine in passenger ships [6]. Most recent application of Stirling engines are for Micro-CHP with high overall efficiency and the ability to use various fuels.

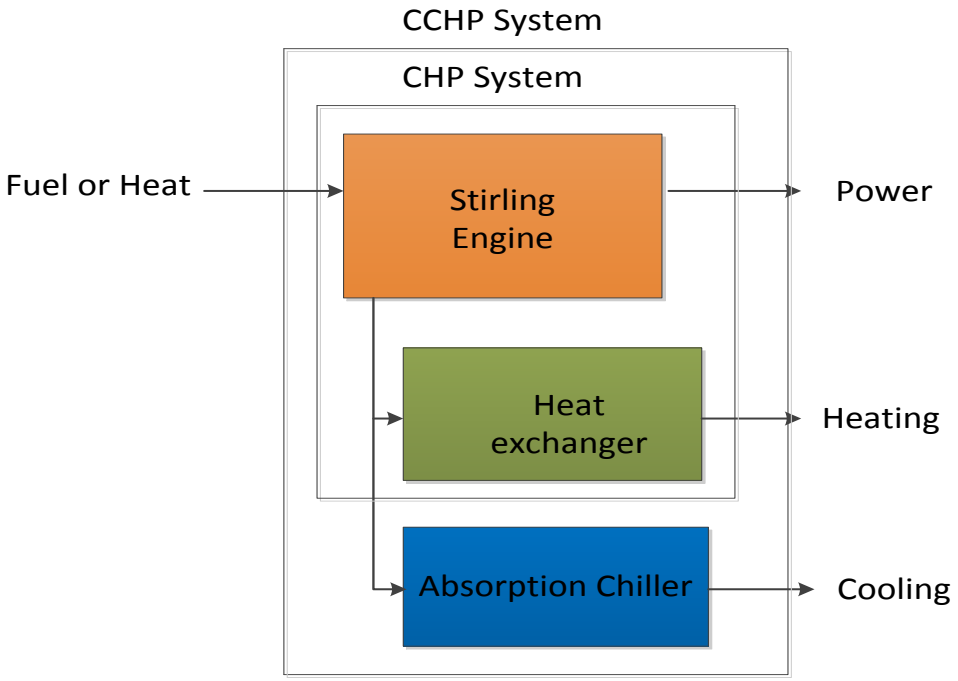

Figure 1.1: A Schematic diagram of a CCHP/CHP system with Stirling engine [7].

Certain features of the Stirling engines, which make these an attractive technology for conversion of energy, are as follows:

(i) A very low level of polluted gases emitted from the exhaust to the environment.

(ii) The operation of the engine is free of vibration and quiet.

(iii) A very low level of fuel consumption.

(iv) Engines are capable of using different fuels as the source of energy along with solar, geothermal and nuclear energy.

(v) The engine has a reversible mode of operation.

(vi) Some types of engines, namely free-piston ones are simple in the design.

1.1 The ideal Stirling cycle

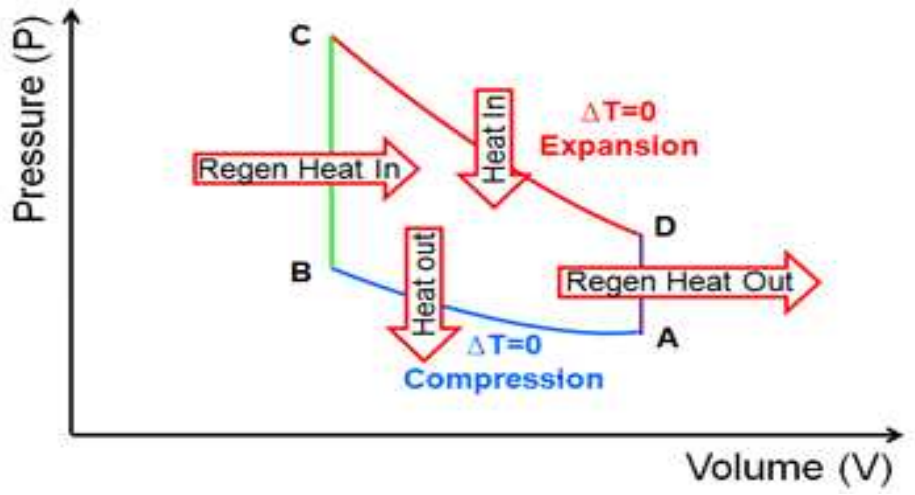

Figure 1.2: P-V diagram of the ideal Stirling cycle. [8]

The ideal Stirling cycle, shown in Figure 1.2, consists of two isochoric and two isothermal processes. In the isothermal processes that occur in AB and CD, the working fluid exchanges heat with the heat source and sink and is maintained at constant temperatures. Whilst in the two isochoric processes that occur in BC and DA, there is an internal exchange of heat transfer between the heat exchangers and working fluid, resulting in the rise or reduction in the temperature of the working fluid. In the engines with drive mechanisms the volume changes are predefined. To model and optimize the free piston Stirling engine is not an easy task because of no mechanical linkage between the piston and displacer, therefore it is difficult to determine their strokes and phase angles. To provide the stable operation of the engine, its design parameters are defined using a simultaneous analysis of the working process and dynamics of moving elements is necessary. The isothermal analysis of the working process is usually employed at initial stages of modelling. In isothermal analysis the dynamic pressure can be obtained as a

function of the positions of the displacer and piston. Hence, the engine performance is obtained deploying linearization methods [9-12]. This analysis does not take into consideration the thermal losses and the effect of heat exchangers on the engine thus leading to an imperfect prediction of the engine performance.

It is required to develop advanced mathematical models to carry out the analysis, taking into consideration the thermodynamic properties of the whole system. In order to predict the accurate performance of the free piston Stirling engine, there is need for application of the second order modelling which takes into account all the pressure and thermal losses within the engine during operation. It still can be achieved by employing thermodynamic isothermal models with the dynamic analysis of the FPSE. A Stirling engine is defined as a mechanical device that produces power through the transfer of heat from a hot temperature region to a cold temperature region [13]. The Figure 1.3 represents the schematic diagram of a simplified Stirling engine for these types of models.

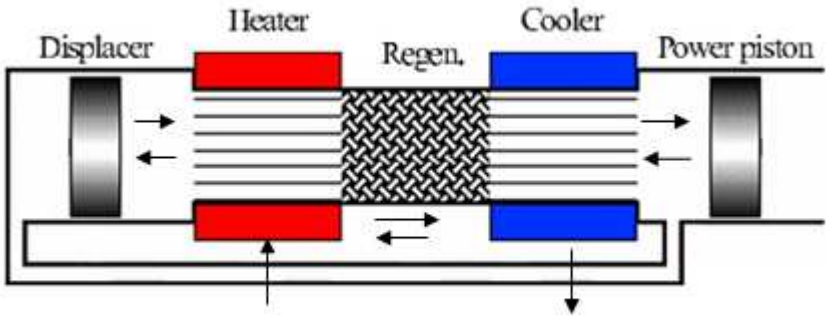

Figure 1.3: The simplified schematic diagram of the Stirling engine [14].

The engine consists of a displacer, a piston, two springs and the engine casing. The displacer and the piston are connected via springs to the casing of the engine. There is no mechanical linkage between the piston and the displacer. Their synchronous motion is achieved by the means of the gas pressure in the working volume of the engine. The

displacer is required to have a low mass for achieving necessary phase angle between motions of pistons. The inner volume of the engine consists of the dead and working volumes. The working volume is made up of the cold and hot volumes and the dead volume consists of volumes of heat exchangers (cooler, regenerator and heater). Heating, regeneration and cooling processes of the working fluid are achieved in corresponding heat exchangers. The regenerative volume can be seen in the figure above as the gap between the cylinder wall and the displacer's side surface.

The working cycle of the engine is produced if the hot end of the cylinder is heated up from an external source of energy to a certain degree of temperature, the pressure in the working volume increases in proportion to the ratio of temperature increase and this causes the movement of the piston and displacer downwards. Due to the smaller mass of the displacer it achieves a higher velocity and forces the working fluid from the cold volume to the hot volume. This results in further rise in the pressure of the working fluid which pushes the displacer and piston further downwards. While the displacer is moving from its equilibrium position, the force the displacer spring exerts on it prevails the pressure force resulting in dispacer deceleration. As displacr deceleration starts the working fluid starts to flow in the oppite direction causing the pressure drop and returning of pistons in their intial position.

The thermodynamic analysis of the free piston Stirling engine has been performed in a number of past studies using different methods. This research work aims to extend further the developed advanced modelling and optimization methods for designing free piston Stirling engines for micro-CHP applications. In the present study isothermal, ideal adiabatic and Quasi steady flow models have been developed and used for investigations.

1.2 Objectives

The main objective is to developed mathematical models required to optimize the design and performance of the free piston Stirling engine operating at steady conditions, by taking into consideration the displacer and piston's dynamics. The tasks are:

- To study the different methods and approaches to the modelling and optimization of free piston Stirling engines.
- To develop mathematical models with the set of equations to describe working process and dynamics of pistons and to analyse the general characteristics and behaviour of a free piston Stirling engine.
- To develop computer programs to perform the isothermal, adiabatic and Quasi steady flow analysis of the free piston Stirling engine's operation using MATLAB environment.
- To produce data to present the performance of the engine.
- To compare the outputs generated from the numerical model to real data available in open published sources in order to validate the developed models.
- Perform a parametric check to examine the impact on the performance of the engine model of key working process and design parameters.
- To develop a method for optimization of the free piston Stirling engine.

1.3 Methodology of research

The work in this study was divided into different stages which are as follows:

1. The isothermal model of the free piston Stirling engine was developed for preliminary analysis.

2. Numerical analysis was carried out to produce feasible values of design parameters of the engine which then could be rectified with deployment of more complex modelling and optimisation methods.

3. The second order mathematical model (based on the adiabatic model) of the free piston Stirling was developed considering the variation in temperatures of the adiabatic working spaces and the gas mass flows of the working fluid during engine's operation.

4. Numerical analysis was carried out to obtain data on using the adiabatic model and the results were compared with the experimental data for the RE-1000 FPSE, published in open literature.

5. The second order mathematical simulation code using the Quasi steady flow model of the free piston Stirling engine was developed, taking into consideration the thermal losses in the cycle, pressure drop and mass flow rates and the dynamics of piston motions.

6. Numerical simulations were carried out using the Quasi steady model and of losses taking place during the engine's operation. Theoretical results were compared with the experimental data of the RE-1000 FPSE, published in open literature, and the model was modified.

7. The developed Quasi steady flow model of the free piston Stirling engine was coupled to a Genetic Algorithm optimization code and optimal design parameters of the engine were obtained.

Thesis structure

The thesis is divided into nine chapters and described below. The structure of the thesis reflects stages of investigations described above.

Chapter 1 Introduction: This chapter is a summary of the aims of the research work performed and describes the structure of this thesis. The contribution to original knowledge was also highlighted in this Chapter.

Chapter 2 Literature review: In this chapter previous studies on the development of the Stirling engine and the free piston Stirling engine were reviewed. Results published from past investigations on the design, experimental tests and numerical simulations of the Stirling and free piston Stirling engines were described. Also different optimization methods used for free piston Stirling engines to obtain the engine's optimal design were reviewed.

Chapter 3 Theory and applications of Stirling engines: In this chapter the theory behind the operation of Stirling engines is described, their applications, different types of Stirling and free piston Stirling engine configurations and factors governing their performance are discussed.

Chapter 4 General principles and isothermal mathematical modelling of the free piston Stirling engine: In this chapter, the principles of the isothermal model for the free piston Stirling engine are discussed. The mathematical model is defined with all the required

equations employed to carry out the numerical simulation. The results generated from the numerical simulations were presented and analysed.

Chapter 5 General principles and mathematical modelling using the adiabatic model of the free piston Stirling engine: In this chapter the principles of the adiabatic model of the free piston Stirling engine are discussed with the mathematical equations presented for the second order modelling of the engine. The results generated were presented and analysed.

Chapter 6 General principles of the second order mathematical modelling using the Quasi steady flow model of the free piston Stirling engine: The principles of the Quasi steady flow model of the free piston Stirling engine are discussed in this chapter. The mathematical equations employed to carry out the numerical simulation of the engine were presented and the results obtained from numerical simulations were analysed.

Chapter 7 The principles of Genetic Algorithm: This chapter presents the general principles of the Genetic Algorithm optimization procedure which was employed for the optimization based on the Quasi steady flow model of the free piston Stirling engine.

Chapter 8 Mathematical modelling and optimization of the free piston Stirling engine based on the Quasi steady flow model: This chapter presents the outcome of simulations using the Genetic Algorithm code employed to obtain the optimal engine design parameters. The optimal design parameters were found and the improvement in the output results was demonstrated.

Chapter 9 Conclusions and recommendations for future work: In this chapter the conclusions drawn from the research and investigations in this study are presented and recommendation for future work is made.

1.5 Original contribution to knowledge

Stirling engines, especially in free-piston configurations, have advantages which make them attractive for micro-CHP applications but currently the technology has a limited use because it is yet to be fully developed. To advance the technology, accurate mathematical methods of its modelling for design purposes should be developed. Due to difficulties in description of the engine's operation, relatively simple models are in use, which simplify the description of processes taking place in the engine. One of the major simplifications is that the analysis of the working process of the engine and of dynamics of pistons is separated. This results in the low accuracy in determination of required design parameters and the engine's performance.

The main contribution of this work is that approach has been developed which allows simultaneous modelling of the working process of free-piston Stirling engines and of pistons dynamics. This is accomplished for models of different levels: the first order, advanced second order and Quasi steady flow model of the free piston Stirling engine. Results of the low level models are then used for modelling at the following stage with deployment of the model of higher level. Finally, the optimisation procedure was developed, based on application of the Quasi steady flow model coupled to Genetic Algorithm approach, which provides determination of optimal design parameters of the engine to achieve the specified power output.

Chapter 2 Literature Review

2.1 Introduction

Previous works related to the development and modelling of Stirling and free Piston Stirling engines are critically reviewed in this chapter. The chapter presents published results on the experiments, designing and simulations of Stirling and free piston Stirling engines.

2.2 Stirling engine modelling

In this section the past studies on the mathematical modelling of the zero order, first, second and third orders of Stirling engines and free piston Stirling engines are presented. Also the use of Genetic Algorithm methods to carry out optimisation of Stirling engines and of other optimisation techniques is described. The fundamentals of the working principles of the free piston Stirling engines are described. Stirling engine simulation and modelling was traditionally performed in the sequence using zero, first and second order models, with each step leading to a more accurate approximation of the engine's operation in the reality.

2.2.1 Zero order modelling

The zero order modelling is an empirical approach to modelling the Stirling engines rather than the mathematical approach. William Beale introduced the zero order modelling of the Stirling engine as a result of processing a large number of statistical experimental data [15]. Its principle requires more experimental observation other than the special mathematical approach. Other related studies have been carried out by Erbay and Yavuz

on the analysis of the engine cycle with focus on the polytropic process in the power piston and displacer volumes [16]. A model was developed by Fiedt et al on the general law of heat transfer at the heat source and heat sink based on the ideal cycle [17]. Timonmi et al performed a research on the Stirling engine model with focus on the incomplete regeneration and irreversibility on the ideal cycle [18].

2.2.2 First order modelling

This is an analytical approach to the study of ideal Stirling cycle. The first order model produces performance outputs of Stirling engines overestimated than in the reality due to us of assumptions to idealise the cycle. Gustav Schmidt produced the first order modelling of the ideal Stirling cycle [19]. The result of the analysis produces information on outputs with a low accuracy, but the approach is generally preferred over the zero order. Though it relies on the assumptions of ideal parameter values, it has proven to be a very productive tool for analysing and predicting the engine cycle to generate realistic performance outputs for the engine. Finkelstein conducted a research on the isothermal model of the engine where he tried to proffer solution to the problems encountered in the Schmidt analysis [20]. Kongratool and Wongwise generated an isothermal model of the engine and established the significance of defective regeneration and dead volumes of the system [21]. A related model was developed by Walker on the engine's four dimensional geometry [13].

The method of approach requires removal of the components of the engine design geometry into a separate subordinate design phase. It proved as an advantage in the engine design but its validity was not generally accepted. [4]. Schmidt's model is not sufficient for use as the major approach for the Stirling engine design because it uses ideal assumptions to predict performance of the engine than in reality. Schmidt proposed a close form

expression for the cyclic work of the Stirling engine by developing a mathematical model based on the mass conservation equation. The analysis predicted the behaviour and characteristics of the Stirling engine [22]. The Carnot efficiency is achieved with the Schmidt model due to made assumptions. The model has shown the possibility to align the ideal model to the performance of the actual engine by employing certain correlation factors. The Schmidt analysis was conducted on the Stirling engine using the dead volume with assumptions for isothermal conditions and ideal regeneration [22]. The isothermal and non-isothermal model of the FPSE was conducted by Ulusoy in order to analyse the nonlinear effects. The effects that were studied are non-linear pressure loss, non-linear damper load and gas spring of the displacer, the coefficient of non-linear load terms was used to obtain the stable operation of the periodic motions for the piston and displacer. The non-isothermal behaviour of the working fluid in the FPSE during operation resulted in the difference in temperature. From the analysis a conclusion was made that an isothermal analysis is suitable and more predictive than the non-isothermal analysis for a qualitative dynamic analysis of the engine because the temperature of the working fluid had no noticeable effect on the engine dynamics [23]. There have been a number of approaches to modify and improve the performance of the Stirling engine. The changes have been applied to Stirling engines over the years.

Heat pipes and capillary pump loops were used by Kroliczek et al to produce a more effective means of heat transfer[24]. Also research was performed by Abdulrahman on the engine regenerator as to design and carry out tests on the material to be used to make it more effective [25]. Also various types of working fluids and materials for displacer and piston have been investigated to find the most suitable ones for better engine performance. Although the Stirling engine might not be efficient enough for applications with expected large power output, their mode of operation can be employed in wider applications. The

general conditions of the practical behaviour of the Stirling engine like the adiabatic internal heat exchangers and heat transfer in the surrounding of the Stirling engine have not been critically examined but the ideal thermodynamics have been analysed. The factors that affect the engine operation in reality need to be considered and examined in order to discover the influence on the actual engine. The temperature of the working fluid in the engine during operation is more likely to behave in an adiabatic manner than isothermal. Thermodynamic evaluation of irreversible Stirling and Ericsson cycles has been performed in [26]. The analysis was based on the perfect and ideal gas regeneration for losses in heat sink with engine power output. The performance of Stirling engine is determined by the various conditions of heat transfer. The research conducted by Costea and Feidt showed that the temperature difference of the engine's hot components varies linearly with the heat transfer coefficient [27].

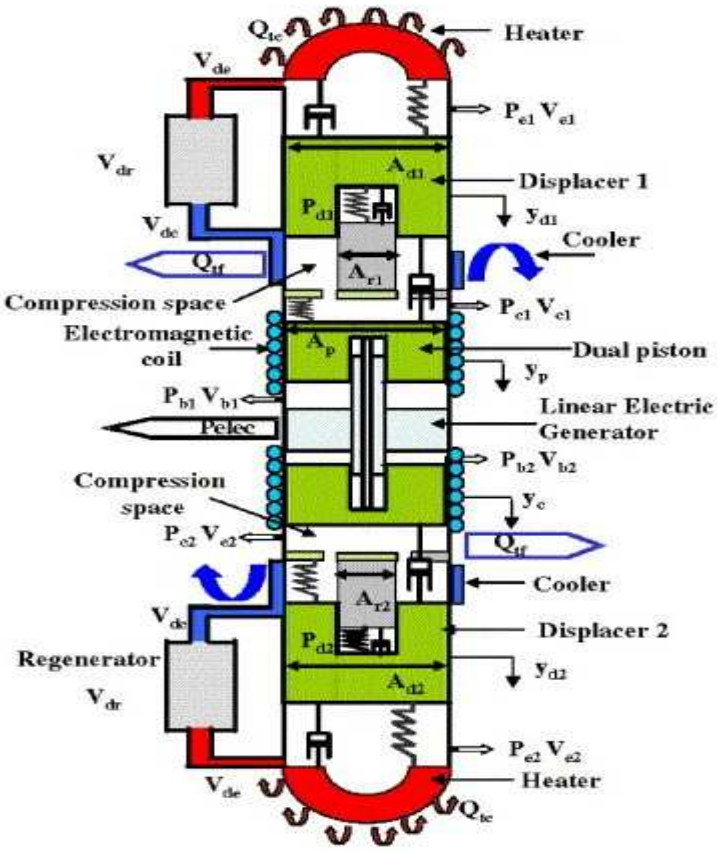

Figure 2.1: Schematic diagram of a dual free piston Stirling engine [2].

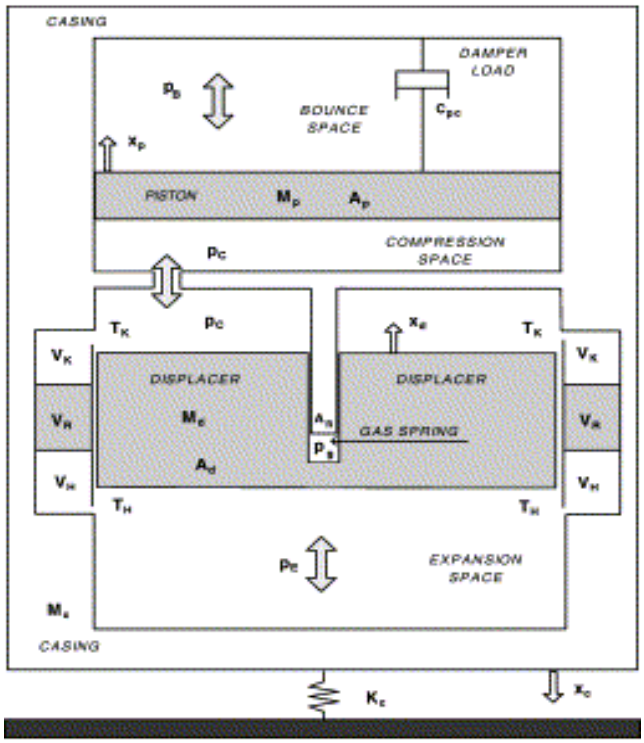

Figure 2.2: Notation of a typical beta type free piston Stirling engine [9].

2.2.3 Second order modelling

The second order modelling of the Stirling engine is a further development of the first order model. It is a more rigor approach to the modelling of Stirling engines which accounts for various losses that occur during engine operation. The second order analysis of the Stirling engine proved to be a more complex approach to the study of the engine's performance. In order to enhance the first order method analysis, the second order modelling provides a detailed description of the losses encountered during engine's operation. A study was conducted by Boucher et al in [2] on a double free piston Stirling engine by developing dynamic balance equations, see Figure 2.1. The non-linear dissipative effects of the fluid and the electromagnetic forces were considered in the model and the equations were solved in the time domain together with the linearized pressure equation in order to achieve a steady operation of the engine. These losses are usually

encountered during the flow of working fluid, power transfer and transfer of heat in the engine during its operation [28]. In this analysis the design of the engines component is of a paramount importance. Various analyses have been carried out on the engines component design such as the displacer, piston, regenerator, cooler, heater and other necessary significant components in [17, 29-31]. Pretescue employed the direct method for processes to analyse the irreversibility that occurs in the non-ideal situation of the Stirling engine cycle [32]. The second order approach was employed by Domingo for the solution of equations to analyse Stirling heat pumps [33]. The method which uses the direct integration of equations resulting from the first law for processes with finite speed was used in the second order approach in [34]. The method was considered to be successful due to the reasonable output results and its ability to predict operation in good agreement which real data of the engine performance. The second order modelling of the Stirling engine was developed by Timouni et al., where the lumped analysis, which took into account all the losses within the engine at the same time, was employed and used to optimize the General motors GPU-3 engine [35]. Martini conducted a second order analysis of the Stirling engine using the non-ideal regeneration to balance the energy equation from the Schmidt analysis. The heat transfer between the engine and the heat exchangers were taken into account. A number of investigations have been performed on the effect of irreversibility and heat losses on the performance of free piston Stirling engines. It was observed that in all the technological parameters of the Stirling engine, non-ideal regeneration and dead volume have the greatest influence on the engine performance [19, 36]**.** According to Popescu et al. the non-adiabatic regenerator has the most effect on the performance reduction of the engine [37]. A research was conducted by Kongtragool on the efficiency of regenerator and dead volumes on the total work done and engine efficiency without taking into consideration the heat transfer within the heat exchangers, heat source and sink [38]**.** The first non-isothermal analysis of the Stirling engine was carried out by

Finkelstain. The model he developed was able to derive the finite heat transfer in the working space of the engine by the use of the heat transfer coefficient. Also the difference in the working gas temperature as it moves through the working space was calculated [39]. A general model for the simulation of Stirling engines was developed by Schulz and Schwendig [40]**.** Kongtragool and Wongwise developed a thermodynamic analysis of the Stirling engine by taking into consideration the dead volume of the working space, including those in the expansion space, heater, regenerator, cooler and compression space [38]**.** Karabulut simulated the operation of the Stirling engine, where he carried out kinematic and nodal thermodynamic analysis on the instantaneous temperatures of the working gas through the working space. For this study a beta type Stirling engine with a lever driven mechanism on its displacer, as shown in Figure 2.3, was used [41]. A solar Stirling engine was investigated by Mahkamov where the working process of the engine was analysed by the axisymmetric computational fluid dynamic approach [42]**.** A detailed analysis of the operational characteristics of a 10kW dish/Stirling system was presented by Reinalter et al [43].

The compressible flow of the working gas through the working space and the oscillations of the piston and displacer using a control-volume-based modelling were analysed by Anderson et al [44]. Schmidt presented a second order approach to the analysis of the ideal cycle of the Stirling engine. In the analysis he assumed the sinusoidal variation of the compression and expansion spaces. It was noted that the proposed analysis could not account for the non-isothermal effects and internal irreversibility caused by difference in pressure and friction of the working fluid in the working spaces of the engine [22]. A numerical study was carried out on regenerator matrix design to improve the efficiency of a Stirling engine. Numerical model of the engine was developed and a new regenerator

design was optimized by dividing the regenerator matrix into three sections. The new design improved the overall temperature oscillations of the matrix, reduced the inflow effect on the matrix oscillations thereby improving the efficiency of the engine [45]**.** An investigation was conducted by Kuosa et al [31] on the impact of heat exchangers fouling on the optimum performance of the Stirling engine for the combined heat and power application. A steady state operation was achieved in the developed model considering the fouling factors of the heat exchangers. The developed model was used to evaluate and predict the fouling factors from the output performance of the engine**.** Formosa [10] conducted a study on the operation of a miniaturized membrane Stirling engine. The steady state operation of the engine was achieved by predicting the starting conditions of the engine and the instability problems with the aid of the stability analysis. The method of approach to obtain a simplified system without exempting the dynamics of the original systems was done by reducing the number of equations**.** An investigation was carried out on the development of a numerical model for a beta type Stirling engine with the rhombic drive mechanism.

This was done by considering the regenerator effectiveness, non-isothermal effects and thermal resistance of heater. The energy equations of the control volumes in the expansion and compression chambers and the regenerative channel were derived and solved. The output of the engine was improved by adjusting certain parameters such as regenerative gap, offset distance from the crank to the center or gear and the temperature of the heat source [46]**.** There are three stages of Stirling engine analysis deployed. The isothermal Schmidt analysis is the first stage, the second order analysis which is adiabatic is deployed at the second stage. Finally, the third order analysis was utilised for calculations [19, 39, 47]. The research conducted by Wu et al. shows the effect of the regeneration, imperfect regeneration and heat transfer on the Stirling engine cycle performance [36]. A new

theoretical method was developed for the evaluation and improvement of the actual Stirling engine performance. Riofiro et al. developed a dynamic model of the free-piston Stirling, shown in Figure 2.4, by conducting linear analysis for the dynamic modelling elements which were employed in place of the equation of state and the output result generated was compared to the output from the experimental results [48]. Investigation was carried out on the FPSE by applying scaling effects which allows for miniaturization, as shown in Figure 2.5.

Major losses such as the heat conduction loss, pressure drop and regenerator reheat loss were defined as a function of the operating and geometrical parameters [49].

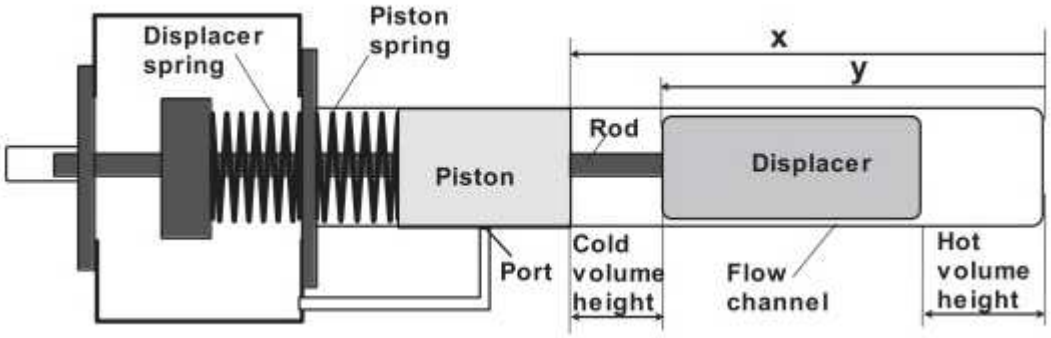

Figure 2.3: Layout diagram of a free piston Stirling engine [41].

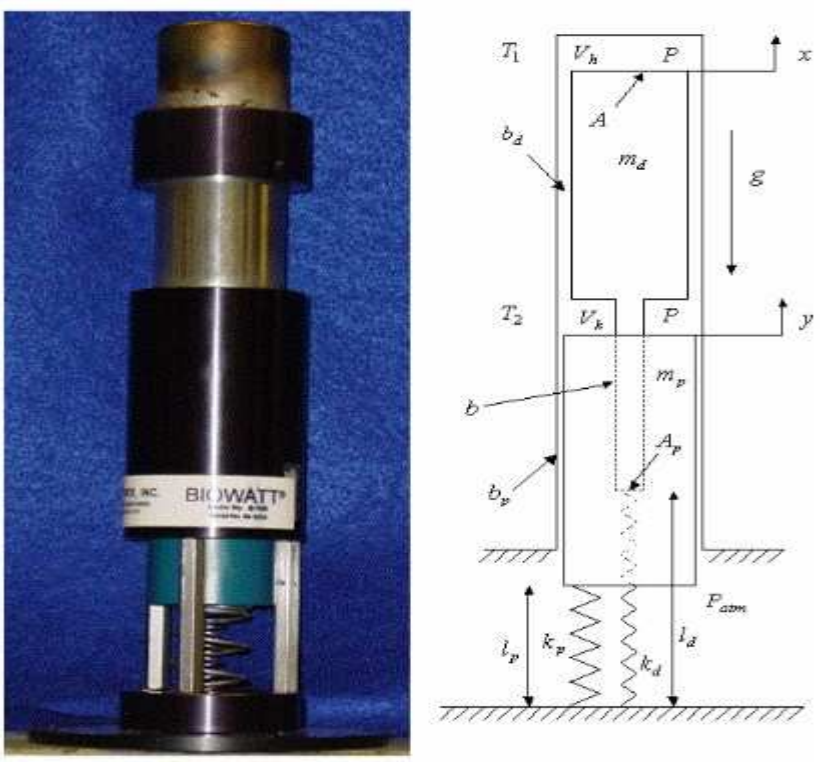

Figure 2.4: Sunpower B-10B free-piston Stirling engine demonstrator [48].

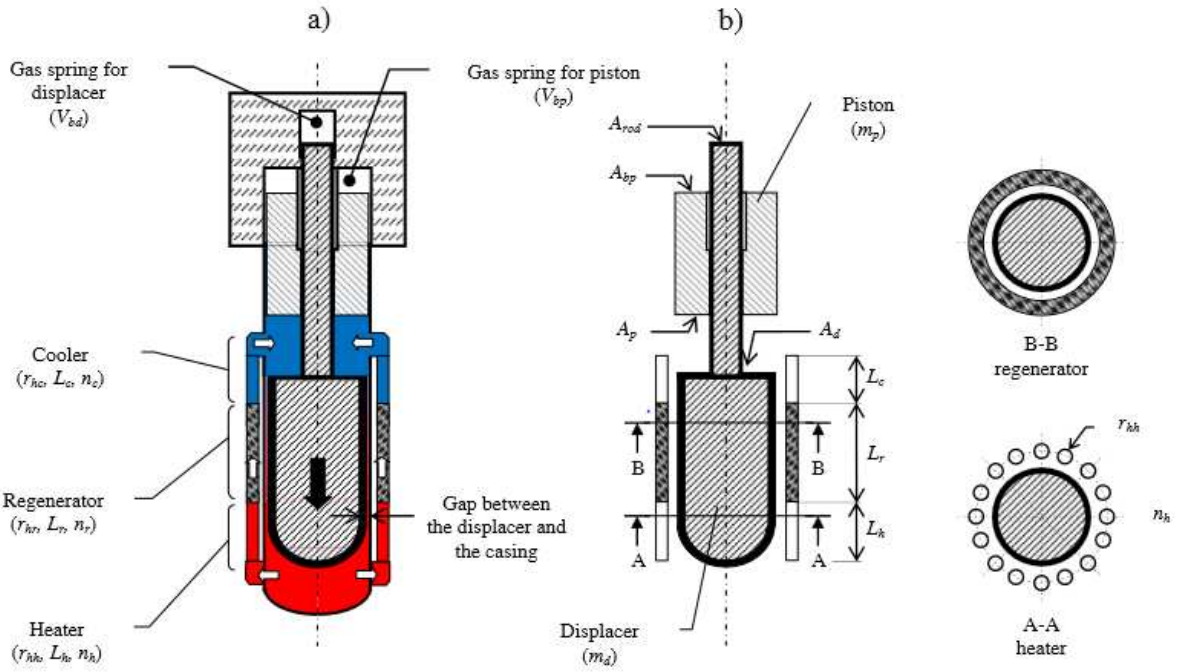

Figure 2.5: Geometry of the free piston Stirling engine [49].

2.2.4 Third order modelling

The third order model is similar to the second order model but it is a more advanced approach to the modelling of Stirling engines. A study was performed on the conventional Stirling engine cycle performance which took into account the effects of incomplete heat regeneration, heat transfers within the heat exchangers and the cycle irreversibility, friction between the displacer and piston with the walls of the engine and pressure losses by Costea et al [50]. A very careful measure is required to understand the working principles of the engine in order to determine the design parameters, losses within the engine and its performance output.

The investigations carried out by Kaushik and Wu exhibited the key factors affecting the performance of the Stirling engine such as the heat transfer within the engine, the regenerator effectiveness and the rate at which the regenerator absorbs and releases the heat during the heat transfer back and forth within the heat exchangers [26, 36]. A study was conducted on a split-Stirling cryocooler with the aid of dynamic simulation by Cun-quan et al. The losses encountered such as shuttle loss, pump pressure loss and losses due to regenerator inefficiency were integrated into the mathematical model. Hence a conclusion was achieved that accounting for such losses improves agreement between the experimental and mathematical model results [51]. A beta-type Stirling engine functioning at atmospheric pressure was produced by Cinar et al and the observation on the parametric check showed that increase in the hot source temperature also increased the speed, torque and output power [52]. Some losses were analysed by Walker in the research he carried out on Stirling engines: shuttle, load and spring hysteresis losses. Due to the difficulty in determining such losses these are not usually considered in detail in the literature [13]. A quasi-stationary and adiabatic model was developed by Urieli and Berchowitz where pressure drops in the heat exchangers were considered. The calculations demonstrated that

though there was difference between the experimental results and the model, agreement was still better than with other models. Hence the performance of the Stirling engine depends on the physical and geometrical properties, the working fluid, pressure drops, heat losses, hysteresis losses and temperature changes. Parlak et al conducted an investigation on a gamma type Stirling engine considering the thermodynamic analysis of its quasi steady flow model. The analysis was performed on the five component parts of the engine namely expansion and compression spaces and heat exchangers (heater, regenerator and cooler). The output results generated from the developed model predicted more accurate results than the models available in literature [53]**.**

Also detailed research was carried out on Stirling engines in order to increase their performance output and analyse their operations.

A numerical simulation model was developed considering the thermal losses to optimize the engine performance. The experimental data from the GPU-3 Stirling engine was used and the results obtained showed a good correlation with prototype of the engines output. Also the influence of the physical and geometrical parameters on the engine performance was investigated in [54]**.** A research was performed on the design of a low temperature differential double acting Stirling engine for solar application. The engine design was determined based on Schmidt analysis and third order analysis was used to establish a complete analytical model during the design optimization stage [55]**.**

2.2.5 Optimisation of Stirling engines

Optimisation research is being performed on improvement of designs of the cold-end and hot-end heat exchangers and regenerator of the Stirling engine based on the thermodynamic and other types of mathematical models. For example, the mathematical

model of the Stirling engine, based on the finite dimension thermodynamics process, was used for optimisation calculations. The engine under steady state condition was analysed using the energy balance equations. Certain parameters such as the thermal efficiency and output power, were considered as the objective function in order to carry out the optimization in [56]. A one dimensional model was produced by Boer [57] for analysing Stirling engine regenerators. This model was developed from the simplified equations considering the thermal and viscous losses.

The output from the optimisation provided the optimal values of the piston phase angle and parameters of the regenerator to achieve maximum power output. A model for optimisation was developed by Senft using the principle of the forced work integrated to the classical Schmidt theory. The results obtained from the optimisation produced maximum brake work considering the optimal values generated for the swept volume ratio and phase angle [58]. Cullen et al. carried out optimisation of the geometry of the gamma-type Stirling engine. To obtain preliminary results of the modelling of an Otto/Stirling cycle hybrid engine, Schmidt model was considered. The results derived from the simulation, using direct method, were compared with the simulations with respect to the engine speed using the Schmidt model [59]. A study was performed by Orunov et al [60] on the design of the tri-generation power unit based on the alpha Stirling cycle for the production of CCHP-combined cooling, heating and power production. At the first stage of the design process, the first order model of the Stirling cycle was developed and hydraulic losses were considered. The second order model which was used after the first order took into account the hydraulic losses in the heat exchangers in order to analyse the process of the working fluid. The optimisation was performed considering dimensionless parameters such as the length of the heat exchangers (heater, regenerator and cooler) as the criteria for the procedure. The Optimisation of 20 kW Stirling engine was carried out by Zarinchang and

Yarmahmoudi. The second order model of the engine was used for optimisation by coupling to the code named OPTIMUM. The sensitivity analysis was used to redesign the heater, cooler and regenerator. A third order program called STRENG was used to recalculate the results obtained from the optimisation with the second order model for more accurate output result prediction [61]. An investigation was conducted by Blank and Wu [62] on an extra-terrestrial Stirling engine using the irreversible thermodynamic cycle analysis powered by a solar heat source.

The optimal values of the power output and overall efficiency were determined using the finite time approach. An analysis was conducted by Erbay and Yavuz on the performance of the Stirling heat engine at maximum operating conditions. The model of the thermodynamic cycle of a Stirling engine with a regenerative heat exchanger was used to determine the power output and efficiency. The engine performance was analysed using the maximum power density technique [16]. The operating temperature for a solar powered Stirling engine was optimised with the use of mathematical model based on Stirling engine thermodynamic cycle by Costea et al [63]. The mechanical losses and fluid friction was considered using empirical correlations in the model. Lagrangian undetermined multiplier method was employed to solve the system of nonlinear equations to obtain output results.

2.3 Free piston Stirling engine modelling

The layout of the free piston Stirling engine that was invented by William T. Beale in the early 1960s resulted to be one of the assuring discoveries in the applications of the Stirling cycle [64]. It consists of a simple mechanism where direct translational vibrations of the piston and displacer produces power output [13]. Different types of heat source such as radioisotope energy, fossil fuels, solar energy, geothermal energy, coal, wood etc. can be used as the source of inut energy. The free piston Stirling engine developed by Sunpower Inc. is shown in Figure 2.6.

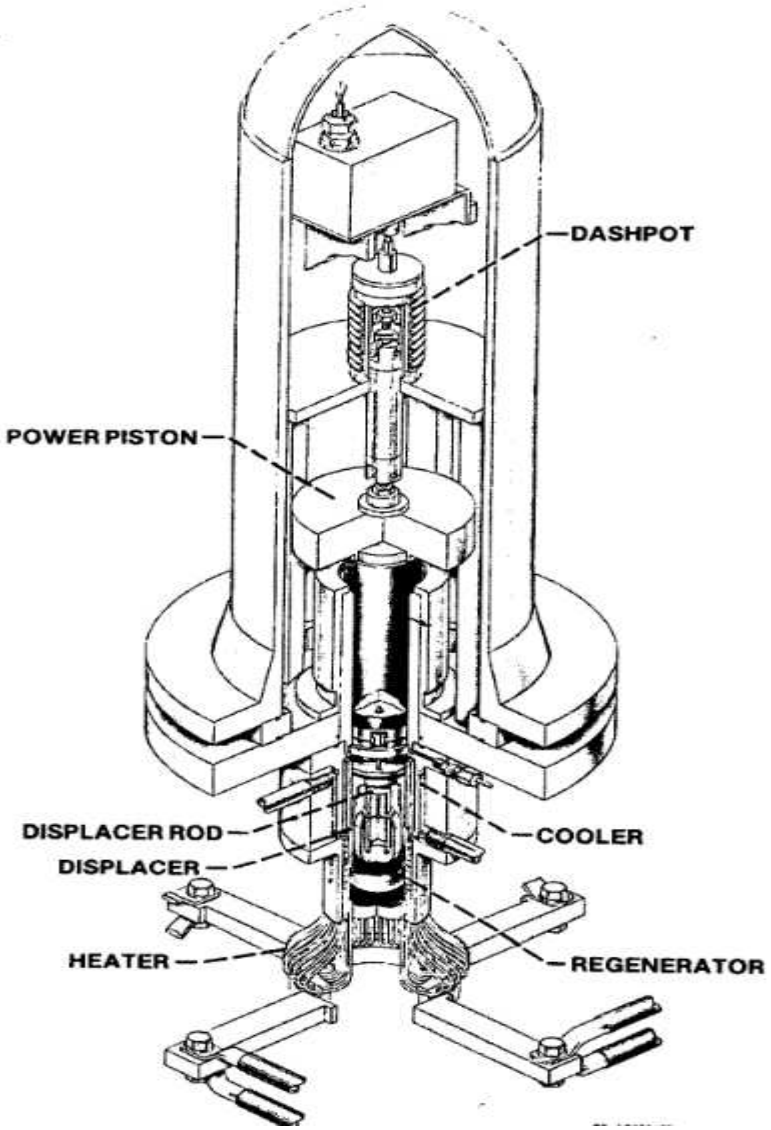

Figure 2.6: Cut away view of RE-1000 free-piston Stirling engine [65].

To perform a thermodynamic analysis on the FPSE the phase angle, expansion and compression swept/clearance volumes need to be determined. In classical Stirling engine these parameters are predetermined by mechanical kinematics. Parameters such as mean pressure, external temperatures and frequency are also determined. The expansion and compression temperatures are defined by the characteristics of the heat exchangers and the properties of the working fluid.

2.3.1 First order model

A linearized model was produced by Urieli and Berchowitz in order to analyse and predict the stable operation of the engine [19]**.** The Linear dynamic analysis of the FPSE produces estimated output which can be used to predict the engine design and performance [66]. The analysis carried out by Redlich and Berchowitz was to linearize the motion equation for the displacer and piston caused by the pressure of the working fluid and the gas springs [67]. The analysis predicted the algebraic relations between the thermodynamic and geometric engine parameters. It can be used to predict the performance stable operation of the engine. Organ carried out an isothermal assumption where he proposed a method to examine the mass flow rate in the engine. The mass flow rates are linked to the piston and displacer strokes, phase angle, operating frequency and temperature [30].

2.3.2 Second order model

The Hopf bifurcation method was used for the non-linear analysis of the FPSE and for its simulation deploying Schmidt and Nodal analysis. Multiple scale method was used on the beta FPSE with cube damping in the power piston chamber to examine the nonlinear system in order to create limited cycle motions. The comparison was carried out between the numerical and analytical results which gave a close prediction of the output generated [68] . Parametric check was also carried out to evaluate the different parameters that could result in instability in the Hopf results.

The thermodynamic model of the engine can be developed for the given sink and heater temperature [69]**.** Realistic results of the FPSE can be produced with the use of dynamic-thermodynamic studies. Thus, Kim et al carried out a study on the thermodynamic performance of a 35W, 80W and 1.1 W solar powered free piston Stirling engines, see

Figures 2.7 and 2.8. The results were presented for the output power over a wide range of temperatures. The engines attained an overall efficiency greater than 55% of Carnot efficiency at their design specifications [70]. A study was conducted by Formosa and Despesse on the free piston Stirling engine configuration by developing an analytical thermodynamic model. In order to achieve a more realistic output result, heat losses and irreversibility during engine operation were taken into consideration. The effectiveness of the heat exchangers, especially the regenerator, was investigated. Optimization was carried out by reducing the losses and improving engine performance [69]. A research was performed on the thermal efficiency of a low mass 35W free piston Stirling engine design. The predictions of the engines output performance in terms of power output and efficiency were similar to that of the Sunpower EG-1000 engine [71]. The study was carried out on the Free piston Stirling engine pumps by Beachely and Fronczak [72]. Another method was deployed by McGee et al. to evaluate the hydraulic power supply by introducing the mono propeller to drive the free piston hydraulic pump [73].

Considerable emissions and high noise occur due to the short combustion of the internal combustion engines.

An analysis was performed on the stable operation of the Stirling engine by Rogdakis et al. where a linear analytical model was developed. The schematic diagram of the beta free piston Stirling engine employed is shown in Figure 2.2 [9]. Linear coefficients were introduced to model the dynamics of the Stirling engine by De Monte and Benvenuto which was equivalent to the nonlinear model [12, 74]. Analysis was carried out using the linearized model of the engine with the nonlinear load by Ulusoy and Mc Caughan in [23].

2.3.3 Third order model

Benvenuto et al proposed a method of analysing the FPSE which gave a good prediction of the stationary oscillations of the displacer and piston taking into consideration the pressure loss within the heat exchangers that in turn produced a steady amplitude of oscillation but the analysis has not been experimentally validated [75]. It also gives room to investigate the engine behaviour under various loading conditions such as change in the parameters of the spring stiffness, instantaneous pressure, damping coefficient and weight of the moving elements [76]. Therefore, an accurate global method using a thermodynamic isothermal model in agreement with the dynamic analysis is required to design a free piston Stirling engine. There is more complexity in the numerical calculations associated with the third order modelling in comparison to the second order. To model an engine in the third order, there is need to form and produce the partial differential equations of the momentum, , mass and energy conservation for a number of gas control volumes in the circuit of engine. A Stirling engine analysis code called H-FAST which employs the harmonic analysis method was developed by Huang [77] . The energy, momentum and mass conservation equations were used in a simplified manner. To obtain the correct output results, the various losses were determined. The software called PROSA developed by Thomas was described by Anderson in [78]. A one- dimensional modelling approach for a Stirling engine was produced by Anderson et al [79] which takes into consideration the compressibility in the unsteady gas flow. The empirical correlations were used to determine the losses due to the finite temperature heat transfer and flow friction. The MusSIM software was used for the modelling approach on the SM5 Stirling engine. The results obtained from the simulation showed a good agreement when compared to experimental data. For accurate prediction of power output and efficiency there is need for correct empirical correlations to calculate friction and heat transfer in the regenerator and

heat transfer in the displacer clearance space. In addition shooting method was employed for the optimisation carried out in this study.

2.4 Optimization of free piston Stirling engines

Certain parameters such as the maximum thermal efficiency, maximum power, minimum entropy generation and maximum exergy efficiency were considered as the objective functions in order to carry out the optimization of the FPSE in [80]. A one dimensional model was produced by Boer [57] for analysing Stirling engine regenerators. The model was developed considering the thermal and viscous losses.

The output from the optimisation calculations provided the optimal values of the piston phase angle and parameters of the regenerator to achieve the maximum output power. A model for optimisation was developed by Senft using the principle of the forced work integrated to the classical Schmidt theory. The design parameters obtained from the optimisation ensured the maximum brake work at the optimal values of the swept volume ratio and phase angle [81]. The optimization of the heat exchangers of the FPSE was performed by Shoureshi on the basis of ratio of the operating temperatures, Mach number and percentage of heat exchanger dead volume [82].

A method was proposed in 1990 by Benevenuto et al for the optimization of the free piston Stirling engine in order to predict design parameters of the engine for space applications. A special consideration was used for the effects of losses due to gas hysteresis in the gas spring space with the temperature variation effect in the working space. The analysis performed resulted in the method to ascertain the dynamic behaviour of the FPSE model [74]. The free piston Stirling engine is one of the forms of the Stirling engines designed by Beale in the 60s [83]. The basic mechanical structure of the FPSE with no lateral loads

reducing wear and providing longer running time, is the major advantage it has over other classical Stirling engines and internal combustion engines [84, 85]**.** To optimize a FPSE is a difficult and challenging task. The piston and displacer are driven by the spring pressure and working gas. The motions of the displacer and piston alter the volume of the working space as well as the pressure and pressure losses through the heat exchangers. Before the dynamic model of the FPSE is developed the thermodynamic properties of the engine must be defined. In order to obtain the performance of the FPSE, linearization methods were employed and behaviour of the engine was determined. With this type of analysis the steady state operation of the engine cannot be predicted accurately [86]**.** The evaluation of the pressure drop during the engine operation is very important for accurate prediction of operation of FPSEs. . The performance of a free piston Stirling engine, powered by the heat from an incinerator, was investigated by Hsu et al [87]. The cycle-averaged heat transfer coefficient's value was used to determine the engine thermal efficiency and the power output for various heat source and sink temperatures. It was discovered that the optimal power output and efficiency were proportional to the temperature of the heat source. The feasibility of power production using the waste heat of an incinerator and a FPSE was investigates by Hsieh et al. The heat transfer with irreversible processes with the Lagrange multiplier method was used to optimise the engine's output power. For this, the FPSE performance was predicted and maximum power was considered as an objective function in the procedure for optimisation [88].

The review of the optimisation methods used for designing engines shows that there has been very limited usage of Genetic algorithm methods.

2.5 Optimization using the Genetic Algorithm procedure

The use of Genetic Algorithm has been applied previously in many engineering fields, but it has not been much used in the design of free piston Stirling engines. A brief review on application of Genetic Algorithm method for designs of engines and thermal machines is discussed in this section and the detailed description of Genetic Algorithm and its procedure in application to the FPSE is provided in Chapter 7. GA was used to optimise four parameters of the turbofan engine, such as the compression pressure ratio, bypass ratio, fan pressure ratio and Mach number. The results generated ensured the best values of the overall efficiency and thrust per mass flow rate and this case demonstrated that GA is a good tool for improving the engine performance [89]. The GA method was employed for the optimisation of a natural gas engine by Kesgin in [90]. The objective functions for optimisation were the efficiency and NOx emissions.

Also the heat exchanger, which is a very essential component of the thermal system of a heat engine, was also optimised using the GA method. A computer program for obtaining the optimal design of heat exchangers was developed by Tayal et al [91]. For the GA optimisation procedure of the ST-5 engine, HTRI program was used to determine the heat transfer area. Different strategies of GA were employed to obtain the overall minimum costs. The simulated annealing (SA) and GA methods were compared and discussed. GA optimisation method was used by Mohagheghe and Shayegan to determine the thermodynamic optimal design of heat exchangers in the heat recovery steam generator (HRSG) of the combined cycle gas turbine (CCGT). Taking into account the non-linearity of the system, the GA turned out to be the best optimisation tool [92]. The optimal design of shell and tube-heat exchangers was determines using GA method by Ponce-Ortega et al [93]. The heat exchanges were designed using the Bell-Delaware method but due to high level of the system nonlinearity, GA was employed for the optimisation. The objective

function was the cost of the heat exchanger and parameters such as standard internal and external tube diameters, number of tube passages, tube pitch and layout, inlet and outlet baffle spacing, shell-side and tube-side pressure drops and number of sealing strips. Kwanchai Kraitong performed and optimisation of the design of LTD and MTD Stirling engines using the GA method, the objective was to maximise the power output and the overall efficiency. The parameters considered for the optimisation were length and diameter of the heat exchangers (heater, regenerator and cooler), porosity of the regenerator matrix and its wire diameter [94].

2.6 Designs of free piston Stirling engine prototypes

Prototypes of the free piston Stirling engines designed and developed by Sunpower for power production are presented in Figures 2.7 and 2.8 below.

Figure 2.7: Sunpower EG-1000 free piston Stirling engine [70].

Figure 2.8: Sunpower EE-35 free piston Stirling engine [70].

2.7 Conclusions

The literature review in the subject area demonstrates that a large volume of investigations has been conducted on the second order modelling of kinematical Stirling engines but there has been limited study on application of the second order modelling for free piston Stirling engines. The second order mathematical models developed have been used to predict the performance of the kinematical Stirling engines and analyse their working process. The accuracy in the output results is achieved at reasonable computing time and is in a good agreement with experimental data. The first order approach only predicts the indicative values of the engine performance but requires less time for computation. The Quasi and third order models might provide a better insight into the working process and better accuracy in the prediction of the engines performance although this method requires significant time for computations. Most of studies on optimisation of engines was carried using closed form solutions for the efficiency or engine power, which are used as the objective functions. There are a number of studies which used high order models to carry out parametric analysis to determine the optimal engine design parameters. Genetic algorithm has been used in the optimisation of the design of kinematical Stirling engines

and other heat engines with the heat exchangers but it has not been used for the free piston Stirling engine.

Few studies conducted the second order modelling of free piston Stirling engines. However results described on the operational performance of the FPSE at a steady state operation were not sufficiently accurate, even those taking into account thermal losses encountered during the engine operation. Very few papers described the complete design procedure of the FPSE with the use of optimisation methods.

Therefore, this present study will focus on the design and development of the first, second and Quasi steady flow model of the free piston Stirling engine and such approach can be considered as an advanced one which takes into consideration the thermal losses and other losses encountered in the cycle and provides better understanding of the working process of the engine. The engine's mathematical model will then be coupled with the GA method to obtain the optimal design parameters to provide better FPSE performance.

Chapter 3 Theory and Applications of Stirling engines

3.1 Introduction

In this chapter, the fundamental operational principles of the kinematical Stirling and free piston Stirling engines are discussed. The in-depth analysis of the design configurations and the fundamental principles of thermodynamics of the Stirling engines are also presented.

3.1.1 Configurations of Stirling engines

The Stirling engines are categorized into three types, namely alpha, beta and gamma. The alpha engines consist of two separate cylinders which contain the two pistons and usually configured into "V" shape. The Beta engine is made up of the piston and displacer in the same cylinder, while the Gamma engine consists of two separate cylinders which house the displacer and piston and compression space is formed in the part of piston cylinder and in the displacer cylinder.

3.1.1.1 Alpha Stirling engine

The alpha configuration of Stirling engines is designed in the such way that the expansion and compression spaces are separated and located in different cylinders, which house the two pistons, see Figure 3.1. The alpha Stirling engine is most suitable for low temperature heat sources, refrigerators and heat pumps. In the alpha engine the changes in the volume of working fluid in expansion and compression spaces are carried out by the combined action of the two pistons.

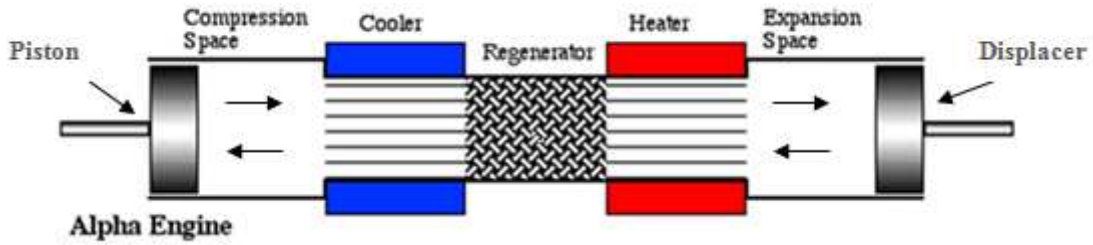

Figure 3.1: A schematic diagram of the alpha type Stirling engine [95].

The Ross yoke engine in Figure 3.2 can be considered as an example of both alpha and gamma engines.

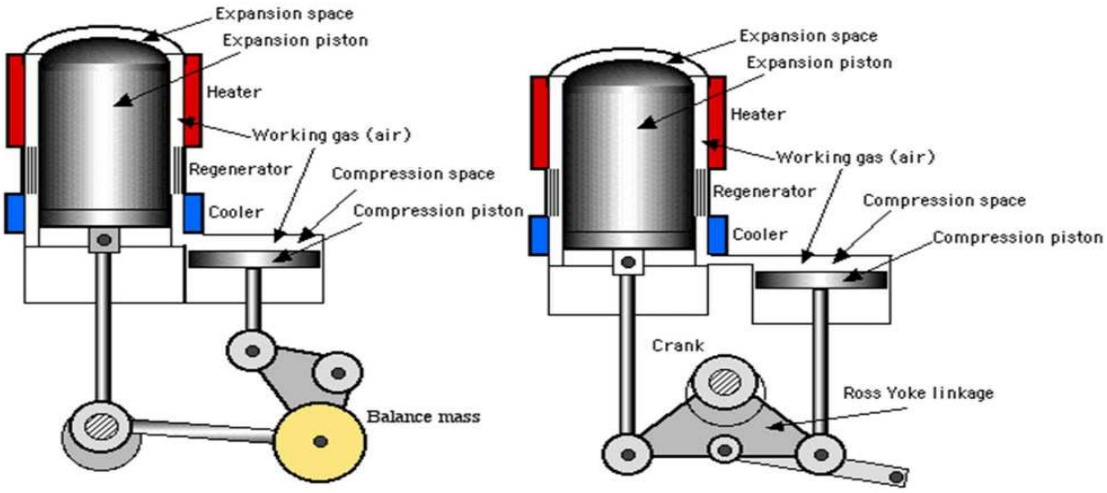

Figure 3.2: The Ross yoke engine [95].

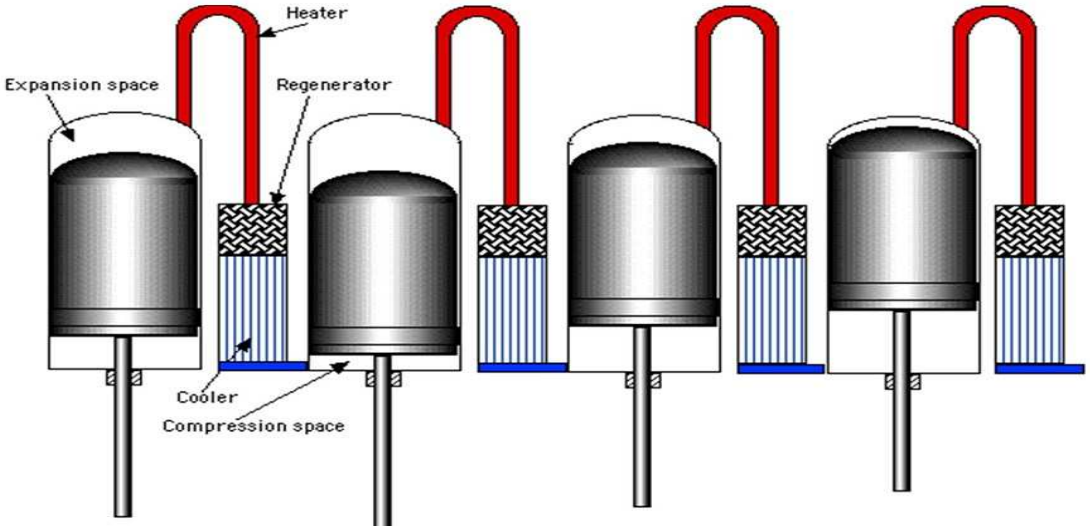

Figure 3.3: A multi cylinder configuration of the alpha type Stirling engine [95].

The power to volume ratio of the alpha engine is high but it can be improved using the assembly of the alpha engines to form a multi cylinder configuration. The Figure 3.3 shows such the typical configuration. The cylinders are connected in a specific way so that the heat exchangers serve as the link between the expansion space of one cylinder to the compression space of the following cylinder.

3.1.1.2 Beta Stirling engine

The beta type of the Stirling engine has been popular since the 19th century, see Figure 3.4. Actually, the original design of the engine developed by Robert Stirling was the beta engine.

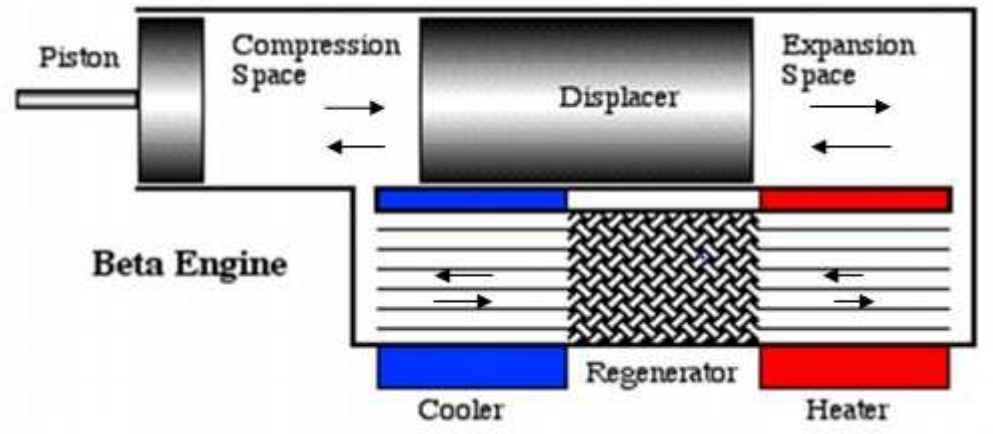

Figure 3.4: A schematic diagram of the beta type Stirling engine [95].

The engine configuration is arranged in the way where the piston and displacer are located in the same cylinder and overlapping in their displacement is allowed. The arrangement is well suited for high temperature machines so as to prolong the durability of the seals. The beta type engine has a higher compression ratio compared to the alpha and gamma engines.

3.1.1.3 Gamma Stirling engine

The gamma engine consists of the displacer and piston in two separate cylinders, as shown in Figure 3.5. The two cylinders can be parallel and coaxial, offset or at an angle to each other. Due to the type of separation between the expansion and compression spaces it results in a larger dead space. Such the separation leads to the reduction in the output power of the engine.

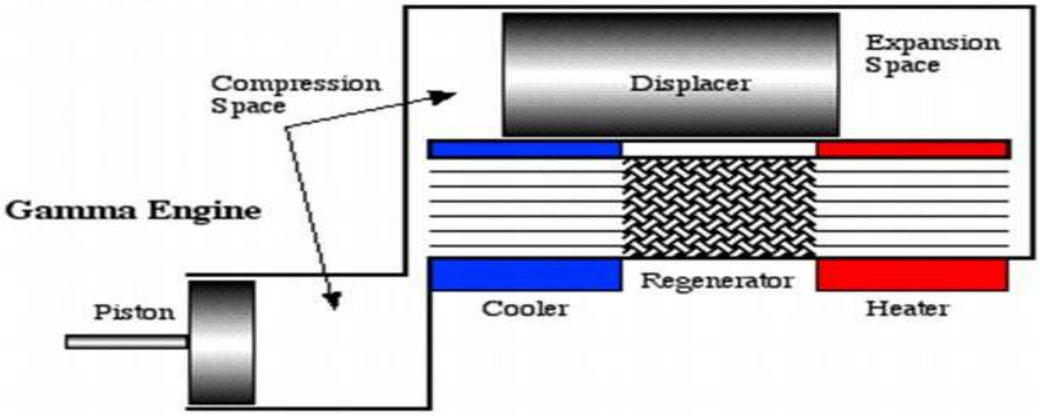

Figure 3.5: A schematic diagram of the gamma type Stirling engine [95].

The Figure 3.5 depicts a Ringbom engine in which the displacer is a free piston and power piston has a kinematical mechanism.

3.1.2 Free piston Stirling engine operational principles

The difference between kinematical and free piston Stirling engines is that in the latter there is no rigid kinematical mechanism which ensures displacement of power and displacer pistons in accordance with prescribed sequence (very often harmonic displacements). These kinematical mechanisms are also used to synchronise motions of these two pistons and to convert reciprocating motion of power piston into rotational motion of the power output shaft. A variety of different kinematical mechanisms are used in modern kinematical Stirling engines.

In free piston Stirling engines pistons are related via gas pressure and mechanical spring forces. The active part of their stroke is carried out due to action of working fluid's pressure variation inside the engine. Pistons are returned to initial positions due to the

action of mechanical springs which balance the action of gas pressure forces. Overall, the free piston Stirling engine is thermal oscillation system with mass-spring mechanism.

The frequency of oscillations is defined by the resonant frequency of the mass-spring system made of pistons and mechanical springs and also by damping forces due to hydraulic losses, frictional losses and load.

By selecting correct masses of pistons and stiffness of their springs it is possible to synchronise their displacements with providing correct phase angle. The displacer is usually significantly lighter than power piston in order to achieve acceptable values of the phase angle between displacements of pistons.

3.1.3 Types of free piston Stirling engines.

Free piston Stirling engine are usually made of gamma or beta configurations.

Gamma Free Piston Engine

The gamma configuration of FPSEs is much more convenient in manufacturing and exploitation since such configuration allows avoid overlap in displacement of pistons since each piston is physically located in its own cylinder.

Beta Free Piston Stirling Engine

The beta FPSE has a smaller dead volume compared to the gamma type but less stable during operation since such design does not include colliding of two pistons during unsteady operation. Usually such engines require high precision electronic and electrical control systems to additionally synchronise motions of pistons.

Overdriven and resonant Free Piston Engines

The configuration is similar to that of the beta FPSE with the heat exchangers situated round the cylinder. The displacer is hollow in shape with a smaller volume. The operation of the engine is similar to that of the gamma FPSE but there is a significant difference due

to the small displacer bounce space. The working fluid pressure is increased as a result of the downward motion of the displacer into the compression space towards the piston. The engine is designed so that the increase or decrease in the working space pressure is smaller compared to the increase or decrease in the bounce space pressure cause by the movement of the displacer. The bounce space pressure in the working space acts as a gas spring which returns it to its original central position when the pressure and working gas temperature destabilizes the movements of the displacer forcing it to its top dead centre in the cylinder. The difference between these effects is the net spring force. The mass of the displacer and net spring rate determines the frequency when it is forced to oscillate from its central position. The gas spring and the restoring forces supplied by the lower bounce space in the working space suspend the power piston. In the overdriven engine, the displacer and piston maintains a phase angle during oscillation despite the losses encountered. During the downward motion of the displacer the working fluid is forced into the expansion space and pressure is increased. This pushes the piston in a downward motion causing the decrease in the pressure of the working fluid and the displacer spring moves the displacer back in an upwards motion. The displacer is prevented from hitting the top of the cylinder by the gas springs that halts the motion. Hence the reversible cycle is repeated in sequence.

3.1.4 Advantages of Stirling engines

There are characteristics of Stirling engine which gives it an advantage over other heat engines.

(i) External heat input: different types of heat sources can be used, including non-traditional ones, renewable energy or waste heat. In case of combustion low emissions are ensured due to steady lean combustion of fuels which is easier to control.

(ii) Low level of noise and vibrations can be achieved in such engines.

(iii) Fuel flexibility: The ability of the Stirling engine to use various sources of heat makes t possible to switch to different types of hydrocarbon fuels during the engine's operation.

3.1.5 Disadvantages of Stirling engines

In the operation of typical Stirling engine certain hindrances are experienced which is not present in other heat engines.

(i) High temperature, high pressure steels are usually required to build the engine with high performance.

(ii) The movement of the working fluid between high and low temperature ends in the engine causes the increased heat losses.

(iii) There is need for a durable and effective sealing element to keep high pressure working fluid in the engine.

(iv) Stirling Engines are heavier and larger in the volume compared to other types of heat engines producing the same power output and efficiency.

3.1.6 The specific characteristics of Stirling engines

The Stirling engine uses a regenerative process of heating and cooling of the working fluid at constant volume, which improves the efficiency of the cycle. A special heat exchanger should be built between the heating and cooling heat exchangers of the engine for this purpose which is called a regenerator.

The working fluid used for the engine should have high heat capacity and low viscosity and preferable gases are hydrogen and helium. Some modern engines are built to use air or nitrogen but these require larger engines to achieve the required levels of power output.

The control of Stirling engines is much more complicated compared to other heat engines and therefore Stirling engines are mostly built to run on a single operational point.

3.1.7 Critical parameters of Stirling engines

Mean cyclic pressure

The output power of the Stirling engine cycle is directly proportional to the mean cyclic pressure. Erbay [16] demonstrated that to derive high densities and power levels, the pressure range of 10 to 20 MPa were required.

The engine developed by Kongtragool [96] powered by low temperature source exhibited that the efficiency of the engine is not very sensitive to the engine speed.

Dead volume

The dead volume which is the un-swept volumes inside the engine accounts for up to 50 % of the total internal gas volume of Stirling engines and reduces the amplitude of pressure variation in the cycle. Wu in [36] developed a criteria to optimize the dead volume at

adequate heat transfer surfaces. If the dead volume is located in the cold zone of the engine its effect is dominant compared to the influence of the dead volume in hot zones.

Mechanical losses

Mechanical losses are caused by the frictional force in rod seals, piston rings, bearings, pumping of oils and other dynamic components. The mechanical efficiency of Stirling engines is lower compared to other heat engines since no lubrication is used inside the gas circuit of engines.

Thermal losses

Mahkamov [42] presented calculations of the hydraulic losses that occur in the cycle. Working fluids with light molecular weights such as hydrogen and helium are required in order to reduce such losses in heat exchangers due to their lower viscosity. These gases are also more difficult to contain in the engine.

3.1.8 Stirling engine heat exchangers

The Stirling engine has three basic heat exchangers, namely the heater, regenerator and cooler and they play a very vital role in the engines operation. The heater transfers heat gained from the heat source to the working fluid, the regenerator takes accumulates heat from the hot working fluid and gives it back as the working fluid moves from cold to hot zone and the cooler dissipates heat from the working fluid.

Heater

The heater needs to have an effective design depending on the type of heat source and its temperature. Usually, its outer surface is exposed to the high temperatures and low

pressure environment while the inner surface is exposed to the high pressure of the working fluid. Therefore expensive stainless steels are required for manufacturing heaters of Stirling engines. The surface requirements results in application of fins and sometimes complex geometry of channels to increase the heat transfer rates through these heat exchangers.

Cooler

The cooler operates at much lower temperatures and therefore can be made of cheaper materials such as copper or aluminium alloys. Its external surface is often exposed to cooling liquids and due to their high densities the coolers does not require such big heat transfer surfaces as heaters. Most engines designs have adopted the water cooling method.

Regenerator

The regenerator represents a metallic casing with a porous material inside. Usually the regenerator matrix is made of metallic wire: gauzes or wool, metal foams etc. The main challenge is to ensure high radial and low axial heat conduction. The matrix also should have high heat capacity at reasonable dimensions. The thermal capacity of the regenerator material determines how effective and efficient it is.

3.1.9 Schmidt's theory

Gustav Schmidt [97] produced first analysis of the Stirling engine cycle resulting in closed solution which can be applied for all three engine configurations, namely the alpha, beta and gamma types. A closed solution was obtained for a sinusoidal variation in the volumes of the working spaces in the engine. The basic assumptions were that compression and expansion processes are isothermal. Results obtained are far realistic than in the ideal

Stirling cycle. As it is seen in Figure 3.6 the temperatures of the working fluid in the expansion space, heater, cooler and compression space is presumed to remain constant.

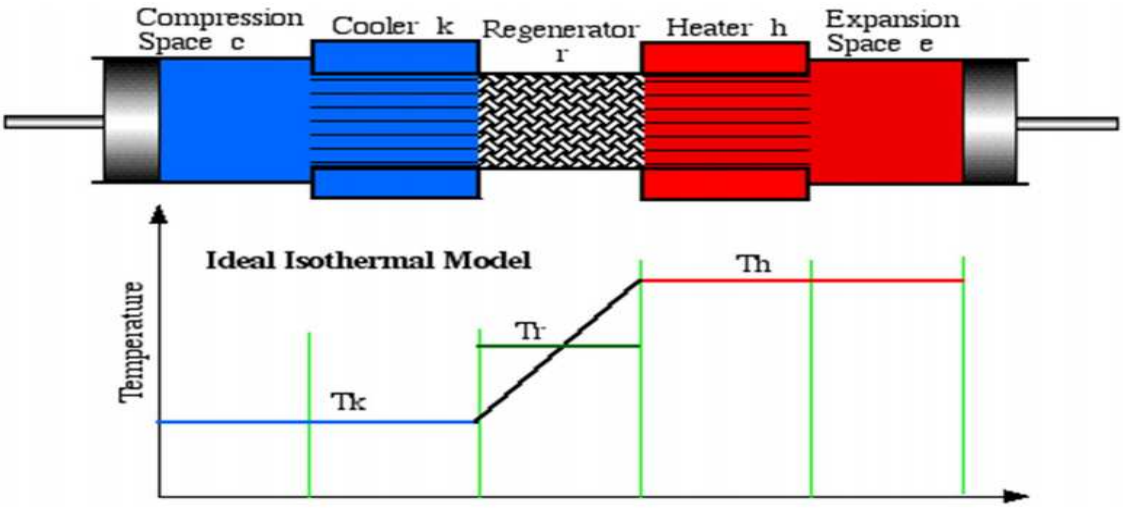

Figure 3.6: A schematic diagram of the Stirling engine isothermal model with temperature distribution [95].

Figure 3.7 shows the variation of the volumes of the compression and expansion spaces assumed in the Schmidt's model.

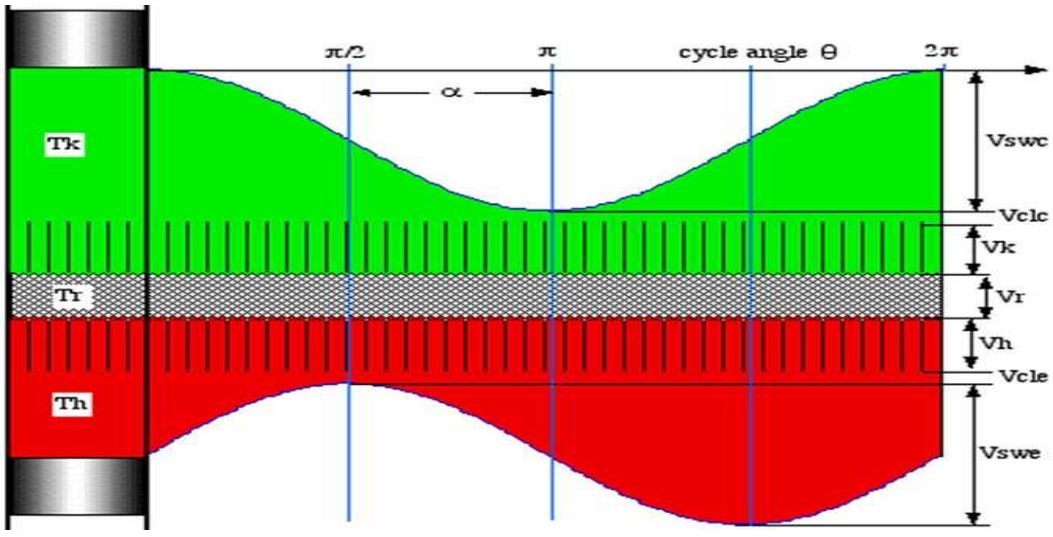

Figure 3.7: Variation of volumes in a Stirling engine [95].

The other assumptions used by Schmidt for the Stirling engine cycle analysis are:

1. There is no leakage in the engine, the mass of gas remains constant in the cycle
2. The working fluid is a perfect gas.
3. The temperatures of the heat exchangers are constant
4. The engine speed is constant
5. Steady state conditions are achieved
6. There is no loss in fluid flow hence no pressure loss or pressure drop.

Using results of the Schmidt's analysis, the predictions can be made of design dimensions for the practical Stirling engine.

3.1.11 Factors which determine performance of Stirling engines

Working Fluids

The working fluid of the Stirling engine should possess high specific heat capacity low viscosity and high thermal conductivity.

Clarke et al in [98] defined the capability factor for working fluid in relation to the specific heat capacity, density and thermal conductivity. This capability is defined as:

Capability factor = thermal conductivity/ specific heat capacity × density of the working fluid

Tables 3.1 and 3.2 shows the relative heat transfer capability of various gases and the relative performance of selected working fluids.

Power and speed control of Stirling engines

The Stirling engines require a mechanism to control and regulate the power output, their speed and torque. The basic methods which can be used for power control are: (i) Mean pressure variation, (ii) Variation in temperature of the working fluid, (iii) Variation in the phase angle, (iv) Variation of the dead volume and (v) Variation of the piston strokes.

Table 3.1: Relative heat transfer characteristics of various gases [99].

Working fluid	Heat transfer	Capability factor
Air	1.0	1.0
Helium	1.42	0.83
Hydrogen	3.42	0.68
Water	1.95	0.39

Table 3.2: Relative performance of selected working fluid [99].

Gas	Nominal molar mass M (kg/kmol)	Gas constant R (kJ/kg K)	Specific heat Cp (kJ/kg K)	Specific heat Cv (kJ/kg K)	Specific heat ratio (Cp/Cv)
H2	1	4.12	14.20	10.08	1.41
He	4	2.08	5.19	3.11	1.67
Ne	20	0.415	1.03	0.62	1.66
N2	28	0.297	1.04	0.74	1.4
CO	28	0.297	1.04	0.75	1.4
Air	29	0.287	1.01	0.72	1.4
O2	32	0.260	0.92	0.66	1.4
Ar	40	0.208	0.52	0.31	1.67
CO2	44	0.189	0.85	0.66	1.28

Mean pressure variation

The output power of the Stirling engine is directly proportional to the cyclic mean pressure of the working fluid. The variation in mean cyclic pressure is not easy to achieve in reality. To achieve this, a gas compressor or gas storage compartment is required in the engine system. To increase power output the working fluid will be supplied to the engine from the storage compartment of from the compressor and to minimize power, the working fluid will be transferred to a reservoir. Such control of the engine is difficult to implement in real life practice due to complexity of the timing of controlling valves opening and closing.

Variation in the temperature of working fluid

The maximum temperature of the working fluid which depends on the heater's temperature can be used to control the output power of the engine. For example, this can be controlled by adjusting the fuel flow, but temperature change results in prolonged time reaction time.

Variation of the dead volume

The output power of the Stirling engine can be changed if the dead volume is increased or decreased, thereby reducing or increasing the pressure's amplitude during operation. The effects of the dead volume variation on the performance of Stirling engine was analysed by Erbay [16] using polytrophic processes**.** The increase in the dead volume within a Stirling engine system results in reduction in output power but does not necessarily reduce the efficiency of the system. However the efficiency can be reduced when there is a considerable amount of dead volume variation. This was observed in the investigation carried out on the DVV (dead volume variation) system developed by United Stirling engine (Alm et al cited [100]). A significant number of gas spaces were incorporated into the main engine block and coupled to the internal working space using ducts with valves in

the engine**.** The capacity of the dead volume was controlled with the extra spaces to give the required amount of dead spaces possible. The system was employed to control one of the first developed United Stirling engines used in a Ford Pinto automobile.

Variation of Stroke

The stroke of the reciprocating piston and displacer can be controlled so as to regulate the output power of the engine. It is suitable for all Stirling engines (single, double acting and free piston Stirling engines). Such method of controlling power output of the engine is widespread in existing engines.

Variation in phase angle

One of the most effective ways of controlling the output power of Stirling engines is the variation of the phase angle. The phase angle is the angle between the oscillations or displacements of the displacer and power piston. The total engine volume variation depens on the phase angle and can be reduced if the phase angle is different from the optimal one. This method can be applied to a single acting machines though requires complex modifications in the kinematical mechanism. However, for double acting engines the variation of phase angle is not applicable.

Effectiveness of the regenerator

The regenerator of the Stirling engines must be designed so that area of the regenerator matrix should have an optimal porosity to balance heat accumulating capacity and minimize gas flow losses. Usually not all the working fluid pass through the regenerator matrix, while some remaining and oscillating inside the regenerator.

Material of the regenerator

The performance of the Stirling engine is influenced by the material used for the regenerator matrix. Usually ceramic and metallic materials are used in the regenerator. Ceramics have a lower rate of permeation than metals. Hence, the efficiency of engines with regenerator made of ceramic coated materials are higher than that with metallic regenerators.

Leakage of the working fluid

In reality the leakage of working fluid in an engine cannot be avoided. Pertescu [32] analysed the effect of pressure loss due to the working fluid leakage during engine operation.

Fluid friction

The regenerator of Stirling engines is very often the source of the highest fluid friction. Isshiki [101] and Muralidhar [102] derived equations to calculate the friction factor of a stacked wire mesh as a function of Reynolds number. The investigation carried out showed that there is a substantial increase in the heat transfer and flow resistance in oscillatory flow in wire meshes of regenerator in Stirling engines.

Engine dynamics

Heat engines analysis requires simultaneous consideration of heat transfer processes and dynamics. The slider-crank mechanism is mostly used in conventional engines, while the Stirling engines employ different forms of drive mechanisms. A general method for Stirling engine optimisation for different engine configurations and operating conditions was presented by Shoureshi in [103]. Gary et al in [104] demonstrated that the engine configuration suitability depends mainly on some certain factors such as output power,

type of fuel, engine speed etc. The relationships for calculation of mechanical efficiency of Stirling engines were investigated by Senft in [105]. Results can be employed for selection of engine mechanism to suit the required application and output.

3.1.12 Losses in Stirling engines

Different types of losses are present during operation of Stirling engines. Due to their complex nature the analysis of these losses usually is not directly included in the simulation rather they are analysed and taken into account separately.

Conduction Losses

These losses are accounted for in large in the simulation process and are also the easiest to calculate. In a generalised analysis, it is often difficult to include every single conduction path. Besides in many components the temperature gradients are quite small and, hence, the conduction losses in these components can be neglected.

The conduction of the regenerator should be considered and calculated carefully and included in the overall heat balance due to its significant value. Conduction losses do not alter the temperature of the working fluid to a great extent and only affect the thermal efficiency of the engine. The losses due to conduction can be considered as an additional thermal load for the cooler and heater.

Gas Spring Hysteresis Losses

There are losses associated with the gas springs because the thermodynamic process that occurs in the gas spring is not totally reversible. A certain quantity of work is dissipated in the case of real gas springs, which can be represented as an area in the relevant Pressure – Volume diagram. This negative work in the diagram is the sum of the gas spring hysteresis

loss which is a function of the temperature and viscous gradient effects in the cavity. The viscous effects are often neglected because they very small. The effect of the gas hysteresis loss can have very little effect on kinematical Stirling engines but may be considerable for free piston engines. The effect should be considered in the analysis of FPSEs due to the fact that the gas hysteresis loss increases damping effects which alter the amplitudes and phase angle in the displacer and piston displacements. The general differential energy equation for the gas in such calculations is (Hughes and Brighton, [106]).

$$\rho c_p \frac{DT}{Dt} = k\nabla^{2T} + \frac{Dp}{Dt} + \emptyset \qquad (1.1)$$

where ρ is the density of gas (kg/m^3), c_p is the gas specific heat at constant pressure (Jk/gK), T is temperature (K), t is time (s), k is thermal conductivity (W/K^3), p is the pressure (Pa), $\emptyset$ is the viscous dissipation (W/m^3)

Seal Leakage

The Stirling engines seals are either of close fitting clearance type or the conventional ring type. The seals are designed in a way that they must be run dry at all times that is without grease or oil lubrication. Therefore certain measures should be taken to reduce their wear. Local heating or gradual seizure of the moving surfaces may occur if the bearing pressure of the seal is not enough. The seals will experience leakages at some point to some level. The effects of the leakage on the thermodynamic cycle are an essential aspect which should be taken into account during engine designing. In cases where ring seals are employed, the leakage experienced is very minor and has no significant effect on the thermodynamic cycle. But the mechanical friction value is considerable. The leakage that occurs in a seal in terms of mass flow is given by

$$\dot{m}_1 = \boldsymbol{\rho} A \bar{u} \text{ (kg/s)} \qquad (1.2)$$

The free piston Stirling engines are usually designed with sliding seals that act as springs and separates the working space from the internal gas volume. Also to prevent the pistons drifting away from its equilibrium position, centering ports are introduced, which causes gas leakage at some instances of the cycle. Therefore, free piston Stirling engines are more prone to leakage power losses than the kinematic machines.

Appendix Gap Losses

The appendix gap losses are caused by the clearance gap between the walls of the displacer and cylinder. There are three main sources of losses in the appendix gap:

(i) Gas enthalpy transfer

(ii) Shuttle enthalpy transfer

(iii) Hysteresis heat transfer

The shuttle heat transfer is a conduction loss caused by the oscillatory motion of the piston or displacer and it occurs down the walls of either of the moving elements. During operation when the displacer is at the top dead centre heat is accumulated by its walls and then dissipated in the cold zone when the piston is at the lowest position.

This type of losses were first calculated by Zimmerman and Longsworth [19].

3.1.13 Friction factor and heat transfer coefficient

The heat transfer coefficient and the flow friction factor can only be analysed for steady laminar flow conditions in plain geometric shape. The Stirling engines exhibit extreme unsteady flow conditions and empirical data is the only solution to calculate the above factors. This data is presented as correlations in terms of dimensionless groups.

Dimensionless groups

Dimensional analysis and similarities are widely used to present data on heat transfer and flow [107]. The set of variables below are considered to analyse heat transfer process and flow-friction under forced convection, which are present in Stirling engines:

g, working gas mass flux ($kgm^{-2}s^{-1}$), d, hydraulic diameter (m), μ, dynamic viscosity of the working fluid ($kgm^{-1}s^{-1}$), h, coefficient of heat transfer ($Jm^{-1}s^{-1}K^{-1}$), k, working fluid thermal conductivity ($Jm^{-1}s^{-1}K^{-1}$) , $c_{p,}$ specific heat capacity of working fluid at constant pressure ($Jkg^{-1}K^{-1}$) .

The hydraulic diameter d is the single variable representing the heat exchanger geometry and its size. It is denoted by

$$d \equiv 4\frac{V}{A_{wg}} \tag{1.3}$$

where V is the void volume and A_{wg} is the wall to gas or wetted area.

The hydraulic diameter will be equal to the internal diameter for flow in a circular pipe to occur.

The variables above are used to determine Reynolds number:

$$Re \equiv |gd/\mu| \quad \text{(Reynolds number)} \tag{1.4}$$

This parameter represents the ratio of the inertial forcers to the viscous forces. The value of Re is used to determine if flow is laminar or turbulent. The heat transfer coefficient and the friction factor are defined by the type of flow, therefore Re is used for heat transfer and flow friction calculations.

The Prandtl number is determined from the ratio of the kinematic viscosity to the thermal diffusivity, and is related to the ratio of the thermal layer to the viscous boundary layers.

$$Pr \equiv c_p \mu / k \text{ (Prandtl Number)} \quad (1.5)$$

Nusselt Number is a heat transfer measure by convection and is defined as product of Reynolds and Prandtl numbers.

$$Nu \equiv \frac{hd}{k} \text{ (Nusselt Number)} \quad (1.6)$$

$$St \equiv |h/(gc_p)| \text{ (Stanton Number)} \quad (1.7)$$

The Stanton number is often used as a substitute to the Nusselt number for analysing data of heat transfer. It can be determined as a function of the Nusselt, Prandtl and Reynolds number.

The Stanton number has a physical importance which can be referred to the ratio of the convective heat transfer to the thermal capacity of the working fluid.

$$St \equiv Nu/(RePr) \quad (1.8)$$

The energy balance of a cooled or heated working fluid flowing through the heat exchanger can be given as:

$$hA_{wg}(T_{w-T}) = c_p g A(T_0 - T_i) \quad (1.9)$$

where A_{wg} is the wetted area, A is the free-flow area, T_w, T are the respective wall and bulk fluid temperatures, T_i, T_0 are the respective input and output fluid temperatures.

Substituting equation 1.8 into equation 1.9

$$St = \frac{A}{A_{wg}}\left(\frac{T_0 - T_i}{T_w - T}\right) \tag{1.10}$$

The value of St can be derived from the temperature measurements and heat exchanger dimensions without including the properties of the working fluid. The Number of transfer units can also be determined as

$$N = hA_{wg}/(c_p g A) \tag{1.11}$$

$$\text{Therefore n} = N = StA_{wg}/A \tag{1.12}$$

The influence of temperature on the fluid properties can be considered in simulations. The thermal conductivity k and the dynamic viscosity μ changes with temperature as presented in [108].

3.1.14 Calculation scheme of the free piston Stirling engine

Figure 3.9 shows the mechanism of the FPSE used in this study. The engine consists of a piston and displacer, two dampers, two springs and the engine casing. The piston and the displacer are connected to the engines casing through springs. There is no form of mechanical linkage between the displacer and piston. The pressure of the working gas volume in the engine results to the concurrent oscillatory movement of the piston and displacer. For effective results the displacer needs to have a low mass. The engine volume is made up of the block volume and working volume. The hot, regenerative and cold volumes make up the working volume of the engine which is provided by the heat exchangers (heater, regenerator and cooler). The working fluid is displaced between the heater and cooler which house the hot and cold volumes through the regenerator which

houses regenerative volume. This is the path where heating regeneration and cooling process of the working fluid is accomplished. Figure 3.9 shows the regenerative volume which is present between the side of the displacer surface and the walls of the cylinder.

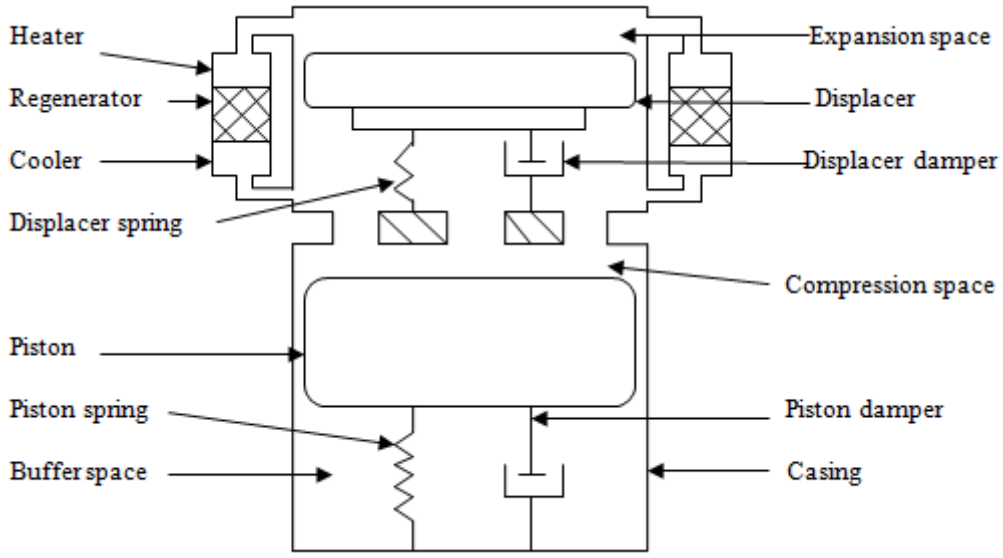

Figure 3.8: A schematic diagram of the gamma type free piston Stirling engine.

As mentioned above a free piston Stirling engine is a mechanical oscillator operating on a Stirling engine cycle which is driven thermally. Three types of forces exist in the FPSE which determine the engines dynamics: the force on masse due to acceleration, the force acting on the moving elements due to their displacements i.e. spring forces, the force acting on the moving elements due to their velocity i.e. damping forces.

The motion of the masses can be derived from Newton's second law of motion which states that $\Sigma F = Ma$ where M is the mass of the element and a, is the acceleration of the mass. Hence, the law provides the motion equation:

$$M\ddot{x} + C\dot{x} + Kx = \Sigma F_p + \Sigma F_e \qquad (1.13)$$

Here C is the damping coefficient, K is the stiffness of the spring, F_p is the thermal driving force and F_e is the primary load or external force.

Stability and Damping

There might be different instability situations in the engine's operation:

(i) Dropout- a state in which oscillation of the engine cease due to constant decrease in the amplitudes of oscillation of moving elements (displacer and piston).

(ii) Blow up- a state in which the collision between the piston and displacer limits the increment in their oscillation.

(iii) Hunting- a state in which the frequency or amplitude increases or decreases periodically.

The engine characteristics and the load it drives determine its stability. If sufficient control measures are not considered in the dynamics of the FPSE, any disturbance such as change of load or pressure can result in poor engine performance.

Vibrating systems can either be linear or non-linear. In the non-linear systems the principle of superposition does not occur. The response of the engine dynamics depends on the amplitude and frequency of excitation and other parameters such as pressure distribution and change in the temperature. In linear systems the principle of superposition applies i.e. any change in the system response by the load applied or periodic excitation of the system results in its linear changes respectively. Also a linear system has just one equilibrium position. The equilibrium state can be altered by any change in the operating conditions. Depending on the conditions of equilibrium non-linear systems can have more than one equilibrium position. In order to analyse a non-linear system, the system will be linearized to simplify it due to the difficulty encountered in solving non-linear conditions. In the FPSE adequate non-linear conditions must be obtained to achieve stability. Though the engine might be linear at some point during operation the steady state of the engine can

only be achieved by the non-linear nature of the load or performance. Losses due to damping or damping forces are a major factor in the performance of the FPSE due to the freedom of oscillation of the displacer and piston. Damping forces can range from the mechanical dampers or the resistance to motion caused by the fluid frictional flow imposed on the engine by loading devices. The dynamic motion of the displacer is influenced by the internal damping forces while that of the piston is influenced by the load resistance. In the FPSE the load dynamics and the engine cannot be separated because the displacer and piston are coupled closely through the pressurized gas. Viscous damping occurs where the resisting force is proportional to the velocity of the moving element. Hysteresis damping exists mostly in vibrating systems with elastic restoring forces. It occurs as a result of internal frictional effects in a gas or mechanical spring system exhibiting reversible cyclic operation. In free piston Stirling engine, hysteresis loss is experienced by the gas springs which consumes considerable amount of energy.

3.1.15 Applications of Stirling engines

Both kinematical and free piston Stirling engines have been employed for different applications due to their specific design and performance features.

Artificial heart power

Considerable research has been undertaken to develop an artificial heart over the years using Stirling engines. The ability of the engine to use an external heat source is an advantage in this application. For supply of blood flow through the body the small Stirling engines was used to drive a small pump. Radio isotopes were used as source of heat to drive the engine in such the application.

Underwater power units.

The low noise and vibration characteristics of the Stirling engine have made it attractive for marine applications. The lower speed is required for the Stirling engines used in marine other than the one used on land, so helium or nitrogen can be employed in place of hydrogen without reducing the engine performance. The sea water can serve as an efficient source of cooling for the engine in the marine applications. Nilsson conducted a research for naval operation on the application of Stirling engines in underwater systems.

The combustion of methanol in pure oxygen was employed as the heat source at a pressure of 3MPa, which is the same as the ambient pressure estimated at the greatest sea depth so that omitted gases are disposed easily. The products of the combustion process are recycled in order to sustain the flame temperature in pure oxygen within a suitable limit that could be as high as 4000° C. Stirling engine is suitable for this purpose due to its usage as both power and generator of hot water in the vessel. Stirling engines were employed by the Swedish defence contractor Kockums to make the quietest submarines for the Navy. The technology used is called air-independent propulsion (AIP) system. It is equipped by the Stirling engine unit with electrical equipment and liquid oxygen (LOX) tanks, see Figure 3.10, installed in the middle section of the submarine.

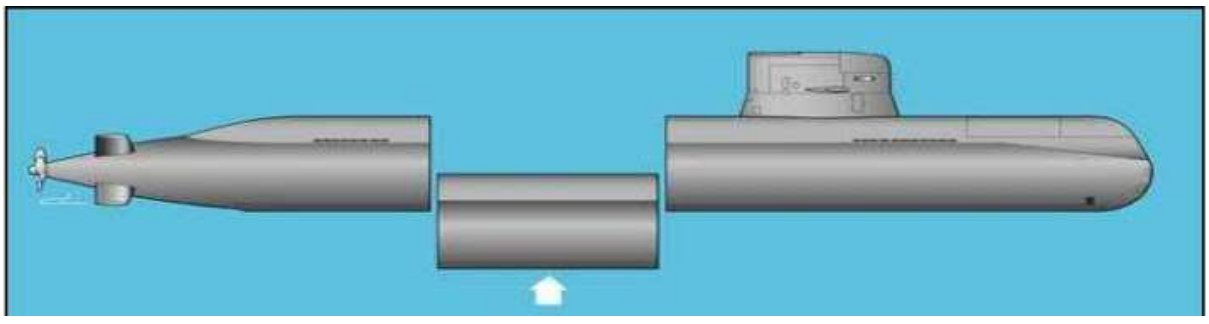

Figure 3.9: The Air Independent Propulsion system [109].

Ground power units

Military considered wide use of Stirling engines for power supply applications. Stirling engines were used for the production of electrical generator units which are quiet in operation; able to use various fuels such as diesel, gasoline etc.; durable; able to operate for a long time before maintenance is required. The research was described by Percival in his report.

Aircrafts

Stirling engines can be also used to power small special aircrafts due to its quiet operation and lo vibrations. Figure 3.11 shows the advantage of Stirling engine in vibrations. For four cylinder IC engine, the shaft torque varies from 350% positive to 100% negative. For the Stirling engine this varies by only 5%, which reduces the fatigue of the airframe and isolator materials and also increases the comfort of passengers.

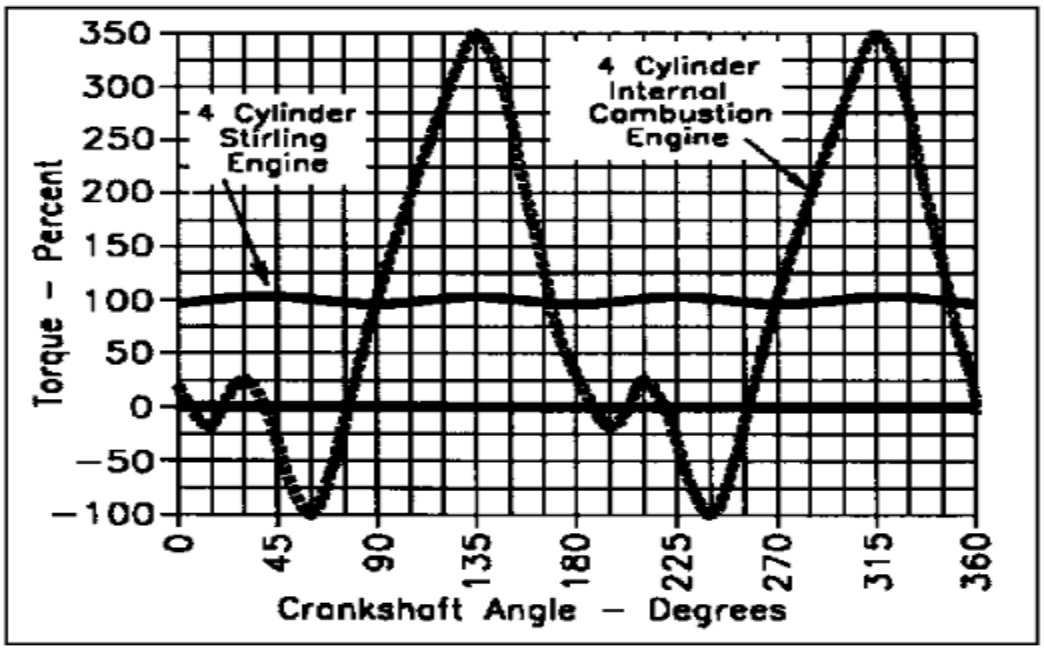

Figure 3.10: The graph of Torque-Crankshaft Angle [109].

Figure 3.12 shows the performance of the Stirling engine compared to the conventional IC engine. The closed cycle of the Stirling engine gives it an advantage as this increases the performance of the engine with altitude. The engine power increases as the outside temperature is reduced. Another additional advantage from this feature of the Stirling engine is a safety room for the aircraft to cruise above the weather rather than through the weather in case of bad weather conditions.

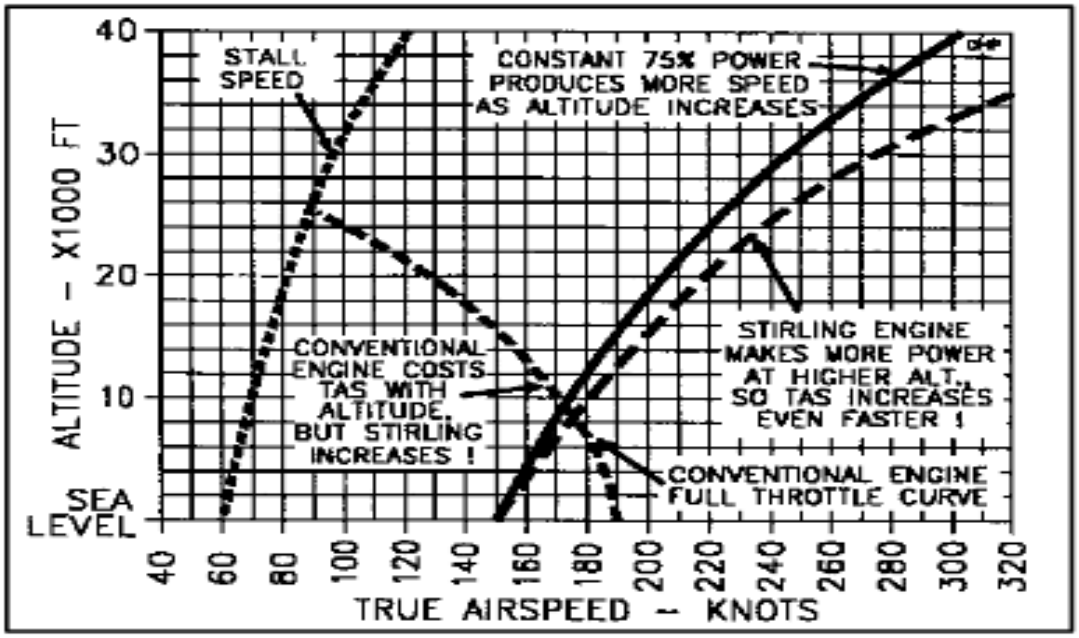

Figure 3.11: The graph of Altitude-Airspeed [109].

Automotive engines

Stirling engines have been tested for automobile applications by Ford in 1970 and 1980 but due to reliability and safety problems of the engine such attempts were unsuccessful.

Nuclear power

Stirling engines can be generally used to replace steam turbines in nuclear plants, so as to increase the efficiency. Stirling Radioisotope Generators were developed by NASA to

generate electricity for long lasting missions in deep space, see Figure 3.13. Nuclear fuel is used to provide the heat source while the space provides cooling. The device generates electricity about four times more than the radioisotope thermoelectric generator. The generators have not yet been used on real missions but have been tested considerably.

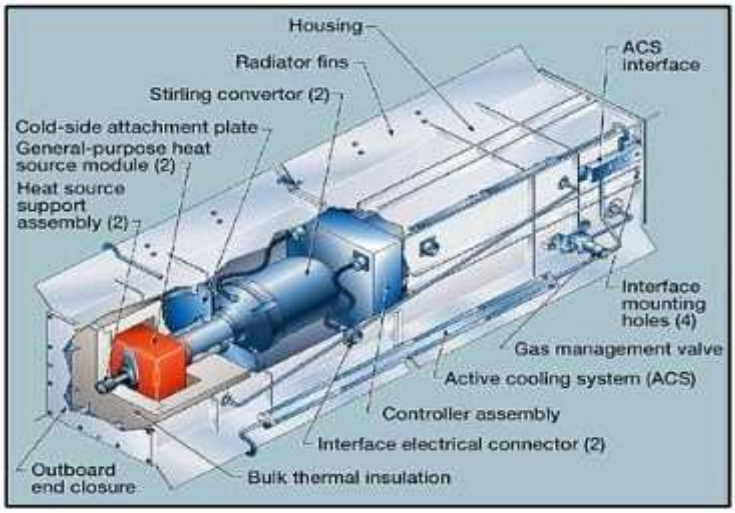

Figure 3.12: Conceptual design of the SRG by Lockheed [109].

Solar thermal conversion

Large scale research has been conducted to produce engines that can transform solar energy to other forms of energy. An advanced method was developed by NASA to collect rays of sunlight, see Figure 3.14. A closed Brayton cycle was the basis of such the system.

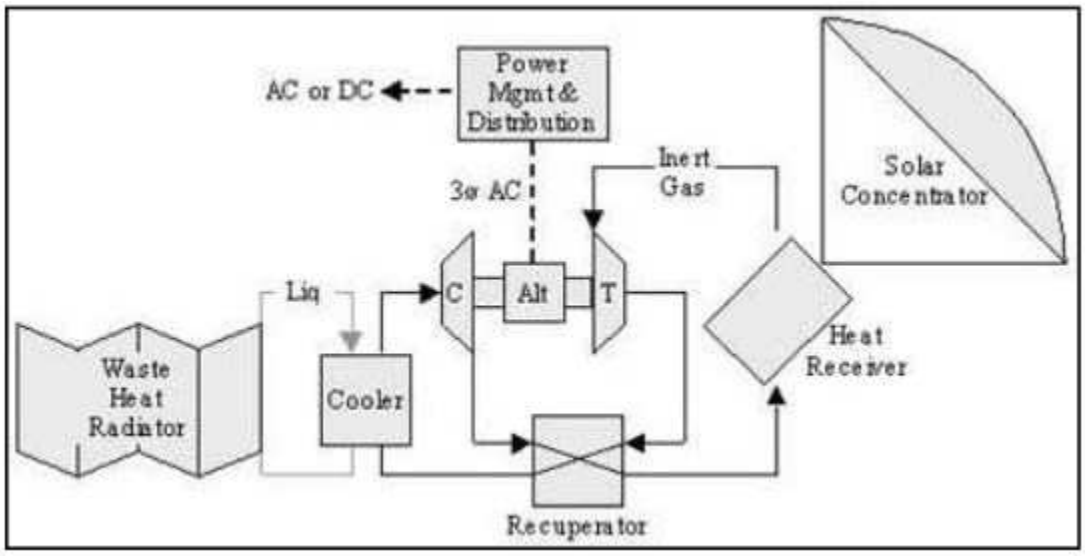

Figure 3.13: A schematic diagram of the solar dynamic Brayton [109].

But the engine with the best efficiency is still the Stirling engine. Stirling engines were coupled with parabolic tracking dishes and units were created with output power from several hundred W to 25 kW.

Combined Heat and Power (CHP) applications

The conversion of the energy simultaneously from a single fuel into two different forms of energy such as electricity and thermal energy simultaneously is referred to as combined heat and power or cogeneration. The Stirling engine CHP system is very productive for use in commercial and domestic buildings. The aim of this unit is to replace the commonly used gas-boilers with Stirling engine plants based CHP commercially. A schematic illustration of the domestic micro CHP application is shown in Figure 3.16

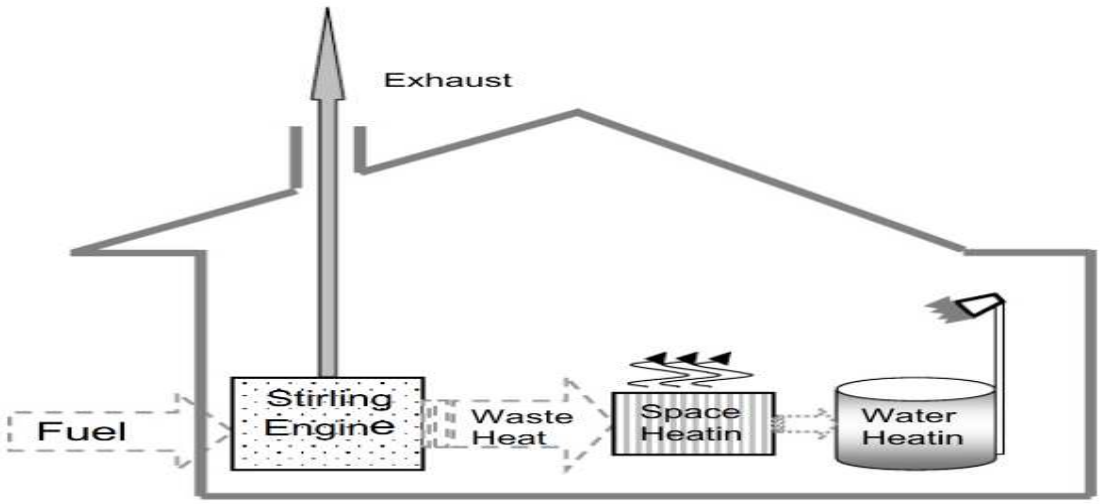

Figure 3.14: A domestic Micro-CHP system [110].

Whispergen produced a MkV AC gas fired device, which is made up of the four cylinder double acting Stirling engine. It supplies thermal output from 7.5 to 12kW with electrical power of 1 kW at 220 -240V. Microgen produces 1 kW FPSE for MCHP manufactured by several boiler manufacturers.

Saving of about £150 per year can be achieved by an average household on power supply using such MCHPs. Carbon dioxide emissions can also be reduced by 1.5 tonnes yearly, which is a good measure towards reducing the effects of global warming [109].

Table 3.3 demonstrates data on 2 types of large Stirling engines which were used for CHP application.

Table 3.3: Parameters of Stirling engine CHP systems [109].

Electric power output – Stirling engine	kW	35	70
Thermal power output – Stirling engine	kW	105	210
Thermal power output – CHP plant	kW	230	460
Fuel power input (based on NCV)	kW	300	600
Electric efficiency – Stirling engine	%	25.0	25.0
Overall electric efficiency – CHP plant	%	11.7	11.7
Overall efficiency – CHP plant	%	88.3	88.3
Working gas	%	Helium	Helium
Mean pressure	Pa	4.5	4.5
Temperature of hot heat exchanger	C	750	750
Revolution speed	pm	1.010	1.010
Engine weight	kg	1.600	3.500

3.2 Conclusions

Stirling engines have a great potential for commercial applications in various areas where traditional engines cannot be used (eg. For utilisation of renewable energies, waste heat etc.). A large number of developments have been undertaken over the years for various applications for Stirling engines, successful and unsuccessful. Currently, free piston Stirling engine based units have most successful applications on the market, compared to conventional kinematical Stirling engines, though the theoretical background of such FPSEs is less developed. To improve performance of FPSEs further development of mathematical modelling of their working process for their designing optimisation is required and this is the purpose of this study. As mentioned above, several levels of mathematical models are developed in this work and calibrated against published experimental and theoretical data to evaluate their accuracy. Finally, GA method of optimisation has been developed for determination of optimal design parameters of the FPSE in order to achieve high level of performance.

Chapter 4 Isothermal Mathematical Modelling of the Free Piston Stirling Engine

4.1 Introduction

In this chapter, the isothermal model of the working process of Stirling engines for determination of their design parameters is described.

4.2 Isothermal model

The isothermal model of the free piston Stirling engine is based on the isothermal model of the working process of Stirling engines developed by Schmidt and modified in [107]. Here, the engine's internal gas circuit is split into five components connected in series, namely the expansion space, heater, regenerator, cooler and compression space, see Figure 4.1 It is assumed that the heat exchangers (heater, regenerator and cooler) are perfectly effective and the temperature in the expansion space and heater are equal and constant during the cycle, temperatures in the compression space and cooler are equal to each other and constant and temperature in the regenerator is constant and equal to the average of temperatures of the heater and cooler.

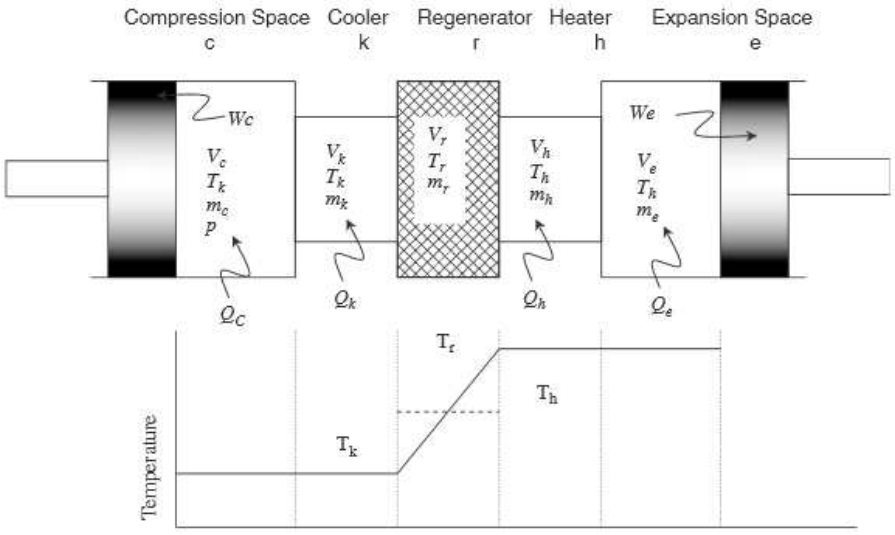

Figure 4.1: The temperature profile of the isothermal model [111] .

Assumptions for the isothermal model

- The engine operates at steady state condition.
- The gas is an ideal gas.
- All processes are reversible
- The mass of the working gas is constant
- There is no pressure drop during engine operation.
- The temperatures of the surrounding walls of the working gas volume do not vary with time.
- The spring's masses are not considered.
- The springs have linear characteristics.
- Gravitational effect is not considered in this analysis.
- The temperature of the regenerator is assumed to be equal to the average of the heater and cooler temperature.
- The motion of the engine casing is neglected.

For analysis of dynamics of the free piston Stirling engine it is presented as a two mass-spring system, oscillations of which are induced by forces due to working fluid pressure in the engine, see Figure 4.2**.** The pressure variation in the engine can be presented as a periodic function and therefore such representation of the dynamics of the engine will result in harmonic motion of pistons. The required phase angle between displacements of the displacer and piston are achieved by selecting certain values of their masses, stiffness of their springs and damping coefficients.

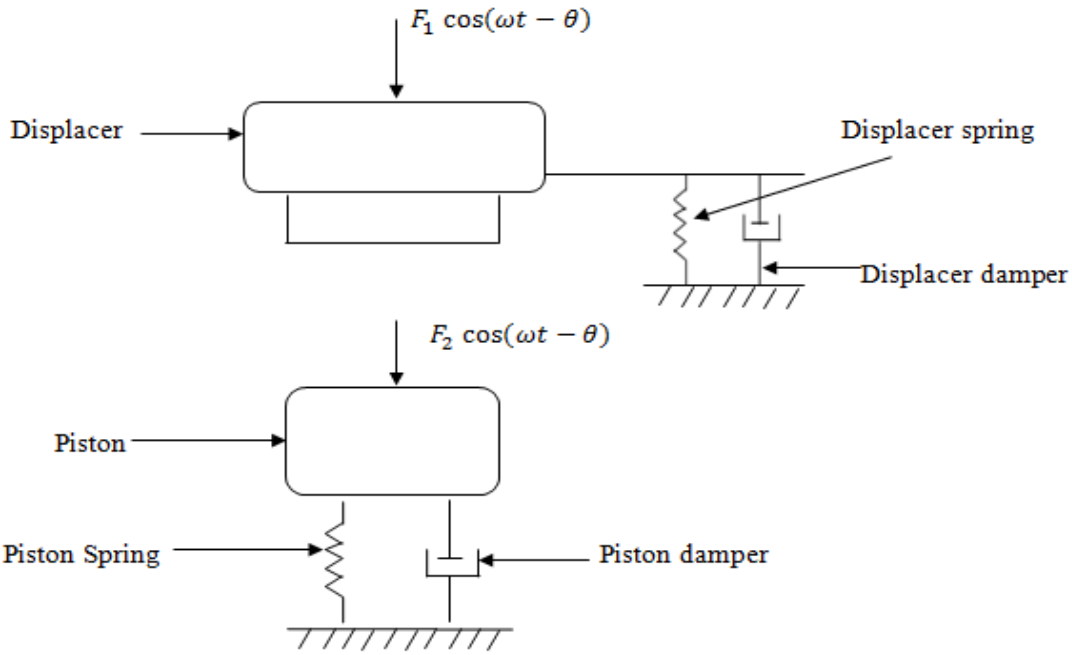

Figure 4.2: The layout diagram for the dynamic analysis of the free piston Stirling engine used in this study.

4.2.1 General analysis

It is important to assume the harmonic motions of the free pistons of the Stirling engine in order to describe its action. The work done by the engine is represented by the force from

the damping device acting on the piston. There are three collinear forces that act on pistons: the spring force, damping force and the gas force[13].

Therefore, using the Newton's second law the motion of the piston and the displacer is

$$\sum F = m\ddot{x} \tag{4.1}$$

or

$$F + F_{damping} + F_{spring} = M\ddot{x} \tag{4.2}$$

The motion of the displacer is a

$$m_d\ddot{x} + K_d x_d + C_d\dot{x} = P(A_d) \tag{4.3}$$

where m_d is the mass of the displacer; K_d is the displacer spring constant; C_d is the displacer damping constant; A_d is the cross sectional area of the displacer upon which the the gas pressure *P* is applied.

Similarly the motion of the piston is

$$m_p\ddot{x} + K_p x_p + C_p\dot{x} = A_p(P - P_b) \tag{4.4}$$

where m_p is the mass of the piston; K_p is the piston spring constant; C_p is the piston damping constant; A_p is the cross sectional area of the piston; P_b is the bounce space (beneath piston) pressure.

In accordance with the assumption made

$T_{ck} = T_k$ $T_{he} = T_h$ $T_{kr} = T_k$ and $T_{rh} = T_h$

where T_k is the cooler temperature and T_h is the heater temperature.

The regenerator has a limited linear profile between the heater temperature T_h and cooler temperature T_k during its length L_r, see Figure 4.3.

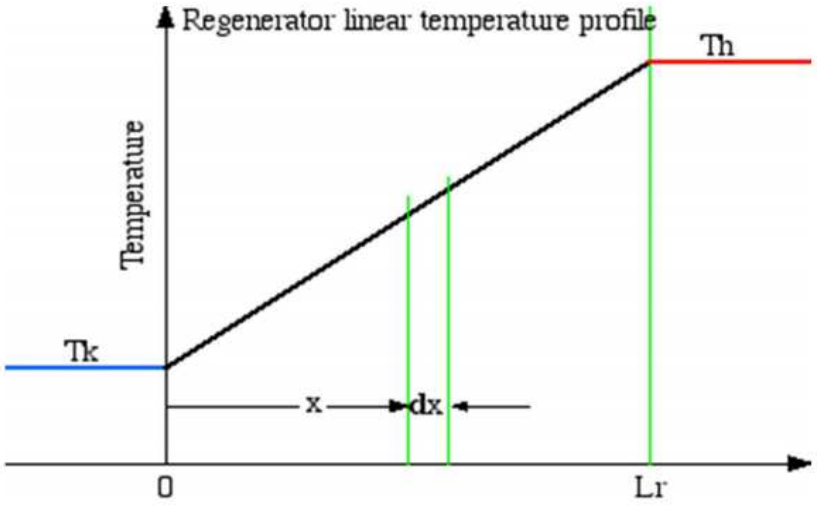

Figure 4.3: The linear profile temperature of the regenerator [95]

The resulting equivalent mean temperature of the gas in the regenerator T_r as a function of T_k and T_h is

$$T_r = \left(\frac{T_h - T_k}{ln\frac{T_h}{T_k}}\right) \tag{4.5}$$

All the equations (4.1) to (4.5) are obtained from Urieli and Berchowitz [4]

It is assumed that the total mass of the working gas in the five parts of the engine volume is constant throughout the cycle:

$$M = m_c + m_k + m_r + m_h + m_e \tag{4.6}$$

where m_c is mass of gas in the compression space; m_k is mass of working fluid in the cooler space; m_r is mass of working fluid in the regenerator space; $m_h$is the mass of the working fluid in the heater space; m_c is mass of the working fluid in the expansion space.

Using the ideal gas law

$$M = \frac{P\left(\frac{V_c}{T_k}+\frac{V_k}{T_k}+\frac{V_r}{T_r}+\frac{V_h}{T_h}+\frac{V_e}{T_h}\right)}{R} \tag{4.7}$$

The cyclic pressure in the engine is then determined as

$$P = MR\left(\frac{V_c}{T_k} + \frac{V_k}{T_k} + \frac{V_r \ln\left(\frac{T_h}{T_k}\right)}{T_h - T_k} + \frac{V_h}{T_h} + \frac{V_e}{T_h}\right)^{-1} \tag{4.8}$$

The work done in the engine is as the sum of the work done in the compression space V_c and expansion space V_e.

$$W = W_e + W_c \tag{4.9}$$

$$W = \oint P dV_e + \oint dV_c \tag{4.10}$$

4.2.2 Methodology for preliminary design of FPSE

Due to its simplicity, the isothermal models does not provide high accuracy in prediction of engine's performance, but results obtained on design and working process parameters can be used as preliminary data and starting point for the second order models of the engine. In this section the methodology is described for determination of preliminary parameters of the working process and design parameters of the FPSE. Equations are presented for a Beta and Gamma Stirling engines with a positive overlap in the motion of pistons as shown in Figure 4.4. Volume changes of other types of engines can be considered as derivations from this general diagram. The figure shows that piston displacements are harmonic with the displacer leading piston in oscillations by angle β. The expansion space is formed by the displacement of the displacer only, whilst the

volume of the compression space is formed by motions of both pistons. Here φ is the angle between the minimum volumes of the expansion and compression spaces.

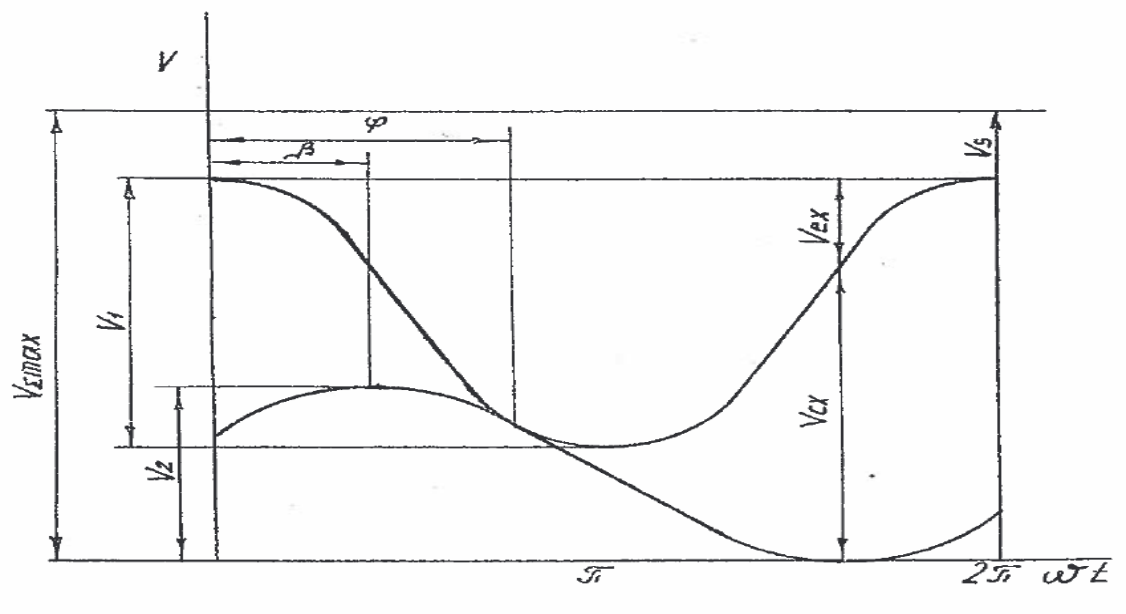

Figure 4.4: Variations in expansion and compression spaces over the cycle [112].

From Figure 4.4 the equations can be derived to describe the volumes of the engine.

The volume of the expansion space:

$$V_e = \frac{1}{2}V_1\,(1 - \cos(\omega\, t)) \tag{4.11}$$

Here V_1 is maximum of the expansion volume.

The volume of the compression space is defined by displacement of two pistons and is defined as

$$V_c = \frac{1}{2}V_1\, Z\,(\cos(\phi - \beta)) - \cos(\omega t - \beta)) + \frac{1}{2}\,(\frac{d}{D})^2 V_1(\cos(\omega t) - cos\phi) \tag{4.12}$$

Here Z is the ratio of maximum volumes displaced by piston (V_2) and displacer (V_1), respectively.

$$V_1 = \frac{\pi D^2}{2}(A_1) \tag{4.13}$$

$$V_2 = \frac{\pi d^2}{2}(A_2) \tag{4.14}$$

Here d is the diameter of the piston in the compression space and D is the diameter of the displacer in the expansion space.

The angle ϕ is defined as

$$\phi = tan^{-1}\left(\frac{Z\sin\beta}{Z\cos\beta-(\frac{d}{D})^2}\right) \tag{4.15}$$

The angular frequency ω of both piston oscillations depends on angular natural frequency ω_i of oscillations of both pistons

$$\omega_i = 2\pi\sqrt{\frac{K_i}{m_i}} \tag{4.16}$$

The displacement of pistons with their amplitudes relative to the pressure variation curve is shown in Figure 4.5. In this figure θ is the pressure angle and is angle between minimum of the expansion space volume and maximum pressure. Angles γ_1 and γ_2 is between maximum pressure and lowest positions of the pistons. For mass-spring oscillating systems with damping device the amplitude A_i and angle γ_i are defined as:

$$A_i = A_2\,\frac{\mu}{Z} \tag{4.17}$$

here A_1 is the amplitude of the displacer;

$$\gamma_i = \pi - \theta \tag{4.18}$$

F_1 and F_2 are maximum pressure forces acting on pistons, ω_i is the natural frequency of oscillation of pistons; n_i is the dimensionless damping coefficient.

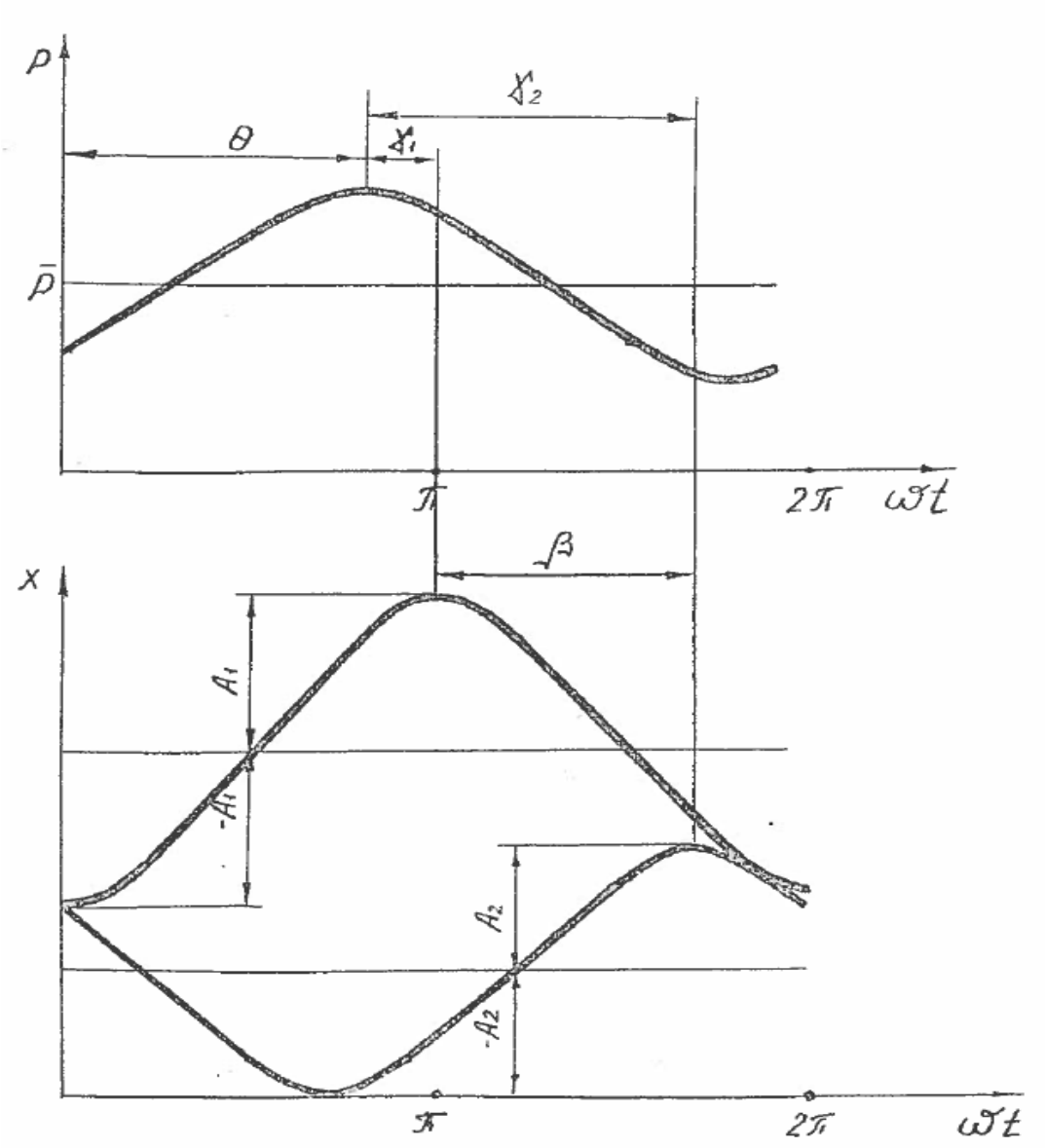

Figure 4.5: Working fluid pressure variation and displacement of pistons over the cycle [112] .

$$F_1 = \frac{\pi(D^2-d^2)}{4}\bar{P}\frac{2\delta}{1+\sqrt{1-\delta^2}}\cos(\omega t-\theta) \tag{4.19}$$

and

$$F_2 = \frac{\pi d^2}{4}\bar{P}\frac{2\delta}{1+\sqrt{1-\delta^2}}\cos(\omega t-\theta) \tag{4.20}$$

$$n_i = \frac{C_i}{2m_i} \tag{4.21}$$

In equations (4.19) and (4.20), $\bar{P}$ is the mean gas pressure over the cycle; δ is the pressure coefficient, which determines the amplitude of pressure variation in the cycle.

$$\bar{P} = P_{max}\sqrt{\frac{1-\delta}{1+\delta}} \tag{4.22}$$

$$\delta = \frac{\sqrt{(\mu Z)^2 - 2\mu\, Z\, (\mu-\tau)\cos\beta + (\mu-\tau)^2}}{\tau + W + S} \tag{4.23}$$

Here P_{max} is the maximum pressure in the cycle.

$$\mu = \left(\frac{d}{D}\right)^2 \tag{4.24}$$

$$Z = \frac{1-\frac{\tau}{\mu}}{\cos\beta - \frac{\sin\beta}{\tan(\theta)}} \tag{4.25}$$

$$\tau = \frac{T_c}{T_H} \tag{4.26}$$

In equation (4.23), W is the ratio of the maximum volume of the compressions and expansion spaces and S is the parameter which determines the influence of dead volumes in the internal gas circuit on the amplitude of pressure variation.

$$W = \mu\sqrt{Z^2 + 1 + 2\,Z\cos\beta} \tag{4.27}$$

$$S = \tau_s v_s \tag{4.28}$$

Here $\tau_s = \tau\, v_{sH} + v_{sc} + \tau_R v_{sR}$ with $v_{sH,} v_{sc}, v_{sR}$ being fractions of the heater, cooler and regenerator in the total dead volume of the engine.

Finally, $\tau_R = \frac{2T_k}{T_k + T_h}$ and $v_s = \frac{2\,V_s}{V_1}$, where V_S is total volume of the dead space in the engine.

The value of the pressure angle can be calculated as

$$\theta = acrtan\left(\frac{sin\beta}{cos\beta - \frac{\mu-\tau}{Z}}\right) \quad (4.29)$$

or from Figure 4.5:

$$\theta = \pi - \gamma_2 + \beta \quad (4.30)$$

In engine calculations the angle γ_2 should be close to 90 degrees to ensure good performance of the engine (as in conventional kinematic drive mechanism engines) but at this angle the mass of the piston might be too large for practical applications.

The relationship between γ_2 and γ_1 is

$$\gamma_2 = \gamma_1 + \beta \quad (4.31)$$

The dimensionless cyclic work in the cycle can be defined as

$$Ly = Z\sqrt{\frac{1-\delta}{1+\delta}}\frac{\delta}{1+\sqrt{1-\delta^2}} \quad (4.32)$$

In calculations the resistance (damping) during the displacer oscillations caused by hydraulic resistance of heat exchangers should be taken into account. It is assumed that the magnitude of pressure losses due to the hydraulic resistance of heat exchangers varies as a harmonic function, see Figure 3.6, and Δp_{max} is equal to 5-10% of P_{max}.

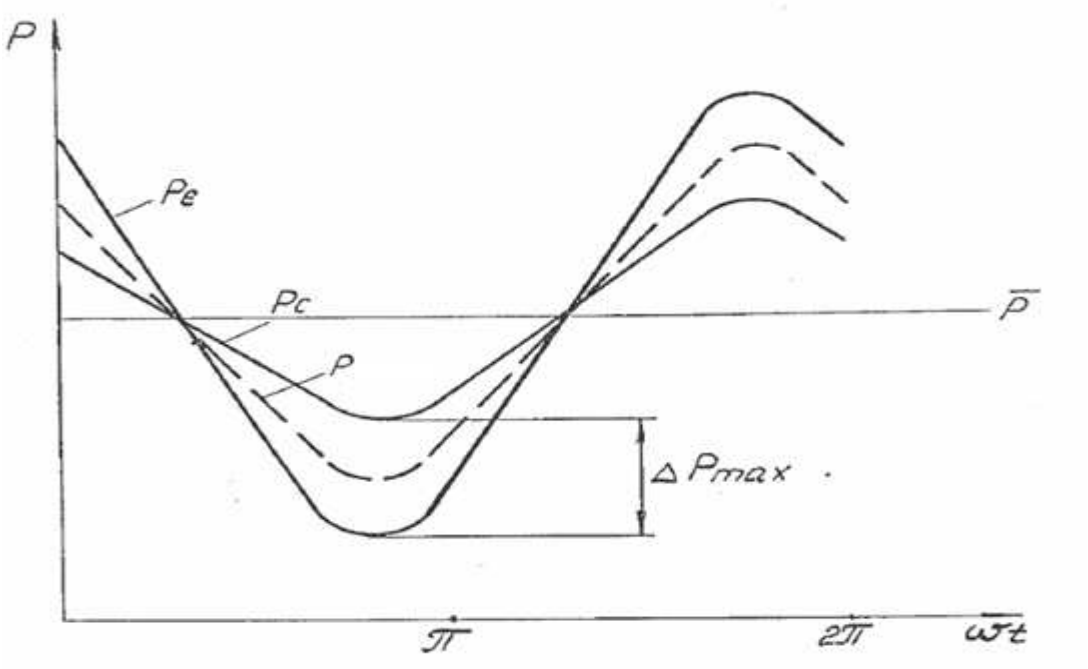

Figure 4.6: Gas pressure variations in the expansion and compression spaces [112].

Using equations (4.12) to (4.32), it is possible to determine the diameter of the piston for the given values of cyclic power output of the engine, frequency of oscillations of pistons, maximum pressure of the gas in the cycle and the amplitude of the piston's displacement:

$$d = \frac{\sqrt{4\,Y\,J}}{2\,Y} \tag{4.33}$$

where

$$Y = 2\,E - \frac{1}{8}\,\Delta p_{max}\,\frac{\pi}{A_2 n_2\,\omega}\,sin\gamma_2 \tag{4.34}$$

and

$$J = \frac{2\,N_e}{n_2 {A_2}^2 \omega^2} \tag{4.35}$$

Here

$$E = \frac{\bar{P}\,\delta\,\pi}{2\,(1+\sqrt{1-\delta^2})A_2\,\sqrt{{n_2}^4+4\,{n_2}^2\omega^2}} \tag{4.36}$$

and

$$n_2 = \frac{2\,\omega}{\tan\gamma_2} \tag{4.37}$$

The mass of the piston is determined as

$$M_2 = \frac{C_2}{2n_2} \tag{4.38}$$

where

$$C_2 = \frac{1}{8} * \Delta p_{max}\,\frac{\pi\,d^2}{A_2\omega}\,sin\gamma_2 + \frac{2\,N_e}{{A_2}^2\omega^2} \tag{4.39}$$

The diameter of the displacer is found as

$$D = \frac{\sqrt{4\,Y\prime J\prime}}{2\,Y\prime} \tag{4.40}$$

where

$$Y' = \frac{1}{2}\bar{P}\frac{\delta\,\pi}{1+\sqrt{1-\delta^2}} - \frac{1}{8}\,\Delta p_{max}\,\pi\sin(\gamma_1)\sqrt{1+\frac{1}{tan^2\gamma_1}} \tag{4.41}$$

$$J' = \frac{1}{2}\bar{P}\frac{\pi\,\delta\,d^2}{1+\sqrt{1-\delta^2}} + \left(\frac{1}{8}\,\Delta p_{max}\,\pi\,d^2\,sin\gamma_1\right)\sqrt{1+\frac{1}{tan^2\gamma_1}} \tag{4.42}$$

The amplitude of the displacer oscillation is

$$A_1 = A_2\,\frac{\mu}{Z} \tag{4.43}$$

The mass of the displacer is

$$M_1 = \frac{C_1}{2n_1} \tag{4.44}$$

where

$$C_1 = \frac{1}{8}\,\Delta p_{max}\,\frac{\pi(D^2-d^2)}{A_1\,\omega}\,sin\gamma_1 \tag{4.45}$$

and

$$n_1 = \frac{2\,\omega}{\tan\gamma_1} \tag{4.46}$$

The convergence criteria used to determine the masses of the piston and displacer is given as

$$\left(\frac{d}{D}\right)^2 - \left(\frac{d_{new}}{D_{new}}\right)^2 \leq 0.01 \tag{4.47}$$

Equations in Section 4.1.3 were used in the developed MATLAB code to determine preliminary design parameters for engines with Beta and Gamma configurations for input data shown in Table 4.1.

Table 4.1: Parametric values used for the numerical modelling of the FPSE.

Engine Data	**Value**
General	
Mean pressure	70 bar
Temperature of the heater	780 K
Temperature of the cooler	320 K
Oscillating frequency	30Hz
Ratio of displacer to piston diameter	0.9
Output Power	1600 W

4.2.3 Procedure for numerical simulation

The iteration procedure is used until the convergence criteria in equation (3.31) are satisfied. Then the cyclic work is calculated, the new diameter of piston and displacer, masses of piston and displacer, area of the piston and amplitude of the displacer are determined. Figure 4.7 presents the procedure for the calculations. Results are dependent on the value of angle β and therefore were repeated for a range of β values from 0^o to γ_2 which was assumed to be 80^o to obtain acceptable value of the piston's mass. Figures 4.8 and 4.9 shows that the maximum value of the dimensionless cyclic work has been obtain for β=40^o. Therefore results were obtained for this optimal angle and these are presented in Table 4.2. Since the engine to be considered in this study is of Gamma configuration the corresponding results on preliminary design parameters were used in further simulations.

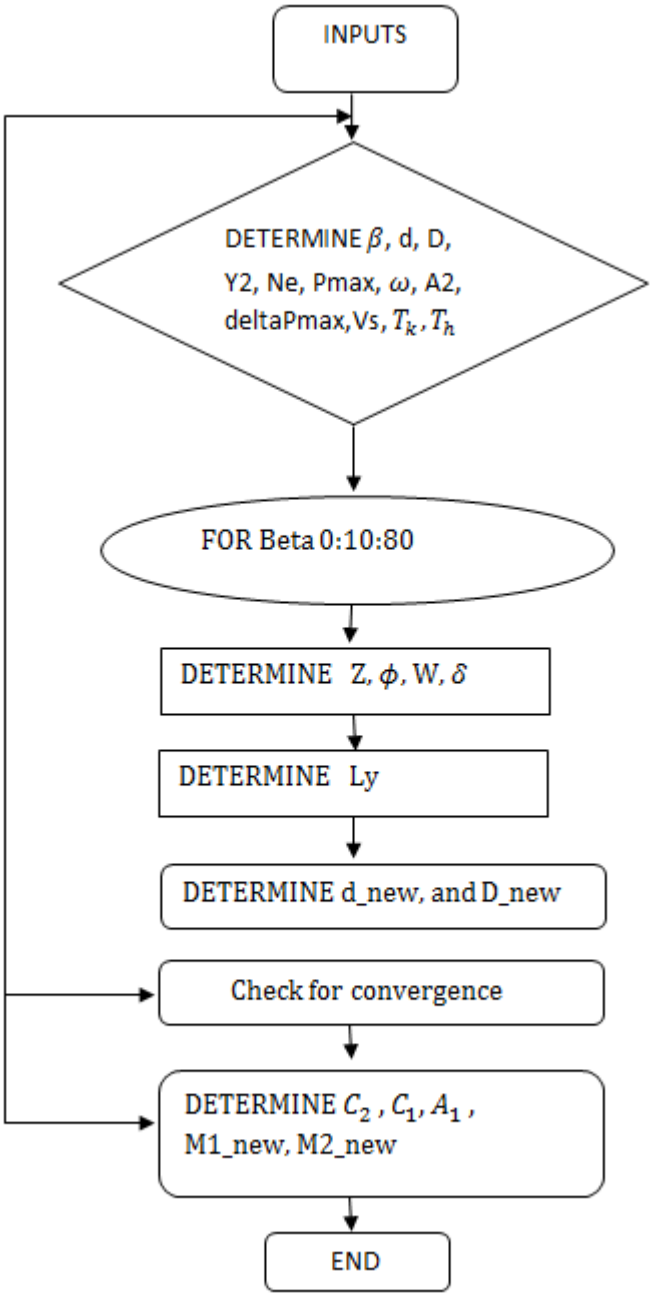

Figure 4.7: The flow chart of the developed isothermal model of the free piston Stirling engine.

4.2.4 Numerical Simulation results

Figures 4.8 and 4.9 illustrate results for the beta and gamma type free piston Stirling engine obtained using the isothermal model. At the specified output power of 1600kW, with temperature of heater at 780K and temperature of cooler at 320 K, mean pressure of 70 bar and ratio of displacer and piston diameter of 0.9. The maximum dimensionless cyclic work was attained when beta angle was 40 degree. Hence, the best output power is generated at this point.

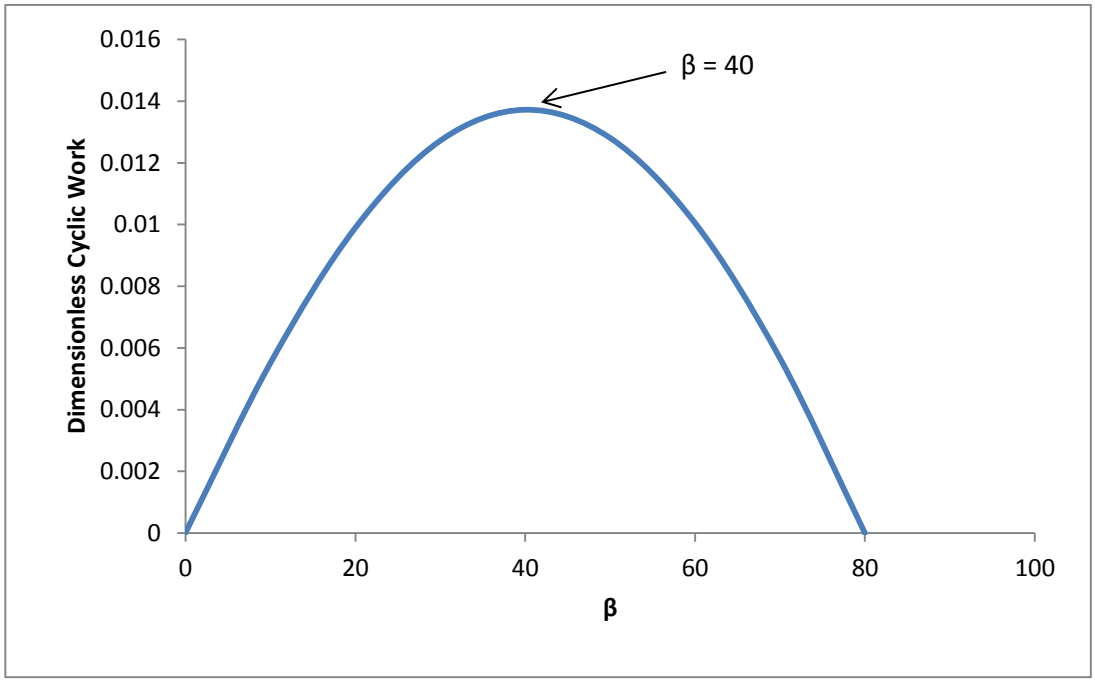

Figure 4.8: The graph of dimensionless cyclic work against β for beta FPSE.

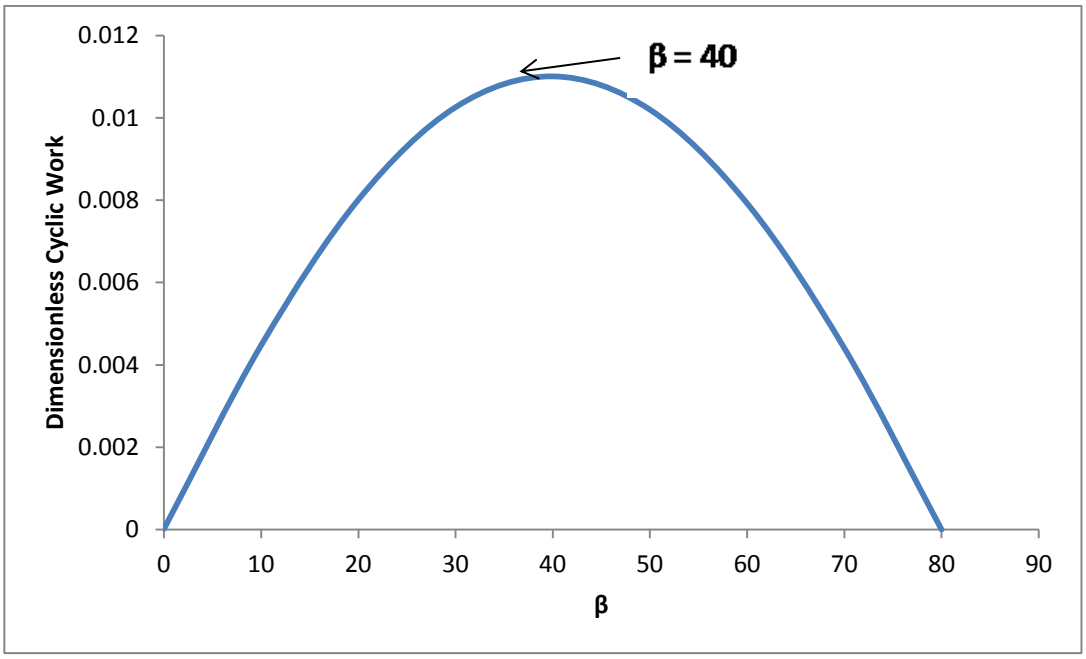

Figure 4.9: The graph of dimensionless cyclic work against β for gamma FPSE.

The parameters which were obtained for the engines are shown in Table 4.2.

Table 4.2: Comparison of the outputs from isothermal model of the β and γ FPSE.

PSE	Beta	Gamma
Frequency	30Hz	30Hz
Output power	1.6kW	1.6kW
Piston diameter	0.099 m	0.113 m
Displacer diameter	0.064 m	0.068 m
Mass of piston	5.1 kg	5.70 kg
Mass of displacer	0.52 kg	0.72 kg
Displacer amplitude	0.02 m	0.021m

4.3 Conclusions

The output results obtained for the Beta and Gamma free piston Stirling engines using coupling of the isothermal model of the working process of Stirling engine and dynamics of two separate mass-spring oscillating systems demonstrated that such approach can be used to produce feasible preliminary values of design parameters of the engine which then can be rectified with deployment of more complex modelling and optimisation methods.

Chapter 5 Mathematical Modelling of the Free Piston Stirling Engine using the Adiabatic Model

5.1 Introduction

In this chapter, the developed adiabatic model of the free piston Stirling engine is presented. The mathematical equations required to model the engine in the numerical simulations are presented.

5.2 Adiabatic model

The ideal adiabatic model of the free piston Stirling engine is the next level of modelling compared to the isothermal model as uses the same five chambers of the engine connected in series to each other. In the isothermal model of the free piston Stirling engine, the compression and expansion space temperatures were assumed to be constant. In the adiabatic model it is assumed that processes in the expansion and compassion spaces are adiabatic and temperature of the gas in these chambers varies due to expansion and compression and gas flow from adjunct chambers. The mass and energy conservation equations form in ordinary differential equations form can only be solved numerically.

The advantage of the adiabatic approach is that it gives more detailed description of the variable parameters during operation and the adiabatic model predicts more accurately the performance of the real life free piston Stirling engine operation.

The heat exchangers (heater, regenerator and cooler) are assumed to be very effective. The heater and cooler maintain the working fluid under isothermal conditions at temperatures T_h and T_k respectively. The regenerator temperature is derived from the logarithmic mean

difference between the heater temperature T_h and cooler temperature T_k. The working fluid in the regenerator matrix and the regenerator void volume possess an identical linear temperature variation. The temperature of the working fluid in the expansion and compression spaces T_e and T_c are assumed to vary in the adiabatic process (as mentioned above). The mass flow of the working fluid through the flow area A (gA) results in the transfer of enthalpy through the four interfaces between the cells of the expansion to heater space *he*, heater to regenerator space *rh*, regenerator to cooler space *kr* and cooler to compression space *ck*. The working fluid flows in the positive direction from the compression space to the expansion space. The flow of enthalpy through the working fluid across the compression to cooler space interface and heater to expansion space interface defines the adjacent upstream temperatures of the cells. Thus T_{he} and T_{ck} are determined by algorithm based on the direction of fluid flow.

$$\text{If } gA_{ck} > 0 \quad \text{then} \quad T_{ck} \leftarrow T_c \quad \text{else } T_{ck} \leftarrow T_k \tag{5.1}$$

$$\text{If } gA_{he} > 0 \quad \text{then} \quad T_{he} \leftarrow T_h \quad \text{else } T_{he} \leftarrow T_e \tag{5.2}$$

Work done on the surroundings is determined by the variation in the volumes of the compression and expansion work spaces V_c and V_e, also the heat transferred in the cooler and heater spaces Q_k and Q_h is transferred from the external environment to the working fluid or vice versa in these spaces, respectively. The internal heat Q_r is transferred from the regenerator matrix to the working fluid flowing through the void volume of regenerator and the regenerator is assumed to be externally adiabatic. The Figure 5.1 shows the layout of the ideal adiabatic model indicating the flow of the working fluid and mass flow across the work spaces and heat exchangers. It also shows the temperature profile from the expansion space through the heat exchangers to the compression space.

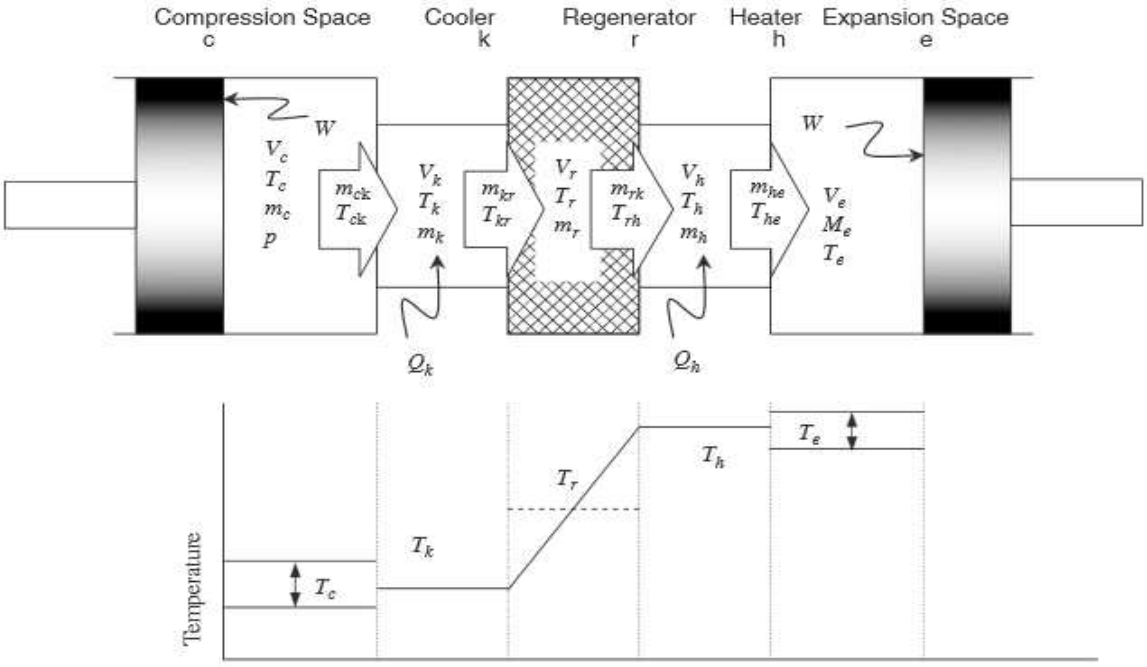

Figure 5.1: The ideal Adiabatic model [111].

Assumptions for the ideal adiabatic model

- The total mass of gas in the engine is constant.
- There is no pressure drop in channels of the engine.
- The engine operates at steady state condition.
- The gas is an ideal gas.
- The spring's masses are not considered.
- The springs in the engine are linear.
- The motion of the engine casing is neglected.

5.2.1 Adiabatic analysis

The adiabatic analysis was performed by Urieli and Berchowitz [19] by applying the equation of state and energy to each of the control volumes to derive the set of differential equations. The continuity equation was also applied across the system to link the resulting equations.

The energy equation applied to a generalised cell is given as:

$$DQ + \left(c_p T_i g A_i - c_p T_o g A_o\right) = dW + c_v D(mT) \tag{5.3}$$

The equation of state is given as

$$pV = mRT \tag{5.4}$$

Some additional equations used are (Rogers and Mayhew [113]):

$$c_p - c_v = R \tag{5.5}$$

$$c_p = R\gamma/(\gamma - 1) \tag{5.6}$$

$$c_v = R\gamma/(\gamma - 1) \tag{5.7}$$

where $\gamma = c_p/c_v$.

Differentiation of equation (5.4) results in

$$\frac{Dp}{p} + \frac{DV}{V} = \frac{Dm}{m} + \frac{DV}{V} \tag{5.8}$$

From the assumption that the total mass of the working fluid is constant

$$m_c + m_k + m_r + m_h + m_e = M \tag{5.9}$$

where m_c is the mass of the working fluid in the compression space, m_k mass of the working fluid in the cooler, m_r mass of the working fluid in the regenerator, m_h mass of the working fluid in the heater and m_e mass of the working fluid in the cooler

By differentiating equation (5.9)

$$Dm_c + Dm_k + Dm_r + Dm_h + Dm_e = 0 \tag{5.10}$$

Since the temperatures and volumes of the heat exchanger cells are constant, the differential form of the equation of state results in

$$\frac{Dm}{m} = \frac{Dp}{p} \tag{5.11}$$

By applying equation (5.11) to the heat exchanger cells and substituting in equation (5.10)

$$Dm_c + Dm_e + Dp\left(\frac{m_k}{p} + \frac{m_r}{p} + \frac{m_h}{p}\right) = 0 \tag{5.12}$$

Also substituting the equation of the state of gas

$$Dm_c + Dm_e + \left(\frac{Dp}{R}\right)\left(\frac{V_k}{T_k} + \frac{V_r}{T_r} + \frac{V_h}{T_h}\right) = 0 \tag{5.13}$$

Applying the energy equation (5.3) to the compression space

$$DQ_c - c_p T_{ck} g A_{ck} = DW_c + c_v D(m_c T_c) \tag{5.14}$$

$DQ_c = 0$ since the compression space is adiabatic. Also the work done in the compression space $DW_c = pDV_c$. Considering the continuity equation the rate of gas accumulation Dm_c is equal to the inflow of gas mass $-gA_{ck}$. The equation is then reduced to:

$$c_p T_{ck} Dm_c = pDV_c + c_v D(m_c T_c) \tag{5.15}$$

Therefore by substituting the equation of state (5.4), and equations (5.5), (5.6) and (5.7) into equation (5.15) and simplifying results new equations for the compression and expansion spaces can be presented as

$$Dm_c = (pDV_c + \frac{V_c D_p}{\gamma})/(RT_{ck}) \tag{5.16}$$

$$Dm_e = (pDV_e + \frac{V_e D_p}{\gamma})/(RT_{he}) \tag{5.17}$$

Now substituting equations (5.16) and (5.17) into equation (5.13) and then simplifying results

$$Dp = -\gamma p(\frac{DV_c}{T_{ck}} + \frac{DV_e}{T_{he}})/[\frac{V_c}{T_{ck}} + \gamma\left(\frac{V_k}{R_k} + \frac{V_r}{T_r} + \frac{V_h}{T_h}\right) + \frac{V_e}{T_{he}}] \tag{5.18}$$

The temperatures between the interface of compression space and cooler space T_{ck} and between the heater space and expansion space T_{he} are based on the conditions of mass flow direction as stated in equation (5.1) and (5.2). To evaluate mass flow and considering the direction of flow, the continuity equation

$$Dm = gA_i - gA_o \tag{5.19}$$

The equation above states that the rate of mass accumulation in a cell is equal to the net mass flow into the cell. Applying equation (5.19) to each cell interface from the compression space through to the expansion space, results in

$$gA_{ck} = -Dm_c \tag{5.20}$$

$$gA_{kr} = gA_{ck} - Dm_k \tag{5.21}$$

$$gA_{rh} = gA_{kr} - Dm_r \tag{5.22}$$

$$gA_{he} = gA_{rh} - Dm_h \tag{5.23}$$

To complete the set of equations heat transferred in the heat exchangers (heater Q_h, regenerator Q_r and cooler Q_k) and work done W should be considered.

The algebraic sum of the work done in the expansion and compression space determines the total work done by the engine.

$$DW = pDV_e + pDV_c \tag{5.24}$$

Taking into consideration the energy equation (5.3) and substituting equations (5.4) and (5.5), a more suitable energy equation is derived:

$$DQ + c_p T_i gA_i - c_p T_o gA_o = (c_p pDV + c_v VDp)/R \tag{5.25}$$

No work is done in the heat exchangers, since their respective volumes are constant. Therefore applying equation (5.25) to each of the heat exchanger spaces

$$DQ_h = \frac{V_h Dpc_v}{R} - c_p(T_{rh} gA_{rh} - T_{he} gA_{he}) \tag{5.26}$$

$$DQ_r = \frac{V_r Dpc_v}{R} - c_p(T_{kr} gA_{kr} - T_{rh} gA_{rh}) \tag{5.27}$$

$$DQ_k = \frac{V_k Dpc_v}{R} - c_p(T_{ck} gA_{ck} - T_{kr} gA_{kr}) \tag{5.28}$$

Since the heat exchangers are isothermal and the regenerator is ideal, the temperature at the interfaces of the regenerator and the heater and cooler

$$T_{kr} = T_k \tag{5.29}$$

$$T_{rh} = T_h \tag{5.30}$$

The above equations of the adiabatic model were used for the numerical simulation of the engine operation.

The calculation scheme used for the analysis of dynamics of the engine is the same as shown in Figure 3.9 The positions of the displacer and piston from the initial equilibrium position at any time *t* are used to define working volumes of the engine.

Equations 4.3 and 4.4 describe the motions of the piston and displacer in this model.

From the engine's geometry the positions of the piston and displacer x_p and x_d define the expansion and compression volumes Ve and Vc:

$$Ve = (V_{cle} + x_d)A_d \tag{5.31}$$

$$Vc = \left(V_{clc} + x_p\right)A_p - (x_d + V_{cle})A_d \tag{5.32}$$

where V_{cle} and V_{clc} are the expansion and compression space clearance volumes.

By differentiating the above equations for Ve and Vc

$$dVe = \dot{x}\ (\ A_d) \tag{5.33}$$

$$dVc = \dot{x}\left(A_p\right) - \dot{x}(A_d) \tag{5.34}$$

The equation for the displacer motion is

$$m_d\ddot{x}_d + K_d x_d + C_d\dot{x}_d = P(A_d) \tag{5.35}$$

or $\ddot{x}_d$ is

$$\ddot{x}_d = \frac{P(A_d)}{m_d} - \frac{K_d x_d}{m_d} - \frac{C_d\dot{x}}{m_d} \tag{5.36}$$

The equation for the piston motion is

$$m_p\ddot{x}_p + K_p x_p + C_p\dot{x}_p = A_p(\ P - P_b) \tag{5.37}$$

and $\ddot{x}_p$ is

$$\ddot{x}_p = \frac{A_p(P-P_b)}{m_p} - \frac{K_p x_p}{m_p} - \frac{C_p \dot{x}_p}{m_p} \tag{5.38}$$

To bounce space pressure P_b can be calculated as

$$P_b = P_{mean}\,(1 + ((\frac{Cap}{Cav})\,(A_p/V_{bo})\,x_p \tag{5.39}$$

where P_{mean} is the mean pressure, Cap is the heat capacity of working fluid at constant pressure, Cav is the heat capacity of working fluid at constant volume, V_{bo} is the bounce space volume and x_p is the displacement of the piston.

The equation for operating pressure in the engine is

$$P = \frac{MR}{\left(\frac{Vc}{Tck}+\frac{Vk}{Tk}+\frac{Vr}{Tr}+\frac{Vh}{Th}+\frac{Ve}{The}\right)} \tag{5.40}$$

where M is the mass of gas, R is the gas constant, Vr is the volume of regenerator, Vk is the volume of cooler, Vh is the volume of heater, Tck is the temperature of the compression space, Tk is the temperature of cooler, Tr is the temperature of regenerator, Th is the temperature of heater and The is the temperature of the expansion space

Therefore the derivative of the pressure is

$$dp = \frac{-\gamma P\left(\frac{dVc}{Tck}+\frac{dVe}{The}\right)}{\left[\frac{Vc}{Tck}+\gamma\left(\frac{Vk}{Tk}+\frac{Vr}{Tr}+\frac{Vh}{Th}\right)+\frac{Ve}{The}\right]} \tag{5.41}$$

The work done in the expansion space

$$dW_e = P_e dV_e \tag{5.42}$$

The work done in the compression space

$$dW_c = P_c dV_c \tag{5.43}$$

The total work in the cycle is

$$W_t = dW_e + dW_c \tag{5.44}$$

or

$$W=P(DV_c + DV_e) \tag{5.45}$$

The indicated output power is

$$Pi = Wf \tag{5.46}$$

where f is the frequency of piston oscillations.

In reality neither the cooling or heating occurs at exactly constant volume and temperature.[114]. Finkelstein developed one of the first adiabatic models in [115] Walker and Kahn [116] performed further research using the theory developed by Finkelstein.

In this chapter the ideal adiabatic model of the working process is coupled with dynamics equations of pistons of the free piston Stirling engine. Table 5.1 shows the parametric data used for the numerical simulation of the adiabatic FPSE in this Chapter.

5.2.2 Procedure for Numerical Simulation

The mathematical equations presented above were employed to analyse the working process of the free piston Stirling engine in accordance with the flow chart shown in Figure 5.2. First, initial values of were determined for both the constant and variable parameters: the initial positions of pistons, the temperatures of the gas in the expansion and compression spaces, regenerator etc. The motion equations were simplified into four first order differential equations and Runge- Kutta (rk4) solver was employed to solve all the equations simultaneously by integrating them using a trial step at interval midpoints to eliminate the errors.

Table 5.1: Engine data of the RE-1000 free piston Stirling [97].

Engine Data	**Value**
General	
Mean pressure	70 bar
Temperature of the heater	780 K
Temperature of the cooler	320 K
Phase angle	120 degree
Oscillating frequency	30Hz
Geometric	
Dead Volume	0.054 mm^3
Volume of the heater	0.016 mm^3
Volume of the regenerator	0.027 mm^3
Volume of the cooler	0.011 mm^3
Piston frontal Area	0.018 m^2
Displacer frontal Area	0.018 m^2
Expansion space clearance volume	0.02 m^2
Compression space clearance volume	0.016 m^3
Mass of the piston	6.2kg
Mass of the displacer	0.426kg
Dynamic	
Piston damping load	461.5 Ns/m
Displacer damping load	35.34Ns/m

The time step was made equal to the 0.001 of the preliminarly estimated period of ocillations and 5 cycles were simulated and check was performed whether the steady state condition was achieved.

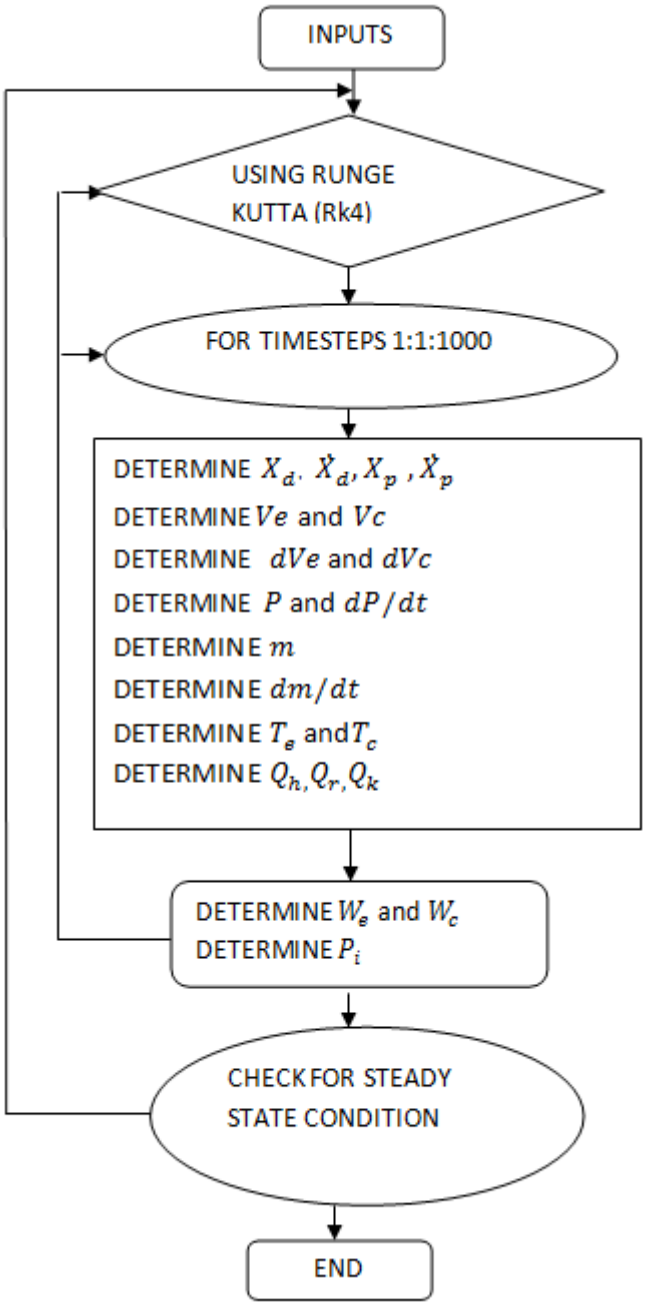

Figure 5.2: The flow chart of the simulation in the accordance with the developed second order adiabatic model of the free piston Stirling engine.

5.2.3 Numerical simulation results

Figure 5.3 shows the variation in the amplitudes of the piston and displacer. The frequency of oscillations is 30 Hz but phase angle between piston displacement is very low. The stroke of the piston is 0.03 m while that of the displacer is 0.055m. The minimum distance between the dispalcer and piston depicts the dead volume which is a negative factor that affects the engine performance.

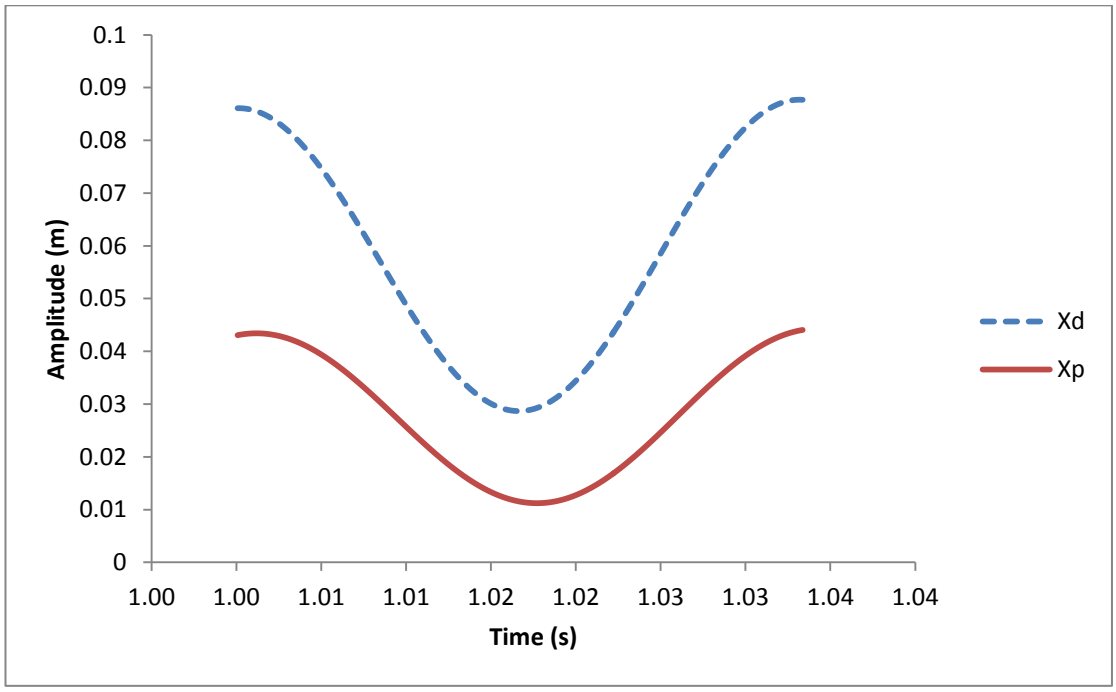

Figure 5.3: The periodic displacements of piston and displacer at the frequency of 30Hz.

Figure 5.4 shows the variation in the temperature of gas in the expansion and compression spaces. The expansion space temperature ranges between 720K to 820K and the in the compression space temperature ranges between 320K to 380K. In the expansion space the mean value is 770K which is less than the heater temperature of 780K. The mean temperature value in the compression space is 350K and is higher than the cooler temperature of 320K.

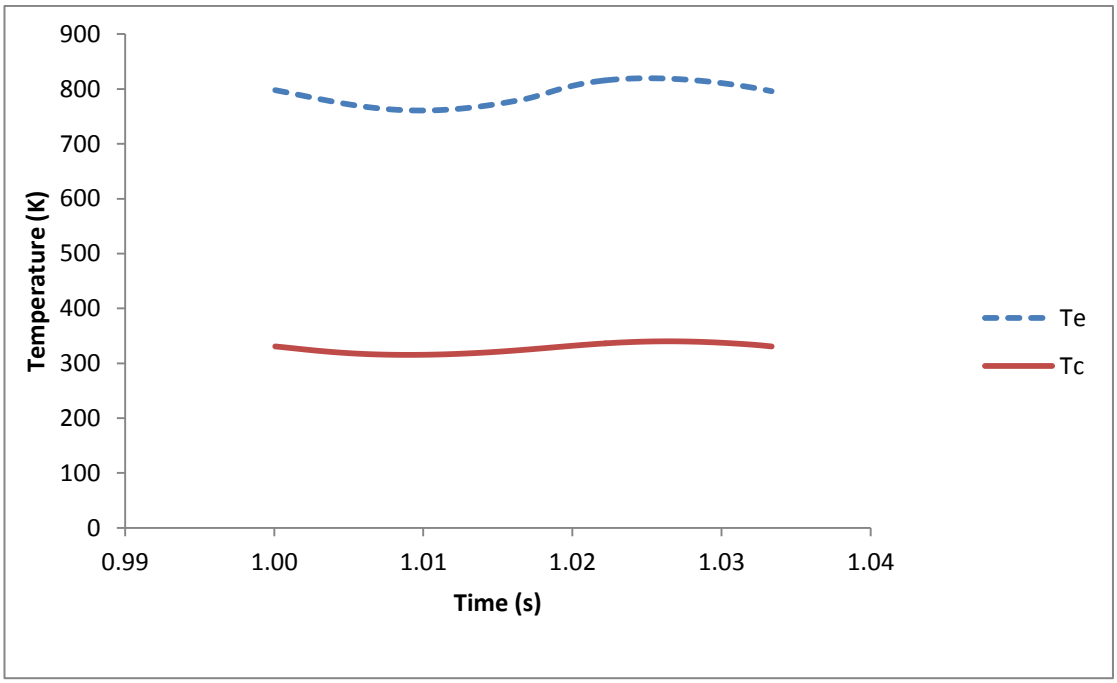

Figure 5.4: The graph of gas temperature variation in the expansion and compression spaces.

Figures 5.5 and 5.6 shows the displacer and piston velocities plotted against their amplitudes. This is done to verify the stable operation of the engine and results indicate such the condition.

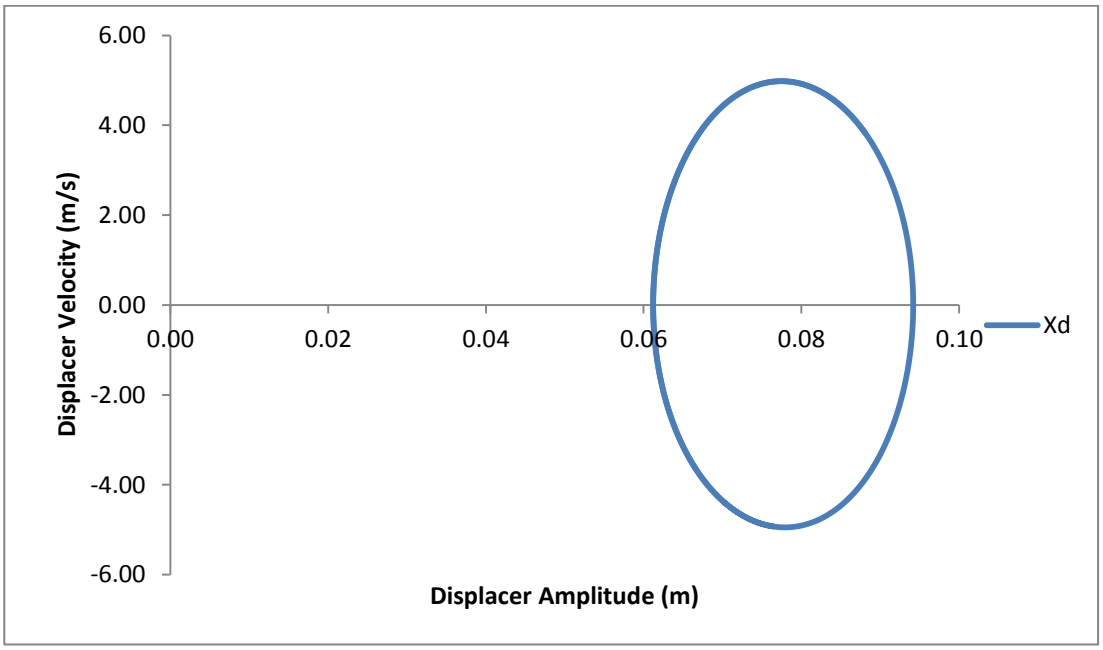

Figure 5.5: The graph of the displacer velocity against displacer amplitude at steady state.

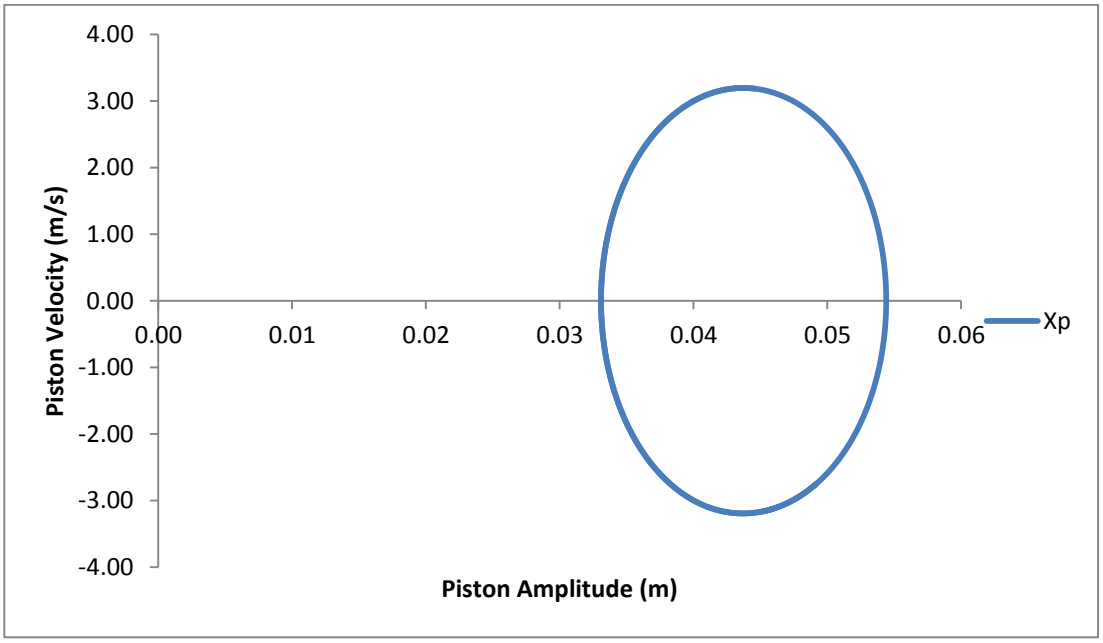

Figure 5.6: The graph of the piston velocity against piston amplitude at steady state.

Figure 5.7 shows the variation in the volumes of the expansion and compression spaces. The volume of the compression space varies from 22 cm^3 to 70 cm^3 while the volume of the expansion space varies from 18 cm^3 to 120 cm^3. As it can be seen on the graph, as the compression volume decreases in a downward motion the expansion volume increases in the other direction with some phase angle.

Figure 5.8 shows the pressure-volume diagram of the free piston engine at the steady state and it indicates that for the given operational conditions the engine generates power of 862 W. The pressure shows a variation between 5.4MPa and 9MPa in the cycle whilst the total volume of the compression space, heater, regenerator, cooler and expansion space varies between 249 cm^3 to 287 cm^3.

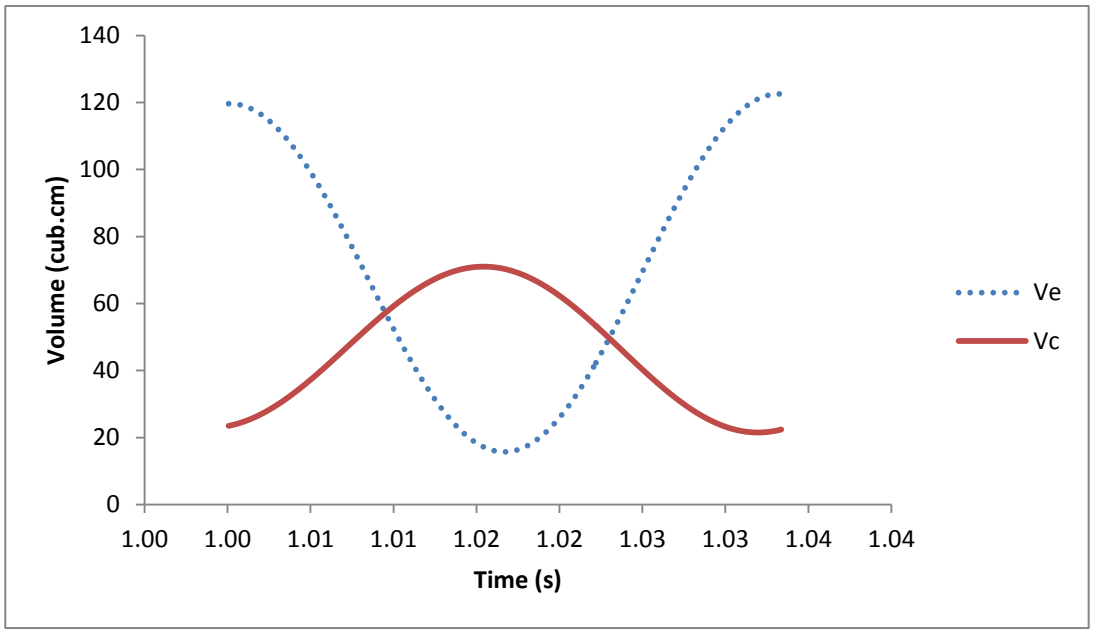

Figure 5.7: The graph of expansion and compression space volumes variation.

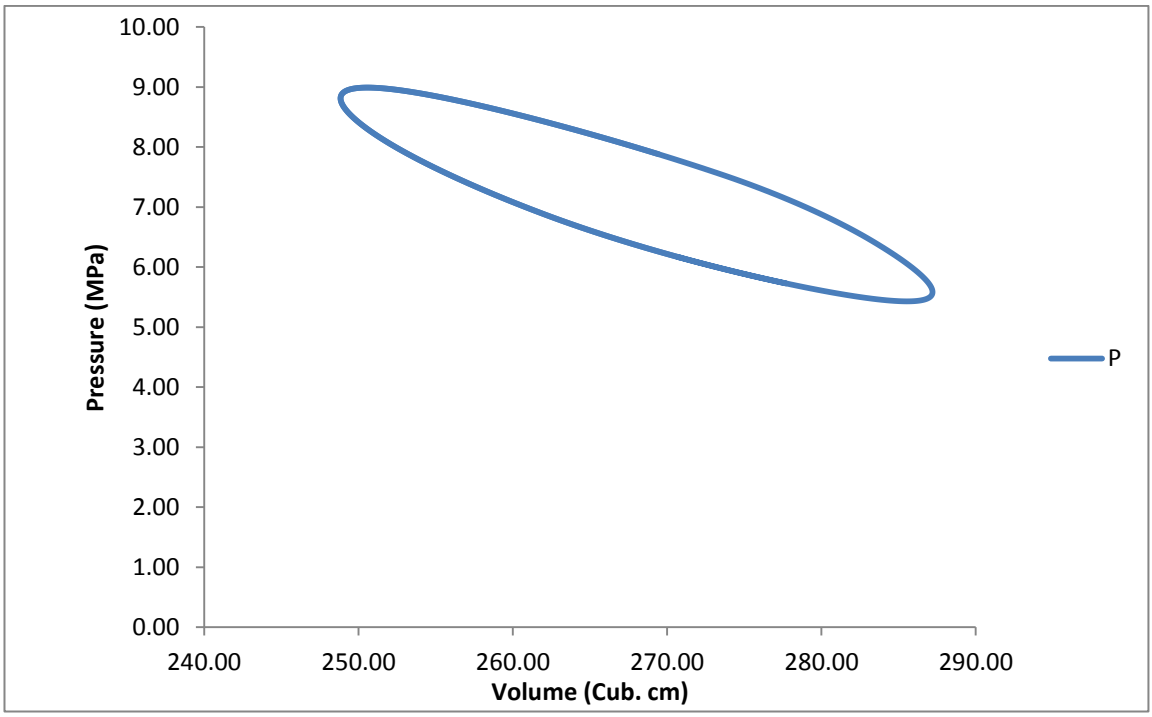

Figure 5.8: The graph of pressure- volume diagram of the engine.

5.2.4 Validation

To validate results from the second order adiabatic modelling performed in this chapter, a documented experimental data for the Sunpower inc. RE-1000 engine was used [106]. The comparison of results is shown in Table 5.2

Table 5.2 Comparison of the Sunpower RE-1000 FPSE results with numerical results from the developed model.

SUNPOWER RE-1000	EXPERIMENT	SIMULATION
Frequency	30Hz	30Hz
Output power	1000W	862W

The geometric data and the operating conditions of the Sunpower RE-1000 FPSE listed in the Table 5.1 above were used for running the developed model and the numerical results are in good agreement with experimental data in terms of output power and frequency of oscillations. This shows that the developed model can return realistic results on the engine's performance.

5.3 Conclusions

The second order adiabatic numerical model of the free piston Stirling engine which was developed in this Chapter provides realistic results for the performance of the engine. This was shown in validation carried out using experimental data for the RE-1000 FPSE. Further work will be carried out on the free piston Stirling engine modelling to improve its accuracy of prediction of power output and this will be done by developing a second order quasi-steady-flow model and considering the losses that occur during the operation of the engine.

Chapter 6 Second Order Quasi Steady Flow Mathematical Modelling of the Free Piston Stirling Engine

6.1 Introduction

In this chapter, the developed quasi steady flow model of the free piston Stirling engine is presented. The physical model of the engine is being studied and results obtained are described. The mathematical equations required to model the engine for numerical simulations are presented.

6.2 Quasi steady flow model

The quasi steady flow model is characterised by the variation in gas temperatures in the heat exchangers and sometimes in their walls. It also takes into consideration all the thermal losses and pressure drops during the engine operation. In the calculation scheme the engine can be split into cells with numbers much greater than 5. The working process equations of this model were coupled with pistons motion equations in this Chapter.

6.2.1 Physical Model

The layout of the RE-1000 FPSE is shown in Figure 6.1 and it is made up of piston and displacer, heat exchangers (heater, regenerator and cooler), gas springs, heat exchangers and load [103]. The physical dimensions of the engine are presented in Table 5.1.

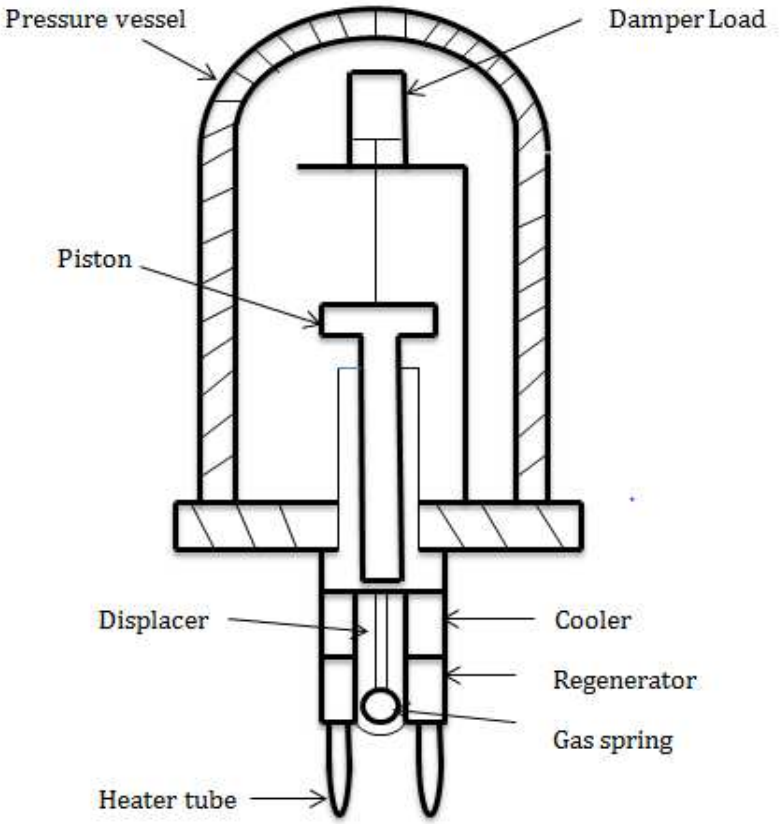

Figure 6.1: The layout diagram of the Re-1000 free piston Stirling engine [103].

6.2.2 The second order mathematical model of the engine

The ideal gas state equation, mass conservation equation, and the energy conservation equations were used to describe the working process in the engine. The engine is divided into fourteen parts. The compression space, expansion space, the heater and cooler spaces are all presented as one cell each whilst ten cells are used for the regenerator space. The regenerator performance determines the engine performance and efficiency. There is a very large temperature gradient is observed in the regenerator and hence the detailed analysis of processes in the regenerator are very important for accuracy of results.

Figures 6.2 and 6.3 show the calculation scheme of the engine used for modelling the temperature profile from the expansion space through the heat exchangers and to the compression space.

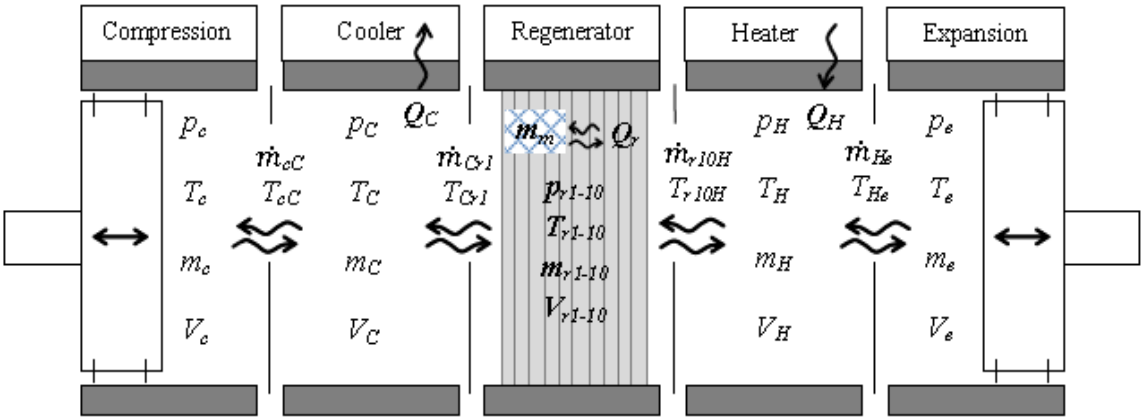

Figure 6.2: The control volumes of the engine [94].

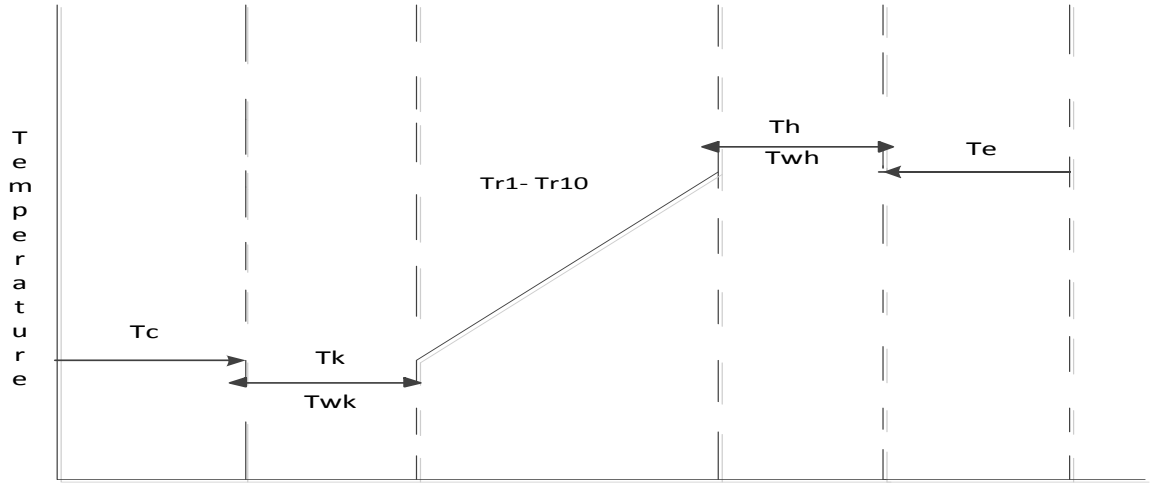

Figure 6.3: Temperature distribution in the work spaces and heat exchangers.

Assumptions of the mathematical model

1. The mass of the gas inside the engine is constant.

2. The working fluid in each control volume is an ideal gas.

3. The engine operates at a steady state condition.

4. Heat losses are calculated separately using superposition principle.

5. The temperatures of the surrounding walls of the working gas volume change with time

6. The derivative pressure in each control volume is the same.

7. The pressure losses are taken into consideration separately.

9. The buffer pressure is the average of the dynamic pressure in the compression space.

Equations 4.1 and 4.2 are used to describe the motions of the piston and displacer.

The gas temperature derivatives in the compression and expansion spaces are

$$dTc = Tc(\frac{dp}{p} + \frac{dVc}{Vc} - \frac{dmc}{mc}) \quad (6.1)$$

$$dTe = Te\ \left(\frac{dp}{p} + \frac{dVe}{Ve} - \frac{dme}{me}\right) \quad (6.2)$$

The total pressure in the engine considering all the losses are:

$$Dp = 1/(C_{av}\ V_t)(R(Q_h + Q_r + Q_c - Q_{hdiss} - Q_{rdiss} - Q_{kdiss}$$

$$-C_{ap}\ P(dV_e + dV_c) \quad (6.3)$$

The temperatue of the working fluid across the boundary between the heater and the expansion space is determined as follows:

$$\text{If } \dot{m}_{he} > 0, T_{he} = T_h \quad (6.4)$$

$$\text{If } \dot{m}_{he} \leq 0, T_{he} = T_e \quad (6.5)$$

where $\dot{m}_{he}$ is the mass flow rate from the heater to the expansion space. (kg/s), T_{he} is the temperature of the mass flow rate from the heater to the expansion space, T_h is the temperature of the heater, T_e is the temperature of the expansion space.

The temperature of the mass flow rate from the last (tenth) part of the regenerator to the heater is described as:

$$\text{If } \dot{m}_{r10h} > 0, T_{r10h} = T_{rh} \tag{6.6}$$

$$\dot{m}_{r10h} \leq 0, T_{r10h} = T_h \tag{6.7}$$

where $\dot{m}_{r10h}$ is the mass flow rate from the tenth part of the regenerator to the heater. (kg/s), T_{r10h} is the temperature of the mass flow rate from the tenth part of the regenerator to the heater. T_{rh} is the temperature of the tenth part of the regerator space to the heater. It is calculated as

$$T_{rh} = 3(T_{r10} - T_{r9})/2 \tag{6.8}$$

The temperature of mass flow rate from the previous part to the following part of the regenerator is

$$T_{r(j)-r(j+1)} = (T_{r(j)} + T_{r(j+1)})/2 \tag{6.9}$$

$T_{r(j)}$ and $T_{r(j+1)}$ represents the working fluid temperature of the (j) and $(j+1)$ part of regenerator space, j is the number of regenerator parts from one to nine**.**

The mas flow rate from the cooler to the first part of the regenerator is obtained as:

$$\text{If } \dot{m}_{kr1} > 0, T_{kr1} = T_k \tag{6.10}$$

$$\text{If } \dot{m}_{kr1} \leq 0, T_{kr1} = T_{rk} \tag{6.11}$$

where $\dot{m}_{kr1}$ is the mass flow from the cooler to the first part of the regenerator (Kg/s), T_{kr1} is the temperature from the cooler to the first part of the regenerator, T_k is the temperature of the cooler space, T_{rk} is the temperature between the first part of the regenerator and the cooler. It is

$$T_{rk} = \frac{3T_{r1} - T_{r2}}{2} \tag{6.12}$$

The mass flow rate from the compression space to the cooler:

$$\text{If} \quad \dot{m}_{ck} > 0, T_{ck} = T_c \tag{6.13}$$

$$\text{If} \quad \dot{m}_{ck} \leq 0, T_{ck} = T_k \tag{6.14}$$

where $\dot{m}_{ck}$ is the mass flow rate from the compression space to the cooler, T_{ck} is the temperature from the compression space to the cooler, T_c is the temperature of the compression space.

The energy conservation equations

The energy conservation equation applied to each of the control volumes (expansion and compression spaces, the ten parts of the regenerator, heater and cooler) can be defined as

$$C_{av} \frac{d(m_c T_c)}{dt} = -\dot{m}_{ck} C_{ap} T_{ck} - \frac{dW_c}{dt} \tag{6.15}$$

$$C_{av} \frac{dm_c T_c}{dt} = dQ_c - dQ_{kdiss} + \dot{m}_{ck} C_{ap} T_{ck} - \dot{m}_{cr1} C_{ap} T_{cr1} \tag{6.16}$$

$$C_{av} \frac{d(m_{r1} T_{r1})}{dt} = dQ_{r1} - dQ_{r1diss} + \dot{m}_{cr1} C_{ap} T_{cr1} - \dot{m}_{r1\_r2} C_{ap} T_{r1\_r2} \tag{6.17}$$

The energy conservation equation for the second to ninth part of the regenerator is derived as:

$$C_{av}\frac{dm_{r(j)}T_{r(j)}}{dt} = dQ_{r(j)} - dQ_{r(j)diss} + \dot{m}_{r(j-1)r(j)}C_{ap}T_{r(j-1)r(j)}$$

$$-\dot{m}_{r(j)r(j+1)}C_{ap}T_{r(j)r(j+1)} \quad (6.18)$$

$$C_{av}\frac{d(m_{r10}T_{r10})}{dt} = dQ_{r10} - dQ_{r10diss} + \dot{m}_{r9\_r10}C_{ap}T_{r9r10} - \dot{m}_{r10h}C_{ap}T_{r10h} \quad (6.19)$$

$$C_{av}\frac{d(m_hT_h)}{dt} = dQ_h - dQ_{hdiss} + \dot{m}_{r10h}C_{ap}T_{r10h} - \dot{m}_{he}C_{ap}T_{he} \quad (6.20)$$

$$C_{av}\frac{(dm_eT_e)}{dt} = \dot{m}_{he}C_pT_{he} - \frac{dW_e}{dt} \quad (6.21)$$

In above eqautions m_c is the mass of working fluid in the cooler, W_c is the work in the compression space, Q_c is the heat transfer in the cooler, Q_r is the heat transfer in the regenerator, $Q_h$is the heat transfer in the heater, Q_{kdiss} is the heat dissipation loss due to friction in the cooler, $Q_{r(j)diss}$ is the heat dissipation loss due to friction in the ten parts of the regenerator, Q_{hdiss} is the heat dissipation loss due to friction in the heater, W_e is the work in the expansion space.

The equations for the conservation of energy for each control volumes is expanded using the ideal gas state equation and equation for the work done in the expansion and compression spaces and the properties of the working fluid.

Ideal gas state equation is

$$(PV = mRT) \quad (6.22)$$

Work done in compression space and expansion spaces are

$$\frac{dW_c}{dt} = P_c\frac{dV_c}{dt} \;\; ; \;\; \frac{dW_e}{dt} = P_e\frac{dV_e}{dt} \quad (6.23)$$

Properties of the working fluid are

$$R = C_{ap} - C_{av} \;\; ; \;\; \gamma = \frac{C_{ap}}{C_{av}} \tag{6.24}$$

The mass flow rate from the expansion space to the compression space is derived as:

$$\dot{m}_{ck} = -\frac{1}{RT_{ck}}\left(P_c \frac{dV_c}{dt} + \frac{V_c}{\gamma}\frac{dp}{dt}\right) \tag{6.25}$$

$$\dot{m}_{kr1} = \frac{1}{RT_{kr1}}\left(\frac{R}{C_{ap}} dQ_k - \frac{R}{C_{ap}} dQ_{kdiss} - \frac{V_k}{\gamma}\frac{dp}{dt} + R\dot{m}_{ck}T_{ck}\right) \tag{6.26}$$

$$\dot{m}_{r1\_r2} = \frac{1}{RT_{rr1}}\left(\frac{R}{C_{ap}} dQ_{r\_1} - \frac{R}{C_{ap}} dQ_{r1diss} - \frac{V_{r\_1}}{\gamma}\frac{dp}{dt} + R\dot{m}_{kr1}T_{kr1}\right) \tag{6.27}$$

The mass flow rate for the second to the ninth part of the regenerator is

$$\dot{m}_{r(j)r(j+1)} = \frac{1}{RT_{r(j)r(j+1)}}\left(\frac{R}{C_{ap}} dQ_{r(j)} - \frac{R}{C_{ap}} dQ_{r(j)diss} - \frac{V_{r_j}}{\gamma}\frac{dp}{dt}\right.$$

$$\left. + R\dot{m}_{r(j-1)r(j)}T_{r(j-1)r(j)}\right) \tag{6.28}$$

$$\dot{m}_{r10\_h} = \frac{1}{RT_{r10\_h}}\left(\frac{R}{C_{ap}} dQ_{r\_10} - \frac{R}{C_{ap}} dQ_{r10diss} - \frac{V_{r\_10}}{\gamma}\frac{dp}{dt} + R\dot{m}_{r9\_r10}T_{r9\_r10}\right) \tag{6.29}$$

$$\dot{m}_{he} = \frac{1}{RT_{he}}\left(\frac{R}{C_{ap}} dQ_h - \frac{R}{C_{ap}} dQ_{hdiss} - \frac{V_{r\_10}}{\gamma}\frac{dp}{dt} + R\dot{m}_{r10\_h}T_{r10\_h}\right) \tag{6.30}$$

The derivative for the total pressure in the engine is obtained by summing all the energy equations and losses:

$$\frac{dp}{dt} = \frac{1}{C_{av}V_t}\left(R\left(dQ_h + \sum dQ_r + dQ_c - \sum dQ_{diss} - dQ_{shtl}\right)\right)$$

$$\left. - C_{ap}\left(P_e \frac{dV_e}{dt} + P_c \frac{dV_c}{dt}\right)\right) \tag{6.31}$$

where $Q_{shtl}$is the shuttle heat loss.

For the regenerator matrix the energy conservation equation can be derived as:

$$\frac{dT_m}{dt} = -dQ_r \frac{1}{\dot{m}_m C_{ap}} \tag{6.32}$$

Hence the energy conservation for each of the regenerator matrix can be written as:

$$\frac{dT_{m(j)}}{dt} = -dQ_{r(j)} \frac{1}{\dot{m}_{m(j)} C_{ap}} \tag{6.33}$$

The mass conservation equations

The equations for mass conservation of the working fluid in each control volume can be obtained as:

$$\frac{dm_c}{dt} = -\dot{m}_{ck} \tag{6.34}$$

$$\frac{dm_k}{dt} = \dot{m}_{ck} - \dot{m}_{kr1} \tag{6.35}$$

$$\frac{dm_{r1}}{dt} = \dot{m}_{kr1} - \dot{m}_{r1r2} \tag{6.36}$$

For the other nine parts of the regenerator

$$\frac{dm_{r(j)}}{dt} = \dot{m}_{r(j-1)r(j)} - \dot{m}_{r(j)r(j+1)} \tag{6.37}$$

$$\frac{dm_{r\_10}}{dt} = \dot{m}_{r9r10} - \dot{m}_{r10h} \tag{6.38}$$

$$\frac{dm_h}{dt} = \dot{m}_{r10h} - \dot{m}_{he} \tag{6.39}$$

$$\frac{dm_e}{dt} = \dot{m}_{he} \tag{6.40}$$

To determine the temperature of the working fluid in the expansion space, compression space and the heat exchangers including all ten parts of the regenerator, the following equations are used:

$$T_e = \frac{P_e V_e}{R_{me}} \qquad T_c = \frac{P_c V_c}{R_{mc}}$$

$$T_k = \frac{P_k V_k}{R_{mk}} \qquad T_h = \frac{P_h V_h}{R_{mh}}$$

$$T_{r(j)} = \frac{Pr_{(j)} V_{r(j)}}{R_{mr(j)}} \tag{6.41}$$

The pressure drop inside the heat exchangers (heater, regenerator and cooler) is determined along with the pressure drops in the expansion and compression work spaces. The pressure drop is calculated in the heater and cooler as

$$\Delta P = \frac{2 f_r \mu U V}{A_{freesurf} {d_h}^2} \tag{6.42}$$

where f_r is the friction coefficient, μ is the viscosity of the working fluid, U is the density of the working fluid, V is the velocity if the working fluid and $A_{freesurf}$ is the free surface area.

$$f_r = f_c Re\text{y} \tag{6.43}$$

Friction coefficient (f_c) for cooler and heater can be obtained as:

If $Re\text{y} < 2000$

$$f_c = \frac{64}{Rey} \tag{6.44}$$

If $2000 < Re\text{y} < 20000$

$$f_c = 0.316\, Rey^{-0.25} \tag{6.45}$$

If Rey >2000

$$f_c = 0.184 Rey^{-0.2} \tag{6.46}$$

Due to the high impact the regenerator has on the Stirlng engine performance, a number of correlations has been obtained by the experimental analysis of the oscillating flow in the regenerator. These were analysed by Thomas and Pittman [118] and in this work the friction factor of the regenerator is defined as

$$f_c = \frac{129}{Rey} + \frac{2.91}{Rey^{0.103}} \tag{6.47}$$

The instantaneous pressure of the working fluid in each of the control volume is derived by:

- In the cooler

$$P_{\boldsymbol{k}} = P_{\boldsymbol{c}} + \frac{\Delta P_k}{2} \tag{6.48}$$

where ΔP_k is the pressure drop in the cooler;

- In the regenerator

$$P_{r\_1} = P_k + \frac{\Delta P_k}{2} + \frac{\Delta P_{r(j)}}{2}\,; \tag{6.49}$$

In the second to the tenth part of the regenerator

$$P_{r(j)} = P_{r(j-1)} + \frac{\Delta P_{r(j-1)}}{2} + \frac{\Delta P_{r(j)}}{2}\,; \tag{6.50}$$

In the heater

$$P_h = P_{r\_10} + \frac{\Delta P_{r\_10}}{2} + \frac{\Delta P_h}{2}\,; \tag{6.51}$$

In the expansion and compression space:

$$P_e = P_h + \frac{\Delta P_h}{2}\,; \tag{6.52}$$

The pressure in the compression space is the same as the calculated pressure in the engine

$$P_c = P \tag{6.53}$$

The following equations are used to calculate the rate of heat transfer in the heat exchangers:

$$dQ_h = h_h A_{surfh}(T_{wh} - T_h) - dQ_{hlir} \tag{6.54}$$

where dQ_{hlir} is the heat loss due to the heat conduction from the part of the heater with higher temperature to the part of the heater with lower temperature;

$$dQ_k = h_k A_{surfk}(T_{wk} - T_k) - dQ_{klir} \tag{6.55}$$

where dQ_{klir} is the heat loss to the heat conduction from the part of the cooler with higher temperature to the part of the cooler with the lower temperature.

The correlation by Colburn was used to determine the heat transfer coefficient for unidirectional flow and it was employed to calculate the coefficient of heat transfer on the surfaces of the heater and cooler. respectively [108]:

$$J = \frac{hPr^{2/3}}{C_{ap}\dot{m}/A_{freesurf}} \tag{6.56}$$

If $Rey < 3000$

$$J = \exp(0.337 - 0.81\log(Rey)) \tag{6.57}$$

If $3000 < Rey < 4000$

$$J = 0.0021 \tag{6.58}$$

If $4000 < Rey < 7000$

$$J = exp(13.31 - 0.861log|(Rey)) \tag{6.59}$$

If $7000 < Rey < 10000$

$$J = 0.0034 \tag{6.60}$$

If $Rey > 10000$

$$J = exp(-3.575 - 0.229log(Rey)) \tag{6.61}$$

To determine the rate of heat transfer in the ten parts of the regenerator, the following equation was used:

$$dQ_r = \varepsilon\, h_{r(j)} A_{surfr(j)} \left(T_{m(j)} - T_{r(j)}\right) - dQ_{r(j)lir} \tag{6.62}$$

where ε is emissivity, h_r is the heat transfer coefficent of the regenerator and $A_{surfr(j)}$ is the free surface area of the regenerator, dQ_{rlir} is the heat loss due to the heat conduction from the part of the regenerator with higher temperature to the part of the regenrator with the lower temperature, (j) represents the ten parts of the regenerator matrix.

The heat dissipation loss due to internal and external conduction and the shuttle loss is accounted for in this second order mathematical model of the free piston Stirling engine (whereas the adiabatic model did not account for these losses). The internal conducton heat loss is the heat transfer from the part of the heat exchanger with higher temperature to the part with lower temperature. The equation used to determine the one- dimensional heat conduction loss along the length of the heat exchanger is given as:

For cooler

$$dQ_{klir} = \frac{k_k A_k}{l_k(T_{kr1} - T_{ck})} \tag{6.63}$$

where k_k is the thermal conductivity of cooler, A_k is the cross sectional area of cooler and l_k is the length of cooler;

For heater

$$dQ_{hlir} = \frac{k_h A_h}{l_h(T_{he} - T_{rh})} \tag{6.64}$$

where k_h is the thermal conductivity of heater, A_h is the cross sectional area of heater and l_h is the length of heater;

For first part of regenerator

$$dQ_{r1lir} = \frac{k_r A_r}{l_{r1}(T_{rr1} - T_{kr1})} \tag{6.65}$$

For second to ninth part of regenerator

$$dQ_{r(j)lir} = \frac{k_r A_r}{l_{r(j)}(T_{rr(j+1)} - T_{rr(j)})} \tag{6.66}$$

For tenth part of regenerator

$$dQ_{r10lir} = \frac{k_r A_r}{l_{r10}(T_{r10h} - T_{rr9)})} \tag{6.67}$$

where k_r is the thermal conductivity of regenerator, A_r is the cross sectional area of regenerator and l_r is the length of regenerator.

The external conducton heat loss is the heat transfer from the part of the regenerator with higher temperature to the part with lower temperature due to heat conduction in relation to the environment. This is only accounted for in the regenerator only:

$$dQ_{r1ext} = (1-\varepsilon)\, h_{r(j)} A_{surfr(j)} \left(T_{m(j)} - T_{r(j)}\right) \tag{6.68}$$

The shuttle heat loss calculation was first introduced by Zimmerman and Longsworth [19]. The shuttle loss accounted for in this as

$$dQ_{sht;} = \frac{0.4 {X_d}^2 k_f d_d}{\Delta g p L_d} \tag{6.69}$$

where X_d is the displacer stroke, k_f is the thermal conductivity of working fluid, d_d is the diameter of displacer and l_d is the length of displacer.

The indicated work in the cycle is

$$W_{in} = \int_0^t \left(P_e \frac{dV_e}{dt} + P_c \frac{dV_c}{dt}\right) \tag{6.70}$$

The indicated power of the engine is

$$P_{in} = W_{in} f \tag{6.71}$$

6.2.3 Procedure for Numerical Simulations

The flow chart of calculations using the above developed model is shwon in Figure 6.4. First, the initial input values for both the constant and variable parameters were determined, initial temperatures in all cells were set.

The inital temperature of the gas in the regenerator cells were obtained using lnear interpolation and values of the heater and cooler temperatures. The Runge Kutta (rk4) solver was used and metodlogy similar t that used in previous Chapter was employed to obtain the engine performance results.

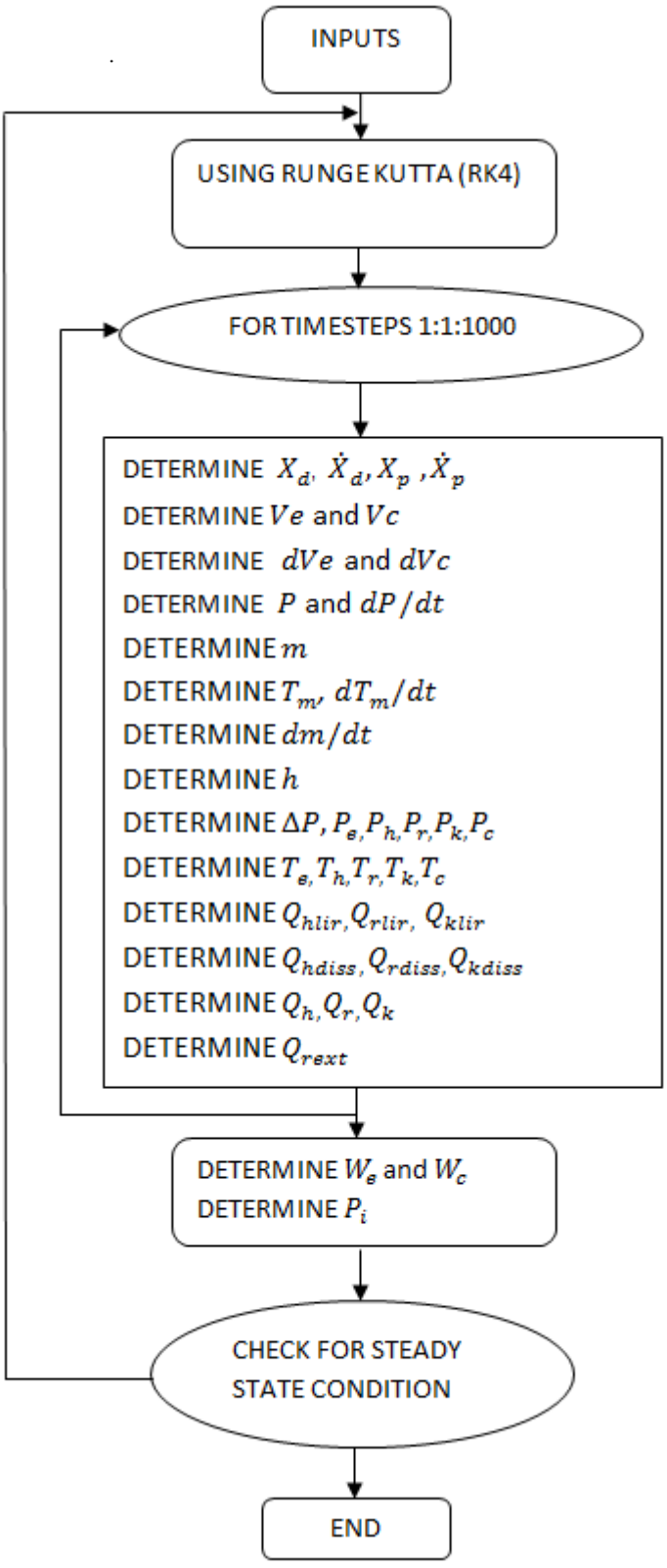

Figure 6.4: The flow chart of calculations using the developed second order Quasi steady flow model of the free piston Stirling engine.

6.2.4 Numerical simulation results

Results obtained on the operational performance of the gamma configuration engine are discussed below. The engine parameters which were used are those of the RE-1000 Sunpower FPSE (see Table 5.1). The values of the heater and cooler temperatures were given as 814.3 K and 322.8 K respectively, the maximum pressure was 70 bar and the working fluid used was helium.

Figure 6.5 shows the pressure-volume diagrams for the expansion and compression spaces. The pressure variation is between 7.25 MPa and 6.75 MPa. The volumes change between $0.3^{-4}(m^3)$ to 0.5^{-4} (m^3). The indicated work from these P-V diagrams is 33.2 J while the indicated output power generated is 996 W at the engine efficiency of 33.67 %.

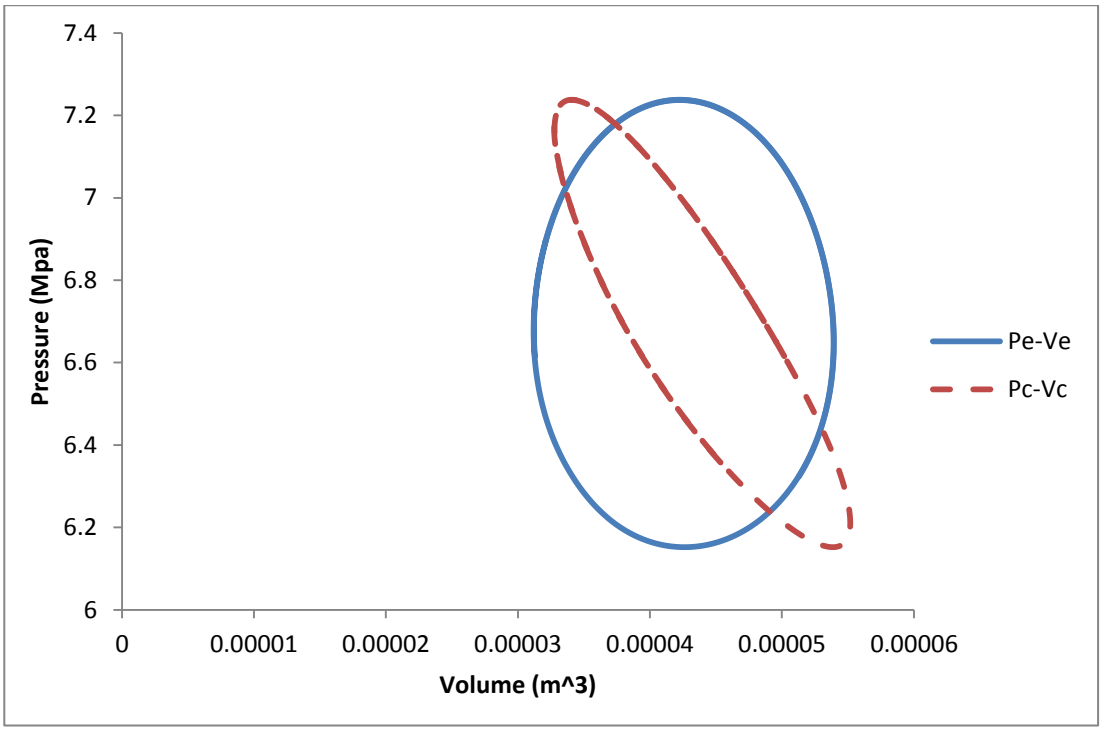

Figure 6.5: The pressure-volume diagrams for expansion and compression spaces.

Figure 6.6 shows the variation in the heat flow rate in the heat exchangers. The heater has the highest heat flow of 4.5 kW while the cooler has the lowest heat flow of 1.2 kW. The 10^{th} part of the regenerator closer to the heater has this value about 3.3 kW and the 1^{st} part closer to the cooler shows 3kW of the heat flow. This shows that overall heat flow in the regenerator is much greater than in heat exchangers, which agrees with other published theoretical and experimental investigations.

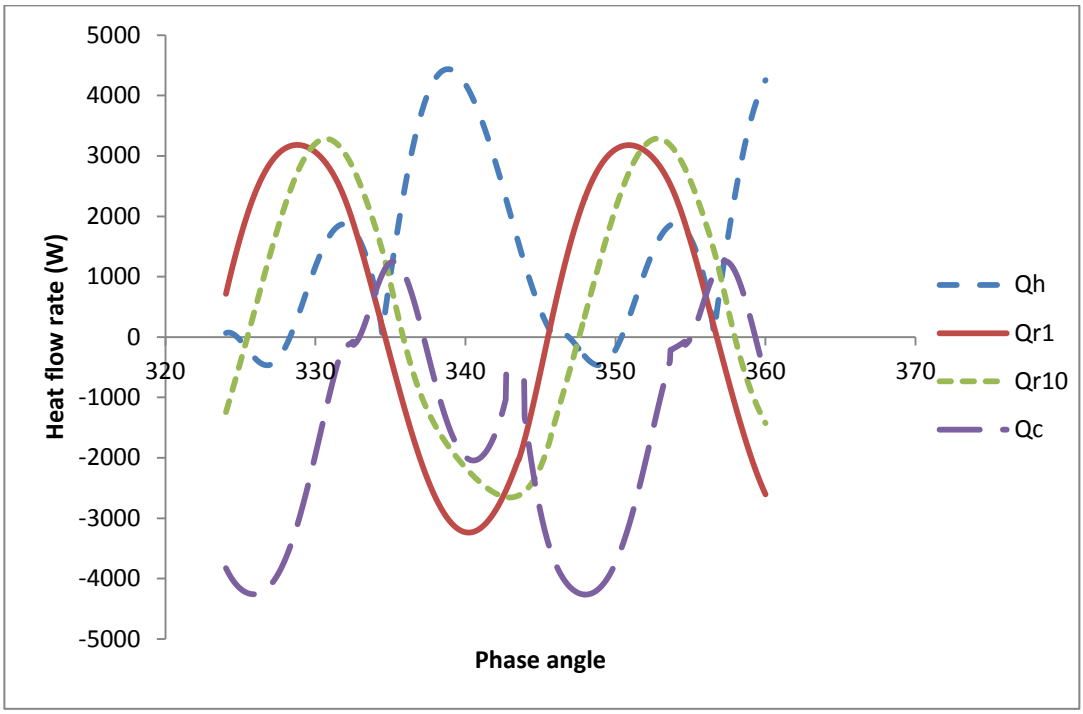

Figure 6.6: Heat flow rate in the heat exchangers.

Figure 6.7 shows the variation in the expansion and compression volumes. The volume of the compression chamber varies from 32 cm^3 to 55 cm^3 whereas the volume of the expansion space varies from 31.5 $cm^3$to 54 cm^3. It can be seen that the phase angle between expansion and compresion volumes has improved and is at about 120 degree. This is due to taking into account different losses in the cycle. Figure 6.8 shows the periodic displacement of the piston with the stroke of 0.005m. The clearances above the piston indicate the prsence of the considerable dead volume during operation of the engine

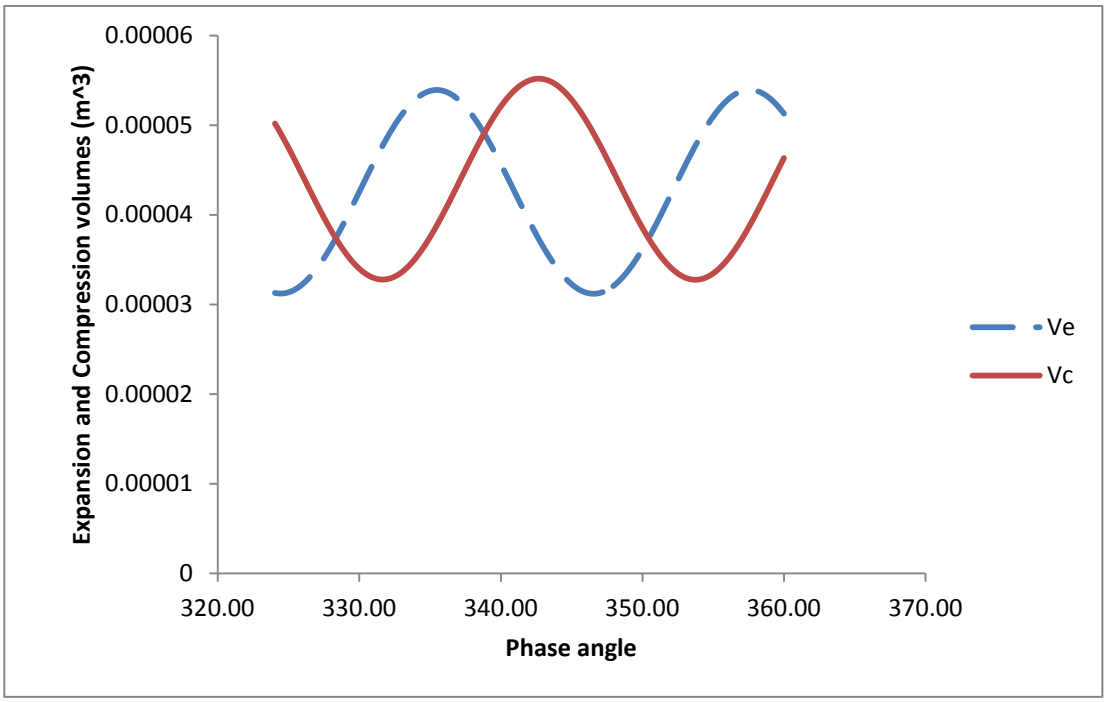

Figure 6.7: Volume variation in expansion and compression spaces.

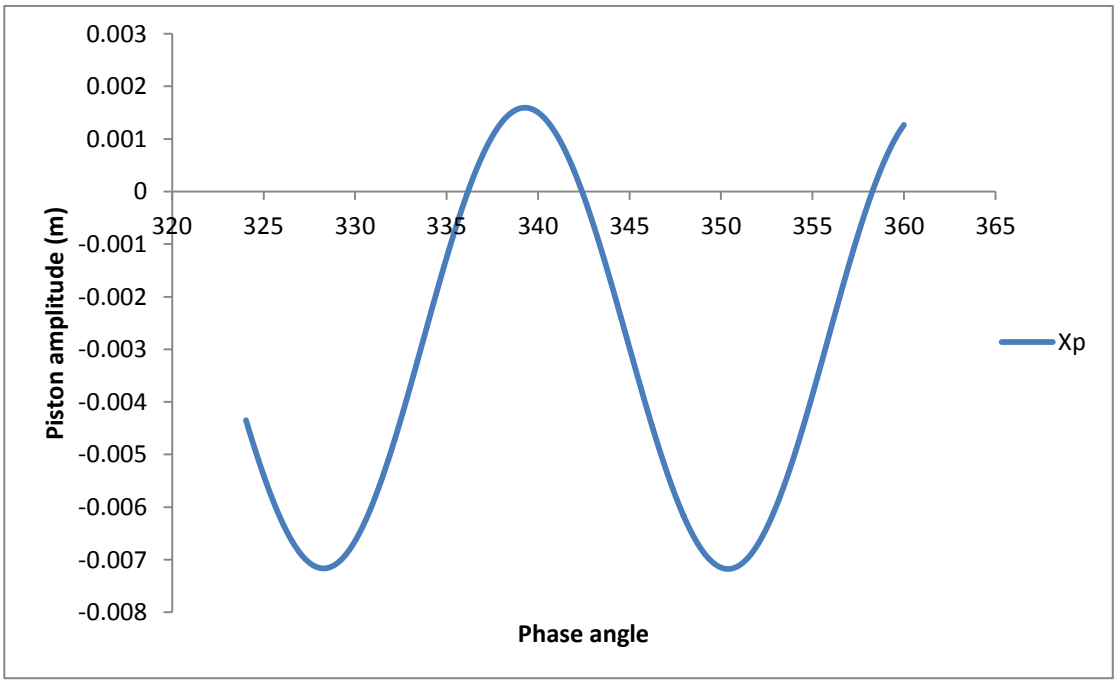

Figure 6.8: The displacement of piston at a frequency of 30Hz.

The amplitude of the displacer oscillations is presented in Figure 6.9. The stroke of the displacer is 0.0037m. The clearance above the displacer indicates the dead volume in the hot part of the cylinder. Figure 6.10 shows the variation in the velocities of the piston and displacer. The piston has a maximum velocity of 1.35 m/s and the displacer has a maximum velocity of 1.38 m/s at the steady state operation.

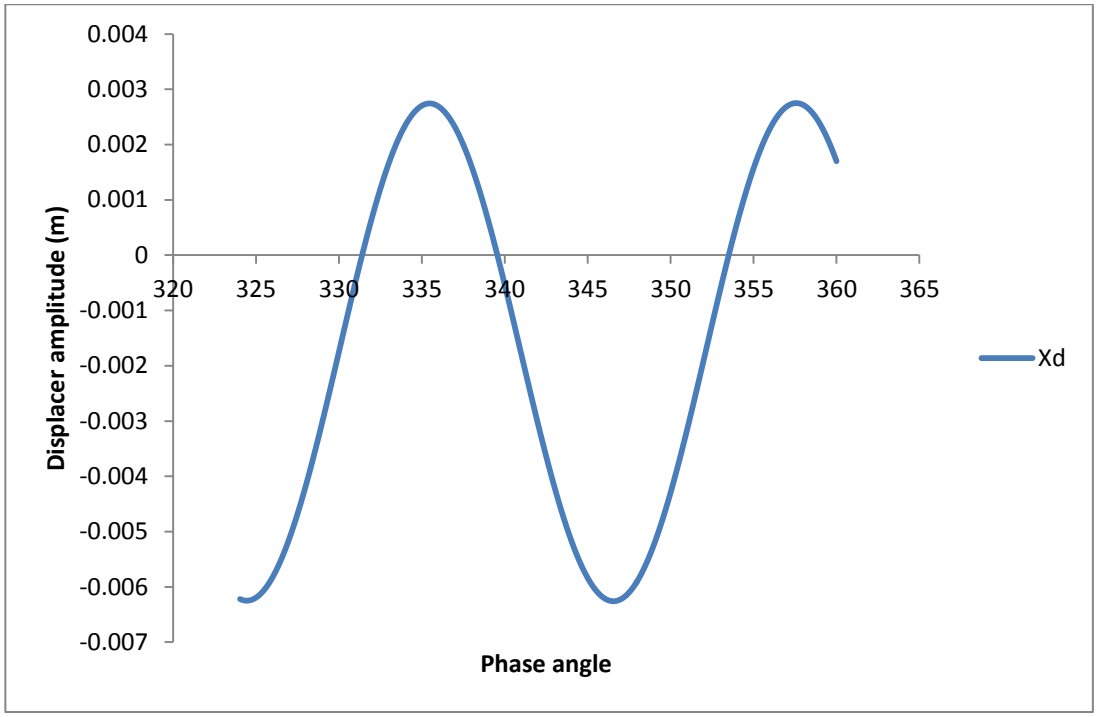

Figure 6.9: The displacement of displacer at an operating frequency of 30Hz.

.

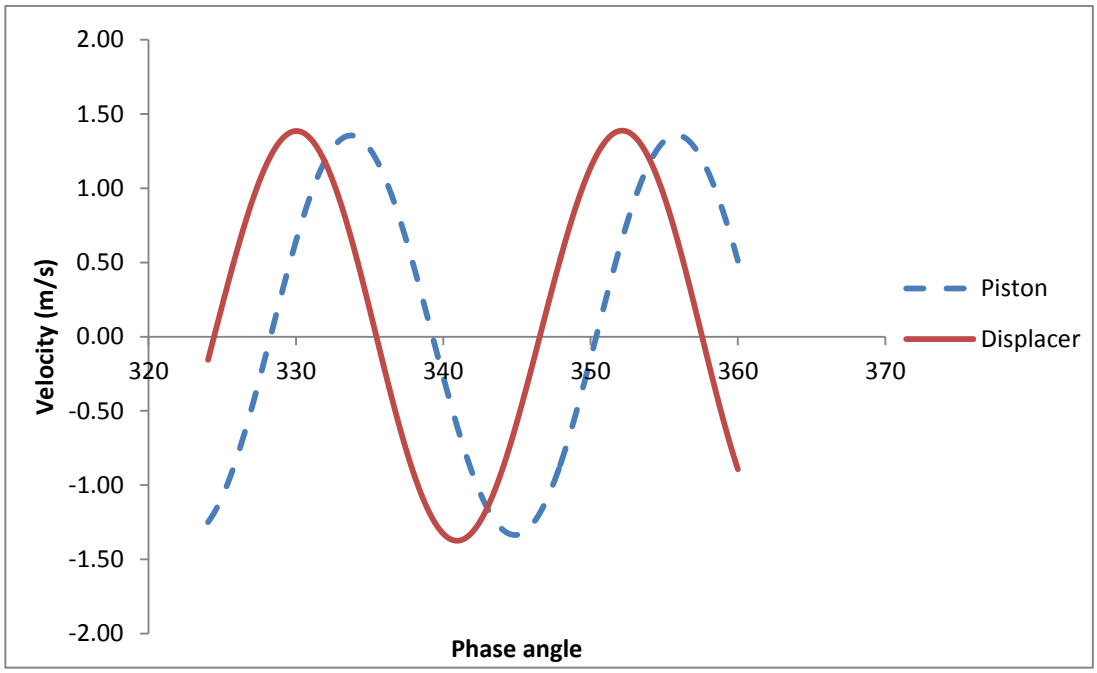

Figure 6.10: The velocity of the piston and displacer.

The mass flow rates of the working fuid in the heat exchangers is shown in Figure 6.1.1. It can be observed that the highest mass flow of the working fluid occurs from the compression space to the cooler which has the value of 0.03 (kg/s), whilst the lowest mass flow rate is observed from the heater to the expansion space.

The Figure 6.12 shows the pressure-total volume diagram for the free piston engine generating a power of 996 W.

The temperature variation in the heat exchangers is presented in Figure 6.13. Temperature levels in the heater and cooler can be observed. The tenth part of the regenerator which is closest to the heater has the temperature at about 770 K, whilst the first part of the regenerator closest to the cooler has the temperature of about 390 K. Also the matrix of the regenerator exhibit similar trend in the temperature variation for the first and tenth part

respectively. Figure 6.14 shows the temperature variation in the expansion and compression spaces. The temperature in the expansion space varies between 760 K and 820 K whilst the temperature in the compression space varies between 320 and 340 K. The variation in the cyclic temperature in the expansion space has the mean value of 790 K which is less than the heater temperature of 814 K, whilst the mean temperature in the compression space is 330 K which is higher than the cooler temperature of 320 K.

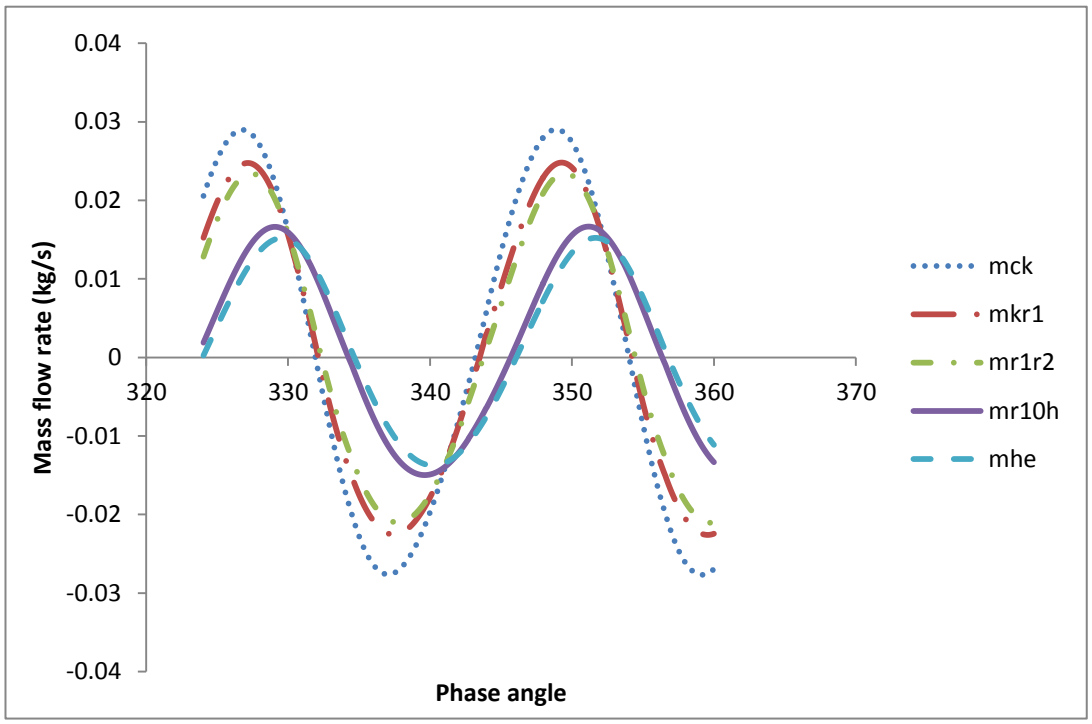

Figure 6.11: Mass flow rates of the working fluid in the heat exchangers.

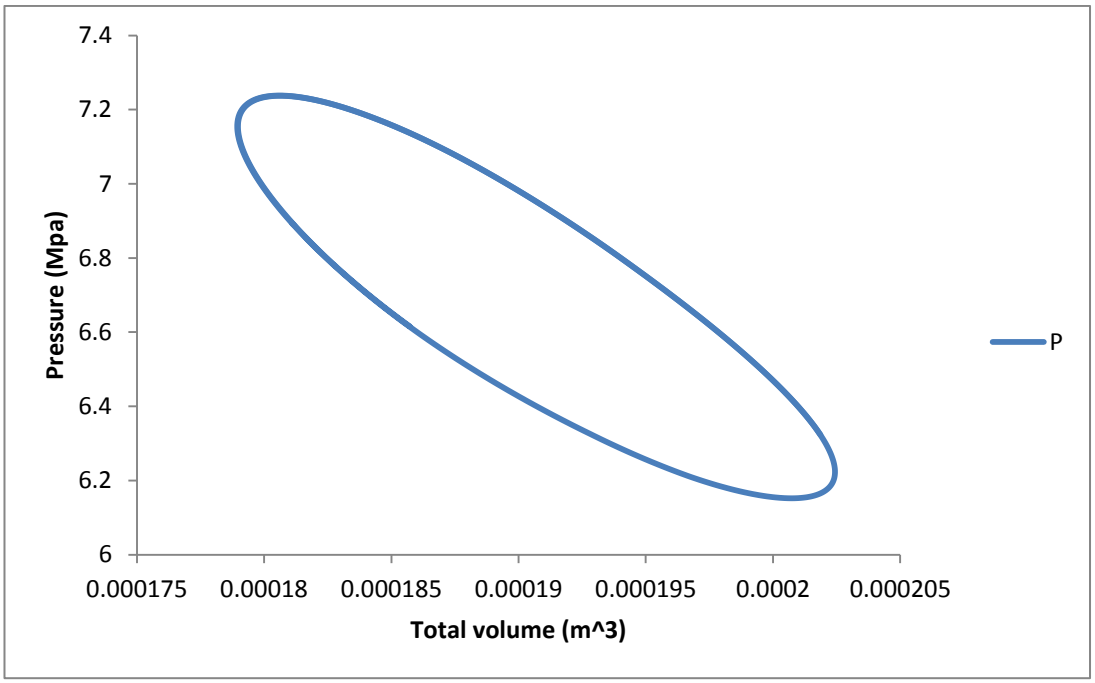

Figure 6.12 The Pressure–total volume diagram.

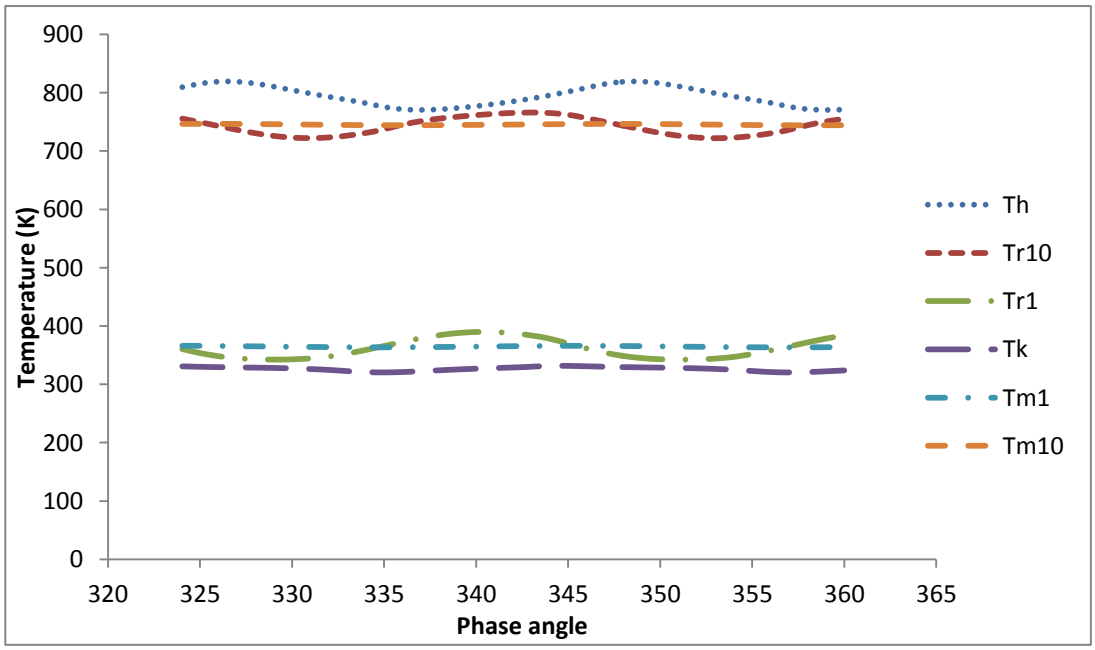

Figure 6.13: Temperature variations in the heat exchangers, the first and tenth parts of the regenerator matrix.

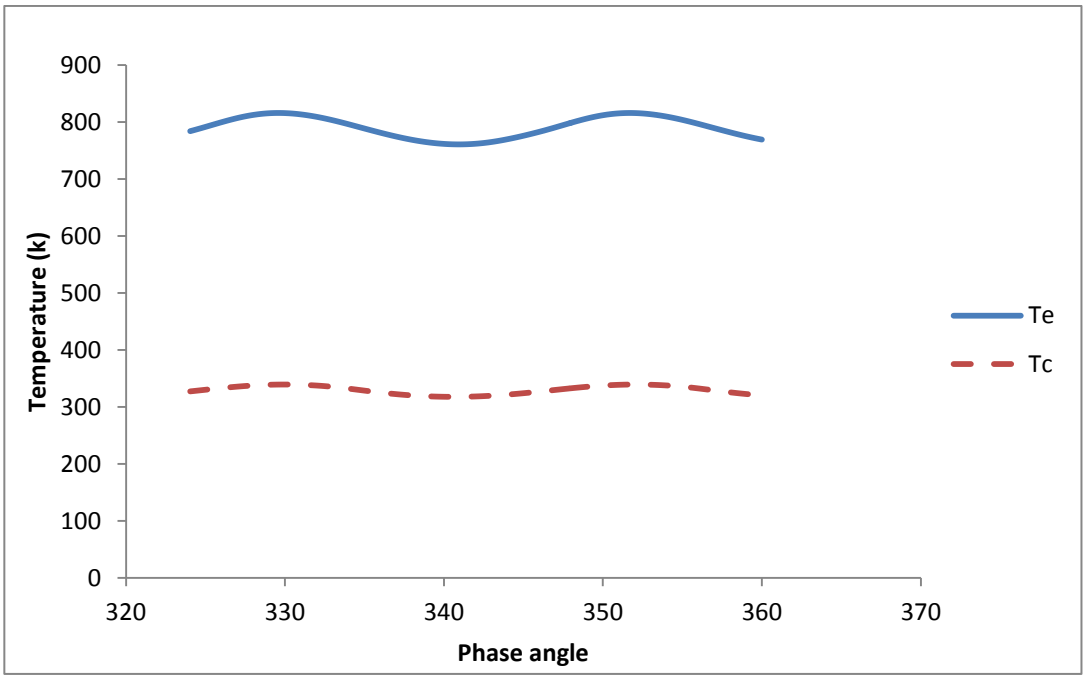

Figure 6.14: Temperature variations in the expansion and compression spaces.

Figure 6.15 illustrates the variation in Reynolds number which is the result of the flow pattern of the working fluid back and forth in the working spaces and heat exchangers. When the Reynolds number is lower than 2000 the flow is laminar and when the Reynolds number is greater than 2000 the flow is turbulent.

Figure 6.16 illustrates the variation of the bounce space pressure in the piston compartnent. The bounce space pressure varies between 6.995 MPa and 7.005 MPa which is on the average is equal to the mean working pressure in the engine. This satisfies the assumptions made in the development of Quasi steady flow model.

Figure 6.17 shows the variation in the masses of the working fluid in the work spaces and heat exchangers. The total amount of mass remains constant. The mass in the expansion space and other hot parts of the engine are lower due to higher temperatures.

Figure 6. 18 illustrates the variation in the internal heat conduction losses in the first, second, ninth and tenth part of the regenerator. The first and second part of the regenerator are closer to the cooler and have internal heat loss of 50 W and 31 W respectively whilst the ninth and tenth part of the regenerator, which are close to the heater have internal heat loss of 48 W and 30 W. This shows on the average the internal conduction loss in the regenrator chambers is constant.

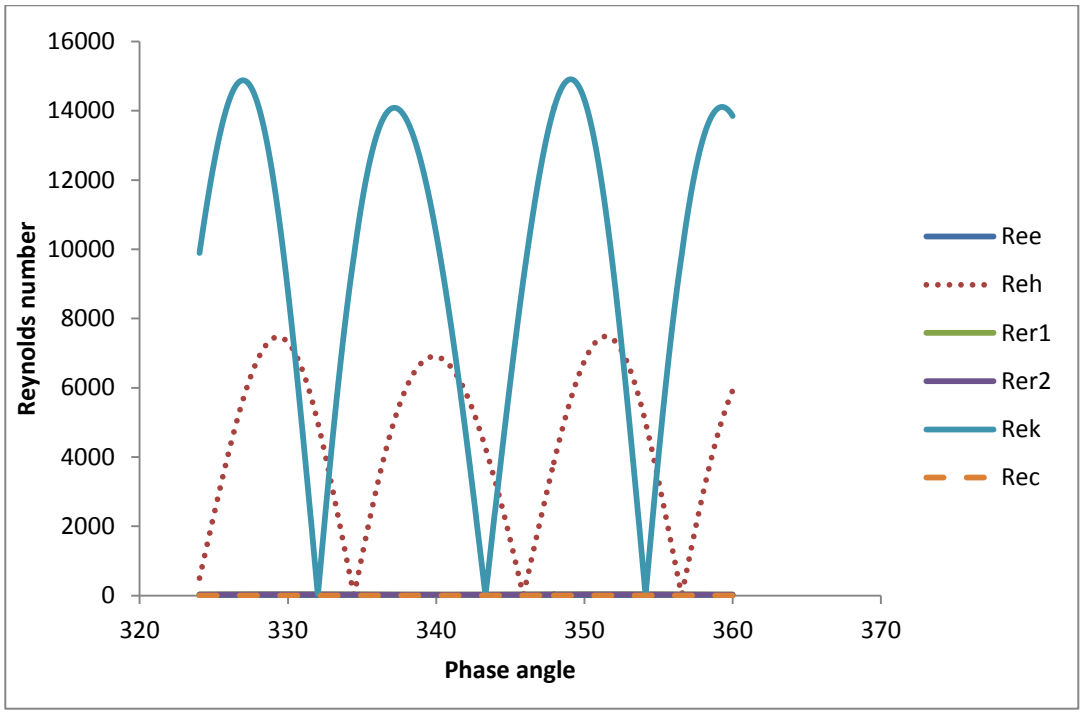

Figure 6.15: Reynolds number variations in the chambers of the engine.

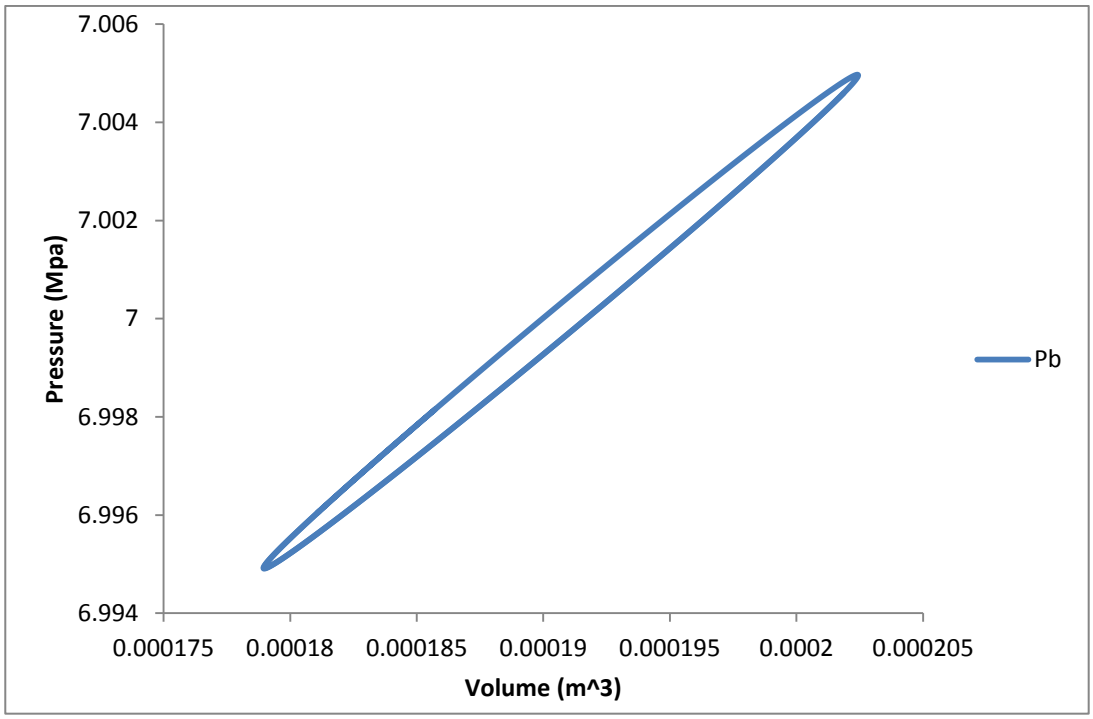

Figure 6.16: The bounce space pressure (buffer pressure) in the piston compartment.

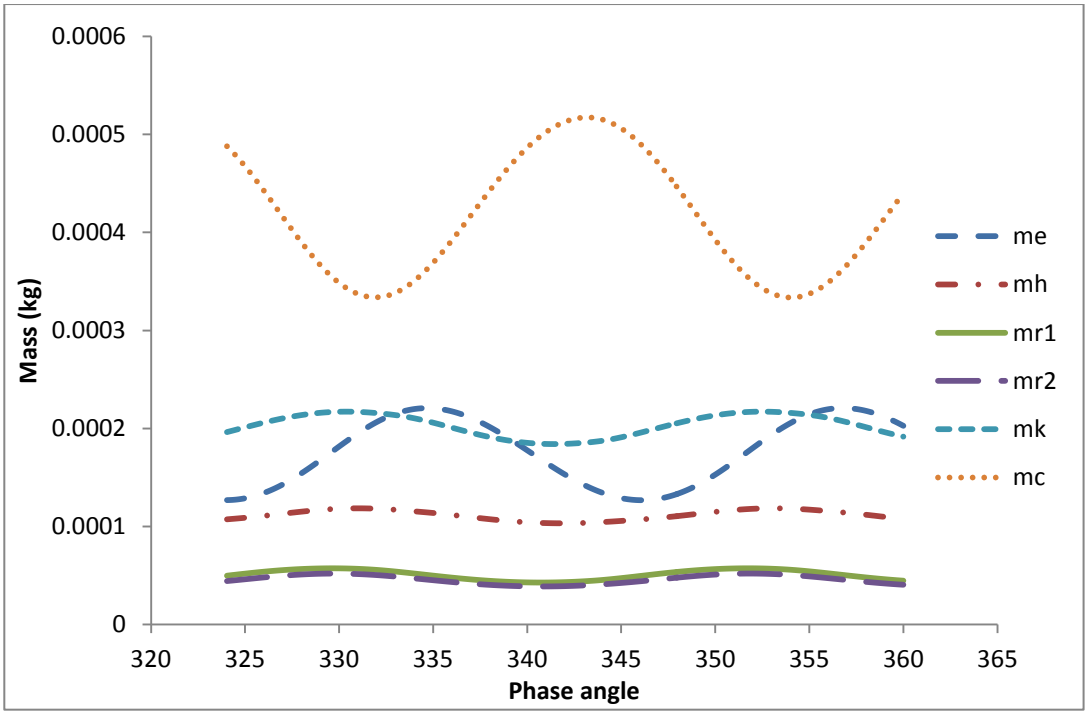

Figure 6.17: The mass of the working fluid in the heat exchangers and work spaces.

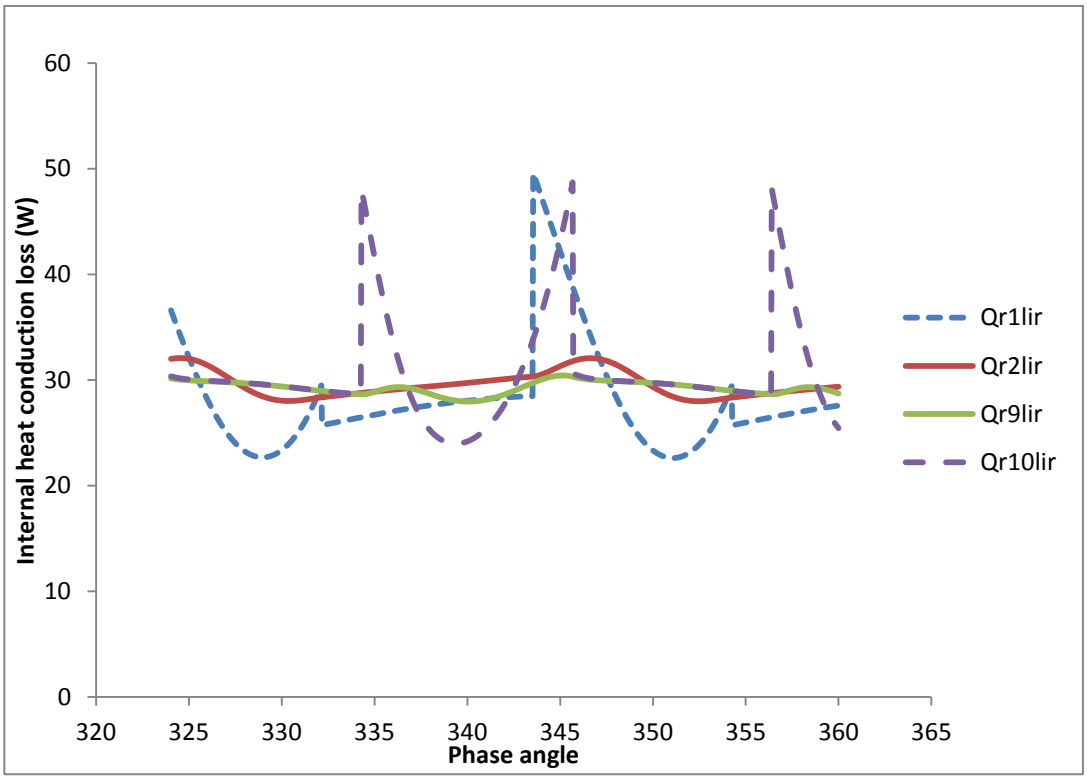

Figure 6.18: Internal heat conduction loss in parts of the regenerator.

Figure 6.19 illustrates the external heat loss by conduction in the first, second, ninth and tenth part of the regenerator to the suroundings as the working fluid flows through these sections. The first and second part of the regenerator which are close to the cooler have higher heat loss than the ninth and tenth parts (close to the heater) due to greater temperature difference. Figure 6.20 shows the variation in the pressure drops in the heat exchangers. The regenerator generates the greater pressure drop of 23,242 Pa than the heater and cooler with pressure drops of 11,016 Pa and 1,213 Pa .The maximum total pressrue drop is 35,471 Pa. The highest pressure drop occurs when the working fluid flows through the regenerator matrix. The power output of the free piston Stirlign engine is greatly affected by the hydraulic ressitance in the regenerator. Hence, the regenerator, heater and cooler shold be investigated and optimised for the better output performance of the whole engine.

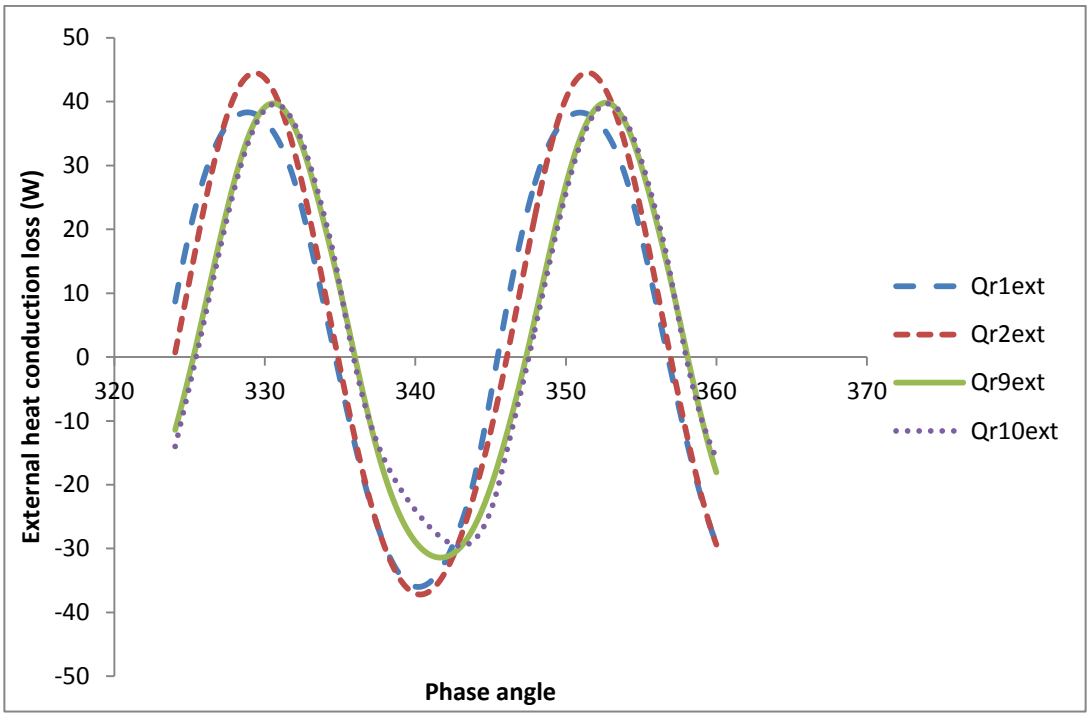

Figure 6.19: External heat conduction loss in parts of the regenerator.

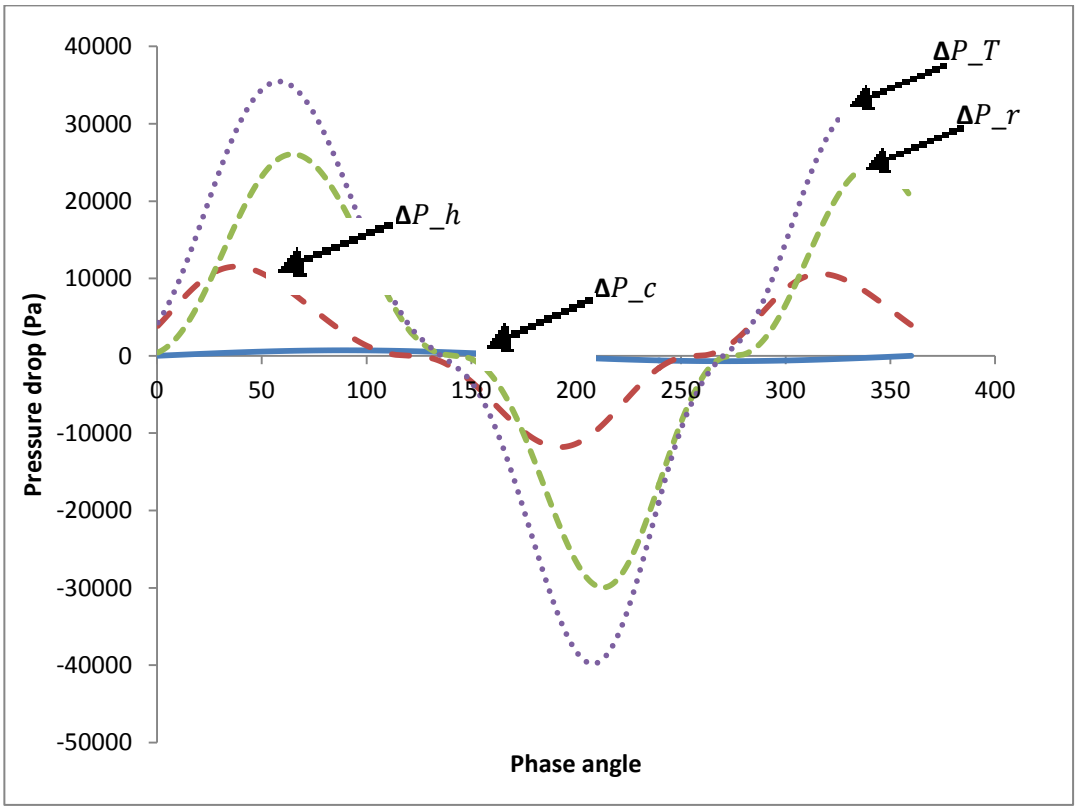

Figure 6.20: The pressure drops in the heat exchangers.

Finally, Figure 6.21 shows relative positions of the displacer and psiton in the engine during its opeation and it can be seen that these can be imporved in order to reduce dead volumes and this task also requires application of optimisation methods.

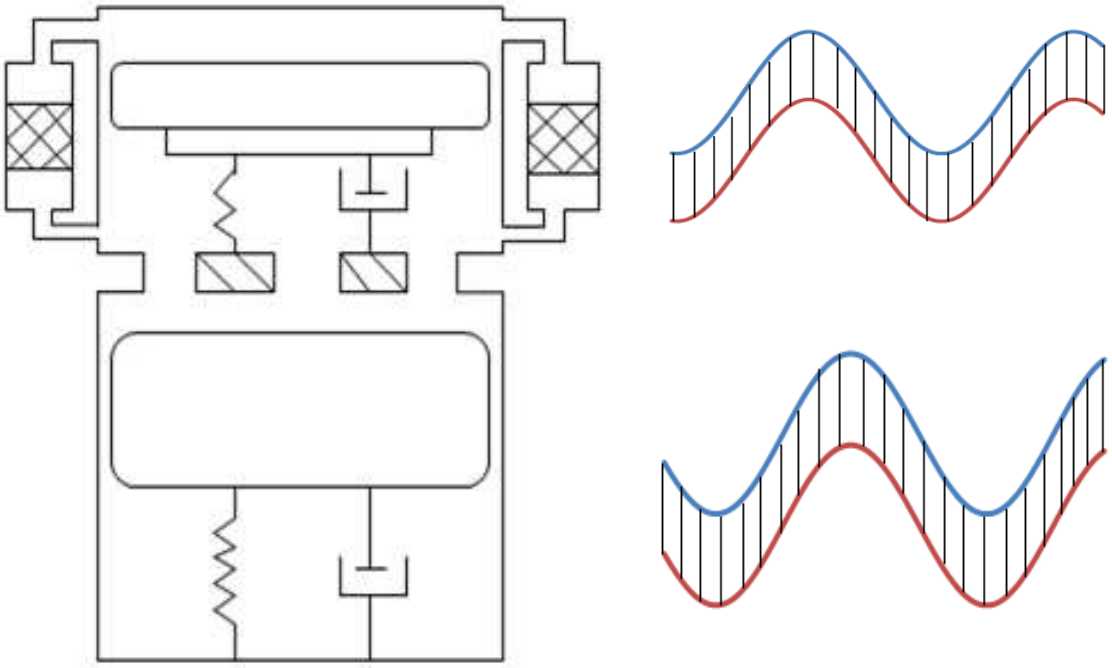

Figure 6.21 Relative positions of the piston and displacer in the engine during its operation.

6.2.5 Parametric Check

The changes in the values of parameters used in the developed second order Quasi steady model affected the calculated performance of the engine accordingly. The parameters that were altered for parametric check are the mean pressure, damping coefficient for the piston and displacer, and the heater temperature and the results obtained are shown.

Mean pressure check

The mean pressure value was altered in the model and the effect on the output power and dynamic pressure is shown in Table 6.1.

Table 6.1: The effects of mean pressure on the engine performance.

Mean pressure	70bar	72bar
Indicated power	996 W	1001 W
Dynamic pressure	7.2MPa	7.7MPa

Piston and displacer damping coeffcients

The piston and displacer damping coefficients were were altered in the model and the effect on the output power and piston displacements is shown in Table 6.2.

Table 6.2:The effects of damping coefficients on the engine performance.

Damping coefficient (Piston)	461.5Ns/m	500Ns/m
Damping coefficient (Displacer)	35.34Ns/m	70Ns/m
Indicated power	996W	778W

Temperature check

The heater temperature was altered in the model and the effect on the output power is shown in Table 6.3.

Table 6.3 The effects of heater temperature on the engine performance.

Temperature of heater (Th)	780K	800K
Indicated power	996W	1074 W

Table 6.1 shows that an increase in the mean pressure of the engine from 70bar to 72bar increases the dynamic pressure from 7.2MPa to 7.7MPa and the indicated power raises 996 W to 1.2kW. It is shown in Table 6.2 that the increase in the damping coefficient of the displacer and piston decreases the indicated power. It can be seen in Table 6.3 that the

increase in the heater temperature from 780K to 800K results in the increase in the indicated power. The change of the above parameters can be used to control the output power of the engine.

6.2.6 The model validation

The results of validation of the model using experimental data for the Sunpower RE-1000 FPSE is shown in Table 6.4

Table 6.4 Comparison of experimental data for the Sunpower RE-1000 FPSE and numerical results obtained using the developed model.

SUNPOWER RE-1000	EXPERIMENT	SIMULATION
Frequency	30Hz	30Hz
Output power	1000W	995.97W

The accuracy of predictions of the performance of the engine is improved and sufficiently high to be used in the design procedure of FPSEs.

6.3 Conclusions

The second order mathematical model based on the Quasi steady flow model of the free piston Stirling engine has been developed and its accuracy is sufficiently high for the model to be used in the designing process. This is due to the fact that the model takes into consideration various losses that occur during the operation of the engine and more accurately describes heat and mass transfer processes in the system. Further work will be carried out on the development of the engine design procedure by coupling the developed model to Genetic Algorithm method for rapid optimisation of the engine design parameters.

Chapter 7 The principles of Genetic Algorithm optimisation method

7.1 Introduction

The general principles of Genetic algorithm (GA) method employed to determine the optimal parameters of the design of the free piston Stirling engine are presented in this Chapter. The procedure for optimization using GA was applied using the Quasi steady flow model of the free piston Stirling engine. GA is selected for optimization procedure due to the advantages it possesses over other optimization methods (listed in this Chapter).

7.2 Genetic Algorithm

Genetic algorithm (GA) is a theoretical optimization method for solving constrained and unconstrained problems based on natural selection, which is a process that stimulates the biological evolution. The theory of Genetic algorithm was first published in 1975 by Holland and the method was successfully implemented by Goldberg in 1989. To produce a new population with better individuals, the Genetic Algorithm modifies population of individual solutions repeatedly. It operates with an initial random population using a stochastic operator to determine the global optimum for the solution to a given problem. The local optimum can be determined using other optimization methods like calculus based methods. GA possesses many advantages over other methods of optimization [119], which are:

- No requirements for derivative information in the GA procedure.
- GA can make use of both constrained and unconstrained variables.

- Large number of variables can be used.
- The objective function in GA can be either in the form of experimental or numerical data and also as an analytical function.
- GA has a time saving advantage when using parallel computing facilities.

The application of GA's procedure for optimization is presented as a natural selection process [120]. The initial population is formed by a random set of individuals called population. The solution to the problem is made up of each individuals or chromosomes that consist of various parameters. The fitness function is determined by the evaluation of each chromosome in the initial population. The fitness value is measured by the objective function. The procedure for selection is performed by using the fitness value ranking. To determine the parents for reproduction, the natural selection process is applied to attain the next generation in the natural process. The recombination of the cross over and mutation operations results in newly generated chromosomes called offsprings. The fitness evaluation is then implemented for the new population. This algorithm is employed to produce several generations until the solution obtained satisfies the termination condition.

7.3 Procedure for determining the optimal design parameters of free piston Stirling engines using genetic algorithm

The binary GA is the most frequently used where the variables are changed into bit numbers with the encoding process and reversed with the decoding process. Significant computation time is required for the encoding and decoding processes, if the binary GA consist of large number of variables in each chromosome.

The continuous or real value GA, where variables are denoted by single floating point numbers is employed in this study [119] in order to reduce computing time and avoid quantitative limitations. The flow chart of the continuous GA procedure for the determination of the optimal design parameters with the use of the Quasi steady model of the free piston Stirling engine is shown in the Figure 7.1.

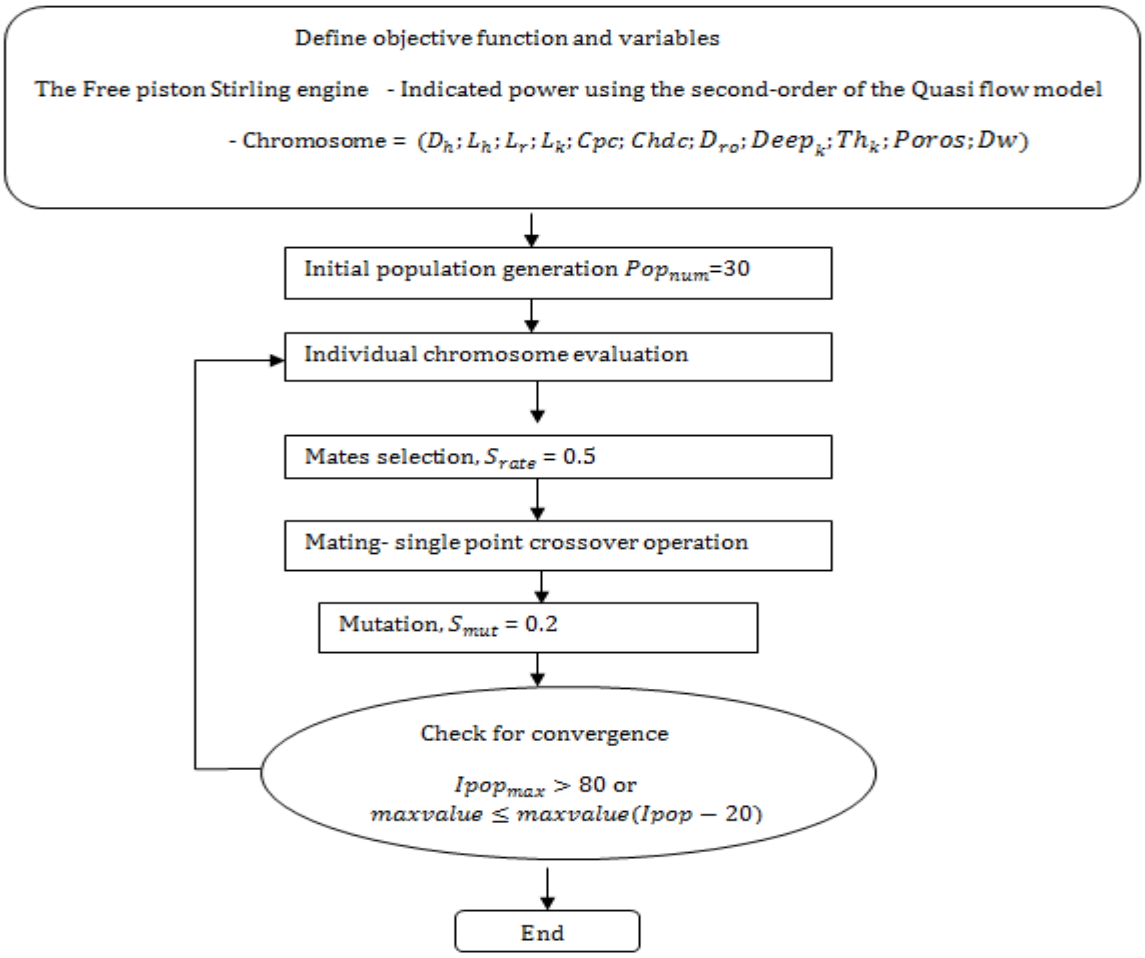

Figure 7.1: Flow chart of Genetic algorithm procedure.

7.3.1 Definition of variables and objective function

The optimization solution procedure uses a set of engine design parameters which form the vectors that represent the variables of GA in each chromosome of the population.

7.3.1.1 Definition of variables and objective function for achieving the optimal design of the free piston Stirling engine using the Quasi steady flow model

The numerical simulations of the free piston Stirling engine are performed for conditions similar to that in the experimental test of the RE-1000 free piston Stirling engine prototype. There is a number of constant parameters and few of such parameters are defined as chromosomes. These include porosity of regenerator matrix, wire diameter, piston and displacer damping coefficients, diameter of the heater tube, cooler and regenerator chamber and their corresponding lengths. The heat exchangers (heater, cooler and regenerator) of the free piston Stirling engine require a careful design, because they strongly influence the engine performance. The values of the dead volume in the expansion and compression spaces, heat transfer area and pressure drops also affect the performance of the engine and will be influenced by the change in geometry of the heat exchangers. The optimal design is focused on dimensions of the piston and displacer damping coefficients and heat exchangers. The chromosome is represented as

$$\text{Indicated power} = \text{f (Chromosome)} = \text{f}(D_h; L_h; L_r; L_k; Cpc; Chdc; D_{ro}; Deep_k; Th_k; Poros; Dw) \quad (7.1)$$

where D_h is the diameter of heater, L_h is the length of heater, L_r is the length of regenerator, L_k is the length of cooler, Cpc is the piston damping coefficient, $Chdc$ is the displacer damping coefficient, D_{ro} is the outside diameter of the regenerator chamber, $Deep_k$ is the depth of cooler slot, Th_k is the thickness of cooler slot, $Poros$ is the porosity of matrix in the regenerator and Dw is the wire diameter.

The constraints are the upper and lower boundaries for each variable and are defined as follows:

1. $0.001 < D_h < 0.007$ (m)
2. $0.2 < L_h < 0.8$ (m)
3. $0.01 < L_r < 0.15$ (m)
4. $0.01 < L_k < 0.1$ (m)
5. $100 < Cpc < 1000$ (Ns/m)
6. $100 < Chdc < 1000$ (Ns/m)
7. $0.01 < D_{ro} < 0.15$ (m)
8. $0.0015 < Deep_k < 0.0035$ (m)
9. $0.0002 < Th_k < 0.001$ (m)
10. $0.3 < Poros < 0.95$ (%)
11. $0.00004 < Dw < 0.001$ (m)

There is a need for a constraint function to be set for the variables based on the engine's prototype design. The indicated power is defined as a chromosome value, which is the performance parameter of the engine. The heat source for the engine might be solar energy hence, the efficiency is not required to be a primary parameter. As mentioned above, the developed second order mathematical model on the basis of the Quasi model of the RE-1000 free piston Stirling engine is employed to determine the value of the indicated power.

Initial population generation

The set of design parameters which is used as the initial population is determined in an absolute random manner and produces a matrix formation of various chromosomes.

$$\text{Population} = \text{rand}\ (Pop_{num};\ Var_{num}) \tag{7.2}$$

where Pop_{num} is the number of chromosomes and Var_{num} is the number of variables.

The population size strongly affects the convergence speed of the solution to the optimization problem, hence this should be carefully defined. When using GA optimization, the recommended number of chromosomes is between 30 and 100 [121]. The chromosome number (Pop_{num}) used in the optimisation procedure is 30 per generation.

Evaluation

The developed Quasi steady flow second order mathematical model of the free piston Stirling engine is used to determine the indicated power. The indicated power which is the chromosome value is evaluated by the fitness function. The fitness value is then determined and ranked in the value map for each generation [122]:

$$\text{Fitness value} = \frac{1}{(1+\max_{value} - value)} \tag{7.3}$$

where max_{value} is the maximum value of chromosome and $value$ is the value of chromosome.

Selection procedure

To determine the survival chromosomes and produce a new generation, the fitness value of each of the chromosome is arranged in descending order:

$$N_{sc} = S_{rate} Pop_{num} \tag{7.4}$$

where N_{sc} is the number of survival chromosomes and S_{rate} is the selection rate of 0.5.

The best chromosomes which are the fittest in the ranking list are selected randomly. The procedure of the random pairing selection for the parents of the reproduction operation employs the rank weighting technique [123].

Procedure for Mating

The process which the operator for reproduction uses parents to generate offsprings for the next generation is called mating. The crossover is the easiest operator in the mating process. The operator with the random position which is used on chromosome parents for new offspring generation is called the single point crossover. The operator selects randomly from the design parameters on different sides from the crossover point between two parents to generate new chromosomes.

Procedure of mutation

Global solution is always the objective in the optimization procedure, but if a rapid convergence occurs then the solution obtained might be a localised minimum or maximum solution. Hence, mutation is the second operator of reproduction process used to avoid finding only local solutions in the optimisation problems. Mutation introduces the random selection of variables to change the value of some certain parameters in the chromosome. Mutation rate of 0.2 is used in this study though it slows down the convergence process. This value is used to ensure that the global solution is obtained [119].

Check for convergence

Convergence is used to determine if the termination condition of a numerical calculation is met. The first number of generations is examined first. In this computation process the maximum number of generations is set at 80 to ensure that the convergence in this algorithm is achieved. The fixed small differences in the values of the indicated power of the free piston Stirling engine for the last twenty generations is used to terminate the numerical calculations before the maximum number of generations is attained in the computing process. If the solution process achieves no convergence, the fitness selection

process is then employed to form population of chromosomes for a new generation. In this study the optimization code was developed by modifying a simple continuous GA code as given in [123].

Chapter 8 Optimization of the of the free piston Stirling engine

8.1 Introduction

The results obtained from the optimization of the RE-1000 free piston Stirling engine are presented in this Chapter. The working process of the engine is simulated using the developed second order Quasi steady state flow model of the free piston Stirling engine, which was validated in the Chapter 6. The numerical results obtained from the optimisation calculations are analysed and discussed in details.

8.2 Results obtained using the developed second order Quasi steady flow model

The working process of the RE-1000 free piston Stirling engine was simulated numerically using the developed second order Quasi steady flow mathematical model, described in Chapter 6.

The geometry and parameters of the engine which were used as input data for the numerical simulations are presented in Table 5.1. The experimental test results for the engine were presented and discussed in [97]. The results obtained from the numerical simulations were compared with data from the experimental tests and these two sets of data are in very good agreement.

8.2.1 Validation of the developed second order mathematical models of the free piston Stirling engine

The comparison between the numerical results obtained from the second order simulations using the adiabatic and Quasi steady flow model with the experimental data obtained from [97] of the free piston Stirling engine is presented and analysed.

The power outputs calculated using the developed second order of the adiabatic and Quasi steady models are compared to the experimental test results in Table 8.1.

Table 8.1: Comparison of the experimental and theoretical results on the FPSE power production.

Output Results	Experiment	Second order adiabatic model	Second order Quasi steady model
Output Power (W)	1,000	862	996

The second order Quasi model predicts the output power of 996 W, which is more accurate than that produced by the developed second order adiabatic model (862 W). The error of prediction of the output power is 13.8 % for the adiabatic model while for Quasi steady flow model this value is about 0.4% which is consistent with other studies in the second order mathematical modelling of the FPSE, namely [4] and [65] . From the numerical simulations of the RE-1000 FPSE developed by Tew, the accuracies of 10.4% and 13.8% were presented from the unconstrained and constrained second order models which did not consider the thermal and dynamic losses [65]**.** The gas hysteresis losses were also not accounted for in these models. As stated by Urieli and Berchowitz in [97], the heat

transfer between the cylinder wall and the working fluid in the compression space of the piston compartment is the gas hysteresis loss. Figures 8.1 and 8.2 show the comparison of predictions by the second order adiabatic and Quasi steady flow modelling. Figure 8.1 shows the pressure variation of the working fluid in the FPSE obtained using the adiabatic and Quasi steady models. It can be observed that the maximum pressure and its amplitude obtained using the adiabatic model is greater than those predicted by the Quasi steady flow model. The low magnitude of the pressure predicted by the Quasi steady model is a result of taking into account various losses in the cycle. The same tendency can be seen in Figure 8.3 which shows the temperature variations in the expansion and compression spaces.

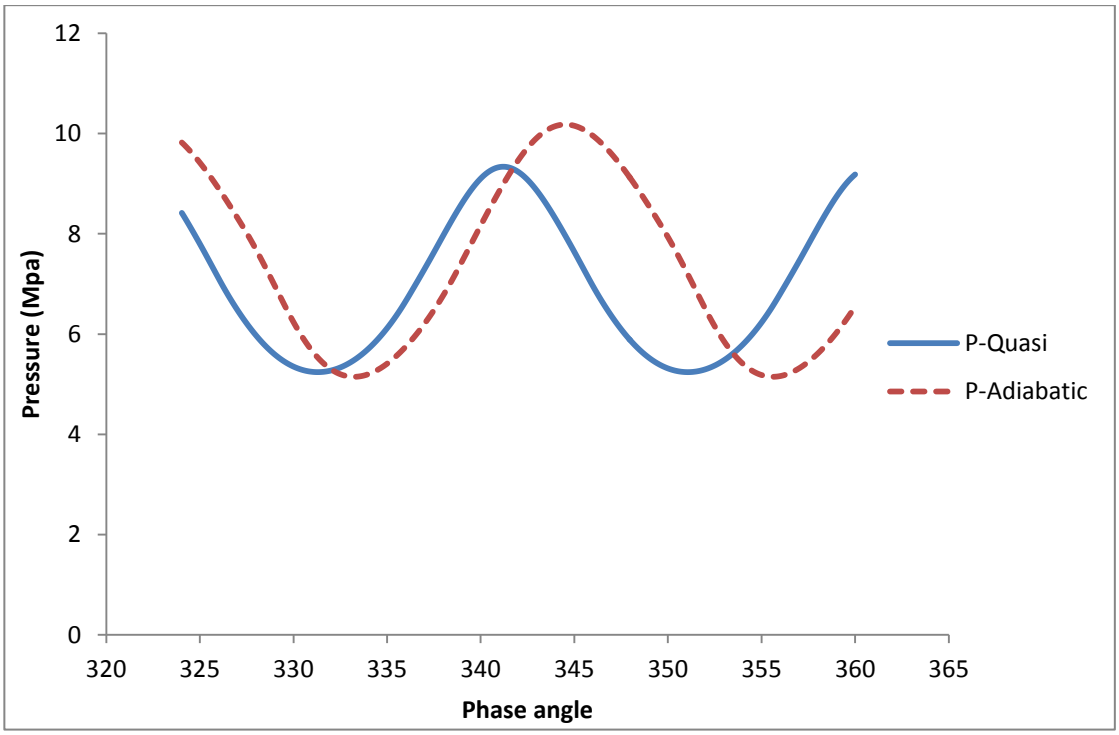

Figure 8.1: Comparison of the pressure variation in FPSE obtained using the developed Quasi steady flow and adiabatic models.

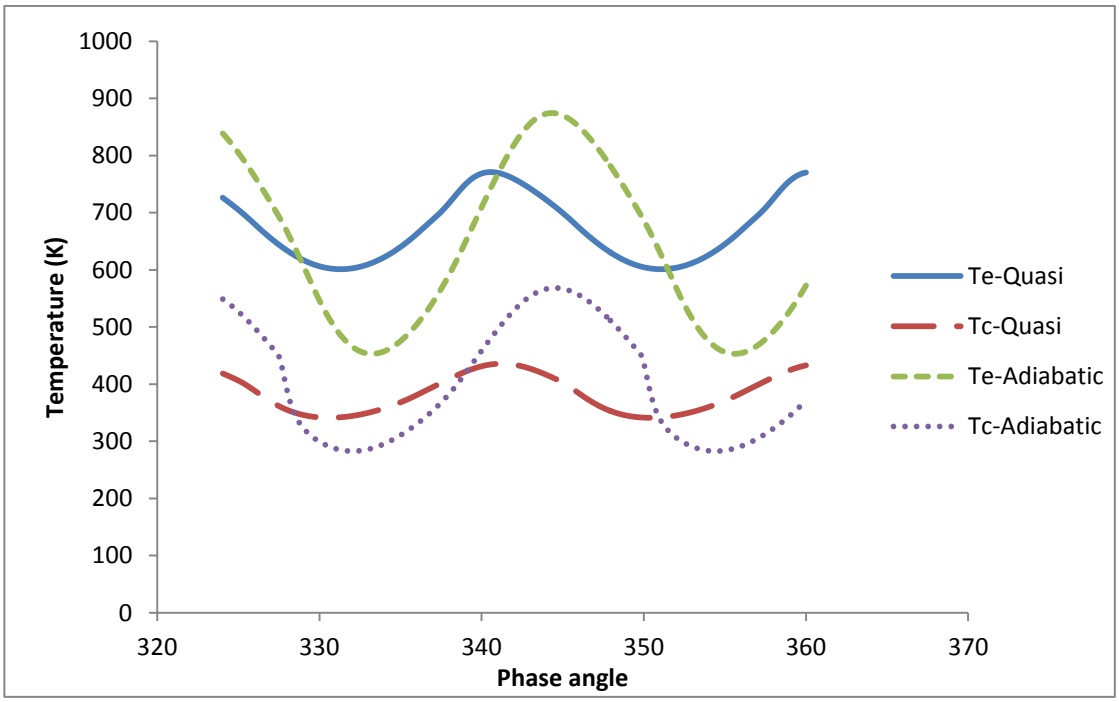

Figure 8.2: Comparison of the temperature variations in the expansion and compression spaces obtained using the developed Quasi steady flow and adiabatic models.

8.2.2 Optimization of the design parameters of the RE-1000 Free Piston Stirling engine

The optimization of the design parameters of the RE-1000 free piston Stirling engine using the GA optimization code coupled with the second order Quasi steady flow model has been carried out. The objective of the optimization is to maximize the indicated power of the FPSE by selecting the optimal set of deign parameters with their values ranging in the diapasons constrained within the upper and lower limits.

Figure 8.3 presents the graph of the change in the value of the engine's indicated power as function of generations. It can be observed that the indicated power rapidly increased for the first number of generations and then rises gradually until the termination condition was met.

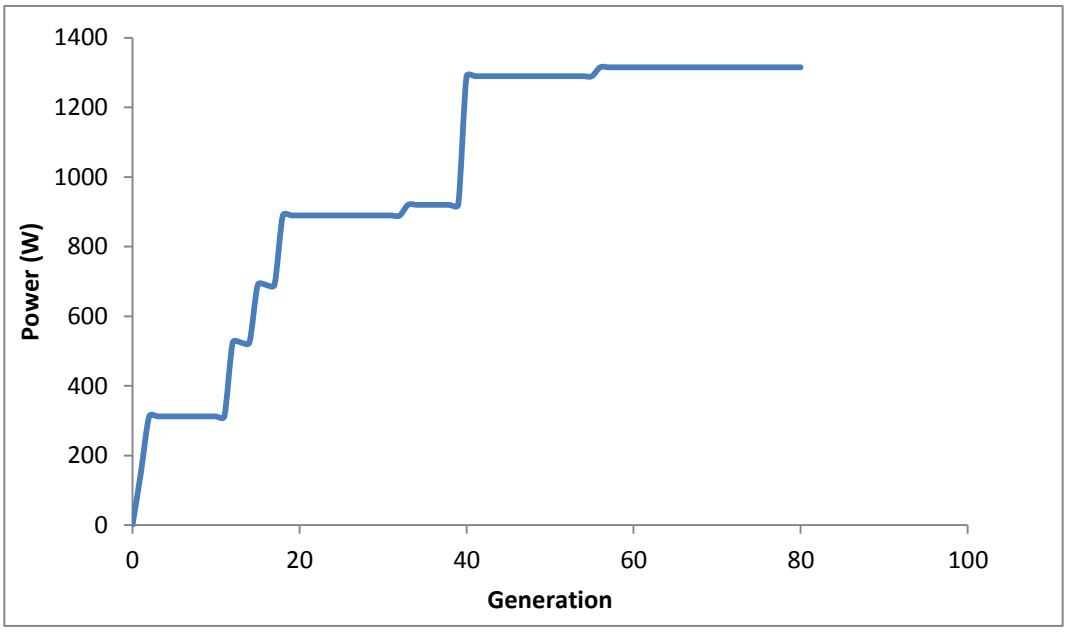

Figure 8.3 Optimal value of Output Power for each generation.

The maximum indicated power of 1360W was obtained at the 80th generation of design parameters and Table 8.2 shows the values of design parameters providing such the improvement. The GA optimization was performed with a selection rate of 0.5 and mutation rate of 0.2 with a population size of 30. The increase in the power output is a result of increase of amplitudes of piston oscillations, reduction of the dead volume in the engine, especially of the cooler, and increase of heat transfer area of heater and regenerator.

Table 8.2: The set of design parameters obtained from GA optimisation procedure.

Engine Parameter	Parameters of the original RE-1000 free piston Stirling engine	Optimal engine parameters
The length of cooler	0.0792 m	0.068 m
length of regenerator	0.065 m	0.013 m
diameter of heater	0.002362 m	0.0029 m
length of heater	0.1834 m	0.3 m
piston damping	461.5 Ns/m	800 Ns/m
displacer damping	85.34 Ns/m	200 Ns/m
outside diameter of the regenerator chamber	0.0718 m	0.12 m
depth of cooler slot	0.00376 m	0.0028 m
thickness of cooler slot	0.000508 m	0.0008 m
porosity of matrix in regenerator	0.759	0.68
wire diameter	0.0000889 m	0.00072 m

8.3 Conclusion

The GA optimisation procedure has been developed on the basis of the second order Quasi steady flow model of the working process of the RE-1000 FPSE to define its optimal set of design parameters which provides a considerable increase of the power output of the engine.

Chapter 9 Conclusions and recommendations for future work

9.1 Introduction

This chapter presents the main conclusions from the study carried out in this research and the recommendations for future work.

9.2 Conclusions from the study on the development of the isothermal model of the free piston Stirling engine

The developed isothermal mathematical model of free piston Stirling engines in this study was applied to calculate the Beta and Gamma configurations of free piston Stirling engines. This was done by coupling of the isothermal model of the working process of Stirling engine and dynamics of two separate mass-spring oscillating systems. The approach demonstrated that it can be used to produce feasible preliminary values of design parameters of the engine which then can be rectified with deployment of more complex modelling and optimisation methods.

9.2.1 Conclusions from the research on the development of the adiabatic model of the free piston Stirling engine

The developed second order adiabatic mathematical model of the free piston Stirling engine is a coupling of the system of differential equations, describing the working process of the engine, and differential equations describing the dynamics of pistons. The major assumption was that processes of expansion and compression of the working fluid in the working spaces of the engine are adiabatic. Various heat losses, taking place in the engine's operation were not taken into account during the modelling process and therefore the accuracy of perditions of the engine performance was about 15%.

9.2.2 Conclusions from the research on the development of the quasi steady flow model of the free piston Stirling engine and its GA optimisation procedure

The developed second order quasi steady mathematical model of the free piston Stirling engine is an advanced approach to numerical simulations of the operation of the engine.

The model provides results on the oscillations of the pistons, variations of the pressure, temperatures, working fluid mass flows, heat flow rates and losses taking place in the engine. The engine is split into a larger number of control volumes, in which heat transfer between the working fluid and chamber walls is taken into account. Variation of temperatures of chambers is also taken into account. The model allows to take into account a wide range of various losses and this provides a high accuracy of prediction of the engine performance (typically on the level of few percent).

The GA optimization code coupled to the second order quasi steady flow mathematical model of the FPSE was developed and used for finding the set of optimal design parameters of the RE-1000 FPSE to significantly increase the power output of the engine. The developed approach can be used in practical engineering activities when designing the FPSE engine for various applications.

9.3 Recommendations for future work

- To improve further accuracy of the developed approach in prediction of engine performance it is recommended to investigate applicability of various published correlations on heat transfer and hydraulic resistance in channels of Stirling engines and on hysteresis losses in FPSEs.
- It is also recommended to validate the developed models using experimental information which becomes available for other types of FPSEs.
- Finally, it is recommended to extend the developed GA optimisation approach for solving multi-objective problems, such as optimisation in terms of both power output and efficiency.

References

[1] M. D. d'Accadia, M. Sasso, S. Sibilio, and L. Vanoli, "Micro-combined heat and power in residential and light commercial applications," *Applied Thermal Engineering,* vol. 23, pp. 1247-1259, Jul 2003.

[2] J. Boucher, F. Lanzetta, and P. Nika, "Optimization of a dual free piston Stirling engine," *Applied Thermal Engineering,* vol. 27, pp. 802-811, Mar 2007.

[3] J. Jackson, "Ensuring emergency power for critical municipal services with natural gas-fired combined heat and power (CHP) systems: A cost-benefit analysis of a preemptive strategy," *Energy Policy,* vol. 35, pp. 5931-5937, Nov 2007.

[4] I. Urieli, D. Berchowitz, "Stirling Cycle Engine Analysis - Urieli,I, Berchowitz,D," *Alternative Sources of Energy,* pp. 71-71, 1984.

[5] H. W. Brandhorst Jr., "Free-Piston Stirling Convertor Technology for Military and Space Applications.," 2007.

[6] G. Chicco, Mancarella, P, "Performance evaluation of cogeneration systems:an Approach Based on Incremental Indicators," *Proceedings of the 6th WSEAS International Conference on Power Systems,,* pp. pp 34 - 39., (2006).

[7] G. Pivec, L. Eisner, and D. Kralj, "Optimization supplying of electricity and heat energy - An aspect of sustainability in the Hospital Maribor," *Lecture Notes on Energy and Environment,* pp. 111-115, 2007.

[8] Woodbank Communications Ltd, "Energy Conversion and Heat Engines," 2005.

[9] E. D. Rogdakis, N. A. Bormpilas, and I. K. Koniakos, "A thermodynamic study for the optimization of stable operation of free piston Stirling engines," *Energy Conversion and Management,* vol. 45, pp. 575-593, Mar 2004.

[10] F. Formosa, "Nonlinear dynamics analysis of a membrane Stirling engine: Starting and stable operation," *Journal of Sound and Vibration,* vol. 326, pp. 794-808, Oct 9 2009.

[11] F. de Monte and G. Benvenuto, "Reflections on free-piston Stirling engines, part 2: Stable operation," *Journal of Propulsion and Power,* vol. 14, pp. 509-518, Jul-Aug 1998.

[12] F. de Monte and G. Benvenuto, "Reflections on free-piston Stirling engines, part 1: Cyclic steady operation," *Journal of Propulsion and Power,* vol. 14, pp. 499-508, Jul-Aug 1998.

[13] G. Walker, "Stirling engines. ," 1980.

[14] R. S. Sanders, "Stirling engines for distributed low-cost solar-thermal-electric power generation," *Journal of Solar Energy Engineering-Transactions of the Asme,* vol. 133, p. 3, 2011.

[15] G. Walker, Fauvel G.R., Reader and E.R. Bingham, "The Stirling alternative," 1994.

[16] H.Yavuz. L. B. Erbay, "Analysis of the Stirling heat engine at maximum power conditions," *Energy,,* vol. 22(7), pp. 645-650., (1997) '.

[17] M. Feidt, Lesaos,K.,Costea,M and S. Petrescu, "Optimal allocation of HEX inventory associated with fixed power output or fixed heat transfer rate input," *International Journal of Applied Thermodynamics,,* vol. 5(1), pp. 25-36., (2002)

[18] Y. Timoumi, Tlili, I. and Ben, S., , "'Design and performance optimization of GPU-3 Stirling engines," *Energy,* vol. 33 (7), pp. . 1100–1114, (2008)

[19] Urieli,I, Berchowitz,D "Stirling Cycle Engine Analysis -," *Alternative Sources of Energy,* pp. 72, 1984.

[20] T. Finkelstein, "A new isothermal theory for Stirling machine analysis and a volume optimization using the concept of ‘ancillary’ and ‘tidal’ domains," *Proceedings of the Institution of Mechanical Engineers, Part C:Journal of Mechanical Engineering Science,,* vol., 212(3),, pp. 225-236, (1998).

[21] B. Kongtragool , S. Wongwises, "Thermodynamic analysis of a Stirling engine including dead volumes of hot space, cold space and regenerator," *Renewable Energy,* vol., 31, pp. . 345–359., (2006).

[22] G. Schmidt, "The theory of Lehmans calorimetric machine," vol. 15(1), 1871.

[23] N, Ulusoy, F. McCaughan, "Nonlinear analysis of free piston stirling engine/alternator system," *Proc 29th Intersoc Energy Convers Eng Conf,* pp. 1847–52, 1994.

[24] E. J. Kroliczek, Nikitkin, M. and Wolf, D. A. , (2010) Patent No. 7,708,053. Washington D.C. U.S. Patent and Trademark Office

[25] A. S. Abdurrahman, " Selection and experimental evaluation of low-cost porous materials for regenerator applications in thermo acoustic engines’, Materials & Design,," vol. 32(1), , (2011).

[26] S. Kaushik, S. Kumar, " Finite time thermodynamic analysis of endoreversible Stirling heat engine with regenerative losses.," *Energy,* vol. 25(10), pp. 989–1003, 2000.

[27] M. Costea, M. Feidt, "The effect of the overall heat transfer coefficient variation on the optimal distribution of the heat transfer surface conductance of area in a Stirling engine," *J Energy Convers Manage,* vol. 39(16–18), pp. 1753–61., 1998.

[28] R. W. Dyson, S.D. Wilson and R. C. Tew‘’, , "Review of computational Stirling analysis methods," *NASA.,* (2004)

[29] J.R. Senft, "A mathematical model for ringbom engine operation," *Gas Turbine Power* vol. 107, pp. 590–5, 1985;.

[30] A. J. Organ, " The regenerator and the stirling engine," 1997.

[31] M. Kuosa, J. Kaikko, and L. Koskelainen, "The impact of heat exchanger fouling on the optimum operation and maintenance of the Stirling engine," *Applied Thermal Engineering,* vol. 27(10), pp. 1671-1676., (2007)

[32] S. Petrescu, M. Costea, C, Harman and T. Florea, "Application of the direct method to irreversible Stirling cycles with finite speed," *International Journal of Energy Research,* vol. 26(7),, pp. 589-609., (2002).

[33] N. Domingo, "Comparative analysis of a stirling heat pump with the second and third order computer models,", 1985)

[34] B. M. Cullen, J. Petrescu, S and Feidt, M. , "Preliminary modelling results for an otto cycle/ Stirling hybrid-engine-based power generation system'," *Efficiency, Cost, Optimization Simulation and Environmental Impact of Energy Systems,,* 31 August to 3 September 2009 (2009).

[35] Y. Timoumi, I. Tlili, and S. Ben Nasrallah, "Design and performance optimization of GPU-3 Stirling engines," *Energy,* vol. 33, pp. 1100-1114, 2008.

[36] F. Wu, L. G. Chen, C. Wu, and F. G. Sun, "Optimum performance of irreversible stirling engine with imperfect regeneration," *Energy Conversion and Management,* vol. 39, pp. 727-732, Jun 1998.

[37] G. Popescu, V. Radcenco, M. Costea, and M. Feidt, "Optimisation thermodynamique en temps fini du moteur de Stirling endo- et exo-irréversible," *Revue Générale de Thermique,* vol. 35, pp. 656-661, 1996.

[38] B. Kongtragool and S. Wongwises, "Thermodynamic analysis of a Stirling engine including dead volumes of hot space, cold space and regenerator," *Renewable Energy,* vol. 31, pp. 345-359, 2006.

[39] T. Finkelstein, "Thermodynamic analysis of stirling engines. ," *Journal of spacecraft and rockets,* vol. 4(9), p. 1184, 1967.

[40] S. Schulz and F. Schwendig, "A general simulation model for stirling cycles," *Journal of Engineering for Gas Turbines and Power-Transactions of the Asme,* vol. 118, pp. 1-7, Jan 1996.

[41] H. Karabulut, F. Aksoy, and E. Öztürk, "Thermodynamic analysis of a type Stirling engine with a displacer driving mechanism by means of a lever," *Renewable Energy,* vol. 34, pp. 202-208, 2009.

[42] K. Mahkamov, "An axisymmetric computational fluid dynamics approach to the analysis of the working process of a solar Stirling engine," *Journal of Solar Energy Engineering-Transactions of the Asme,* vol. 128, pp. 45-53, Feb 2006.

[43] W. Reinalter, "Detailed performance analysis of a 10 kW dish/Stirling system.," *Journal of Solar Energy Engineering-Transactions of the ASME,* vol. 130(1). 2008;.

[44] S. K. Andersen, H. Carlsen, and P. G. Thomsen, "Control volume based modelling in one space dimension of oscillating, compressible flow in reciprocating machines," *Simulation Modelling Practice and Theory,* vol. 14, pp. 1073-1086, 2006.

[45] S. K. Andersen, P.G. Thomsen, "Numerical study on optimal Stirling engine regenerator matrix designs taking into account the effects of matrix temperature oscillations," *Energy Conversion and Management,* vol. 47, pp. 894-908, 2006.

[46] C.Cheng, Y. Yu, "Numerical model for predicting thermodynamic cycle and thermal efficiency of a beta-type Stirling engine with rhombic-drive mechanism " *Renewable energy,* vol. 35, pp. 2590-2601, 2010.

[47] K. Kawajiri, M. Fujiwara, and T. Suganami, "Analysis of Stirling engine performance," *IEEE,* 1989.

[48] J.A. Riofrio, K. Al-Dakkan, E. Mar, Hofacker, and E. J. Barth, "Control-Based Design of Free-Piston Stirling Engines," *American Control Conference,* June 11-13, 2008 2008.

[49] Fabien Formosaa L. G. Frechetteb. "Scaling laws for free piston Stirling engine design: Benefits and challenges of miniaturization," *Energy,* vol. 57, pp. 796 - 808, 2013.

[50] M. Costea, S. Petrescu, and C. Harman, "The effect of irreversibilities on solar Stirling engine cycle performance," *Energy Conversion and Management,* vol. 40, pp. 1723-1731, 1999.

[51] Z. Cun-quan, W. Yi-nong, J. Guo-lin, "Dynamic simulation of one-stage Oxford split-Stirling cryocooler and comparison with experiment Cryogenics," vol. 42 (2002), pp. 377–586.

[52] C. Cinar, S. Yucesu, T. Topgul, M. Okur, "Beta-type Stirling engine operating at atmospheric pressure," *Applied Energy,* vol. 81 (2005), pp. 351–357.

[53] N. Parlak, A. Wagner, M. Elsner, and H. S. Soyhan, "Thermodynamic analysis of a gamma type Stirling engine in non-ideal adiabatic conditions," *Renewable Energy,* vol. 34, pp. 266-273, 2009.

[54] Y. Timoumi, I. Tilli, S. B. Nasrallah, "Performance optimization of Stirling engines," *Renewable energy,* vol. 34, pp. 2134-2144, 2008.

[55] S. Abdullah, B. F. Yousif, K. Sopian, "Design consideration of low temperature differential double-acting Stirling engine for solar application," *Renewable Energy,* vol. 30, pp. 1923-1941, 2005.

[56] N. Martaj, P. Rochelle, "Exegetical analysis and design optimisation of the Stirling engine," *International Journal of Exergy,* vol. 3, pp. 45-67, 2006.

[57] P. C. T. de Boer., "Optimal regenerator performance in Stirling engines," *International Journal of Energy Research,* vol. 33, pp. 813-820, 2009.

[58] J. R. Senft, "Optimum Stirling engine geometry," *International Journal of Energy Research,* vol. 26(12), pp. 1087-1101., (2002)

[59] B. Cullen, J. McGovern, "Development of a theoretical decoupled Stirling cycle engine," *Simulation Modelling Practice and Theory,* vol. 19, pp. 1227-1234, 2011.

[60] B. Orunov, V. T. Krykov. A.P. Korobkov, K. Mahkamov, D. Djumanov, " The first stage of the development of a small Stirling tri-generation power unit," *Proceeding of 12th international Stirling engine conference,* pp. 416-423, 2005.

[61] J. Zarinchang, A.Yarmahmoudi "Optimization of Thermal Components in a Stirling Engine," *WSEA Transactions on Heat and Mass Transfer,* vol. 4, pp. 1-10, 2009.

[62] D.A. Blank, C. Wu, "Power optimization of an extra-terrestrial solar-radiant stirling heat engine," *Energy,* vol. 20, pp. 523-530, 1995.

[63] M. Costea, S. Petrescu. C. Harman, "The effect of irreversibilities on solar Stirling engine cycle performance," *Energy Conversion and Management,,* vol. 40, pp. 1723-1731, 1999.

[64] W. T. Beale, "Free piston Stirling- some model tests and simulation," *International Automotive Engineering Congress,* vol. 690230, January 13–17 1969.

[65] R. C. Tew, "Comparison of Free-Piston Stirling Engine Model Predictions with RE 1000 Engine Test Data," *Nineteenth Intersociety Energy Conversion Engineering Conference,* 1984.

[66] M. D. Kankam and J. S. Rauch, "Comparative Survey of Dynamic Analyses of Free-Piston Stirling Engines," *Proceedings of the 26th Intersociety Energy Conversion Engineering Conference, Vols 1-6,* pp. E314-E319, 1991.

[67] R. W. Redlich and D. M. Berchowitz, "Linear Dynamics of Free-Piston Stirling Engines," *Proceedings of the Institution of Mechanical Engineers Part a-Journal of Power and Energy,* vol. 199, pp. 203-213, 1985.

[68] F. Choudhary, " Dynamics of Free Piston Stirling Engines," (2009).

[69] F. Formosa and G. Despesse, "Analytical model for Stirling cycle machine design," *Energy Conversion and Management,* vol. 51, pp. 1855-1863, 2010.

[70] . S. Kim, J. Huth, J.G. Wood, "Performance characterization of sunpower free-piston Stirling engine," *International Energy Conversion Engineerung Conference,* 2005.

[71] J.G. Wood, N. Lane, "Advanced 35 W Free-Piston Striling Engine for Space Power Applications," *American Institute of Physics,* 2003.

[72] N. H. Beachley, F.J. Fronczak, "Design of a free-piston engine-pump,", *International off-highway and powerplant congress and exposition,* p. 921740., 1992.

[73] T.G. McGee, J. W. Raade, H. Kazerooni, "Monopropellant-driven free piston hydraulic pump for mobile robotic systems," *Journal of Dynamic Systems, Measurement and Control,* vol. 126 (1), pp. 75–81, (2004).

[74] G. Benvenuto, and F. de Monte, " Analysis of Free-Piston StirlingEngines/Linear Alternator Systems Part 1," *Theory.Journal of Propulsion and Power,* vol. 11: , pp. 1036-1046, (1995).

[75] G. Benvenuto, F. De Monte F. Farina, "Study of the response to load variation of a free-piston Stirling engine," *IECEC '91; Proceedings of the 26th Intersociety Energy Conversion Engineering Conference,* vol. 5, pp. pp. 337 - 342 1991.

[76] G. Benvenuto, F. Demonte, and F. Farina, "Dynamic Behavior Prediction of Free-Piston Stirling Engines," *Proceedings of the 25th Intersociety Energy Conversion Engineering Conference, Vols 1-6,* pp. 346-351, 1990.

[77] R.W. Dyson, S. D. Wilson, R.C. Tew. , "Review of Computational Stirling Analysis Methods.," *Proceedings of 2nd International Energy Conversion Engineering Conference,,* pp. 1 - 21, 2004.

[78] S. K. Anderson, "Numerical Simulation of Cyclic Thermodynamic Processes," 2006.

[79] S. K. Andersen, H. Carlsen. P.G. Thomsen, "Control volume based modelling in one space dimension of oscillating, compressible flow in reciprocating machines," *Simulation Modelling Practice and Theory,,* vol. 14, pp. 1073-1086., 2006.

[80] N. Martaj, L. Grosu, P. Rochelle, " Exergetical analysis and design optimisation of the Stirling engine," *International Journal of Exergy,* vol. 3 pp. 45-67, 2006.

[81] J. R. Senft., "Optimum Stirling engine geometry.," *International Journal of Energy Research,* vol. 26, pp. 1087-1101, 2002.

[82] R. Shoureshi, "General Method for Optimization of Stirling Engine," *Seventeenth intersociety energy conversion engineering conference,* vol. 829279, pp. 1688–93, 1982.

[83] W. Beale, " Stirling cycle type thermal device," 1971.

[84] R. G. Lange and W. P. Carroll, "Review of recent advances of radioisotope power systems," *Energy Conversion and Management,* vol. 49, pp. 393-401, 2008.

[85] G. R. Schmidt, D. H. Manzella, H. Kamhawi, T. Kremic, S. R. Oleson, J. W. Dankanich, and L. A. Dudzinski, "Radioisotope electric propulsion (REP): A near-term approach to nuclear propulsion," *Acta Astronautica,* vol. 66, pp. 501-507, 2010.

[86] D. Berchowitz , " Operational characteristics of free-piston stirling engines," *Proceedings of the 23rd intersociety energy conversion engineering,* 1988.

[87] S.T. Hsu, F. Y. Lin, J.S. Chiou, " Heat-transfer aspects of Stirling power generation using incinerator waste energy," *Renewable Energy,* vol. 28, pp. 59-69, 2003.

[88] Y.C. Hsieh, T. C. Hsu, J.S. Chiou, " Integration of a free-piston Stirling engine and a moving grate incinerator," *Renewable Energy,* vol. 33, pp. 48-54, 2008.

[89] A. Homaifar, H. Y. Lai, E. McCormick, "System optimization of turbofan engines using genetic algorithms," *Applied Mathematical Modelling,* vol. 18, pp. 72-83., 1994.

[90] U. Kesgin, "Genetic algorithm and artificial neural network for engine optimisation of efficiency and NOx emission," *Fuel,* vol. 83, pp. 885-895, 2004.

[91] M.C. Tayal, Y. Fu, U.M. Diwekar, "Optimal Design of Heat Exchangers: A Genetic Algorithm Framework," *Industrial & Engineering Chemistry Research,* vol. 38, pp. 456-467, 1998.

[92] M. Mohagheghi, J. Shayegan, " Thermodynamic optimization of design variables and heat exchangers layout in HRSGs for CCGT using genetic algorithm," *Applied Thermal Engineering,* vol. 29 pp. 290-299, 2009.

[93] J.M. Ponce-Ortega, M. Serna-Gonzalez, A. Jiménez-Gutiérrez., "Use of genetic algorithms for the optimal design of shell-and-tube heat exchangers," *Applied Thermal Engineering,* vol. 29 pp. 203-209, 2009.

[94] K. Kraitong, "Numerical Modelling and Design Optimisation of Stirling Engines for Power Production," *Doctoral thesis,* 2012.

[95] Ohio University, "Stirling Cycle Machine Analysis," 2012.

[96] B. Kongtragool, S. Wongwises, "A review of solar-powered Stirling engines and low temperature differential Stirling engines" *Renew Sustain Energy* vol. 2, pp. 131–154, 2003.

[97] I.Ureli, "Stirling cycle engine analysis," 1984.

[98] M. A. Clarke, G. T. Reader, D.R. Taylor, " Experiences in the commissioning of a prototype 20 kW helium charged Stirling engine. ," *Seventeenth intersociety energy conversion engineering conference,* vol. 829298, pp. 1796–1800, 1982.

[99] D. G. Thombare, S. K. Verma, "Technological development in the Stirling cycle engines," *Renewable and Sustainable Energy Reviews,* vol. 12, pp. 1-38, 2008.

[100] G. T. Reader, C. Hooper, " Stirling Engines," 1983.

[101] S. Isshiki, A. Sakano, I. Ushiyama, and N. Isshiki, "Studies of flow resistance and heat transfer of regenerator wire meshes of Stirling engines in oscillatory flow" *JSME Int J Fluid Therm Eng,* vol. 40, pp. 281–289, 1997.

[102] K. Muralidhar, K. Suzuki, "Analysis of flow and heat transfer in a regenerator mesh using a non Darcy thermally non-equilibrium model" *Int J Heat Mass Transfer,* vol. 44, pp. 2493–2504, 2001.

[103] R. Shoureshi, " General method for optimization of Stirling engine.," *Seventeenth intersociety energy conversion engineering conference,* vol. 829279, pp. 1688–93, 1982.

[104] J. Wood, B. Changnot, and L.B. Penswick, "Design of a low pressure air engine for third world use," *Seventeenth intersociety Energy conversion engineering conference,* vol. 829289, pp. 1744–48, 1982.

[105] J. Senft, "Extended mechanical efficiency theorem for engines and heat pump," *J energy* pp. 679–693, 2000).

[106] C. D. West, "Principles and applications of Stirling engines," 1986.

[107] H. L. Langhaar, "Dimensional Analysis and Theory of Models," 1951.

[108] W.M. Kays, A. L. London, "Compact Heat Exchangers," vol. 2, 1964.

[109] C. Maier, A. Gil, R. Aguilera, L. Shuang, and X. Yu, "Stirling engine," *University of Gavle,* 2007.

[110] D. Thombare, "Stirling engine: Micro-CHP System for Residential Application," *Encyclopedia of Materials: Science and Technology*.

[111] D. G. Thombre, S. K. Verma, "Technological developement in the Stirling cycle engines," *Renewable and Sustainable Energy Reviews,* vol. 12, pp. 1-38, 2008.

[112] K. Mahkamov, "Doctoral Thesis," 1990.

[113] G. F. Rogers Y. R. Mayhew, "Engineering Thermodynamics, work and heat transfer," 1967.

[114] W. J. M. Rankine, "Thermodynamics of Stirling cycle engine," pp. 140-146, 1859.

[115] T. Finkelstein and . "Optimisation of phase angle and volume ratio for Stirling engine," *SAE Winter Annual Meeting,* 1960.

[116] G. Walker, M. I. Kahn, "Theoretical performance of Stirling cycle engine," *Proceedings of SAE International Automotive Congress,* 1965.

[117] I. Urieli, "Stirling cycle machine analysis," (2001).

[118] B. Thomas, D. Pittman. "Update on the evaluation of different correlations for the flow friction factor and heat transfer of Stirling engine regenerators," *Proceedings of the 35th Intersociety Energy Conversion Engineering Conference and Exhibition, Las-Vegas, USA.,* vol. .71, pp. 76-84, 2000.

[119] S. E. Haupt. R.L. Haupt, . "Practical Genetic Algorithms," 2004.

[120] D. E. Goldberg., "Genetic algorithms in search, optimization, and machine learning," 1989.

[121] A. M. S. Zalzala, P. J. Flemming, "Genetic Algorithms in Engineering Systems," *Institution of Electrical Engineers.* 1997.

[122] E.G. Shopova, N. G. Vaklieva-Bancheva, "BASIC—A genetic algorithm for engineering problems solution," *Computers & Chemical Engineering,* vol. 30, pp. 1293-1309, 2006.

[123] "Fluent 6.3 User's Guide Manual," 2006.

[124] W. T. Beale, "'Free piston Stirling- some model tests and simulation' " *International Automotive Engineering Congress, Society of Automotive Engineers Inc. ,* January 13–17 1969.

Appendix A MATLAB codes for the second order mathematical model of the adiabatic and quasi steady model of the free piston Stirling engine

The developed model consists of different codes in each subprogram:

GA_optimisation_FPSE

This includes the optimization codes for the quasi FPSE model

global_file_FPSE

This includes all the parameters considered for the numerical simulation

inputdata_FPSE

This includes all the input design parameters for the numerical simulation of the free piston Stirling engine

FPSE_modelling_quasi

This file solves all the equations listed in the cal_function_FPSE file

define_y_parameter_FPSE

This file defines the matrix of the parameters and equations to be solved by rk4.

objective_function_FPSE

This consists of the objective function of the optimization using GA

cal_function_FPSE

This file consists of all the differential equations in the numerical simulation

rk4.

This file simultaneaously solves all the differential equations of the model

GA_optimisation_FPSE

```
function []=GA_optimisation_FPSE
tic
%   GA
%   Single objective function
%   Edited by Ayodeji Sowale 2015 and modified from Haupt & Haupt
2003

% Public parameter
global_file_FPSE_GA
inputdata_FPSE_GA
%_____________________________________________________________________
%                         I Setup the GA
ff='objective_function_FPSE_GA';    % objective function
% variable
limits**************************************************
varhi=zeros(popsize,npar);
varlo=zeros(popsize,npar);
for i = 1:1:popsize
    varhi(i,:)=var_hi;
    varlo(i,:)=var_lo;
end
%_____________________________________________________________________
%                         II Stopping criteria
maxvalue=9999999;       % maximum cost
%_____________________________________________________________________
%                         III GA parameters
Nt=npar;                % continuous parameter GA Nt=#variables
%*********************************************************************
% objective function
%*********************************************************************
keep=floor(selection*popsize);      % #population members that
survive
nmut=ceil((popsize-1)*Nt*mutrate);  % total number of mutations
M=ceil((popsize-keep)/2);           % number of matings
%_____________________________________________________________________
%               Create the initial population
iga=0;              % generation counter initialized
par=(varhi-varlo).*rand(popsize,npar)+varlo;  % random

result=feval(ff,par);       % calculates population value using f

value1=result(:,1);         % reult 1 from the objective function
(poweri)
value2=result(:,2);         % reult 2 from the objective function
(eff)
value3=result(:,3);         % reult 3 from the objective function
(Nhtube)
value4=result(:,4);         % reult 4 from the objective function
(Nktube)
value5=result(:,5);         % reult 5 from the objective function
(pressure drop)

%*********************************************************************
```

```
%*************************************************************
% single objective function
max_value1 = max(value1);
value = 1./(1+max_value1-value1); % evaluate fitness value for the
maximum problem
%*************************************************************
%*************************************************************
[value,inx]=sort(value,'descend');  % max value in element 1
par=par(inx,:);                     % sort continuous
value1= value1(inx,:);
value2= value2(inx,:);
value3= value3(inx,:);
value4= value4(inx,:);
value5= value5(inx,:);
Dpar1(1)=par(1,1);
Dpar2(1)=par(1,2);
Dpar3(1)=par(1,3);
Dpar4(1)=par(1,4);
Dpar5(1)=par(1,5);
Dpar6(1)=par(1,6);
Dpar7(1)=par(1,7);
Dpar8(1)=par(1,8);
Dpar9(1)=par(1,9);
Dpar9(1)=par(1,10);
Dvalue1(1)=value1(1);
Dvalue2(1)=value2(1);
DNhtube(1)=value3(1);
DNktube(1)=value4(1);
DdeltaPsummax(1)=value5(1);

maxvalue(1)=max(value1);            % maxvalue contains maximum of
population
meanvalue(1)=mean(value1);          % meanvalue contains mean of
population
disp(['#generations=' num2str(iga) ' best value='
num2str(value(1)) ' mean value=' num2str(mean(value))])
disp([                              ' Indicated power ='
num2str(value1(1))])
disp([                              ' Thermal efficiency ='
num2str(value2(1))])
%_____________________________________________________________
%_____________________________________________________________
%               Iterate through generations
while iga<maxit
   iga=iga+1;               % increments generation counter
%_____________________________________________________________
%                        Pair and mate
M=ceil((popsize-keep)/2);       % number of matings
prob=flipud([1:keep]'/sum([1:keep]));   % weights chromosomes
odds=[0 cumsum(prob(1:keep))']; % probability distribution
function
pick1=rand(1,M);                        % mate #1
pick2=rand(1,M);                        % mate #2
% ma and pa contain the indicies of the chromosomes that will mate
ic=1;
```

```
while ic<=M
  for id=2:keep+1
    if pick1(ic)<=odds(id) && pick1(ic)>odds(id-1)
      ma(ic)=id-1;
    end
    if pick2(ic)<=odds(id) && pick2(ic)>odds(id-1)
      pa(ic)=id-1;
    end
  end
  ic=ic+1;
end
%_____________________________________________________________________
%           Performs mating using single point crossover
ix=1:2:keep;                          % index of mate #1
xp=ceil(rand(1,M)*Nt);                % crossover point
r=rand(1,M);                          % mixing parameter
for ic=1:M
    xy=par(ma(ic),xp(ic))-par(pa(ic),xp(ic));  % ma and pa mate
    par(keep+ix(ic),:)=par(ma(ic),:);          % 1st offspring
    par(keep+ix(ic)+1,:)=par(pa(ic),:);        % 2nd offspring
    par(keep+ix(ic),xp(ic))=par(ma(ic),xp(ic))-r(ic).*xy; % 1st
    par(keep+ix(ic)+1,xp(ic))=par(pa(ic),xp(ic))+r(ic).*xy; % 2nd
        if xp(ic)<npar % crossover when last variable not selected
            par(keep+ix(ic),:)=[par(keep+ix(ic),1:xp(ic))
par(keep+ix(ic)+1,xp(ic)+1:npar)];
            par(keep+ix(ic)+1,:)=[par(keep+ix(ic)+1,1:xp(ic))
par(keep+ix(ic),xp(ic)+1:npar)];
        end
end
%_____________________________________________________________________

%_____________________________________________________________________
%                          Mutate the population
mrow=sort(ceil(rand(1,nmut)*(popsize-1))+1);
mcol=ceil(rand(1,nmut)*Nt);
for ii=1:nmut
    par(mrow(ii),mcol(ii))=(varhi(mrow(ii),mcol(ii))-
varlo(mrow(ii),mcol(ii)))*rand+varlo(mrow(ii),mcol(ii));  %
mutation
end % ii

%_____________________________________________________________________
%   The new offspring and mutated chromosomes are evaluated
result=feval(ff,par);       % calculates population value using f
value1=result(:,1);         % reult 1 from the objective function
(poweri)
value2=result(:,2);         % reult 2 from the objective function
(eff)
value3=result(:,3);         % reult 3 from the objective function
(Nhtube)
value4=result(:,4);         % reult 4 from the objective function
(Nktube)
value5=result(:,5);         % reult 5 from the objective function
(pressure drop)

%*************************************************************
```

```
% single objective function
%value=value1;
maxvalue1 = max(value1);
if maxvalue1>max_value1
    max_value1=maxvalue1;
end
value = 1./(1+max_value1-value1);   % evaluates fitness value for
the maximum problem
[value,inx]=sort(value,'descend') ; % max value in element 1
par=par(inx,:)  ;                   % sort continuous
value1= value1(inx,:);
value2= value2(inx,:);
value3= value3(inx,:);
value4= value4(inx,:);
value5= value5(inx,:);

%_____________________________________________________________________
%           Do statistics for a single nonaveraging run
Dpar1(iga+1)=par(1,1);
Dpar2(iga+1)=par(1,2);
Dpar3(iga+1)=par(1,3);
Dpar4(iga+1)=par(1,4);
Dpar5(iga+1)=par(1,5);
Dpar6(iga+1)=par(1,6);
Dpar7(iga+1)=par(1,7);
Dpar8(iga+1)=par(1,8);
Dpar9(iga+1)=par(1,9);
Dpar10(iga+1)=par(1,10);
Dpar11(iga+1)=par(1,11);
Dvalue1(iga+1)=value1(1);
Dvalue2(iga+1)=value2(1);
DNhtube(iga+1)=value3(1);
DNktube(iga+1)=value4(1);
DdeltaPsummax(iga+1)=value5(1);
maxvalue(iga+1)=max(value1);
meanvalue(iga+1)=mean(value1);

disp(['#generations=' num2str(iga) ' best value='
num2str(value(1)) ' mean value=' num2str(mean(value))])
disp([                              ' Indicated power ='
num2str(value1(1))])
disp([                              ' Thermal efficiency ='
num2str(value2(1))])
%_____________________________________________________________________
%                         Stopping criteria
    if iga>10 && iga<=maxit
        if maxvalue<=maxvalue(iga-10)
        break
        end
    elseif iga>maxit
        break
    end
end
%_____________________________________________________________
%
```

```
Dpara1=Dpar1';                                  % Cpc - Piston
Damping
Dpara2=Dpar2';                                  % CHdc - Displacer
Damping
Dpara3=Dpar3';                                  % lh - length of
heater, m
Dpara4=Dpar4';                                  % lr - length of
regenerator, m
Dpara5=Dpar5';                                  % lk - length of
cooler, m
Dpara6=Dpar6';                                  % Dh - diameter of
heater tube, m
Dpara7=Dpar7';                                  % Dr - Outside
diameter of regenerator chamber, m
Dpara8=Dpar8';                                  % Deepk - Depth of
cooler slot, m
Dpara9=Dpar9';                                  % Wk - thickness of
cooler slot, m
Dpara10=Dpar10';                                % poros - porosity
of matrix in the regenerator
Dpara11=Dpar11';                                % Dw - wire
diameter of matrix in the regenerator, m

iters=0:length(maxvalue)-1;
save Indicated_power-G.xls iters Dvalue1 -ascii;
save eff-G.xls iters Dvalue2 -ascii;
save Nhtube-G.xls iters DNhtube -ascii;
save Dh-G.xls iters Dpar6 -ascii;
save lh-G.xls iters Dpar3 -ascii;
save Nktube-G.xls iters DNktube -ascii;
save Dr-G.xls iters Dpar7 -ascii;
save lk-G.xls iters Dpar5 -ascii;
save poros-G.xls iters Dpar10 -ascii;
save lr-G.xls iters Dpar4 -ascii;
save delP-G.xls iters DdeltaPsummax -ascii;
save Cpc-G.xls iters Dpar1 -ascii;
save CHdc-G.xls iters Dpar2 -ascii;
save Deepk-G.xls iters Dpar8 -ascii;
save Dw-G.xls iters Dpar11 -ascii;
save Wk-G.xls iters Dpar9 -ascii;

figure(1)
plot(gen,Dvalue1,'r-')                      % plot graph between
best value and generation
xlabel('generation');
ylabel('Value1');
title('Value - generation')

figure(2)
plot(gen,Dvalue2,'r-')                          % plot graph
between efficiency and generation
xlabel('generation');
ylabel(' Brake efficiency');
title('efficiency - generation')
```

```
figure(15)
plot(gen,Dvalue1,'b-')                    % plot graph between
Power and generation
xlabel('generation');
ylabel('Brake power');
title('power - generation')

%disp(['best solution'])
%fprintf('stroke of displacer= %12.9f m \n',par(1,1));
%fprintf('stroke of displacer= %12.9f m \n',par(1,2));


Dpara=[Dpara1 Dpara2 Dpara3 Dpara4 Dpara5 Dpara6 Dpara7 Dpara8
Dpara9 Dpara10 Dpara11];
Dvalue1=Dvalue1';
Dvalue2=Dvalue2';
meanvalue=meanvalue';
maxvalue=maxvalue';
disp('the best value in each generation');
disp(Dvalue1);                          %show best value in each
generation
disp('The maximum power');
disp(Dvalue1);                          %show maximum power
disp('The maximum efficiency');
disp(Dvalue2);                          %show maximum efficiency
disp('The optimal parameters');
disp(Dpara);                            % show best parameter
disp('number of generation');
disp(iga);                              % show number of generation

disp('the optimal number of heater tube in each generation');
disp(DNhtube);                                  % show best number
of heater tube
disp('the optimal  of cooler tube in each generation');
disp(DNktube);                                  % show best number
of cooler tube
toc
end
```

Global_file_FPSE

```
% global_file_FPSE

global DD           % diameter of displacer [m]
global R            % gas constant [J/kg.K]
global Capm         % specific heat capacity of matrix, constant
pressure [J/kg.K]
global M            % mass of gas inside the engine [kg]
global VswD         % swept volume of displacer [m3]
global VswP         % swept volume of power piston [m3]
global f            % frequncy (Hz)
global theta        % shaft angle (degree)
```

```
global mm1          % mass of matrix part 1
global mm2          % mass of matrix part 2
global mm3          % mass of matrix part 3
global mm4          % mass of matrix part 4
global mm5          % mass of matrix part 5
global mm6          % mass of matrix part 6
global mm7          % mass of matrix part 7
global mm8          % mass of matrix part 8
global mm9          % mass of matrix part 9
global mm10         % mass of matrix part 10
global Vr1          % gas volume of regenerator part 1
global Vr2          % gas volume of regenerator part 2
global Vr3          % gas volume of regenerator part 3
global Vr4          % gas volume of regenerator part 4
global Vr5          % gas volume of regenerator part 5
global Vr6          % gas volume of regenerator part 6
global Vr7          % gas volume of regenerator part 7
global Vr8          % gas volume of regenerator part 8
global Vr9          % gas volume of regenerator part 9
global Vr10         % gas volume of regenerator part 10
global Vr           % gas volume of regenerator
global Vk           % gas volume of heater space
global Vh           % gas volume of cooler space
global degree       % shaft angle
global poros        % porosity of matrix
global fshp         % shape factor
global kr           % thermal conductivity of matrix [W/mK]
global kC           % thermal conductivity of cooler [W/mK]
global kH           % thermal conductivity of heater [W/mK]
global N            % engine speed [rpm]
global lr           % length of regenerator chamber[m]
global lh           % length of heater tube [m]
global lr1          % length of regenerator part 1 [m]
global lr2          % length of regenerator part 2 [m]
global lr3          % length of regenerator part 3 [m]
global lr4          % length of regenerator part 4 [m]
global lr5          % length of regenerator part 5 [m]
global lr6          % length of regenerator part 6 [m]
global lr7          % length of regenerator part 7 [m]
global lr8          % length of regenerator part 8 [m]
global lr9          % length of regenerator part 9 [m]
global lr10         % length of regenerator part 10 [m]
global lk           % length of cooler tube [m]
global De           % diameter of expansion chamber [m]
global Dh           % diameter of heater tube [m]
global Dr           % outer diameter of regenerator chamber [m]
global dr           % inner diameter of regenerator chamber [m]
global Dc           % diameter of compression chamber [m]
global Dk           % diameter of cooler tube [m]
global SpaceBLayers
global TypeOfReg    % type of regenerator
global TypeOfEngine     % type of engine
global TypeOffriction_hk    % type of friction correlation for
heater and cooler
global TypeOffriction_reg   % type of friction correlation for
regenerator
```

```
global TypeOfheatcof_h     % type of heat correlation for heater
global TypeOfheatcof_k     % type of heat correlation for cooler
global TypeOfheatcof_reg    % type of heat correlation for
regenerator
global Vcleh        % dead volume of tube connection between
expansion and heater spaces [m]
global Vclhr        % dead volume of tube connection betweenheater
and regenerator spaces [m]
global Vclrk        % dead volume of tube connection between
regenerator and compression spaces [m]
global Vclkc        % dead volume of tube connection between
compression and cooler spaces [m]
global Vclc1        % dead volume of compression spaces part 1 [m]
global Vclc2        % dead volume of compression spaces part 2 [m]
global alfa         % phase angle [degree]
global Tmu          % temerature for calculation viscosity [K]
global Tku          % temerature for calculation thermal
conductivity of gas [K]
global mu0          % initial viscosity
global k0           % initial thermal conductivity
global Cap          % specific heat capacity at constant pressure
[J/kg.K]
global Cav          % specific heat capacity at constant volume
[J/kg.K]
global Ze           % stroke of hot piston [m]
global Zc           % stroke of cold piston [m]
global Twh          % temperature of heater wall [K]
global Twk          % temperature of cooler wall [K]
global Nhtube       % number of heater tube
global Nktube       % number of cooler tube
global Nr           % number of regenerator unit
global VswD_c       % swept volume of displacer deducted with rod
volume [m3]
global Dw           % wire diameter [m]
global HD           % thickness of displacer [m]
global romr         %
global popsize      % size of population
global Drod         % diameter of rod in displacer chamber [m]
global dt           % time interval [s]
global num          % number of time step
global tT           % cyclic time
global timestep     % time per time step
global pO           % limitation pressure [Pa]
global Dhi          % inner diameter of heater [m]
global Dho          % outer diameter of heater [m]
global hgap         % gap of heater annular [m]
global pA
global HringD           % height of sealing ring of the Displacer
[m
global Hringp           % height of sealing ring of the power
piston [m]
global Pspr         % additional pressure due to the sealing ring
[Pa]
global Dp           % diameter of power piston [m]
global dirod        % outside dinameter of rod [m]
```

```
global g            %
global theta1       %  phase angle
global Dhh          %heat flow in heater
global Dhk          %heat flow in cooler
global Wh           %thickness of heater slot [m]
global Wk           %thckness of cooler slot [m]
global Deeph         %depth of heater slot [m]
global Deepk         %depth of cooler slot [m]
global gen %number of generations
global Ad  %area of displacer
global Ap  %area of piston
global Mp  %mass of piston
global Md  %mass of displacer
global Cpc
global CHpc  piston damping load
global CHdc  %displacer damping load
global gammaa
global Vbo   %bounce space volume
global cycle  %number of cycles
global Adr  %Area of displacer rod
global Vdo
global Pmean %mean pressure
global Pmen   %mean pressure
global Mc
global CC  %clearance volume in compression space
global EE  clearance volume in expansion space
global HD %thickness of displacer
```

Inputdata_FPSE

```
  %*********************************************
%inputdata_FPSE
%*********************************************
global_file_FPSE
%constant values
 g=9.806;   % gravitation accerelation[ m/s2]
 pi=3.1415926535897;
%choose the working gas from 1-9
 TypeOfGas=2; %1=Hydrogen, 2=Helium, 3=Neon, 4=Nitrogen, 5=
Carbonmonxide, 6=air,
 %7=Oxygen , 8=argon, 9=Carbondioxide
constantR=[4120;2080;415;297;297;287;260;208;189];
constantCap=[14200;5190;1030;1040;1040;1010;920;520;850];
constantCav=[10080;3110;620;740;750;720;660;310;660];
constantmu0=[0.000009;0.0000178;0.0000313;0.0000179;0.0000179;0.00
000184;0.0000208;0.0000229;0.0000150];
constantTmu=[84.4;80;0;106;136;112;139;144;222];
constantk0=[0.163;0.151;0.049;0.024;0.023;0.024;0.025;0.016;0.015]
;
constantTku=[166;0;0;166;177;194;222;150;222];
```

```
Cap=constantCap(TypeOfGas);
Cav=constantCav(TypeOfGas);
R=constantR(TypeOfGas);
mu0=constantmu0(TypeOfGas);
Tmu=constantTmu(TypeOfGas);
k0=constantk0(TypeOfGas);
Tku=constantTku(TypeOfGas);
%*******************************************
%chosse type of engine
%1-Alfa, 2-Beta, 3-Gamma, 4-Free piston
TypeOfEngine=4;
%chosse type of regenrator
%1-wire, 2-foil
TypeOfReg=1;
%chosse type of Heat transfer coeficient of the heat exchanger in
the heater chamber
%1-Dittus-Boelter -unidirectional flow, 2-Colburn correlation -
unidirectional
%flow, 3- Kays&London -unidirectional flow ,4- Annular gap
TypeOfheatcof_h=1;
%chosse type of Heat transfer coeficient of the heat exchanger in
the cooler chamber
%1-Dittus-Boelter -unidirectional flow, 2-Colburn correlation -
unidirectional
%flow, 3- Kays&London -unidirectional flow
TypeOfheatcof_k=4;
%choose type of friction factor determination in heater and cooler
%[1-Kay&London unidirectional flow, 2-Frank Incopera
unidirectional flow,
%3-Schulz&Schwendig oscillation flow]
TypeOffriction_hk=1;
%choose type of Heat transfer coeficient of the metrix in the
regenerator
% 1-Tanaka correlation -oscillation flow, 2- Gedeon&Wood
oscillation flow
TypeOfheatcof_reg=1;
%choose type of friction factor determination in regenerator
% 1-Tanaka correlation -oscillation flow, 2-%Kay&London
correlation -unidirectional flow, 3- Gedeon&Wood oscillation flow
TypeOffriction_reg=1;

%*************************************************************
*********
%operating condition
Twh=814.3;  %Temperature of the chamber wall inside heater space
in the beginning of the cycle, K
Twk=322.8;            %Temperature of the chamber wall inside
cooler space in the beginning of the cycle, K
f=30;                %frequency, Hz
N=f*60;              %engine speed, rpm
pO=71*100000;        %maximum pressure
emit = 0.55;        %absorptance of heat cylinder wall
TA=305.5;           %Ambient temperature
pA=101325;          %Ambient pressure
%regenerator properties
```

```
%*************wire matrix**********************
Nr=1;                %Number of regenerator
poros = 0.759;%porosity of matrix in the regenerator
Dw=0.0000889;           %wire diameter, m
Capm=600;            %Heat capacity of matrix
romr= 7860;          %matrix density
fshp = 4;            %shape factor -wire
%**********foil matrix************************
NumberOfLayers = 100;       %Number of layer
SpaceBLayers = 0.00015;     %Space layer
%*****************************************************************
*******
%properties of material
kD=36;               % thermal conductivity of displacer[W/mK]
kr=16.3;             % thermal conductivity of matrix[W/mK]
kH=36;               % thermal conductivity of heater tube[W/mK]
kC=36;               % thermal conductivity of cooler tube[W/mK] r
tube[W/mK]
%*********************************************
%Simulation parameter
num=1000;    %number of timesteps
tT=1/f;      %period of oscillation
timestep =tT/num;
dt=timestep;
cycle = 1; %number of cycles
%*****************************************************************
*********
%GA parameters
%popsize=input('population size =');
popsize=30;              % set population size
mutrate=.2;             % set mutation rate
selection=0.5;          % fraction of population kept
maxit=80;               % max number of generation
%*****************************************************************
*********
%geometric data
%*****************************************************************
*********
Vcleh=0.00000302;   %Dead space between expansion space and
heater, m3
Vclhr=0.0000359;    %Dead space between heater space and
regenerator, m3
Vclrk=0.0000151;    %Dead space between regenerator space and
cooler, m3
Vclkc=0.0000276;    %Dead space between cooler and cold space, m3
Vclc1=0.00000765;   %Dead space between two parts of the cold
space, m3
Vclc2=0.00000302;   %Dead space of the cold space, m3

%*****************************************************************
*********
    %disp ('Choose optimal engine parameters and define upper and
lower bounds')
%diameter of displacer piston, m
%M_De=input('diameter of displacer is optimal engine parameter :
```

```
enter 1 if not enter 0');
De=0.0567;
%diameter of power piston , m
%M_Dc=input('diameter of power piston is optimal engine parameter
: enter 1 if not enter 0');
Dc=0.05718;
%diameter of regenerator chamber, m
Dr = 0.0718;          %outer diameter of regenerator,m
dr=0.0607;           %inner diameter of regenerator,m
Dh=0.002362;           %diameter of heater chamber, m
Wk = 0.000508;
Deepk = 0.00376;     %depth of cooler slot


lh=0.1834;             %heater length, m
lr=0.06446;             %regenerator length, m
lk=0.0792;             %cooler length, m
Nktube=135;          %Number of cooler tubes
Nhtube=34;           %Number of heater tubes
alfa=90*pi/180;      %phase angle between pistons
Drod=0.01806;  %diameter of rod in hot piston chamber, m
Adr = 2.176e-4; % Area of displacer rod
HD = 0.15;           %diameter of rod in hot piston chamber, m
Md = 0.426;           %mass of displacer
Mp =6.355;            %mass of piston
Mc = 416;
CC = 18.3e-3;         %clearance volume in compression space
EE = 18.61e-3;        %clearance volume in expansion space
Cpc = 500;            %piston damping load

CHdc=100;    %displacer damping load
Vbo=20500E-6; %bounce space volume
Vdo=31.79e-6;
Pmen=71E5;  %mean pressure
%*****************************************************************
*********
```

FPSE_modelling_Quasi

```
function [Pmax, Pmin,Poweri,effi,deltaPsummax, Pmean]=
FPSE_modelling_quasi
% Second-order model of the Free piston Stirling engine based on
% Quasi-steady flow model by Urieli [1984]and Timoumi et.al [2008]
% main file for analysis of working process and prediction of
power output
% Engine space is divided into five main spaces-one compression
space, one
% cooler space, ten regenerator spaces, one heater space and one
expansion space
% edited by Ayodeji Sowale
% last modified 11.09.2015
%tic
```

```
%*****************************************************************
*********
%Public parameter
global_file_FPSE
%*****************************************************************
*********
%define y-parameter
define_y_parameter_FPSE
%define_y_parameter_FPSEc
%*****************************************************************
*********
%inputdata
inputdata_FPSE
%*****************************************************************
*********
graphworking = 1;
%calculation constant parameter
DD=De;
if TypeOfheatcof_h==4;
    Dho=Dhi+hgap;          %outer diameter of heater annular, m
    Dh=Dho-Dhi;            %hydraulic diameter of heater tube, m
end
if TypeOfheatcof_h ==5
    Dhh=4*(Wh*Deeph)/(2*Wh+2*Deeph);
else
    Dhh=Dh;
end
if TypeOfheatcof_k ==4
    Dhk=4*(Wk*Deepk)/(2*Wk+2*Deepk);
else
    Dhk=Dk;
end
lr1=lr/10; lr2=lr/10; lr3=lr/10; lr4=lr/10; lr5=lr/10; lr6=lr/10;
lr7=lr/10;
lr8=lr/10; lr9=lr/10; lr10=lr/10;
Ad=pi*De^2/4;
Ap =pi*Dc^2/4;
y(Xd)=EE;
y(Veld)=0;
y(Velp)=0;
y(Xp)=CC;

VswD_c=pi*(De^2-Drod^2)/4*y(Xd);
VswP=pi*(Dc)^2/4*y(Xp);
VswD=pi*(De)^2/4*y(Xd);
Vr1=pi/4*(Dr^2-dr^2)*lr1*Nr*poros;
Vr2=pi/4*(Dr^2-dr^2)*lr2*Nr*poros;
Vr3=pi/4*(Dr^2-dr^2)*lr3*Nr*poros;
Vr4=pi/4*(Dr^2-dr^2)*lr4*Nr*poros;
Vr5=pi/4*(Dr^2-dr^2)*lr5*Nr*poros;
Vr6=pi/4*(Dr^2-dr^2)*lr6*Nr*poros;
Vr7=pi/4*(Dr^2-dr^2)*lr7*Nr*poros;
Vr8=pi/4*(Dr^2-dr^2)*lr8*Nr*poros;
Vr9=pi/4*(Dr^2-dr^2)*lr9*Nr*poros;
Vr10=pi/4*(Dr^2-dr^2)*lr10*Nr*poros;
```

```
Vr = pi/4*(Dr^2-dr^2)*lr*Nr*poros;
if TypeOfheatcof_h==4;
    Vh=pi/4*(Dho^2-Dhi^2)*lh*Nhtube;
else

    Vh=pi/4*(Dhh^2)*lh*Nhtube;
end
Vk=Wk*Deepk*lk*Nktube;
mm1=(1-poros)*pi/4*(Dr^2-dr^2)*lr1*Nr*romr;
mm2=(1-poros)*pi/4*(Dr^2-dr^2)*lr2*Nr*romr;
mm3=(1-poros)*pi/4*(Dr^2-dr^2)*lr3*Nr*romr;
mm4=(1-poros)*pi/4*(Dr^2-dr^2)*lr4*Nr*romr;
mm5=(1-poros)*pi/4*(Dr^2-dr^2)*lr5*Nr*romr;


mm6=(1-poros)*pi/4*(Dr^2-dr^2)*lr6*Nr*romr;
mm7=(1-poros)*pi/4*(Dr^2-dr^2)*lr7*Nr*romr;
mm8=(1-poros)*pi/4*(Dr^2-dr^2)*lr8*Nr*romr;
mm9=(1-poros)*pi/4*(Dr^2-dr^2)*lr9*Nr*romr;
mm10=(1-poros)*pi/4*(Dr^2-dr^2)*lr10*Nr*romr;
% Initial conditions:
t = 0;
%*****************************************************************
*********
%Calulate Volume  t=0
%degree=theta*180/pi;
if TypeOfEngine==2
   Ldead=0.00;
else
   Ldead=Vclc1;
end
DeadspaceE=Vcleh+Vclhr;
if TypeOfEngine==3
   DeadspaceC=Vclrk+Vclkc++Vclc2+Vclc1;
else
   DeadspaceC=Vclrk+Vclkc+Vclc2;
end
t=t+dt;
theta=2*pi*f*t;
switch(TypeOfEngine)
%Alfa
    case 1
            y(Ve)=0.5*VswD*(1+cos(theta))+DeadspaceE;
            y(Vc)=0.5*VswP*(1+cos(theta-alfa))+DeadspaceC;
%Beta
    case 2
            y(Ve)=0.5*VswD*(1+cos(theta))+DeadspaceE;
            y(Vc)=pi*Dc^2/4*(Ze/2*(1-
cos(theta))+Zc/2*(1+cos(theta-alfa))+Ldead)+DeadspaceC;
%Gamma
    case 3
  %Hamonic
            y(Ve)=0.5*VswD*(1+cos(theta))+DeadspaceE;
            y(Vc)=0.5*VswP*(1+cos(theta-alfa))+0.5*(VswD_c)*(1-
cos(theta))+DeadspaceC;
```

```
%Free piston
    case 4


            y(Ve)=(0.01861+y(Xd))*Ad  ;            % expansion
space volume

            y(Vc)=(0.0183+y(Xp))*Ap-(Ad-Adr)*y(Xd); %compression
volume


end
y(Te)= Twh;    y(Th) =Twh;   y(Tk)= Twk;  y(Tc) =Twk;
y(Tr1) =Twk+(Twh-Twk)/20 ;   y(Tr2) =Twk+3*(Twh-Twk)/20;
y(Tr3) =Twk+5*(Twh-Twk)/20;  y(Tr4) =Twk+7*(Twh-Twk)/20;
y(Tr5) =Twk+9*(Twh-Twk)/20;  y(Tr6) =Twk+11*(Twh-Twk)/20;
y(Tr7) =Twk+13*(Twh-Twk)/20; y(Tr8) =Twk+15*(Twh-Twk)/20;
y(Tr9) =Twk+17*(Twh-Twk)/20; y(Tr10)=Twk+19*(Twh-Twk)/20;
y(Tm1) =Twk+1*(Twh-Twk)/20;  y(Tm2) =Twk+3*(Twh-Twk)/20;
y(Tm3) =Twk+5*(Twh-Twk)/20;  y(Tm4) =Twk+7*(Twh-Twk)/20;
y(Tm5) =Twk+9*(Twh-Twk)/20;  y(Tm6) =Twk+11*(Twh-Twk)/20;
y(Tm7) =Twk+13*(Twh-Twk)/20; y(Tm8) =Twk+15*(Twh-Twk)/20;
y(Tm9) =Twk+17*(Twh-Twk)/20; y(Tm10)=Twk+19*(Twh-Twk)/20;
y(epsilon)=1;
y(hr1)=3000; y(hr2)=3000; y(hr3)=3000; y(hr4)=3000; y(hr5)=3000;
y(hr6)=3000; y(hr7)=3000; y(hr8)=3000; y(hr9)=3000; y(hr10)=3000;
y(hh)=3000; y(hk)=3000;
y(mc)=pO*y(Vc)/(R*y(Tc)); y(mk)=pO*Vk/(R*y(Tk));
y(mr1)=pO*(Vr1)/(R*y(Tr1)); y(mr2)=pO*(Vr2)/(R*y(Tr2));
y(mr3)=pO*(Vr3)/(R*y(Tr3)); y(mr4)=pO*(Vr4)/(R*y(Tr4));
y(mr5)=pO*(Vr5)/(R*y(Tr5)); y(mr6)=pO*(Vr6)/(R*y(Tr6));
y(mr7)=pO*(Vr7)/(R*y(Tr7)); y(mr8)=pO*(Vr8)/(R*y(Tr8));
y(mr9)=pO*(Vr9)/(R*y(Tr9)); y(mr10)=pO*(Vr10)/(R*y(Tr10));
y(mh)=pO*Vh/(R*y(Th)); y(me)=pO*y(Ve)/(R*y(Te));
y(mck)=0.00001; y(mkr1)=0.00001; y(mr1r2)=0.00001;
y(mr2r3)=0.00001;
y(mr3r4)=0.00001; y(mr4r5)=0.00001; y(mr5r6)=0.00001;
y(mr6r7)=0.00001;
y(mr7r8)=0.00001; y(mr8r9)=0.00001; y(mr9r10)=0.00001;
y(mr10h)=0.00001;
y(mhe)=0.00001;
y(P)=pO; y(Pbounce)=pO;y(Pdbounce)=pO;
Pmean = pO;
conv(1)=1; conv(2)=1; conv(3)=1; conv(4)=1; conv(5)=1; conv(6)=1;
conv(7)=1; conv(8)=10000; conv(9)=10000; conv(10)=10000;
conv(11)=10000;
conv(12)=10000; conv(13)=10000; conv(14)=10000; conv(15)=10000;
conv(16)=10000; conv(17)=10000; conv(18)=10000; conv(19)=10000;
conv(20)=1000; conv(21)=1000;conv(22)=1000;conv(23)=1000;
Form3text11=30; Form3text12=20; Form3text13=10; Form3text14=10;
Form3text15=10; Form3text16=10; Form3text17=10; Form3text18=10;
Form3text19=20; Form3text20=30;
Form3text21=50000;Form3text22=1;Form3text23=1;
pOnew=pO;
Xpmax=y(Xp);
```

```
Xdmax=y(Xd);
%increm=Form3text11;
convpr(8)=conv(8);  convpr(9)=conv(9);  convpr(10)=conv(10);
convpr(11)=conv(11);  convpr(12)=conv(12); convpr(13)=conv(13);
convpr(14)=conv(14);  convpr(15)=conv(15); convpr(16)=conv(16);
convpr(17)=conv(17);  convpr(18)=conv(18);
convpr(22)=conv(22);    convpr(23)=conv(23);
it= 1; Cq=1; QHcyl=2;checking=0; t = 0; Cq2 =1; Cq3 =1;
while (abs(conv(1))>=1 || abs(conv(2))>=1 ||abs(conv(3))>=1 ||
abs(conv(4))>=1 ||abs(conv(5))>=1 ||abs(conv(6))>=1 ||
abs(conv(8))>=10000 || abs(conv(9))>=Cq  ||abs(conv(10))>=Cq
||abs(conv(11))>=Cq ||abs(conv(12))>=Cq ||abs(conv(13))>=Cq
||abs(conv(14))>=Cq ||abs(conv(15))>=Cq ||abs(conv(16))>=Cq
||abs(conv(17))>=Cq ||abs(conv(18))>=Cq ||abs(conv(19))>=0.0005
||abs(conv(20))>=0.0005 ||abs(conv(22))>=0.0001
||abs(conv(23))>=0.0001) && it <=90 && abs(conv(21))>(QHcyl*0.01)
        %fprintf('N = %6.3f\n',N)
        Te0=y(Te); Tc0=y(Tc); Tr1o=y(Tr1); Tr2o=y(Tr10);
Th0=y(Th); Tk0=y(Tk);
        P0=y(P); Xp0max=Xpmax; Xd0max=Xdmax;
        dy(We) = 0; dy(Wc) = 0; dy(W)=0; y(We)=0; y(Wc)=0;
        y(Qr1)=0; y(Qr2)=0; y(Qr3)=0; y(Qr4)=0; y(Qr5)=0;
y(Qr6)=0;
        y(Qr7)=0; y(Qr8)=0; y(Qr9)=0; y(Qr10)=0;
        y(Qr1ext)=0; y(Qr2ext)=0; y(Qr3ext)=0; y(Qr4ext)=0;
y(Qr5ext)=0;
        y(Qr6ext)=0; y(Qr7ext)=0; y(Qr8ext)=0; y(Qr9ext)=0;
y(Qr10ext)=0;
        y(QH)=0; y(QC)=0;

y(Qkdiss)=0;y(Qr1diss)=0;y(Qr2diss)=0;y(Qr3diss)=0;y(Qr4diss)=0;

y(Qr5diss)=0;y(Qr6diss)=0;y(Qr7diss)=0;y(Qr8diss)=0;y(Qr9diss)=0;
        y(Qr10diss)=0;y(Qhdiss)=0;
        y(Qshtl)=0;

y(deltaP)=0;y(deltaPk)=0;y(deltaPr1)=0;y(deltaPr2)=0;y(deltaPh)=0;

y(Qklir)=0;y(Qr1lir)=0;y(Qr2lir)=0;y(Qr3lir)=0;y(Qr4lir)=0;y(Qr5li
r)=0;

y(Qr6lir)=0;y(Qr7lir)=0;y(Qr8lir)=0;y(Qr9lir)=0;y(Qr10lir)=0;y(Qhl
ir)=0;


      for j=1:1:cycle
           fprintf('cycle = %6.3f\n',j)
        for i = 1:1:num
            [t,y,dy] = rk4('cal_function_FPSE',29,t,dt,y);
            DdQr1(i)=y(Qr1); DdQr2(i)=y(Qr2); DdQr3(i)=y(Qr3);
DdQr4(i)=y(Qr4);
            DdQr5(i)=y(Qr5); DdQr6(i)=y(Qr6); DdQr7(i)=y(Qr7);
DdQr8(i)=y(Qr8);
            DdQr9(i)=y(Qr9); DdQr10(i)=y(Qr10);
            DdQH(i)=y(QH);  DdWe(i)=y(We); DdQC(i)=y(QC);
```

```
DdWc(i)=y(Wc);
            DTm1(i)=y(Tm1);DTm10(i)=y(Tm10);
            DTh(i)=y(Th); DTk(i)=y(Tk);DTc(i)=y(Tc); DTe(i)=y(Te);
DTr1(i)=y(Tr1);DTr10(i)=y(Tr10);
            DdQr1ext(i)=y(Qr1ext); DdQr2ext(i)=y(Qr2ext);
DdQr3ext(i)=y(Qr3ext);
            DdQr4ext(i)=y(Qr4ext); DdQr5ext(i)=y(Qr5ext);
DdQr6ext(i)=y(Qr6ext);
            DdQr7ext(i)=y(Qr7ext); DdQr8ext(i)=y(Qr8ext);
DdQr9ext(i)=y(Qr9ext);DdQr10ext(i)=y(Qr10ext);
            Dmc(i)=y(mc);Dmk(i)=y(mk);Dmr1(i)=y(mr1);
Dmr2(i)=y(mr2);Dmh(i)=y(mh);Dme(i)=y(me);Ddmc(i)=dy(mc);

Ddmk(i)=dy(mk);Ddmr1(i)=dy(mr1);Ddmr2(i)=dy(mr2);Ddmh(i)=dy(mh);Dd
me(i)=dy(me);Dmck(i)=y(mck);Dmkr1(i)=y(mkr1);
            Dmr10h(i)=y(mr10h);Dmr1r2(i)=y(mr1r2); Dmhe(i)=y(mhe);
            Dtheta(i) = theta;Ddegree(i)= degree;
            DP(i)=y(P);DPe(i)=y(Pe);
DPc(i)=y(Pc);DPr1(i)=y(Pr1);DPr10(i)=y(Pr10);DPh(i)=y(Ph);DPk(i)=y
(Pk);
            DVe(i)=y(Ve);DVc(i)=y(Vc);DVt(i)=y(Vt);
DdVe(i)=dy(Ve); DdVc(i)=dy(Vc); DdVt(i)=dy(Vt);
    DdeltaP(i)=y(deltaP);
    DdeltaPr1(i)=y(deltaPr1);
    DdeltaPr(i)=y(deltaPr);
    DdeltaPr10(i)=y(deltaPr10);
    DdeltaPk(i)=y(deltaPk);
    DdeltaPh(i)=y(deltaPh);
    DdWe(i)=y(We);
    DdWc(i)=y(Wc);
    DdW(i)=y(W);
    DdQH(i)=y(QH);
    DdQC(i)=y(QC);
    DdQr1(i)=y(Qr1);
    DdQr2(i)=y(Qr2);
    DdQr3(i)=y(Qr3);
    DdQr4(i)=y(Qr4);
    DdQr5(i)=y(Qr5);
    DdQr6(i)=y(Qr6);
    DdQr7(i)=y(Qr7);
    DdQr8(i)=y(Qr8);
    DdQr9(i)=y(Qr9);
    DdQr10(i)=y(Qr10);

DdQr(i)=y(Qr1)+y(Qr2)+y(Qr3)+y(Qr4)+y(Qr5)+y(Qr6)+y(Qr7)+y(Qr8)+y(
Qr9)+y(Qr10);
    DQklir(i)=y(Qklir);
    DQr1lir(i)=y(Qr1lir);
    DQr2lir(i)=y(Qr2lir);
    DQr3lir(i)=y(Qr3lir);
    DQr4lir(i)=y(Qr4lir);
    DQr5lir(i)=y(Qr5lir);
    DQr6lir(i)=y(Qr6lir);
    DQr7lir(i)=y(Qr7lir);
    DQr8lir(i)=y(Qr8lir);
```

```
DQr9lir(i)=y(Qr9lir);
    DQr10lir(i)=y(Qr10lir);
    DQhlir(i)=y(Qhlir);

DQlir(i)=y(Qklir)+y(Qr1lir)+y(Qr2lir)+y(Qr3lir)+y(Qr4lir)+y(Qr5lir
)+y(Qr6lir)+y(Qr7lir)+y(Qr8lir)+y(Qr9lir)+y(Qr10lir)+y(Qhlir);
    DQhdiss(i)=y(Qhdiss);
    DQr1diss(i)=y(Qr1diss);
    DQr2diss(i)=y(Qr2diss);
    DQr3diss(i)=y(Qr3diss);
    DQr4diss(i)=y(Qr4diss);
    DQr5diss(i)=y(Qr5diss);
    DQr6diss(i)=y(Qr6diss);
    DQr7diss(i)=y(Qr7diss);
    DQr8diss(i)=y(Qr8diss);
    DQr9diss(i)=y(Qr9diss);
    DQr10diss(i)=y(Qr10diss);
    DQkdiss(i)=y(Qkdiss);

DQdiss(i)=y(Qkdiss)+y(Qr1diss)+y(Qr2diss)+y(Qr3diss)+y(Qr4diss)+y(
Qr5diss)+y(Qr6diss)+y(Qr7diss)+y(Qr8diss)+y(Qr9diss)+y(Qr10diss)+y
(Qhdiss);
    DQshtl(i)=y(Qshtl);
    DReh(i)=y(Reh);
    DRee(i)=y(Ree);
    DRek(i)=y(Rek);
    DRer2(i)=y(Rer2);
    DRer1(i)=y(Rer1);
    DRec(i)=y(Rec);
    Dhh(i)=y(hh);
    Dhe(i)=y(he);
    Dhk(i)=y(hk);
    Dhr1(i)=y(hr1);
    Dhr2(i)=y(hr2);
    Dhc(i)=y(hc);
    DdQr1ext(i)=y(Qr1ext);
    DdQr2ext(i)=y(Qr2ext);
    DdQr3ext(i)=y(Qr3ext);
    DdQr4ext(i)=y(Qr4ext);
    DdQr5ext(i)=y(Qr5ext);
    DdQr6ext(i)=y(Qr6ext);
    DdQr7ext(i)=y(Qr7ext);
    DdQr8ext(i)=y(Qr8ext);
    DdQr9ext(i)=y(Qr9ext);
    DdQr10ext(i)=y(Qr10ext);

DdQrext(i)=(y(Qr1ext)+y(Qr2ext)+y(Qr3ext)+y(Qr4ext)+y(Qr5ext)+y(Qr
6ext)+y(Qr7ext)+y(Qr8ext)+y(Qr9ext)+y(Qr10ext));
    DdQpirrc(i)=y(Wpirrc);
    DdQpirre(i)=y(Wpirre);
    DXp(i) = y(Xp);
    DXd(i) = y(Xd);
    DVelp(i)=y(Velp);
    DVeld(i)=y(Veld);
    DPbounce(i)=y(Pbounce);
```

```
   %fprintf('Xp= %12.9f Xd= %12.9f Vp= %12.9f Vd= %12.9f
\n\n',y(Xp), y(Xd),y(Velp), y(Veld));

            if y(Ph)<0 || y(Pk) <0 || y(Pr1)<0 ||y(Pr2)< 0 ||
y(Pr3)< 0 || y(Pr4)< 0 || y(Pr5)<0 || y(Pr6)< 0 || y(Pr7)< 0 ||
y(Pr8)< 0 || y(Pr9)< 0 || y(Pr10)< 0 || y(Reh)== inf || y(Rek)==
inf
                break;
            end
        end

    fig15=figure(15);
     plot(Ddegree,DXp,'k',Ddegree,DXd,'--')
 xlabel('Crank angle (degree)')
 ylabel('XP,Xd')
 legend ('Xp','Xd');
      end

      if y(Ph)<0 || y(Pk) <0 || y(Pr1)<0 ||y(Pr2)< 0 || y(Pr3)< 0
|| y(Pr4)< 0 || y(Pr5)<0 || y(Pr6)< 0 ||y(Pr7)< 0 || y(Pr8)< 0 ||
y(Pr9)< 0 || y(Pr10)< 0 || y(Reh)== inf || y(Rek)== inf
            error=1;
            break;
      end

        Qr1extcyl=sum(DdQr1ext)*timestep;
        Qr2extcyl=sum(DdQr2ext)*timestep;
        Qr3extcyl=sum(DdQr3ext)*timestep;
Qr4extcyl=sum(DdQr4ext)*timestep;
Qr5extcyl=sum(DdQr5ext)*timestep;
Qr6extcyl=sum(DdQr6ext)*timestep;
Qr7extcyl=sum(DdQr7ext)*timestep;
Qr8extcyl=sum(DdQr8ext)*timestep;
Qr9extcyl=sum(DdQr9ext)*timestep;
Qr10extcyl=sum(DdQr10ext)*timestep;
      Qr1cyl=sum(DdQr1)*timestep ;Qr2cyl=sum(DdQr2)*timestep;
      Qr3cyl=sum(DdQr3)*timestep; Qr4cyl=sum(DdQr4)*timestep;
      Qr5cyl=sum(DdQr5)*timestep; Qr6cyl=sum(DdQr6)*timestep;
      Qr7cyl=sum(DdQr7)*timestep; Qr8cyl=sum(DdQr8)*timestep;
      Qr9cyl=sum(DdQr9)*timestep; Qr10cyl=sum(DdQr10)*timestep;
      QHcyl=sum(DdQH)*timestep;   QCcyl=sum(DdQC)*timestep;

Qrcyl=(Qr1cyl+Qr2cyl+Qr3cyl+Qr4cyl+Qr5cyl+Qr6cyl+Qr7cyl+Qr8cyl+Qr9
cyl+Qr10cyl);

Qrextcyl=(Qr1extcyl+Qr2extcyl+Qr3extcyl+Qr4extcyl+Qr5extcyl+Qr6ext
cyl+Qr7extcyl+Qr8extcyl+Qr9extcyl+Qr10extcyl);
      Pmean=sum(DP*timestep)/tT;
      Xpmax=max(DXp);
      Xdmax=max(DXd);
      Xpmin=min(DXp);
      Xdmin=min(DXd);
      Xpmean=(Xpmax+Xpmin)/2;
      Xdmean=(Xdmax+Xdmin)/2;
      Twc=mean(DTc);
```

```
Wcyle=sum(DdWe)*timestep;
      Wcylc=sum(DdWc)*timestep;
      Wcyli=(Wcyle+Wcylc);
      Pmax=max(DP);
      Poweri=Wcyli*f;           %total cyclic indicated power (W)
      effi=(Poweri/((QHcyl+Qrcyl+Qrextcyl)*f))*100;
      if y(Ph)<0 || y(Pk) <0 || y(Pr1)<0 ||y(Pr2)< 0 || y(Pr3)< 0
|| y(Pr4)< 0 || y(Pr5)<0 || y(Pr6)< 0 ||y(Pr7)< 0 || y(Pr8)< 0 ||
y(Pr9)< 0 || y(Pr10)< 0 || y(Reh)== inf || y(Rek)== inf  %||
isnan(Poweri)==1 || isnan(Pmean)==1 || isreal(Poweri)== 0 ||
Poweri < 0  %|| Wcyle <0
            error=1;
            break;
      else
            error=0;
      end

    fprintf('t= %12.9f  it= %6.3f Xpmax= %12.9f Xdmax= %12.9f
Xpmean= %12.9f Xdmean= %12.9f P= %12.9f Pmax= %12.9f Pmean= %12.9f
QHcyl= %8.8f  Wcyle= %8.8f  QCcyl= %8.8f  Wcylc= %8.8f  Power=
%8.8f   \n\n',t,it,Xpmax, Xdmax,Xpmean, Xdmean,
y(P),Pmax,Pmean,QHcyl,Wcyle,QCcyl,Wcylc,Poweri);
    fprintf('Qr1cyl= %12.9f J Qr2cyl= %6.3f  Qr3cyl= %12.9f
Qr4cyl= %12.5f   Qr5cyl= %6.3f   Qr6cyl= %6.3f  Qr7cyl= %6.3f
Qr8cyl= %6.3f Qr9cyl= %6.3f   Qr10cyl= %6.3f
\n\n',(Qr1cyl+Qr1extcyl),Qr2cyl+Qr2extcyl,Qr3cyl+Qr3extcyl,Qr4cyl+
Qr4extcyl,Qr5cyl+Qr5extcyl,Qr6cyl+Qr6extcyl,Qr7cyl+Qr7extcyl,Qr8cy
l+Qr8extcyl,Qr9cyl+Qr9extcyl,Qr10cyl+Qr10extcyl);
    fprintf('Tm1= %12.9f  Tm2= %6.3f  Tm3= %12.9f  Tm4= %12.5f
Tm5= %6.3f   Tm6= %6.3f  Tm7= %6.3f   Tm8= %6.3f Tm9= %6.3f
Tm10= %6.3f
\n\n',y(Tm1),y(Tm2),y(Tm3),y(Tm4),y(Tm5),y(Tm6),y(Tm7),y(Tm8),y(Tm
9),y(Tm10));


      conv(1)=(y(Te)-Te0); conv(2)=(y(Tc)-Tc0); conv(3)=(y(Tr1)-
Tr1o);
      conv(4)=(y(Tr10)-Tr2o); conv(5)=(y(Th)-Th0); conv(6)=(y(Tk)-
Tk0);
      conv(19)= (Xpmax-Xp0max);    conv(20)= (Xdmax-Xd0max);

      if  it==1
            conv(9)=(Qr1cyl+Qr1extcyl); conv(8)=(Pmean-pO);
            conv(10)=(Qr2cyl+Qr2extcyl);
conv(11)=(Qr3cyl+Qr3extcyl);
            conv(12)=(Qr4cyl+Qr4extcyl);
conv(13)=(Qr5cyl+Qr5extcyl);
            conv(14)=(Qr6cyl+Qr6extcyl);
conv(15)=(Qr7cyl+Qr7extcyl);
            conv(16)=(Qr8cyl+Qr8extcyl);
conv(17)=(Qr9cyl+Qr9extcyl);
            conv(18)=(Qr10cyl+Qr10extcyl);  conv(22)=Xpmean-0;
conv(23)=Xdmean-0;
      else
            convpr(8)=conv(8);  convpr(9)=conv(9);
convpr(10)=conv(10);
```

```
            convpr(11)=conv(11);
convpr(12)=conv(12);convpr(13)=conv(13);
            convpr(14)=conv(14);
convpr(15)=conv(15);convpr(16)=conv(16);
            convpr(17)=conv(17);
convpr(18)=conv(18);convpr(22)=conv(22);convpr(23)=conv(23);
            conv(9)=(Qr1cyl+Qr1extcyl); conv(8)=(Pmean-pO);

conv(10)=(Qr2cyl+Qr2extcyl);conv(11)=(Qr3cyl+Qr3extcyl);

conv(12)=(Qr4cyl+Qr4extcyl);conv(13)=(Qr5cyl+Qr5extcyl);

conv(14)=(Qr6cyl+Qr6extcyl);conv(15)=(Qr7cyl+Qr7extcyl);

conv(16)=(Qr8cyl+Qr8extcyl);conv(17)=(Qr9cyl+Qr9extcyl);
            conv(18)=(Qr10cyl+Qr10extcyl);  conv(22)=Xpmean-0;
conv(23)=Xdmean-0;
      end

conv(21)=abs(conv(9))+abs(conv(10))+abs(conv(11))+abs(conv(12))+ab
s(conv(13))+abs(conv(14))+abs(conv(15))+abs(conv(16))+abs(conv(17)
)+abs(conv(18));




%*****************************************************************
*************************************
      if abs(conv(9))<Cq
            Form3text11=0;
      elseif abs(conv(9))>=Cq  && fix(Form3text11)==0
            Form3text11=1.5;
      elseif (sign(conv(9))~= sign(convpr(9))) &&
abs(conv(9))<=abs(convpr(9))
            Form3text11=Form3text11/10;
      elseif (sign(conv(9))== sign(convpr(9)) )&& abs(conv(9))-
abs(convpr(9))<2
            Form3text11=Form3text11.*3;
      end
      increm1=Form3text11;
      if abs(conv(10))<Cq
            Form3text12=0;
      elseif abs(conv(10))>=Cq  && fix(Form3text12)==0
            Form3text12=1.5;
      elseif (sign(conv(10))~= sign(convpr(10))) &&
abs(conv(10))<=abs(convpr(10))
            Form3text12=Form3text12/10;
      elseif (sign(conv(10))== sign(convpr(10)) )&& abs(conv(10))-
abs(convpr(10))<2
            Form3text12=Form3text12.*2;
      end
      increm2=Form3text12;
      if abs(conv(11))<Cq
            Form3text13=0;
      elseif abs(conv(11))>=Cq  && fix(Form3text13)==0
            Form3text13=1.5;
```

```
      elseif (sign(conv(11))~= sign(convpr(11))) &&
abs(conv(11))<=abs(convpr(11))
            Form3text13=Form3text13/10;
      elseif (sign(conv(11))== sign(convpr(11)) )&& abs(conv(11))-
abs(convpr(11))<2
            Form3text13=Form3text13.*2;
      end
      increm3=Form3text13;
      if abs(conv(12))<Cq
            Form3text14=0;
      elseif abs(conv(12))>=Cq  && fix(Form3text14)==0
            Form3text14=1.5;
      elseif (sign(conv(12))~= sign(convpr(12))) &&
abs(conv(12))<=abs(convpr(12))
            Form3text14=Form3text14/10;
      elseif (sign(conv(12))== sign(convpr(12)) )&& abs(conv(12))-
abs(convpr(12))<2
            Form3text14=Form3text14.*2;
      end
      increm4=Form3text14;
      if abs(conv(13))<Cq
            Form3text15=0;
      elseif abs(conv(13))>=Cq  && fix(Form3text15)==0
            Form3text15=1.5;
      elseif (sign(conv(13))~= sign(convpr(13))) &&
abs(conv(13))<=abs(convpr(13))
            Form3text15=Form3text15/10;
      elseif (sign(conv(13))== sign(convpr(13)) )&& abs(conv(13))-
abs(convpr(13))<2
            Form3text15=Form3text15.*2;
      end
      increm5=Form3text15;
      if abs(conv(14))<Cq
            Form3text16=0;
      elseif abs(conv(14))>=Cq  && fix(Form3text16)==0
            Form3text16=1.5;
      elseif (sign(conv(14))~= sign(convpr(14))) &&
abs(conv(14))<=abs(convpr(14))
            Form3text16=Form3text16/10;
      elseif (sign(conv(14))== sign(convpr(14)) )&& abs(conv(14))-
abs(convpr(14))<2
            Form3text16=Form3text16.*2;
      end
      increm6=Form3text16;
      if abs(conv(15))<Cq
            Form3text17=0;
      elseif abs(conv(15))>=Cq && fix(Form3text17)==0
            Form3text17=1.5;
      elseif (sign(conv(15))~= sign(convpr(15))) &&
abs(conv(15))<=abs(convpr(15))
            Form3text17=Form3text17/10;
      elseif (sign(conv(15))== sign(convpr(15)) )&& abs(conv(15))-
abs(convpr(15))<2
            Form3text17=Form3text17.*2;
      end
```

```
increm7=Form3text17;
      if abs(conv(16))<Cq
            Form3text18=0;
      elseif abs(conv(16))>=Cq  && fix(Form3text18)==0
            Form3text18=1.5;
      elseif (sign(conv(16))~= sign(convpr(16))) &&
abs(conv(16))<=abs(convpr(16))
            Form3text18=Form3text18/10;
      elseif (sign(conv(16))== sign(convpr(16)) )&& abs(conv(16))-
abs(convpr(16))<2
            Form3text18=Form3text18.*2;
      end
      increm8=Form3text18;
      if abs(conv(17))<Cq
            Form3text19=0;
      elseif abs(conv(17))>=Cq  && fix(Form3text19)==0
            Form3text19=1.5;
      elseif (sign(conv(17))~= sign(convpr(17))) &&
abs(conv(17))<=abs(convpr(17))
            Form3text19=Form3text19/10;
      elseif (sign(conv(17))== sign(convpr(17)) )&& abs(conv(17))-
abs(convpr(17))<2
            Form3text19=Form3text19.*2;
      end
      increm9=Form3text19;
      if abs(conv(18))<Cq
            Form3text20=0;
      elseif abs(conv(18))>=Cq  && fix(Form3text20)==0
            Form3text20=1.5;
      elseif (sign(conv(18))~= sign(convpr(18))) &&
abs(conv(18))<=abs(convpr(18))
            Form3text20=Form3text20/10;
      elseif (sign(conv(18))== sign(convpr(18)) )&& abs(conv(18))-
abs(convpr(18))<2
            Form3text20=Form3text20.*2;
      end
      increm10=Form3text20;
      if  (Qr1cyl+Qr1extcyl)>0
            y(Tm1)=y(Tm1)-increm1;
      else
            y(Tm1)=y(Tm1)+increm1;
      end
      if  (Qr2cyl+Qr2extcyl)>0
            y(Tm2)=y(Tm2)-increm2;
      else
            y(Tm2)=y(Tm2)+increm2;
      end
      if  (Qr3cyl+Qr3extcyl)>0
            y(Tm3)=y(Tm3)-increm3;
      else
            y(Tm3)=y(Tm3)+increm3;
      end
      if  (Qr4cyl+Qr4extcyl)>0
            y(Tm4)=y(Tm4)-increm4;
      else
```

```
      y(Tm4)=y(Tm4)+increm4;
      end
      if  (Qr5cyl+Qr5extcyl)>0
            y(Tm5)=y(Tm5)-increm5;
      else
         y(Tm5)=y(Tm5)+increm5;
      end
      if  (Qr6cyl+Qr6extcyl)>0
            y(Tm6)=y(Tm6)-increm6;
      else
            y(Tm6)=y(Tm6)+increm6;
      end
      if  (Qr7cyl+Qr7extcyl)>0
            y(Tm7)=y(Tm7)-increm7;
      else
            y(Tm7)=y(Tm7)+increm7;
      end
      if  (Qr8cyl+Qr8extcyl)>0
            y(Tm8)=y(Tm8)-increm8;
      else
            y(Tm8)=y(Tm8)+increm8;
      end
      if  (Qr9cyl+Qr9extcyl)>0
            y(Tm9)=y(Tm9)-increm9;
      else
            y(Tm9)=y(Tm9)+increm9;
      end
      if  (Qr10cyl+Qr10extcyl)>0
            y(Tm10)=y(Tm10)-increm10;
      else
            y(Tm10)=y(Tm10)+increm10;
      end

      if abs(conv(8))<5000
            Form3text21=0;
      elseif abs(conv(8))>=5000 && abs(conv(8))<10000
            Form3text21=1000;
      elseif abs(conv(8))>=10000 && abs(conv(8))<20000
            Form3text21=2000;
      elseif abs(conv(8))>=20000 && abs(conv(8))<30000
            Form3text21=3000;
      elseif abs(conv(8))>=30000 && abs(conv(8))<40000
            Form3text21=4000;
      elseif abs(conv(8))>=40000 && abs(conv(8))<50000
            Form3text21=5000;
      elseif abs(conv(8))>=50000 && abs(conv(8))<100000
            Form3text21=10000;
      elseif abs(conv(8))>=100000 && abs(conv(8))<500000
            Form3text21=50000;
      elseif abs(conv(8))>=500000
            Form3text21=100000;
      elseif (sign(conv(8))== sign(convpr(8)) )&& abs(conv(8))-
abs(convpr(8))<10000
            Form3text21=Form3text21.*2;
      end
```

```
incremP=Form3text21;
      if  Pmean<pO
            pOnew=pOnew+incremP;
      else
            pOnew=pOnew-incremP;
      end
       abs(conv(22))
      if abs(conv(22))<0.0001
            Form3text22=0;
      elseif abs(conv(22))>=0.0001  && fix(Form3text22)==0
            Form3text22=0.5;
      elseif (sign(conv(22))~= sign(convpr(22))) &&
abs(conv(22))<=abs(convpr(22))
            Form3text22=Form3text22/10;
      %elseif (sign(conv(22))== sign(convpr(22)) )&&
abs(conv(22))-abs(convpr(22))<2
       %    Form3text22=Form3text22.*1.5;
      end


incremXp=Form3text22
       if  Xpmean-0>0
            Cpc=Cpc+incremXp;
       else
            Cpc=Cpc-incremXp;
       end
      Cpc
            abs(conv(23))
      if abs(conv(23))<0.0001
            Form3text23=0;
      elseif abs(conv(23))>=0.0001  && fix(Form3text23)==0
            Form3text23=0.5;
      elseif (sign(conv(23))~= sign(convpr(23))) &&
abs(conv(23))<=abs(convpr(23))
            Form3text23=Form3text23/10;
      end



incremXd=Form3text23
       if  Xdmean-0>0
            CHdc=CHdc+incremXd;
       else
            CHdc=CHdc-incremXd;
       end
      CHdc
      y(P)= pOnew;

      y(mc)=y(P)*y(Vc)/(R*y(Tc)); y(mk)=y(P)*Vk/(R*y(Tk));
      y(mr1)=y(P)*(Vr1)/(R*y(Tr1)); y(mr2)=y(P)*(Vr2)/(R*y(Tr2));
      y(mr3)=y(P)*(Vr3)/(R*y(Tr3)); y(mr4)=y(P)*(Vr4)/(R*y(Tr4));
      y(mr5)=y(P)*(Vr5)/(R*y(Tr5)); y(mr6)=y(P)*(Vr6)/(R*y(Tr6));
      y(mr7)=y(P)*(Vr7)/(R*y(Tr7)); y(mr8)=y(P)*(Vr8)/(R*y(Tr8));
      y(mr9)=y(P)*(Vr9)/(R*y(Tr9));
y(mr10)=y(P)*(Vr10)/(R*y(Tr10));
      y(mh)=y(P)*Vh/(R*y(Th));      y(me)=y(P)*y(Ve)/(R*y(Te));
```

```
      Cq=(QHcyl*0.01);
      Cq2=(Xpmean-0)/(Xpmax-Xpmean);
        Cq3=(Xdmean-0)/(Xdmax-Xdmean);
      it=it+1;
end

if   error ==1
      Pmax=0; Pmin=0;Pmean = 0;
      Wcyl=0;
      Poweri=-99999999999 ;
      Poweri_nodp=-9999999999;Powerb=-999999;
      effb=-100;
      deltaPsummax=0;
else

      QHcyl=sum(DdQH)*timestep;
      Wcyle=sum(DdWe)*timestep;
      Pmean=sum(DP*timestep)/tT;
      Twc=mean(DTc);
      Pmax=max(DP); Pmin=min(DP);
      Wcyle=sum(DdWe*timestep); Wcylc=sum(DdWc*timestep);
      Wcyl=Wcyle+Wcylc;
      Wcyl_nodelP=sum(DdW*timestep);
      Poweri=(Wcyl)*f;
      deltaPsummax=max(DdeltaP);
QHcyl=sum(DdQH)*timestep;
QCcyl=sum(DdQC)*timestep;
Qr1cyl=sum(DdQr1)*timestep;
Qr2cyl=sum(DdQr2)*timestep;
Qr3cyl=sum(DdQr3)*timestep;
Qr4cyl=sum(DdQr4)*timestep;
Qr5cyl=sum(DdQr5)*timestep;
Qr6cyl=sum(DdQr6)*timestep;
Qr7cyl=sum(DdQr7)*timestep;
Qr8cyl=sum(DdQr8)*timestep;
Qr9cyl=sum(DdQr9)*timestep;
Qr10cyl=sum(DdQr10)*timestep;
Qkdisscyl=sum(DQkdiss)*timestep;
Qr1disscyl=sum(DQr1diss)*timestep;
Qr2disscyl=sum(DQr2diss)*timestep;
Qr3disscyl=sum(DQr3diss)*timestep;
Qr4disscyl=sum(DQr4diss)*timestep;
Qr5disscyl=sum(DQr5diss)*timestep;
Qr6disscyl=sum(DQr6diss)*timestep;
Qr7disscyl=sum(DQr7diss)*timestep;
Qr8disscyl=sum(DQr8diss)*timestep;
Qr9disscyl=sum(DQr9diss)*timestep;
Qr10disscyl=sum(DQr10diss)*timestep;
Qhdisscyl=sum(DQhdiss)*timestep;
Qshtlcyl=sum(DQshtl)*timestep;
Qklircyl=sum(DQklir)*timestep;
Qr1lircyl=sum(DQr1lir)*timestep;
Qr2lircyl=sum(DQr2lir)*timestep;
Qr3lircyl=sum(DQr3lir)*timestep;
```

```
Qr4lircyl=sum(DQr4lir)*timestep;
Qr5lircyl=sum(DQr5lir)*timestep;
Qr6lircyl=sum(DQr6lir)*timestep;
Qr7lircyl=sum(DQr7lir)*timestep;
Qr8lircyl=sum(DQr8lir)*timestep;
Qr9lircyl=sum(DQr9lir)*timestep;
Qr10lircyl=sum(DQr10lir)*timestep;
Qhlircyl=sum(DQhlir)*timestep;
Qr1extcyl=sum(DdQr1ext)*timestep;
Qr2extcyl=sum(DdQr2ext)*timestep;
Qr3extcyl=sum(DdQr3ext)*timestep;
Qr4extcyl=sum(DdQr4ext)*timestep;
Qr5extcyl=sum(DdQr5ext)*timestep;
Qr6extcyl=sum(DdQr6ext)*timestep;
Qr7extcyl=sum(DdQr7ext)*timestep;
Qr8extcyl=sum(DdQr8ext)*timestep;
Qr9extcyl=sum(DdQr9ext)*timestep;
Qr10extcyl=sum(DdQr10ext)*timestep;
Qrcyl=(Qr1cyl+Qr2cyl+Qr3cyl+Qr4cyl+Qr5cyl+Qr6cyl+Qr7cyl+Qr8cyl+Qr9
cyl+Qr10cyl);
Qrextcyl=(Qr1extcyl+Qr2extcyl+Qr3extcyl+Qr4extcyl+Qr5extcyl+Qr6ext
cyl+Qr7extcyl+Qr8extcyl+Qr9extcyl+Qr10extcyl);
Qdisscyl=
Qkdisscyl+Qr1disscyl+Qr2disscyl+Qr3disscyl+Qr4disscyl+Qr5disscyl+Q
r6disscyl+Qr7disscyl+Qr8disscyl+Qr9disscyl+Qr10disscyl+Qhdisscyl;
Qlircyl=Qklircyl+Qr1lircyl+Qr2lircyl+Qr3lircyl+Qr4lircyl+Qr5lircyl
+Qr6lircyl+Qr7lircyl+Qr8lircyl+Qr9lircyl+Qr10lircyl+Qhlircyl;
Qlosstotal =Qdisscyl+Qshtlcyl+Qlircyl+Qrextcyl;
Heatbalance=QHcyl+QCcyl+Qrcyl-Qrextcyl-Qdisscyl-Qshtlcyl-Wcyl;
effi=(Poweri/((QHcyl+Qrcyl+Qrextcyl)*f))*100;
%fprintf('j= %12.9f \n',j);
      %print on screen
      printsc=1;
if printsc==1
fprintf('Pmax= %12.9f Pa\n',Pmax);
fprintf('Pmean= %12.9f Pa \n',Pmean);
fprintf('Worke= %12.9f J\n',Wcyle);
fprintf('Workk= %12.9f J\n',Wcylc);
fprintf('Work= %12.9f J\n',Wcyl);
fprintf('Power from PV diagram= %12.9f W\n',Poweri);
fprintf('Heat input= %12.9f J\n',QHcyl);
fprintf('Heat output= %12.9f J\n',QCcyl);
fprintf('Heat regenerator1= %12.9f J\n',Qr1cyl);
fprintf('total Heat regenerator= %12.9f J\n',Qrcyl);
fprintf('K Dissipation loss= %12.9f J\n',Qkdisscyl);
fprintf('Re1 Dissipation loss= %12.9f J\n',Qr1disscyl);
fprintf('Re2 Dissipation loss= %12.9f J\n',Qr2disscyl);
fprintf('H Dissipation loss= %12.9f J\n',Qhdisscyl);
fprintf('total Dissipation loss= %12.9f J\n',Qdisscyl);
fprintf('Shuttle loss= %12.9f J\n',Qshtlcyl);
fprintf('K Internal conduction loss= %12.9f J\n',Qklircyl);
fprintf('R1 Internal conduction loss= %12.9f J\n',Qr1lircyl);
fprintf('R2 Internal conduction loss= %12.9f J\n',Qr2lircyl);
fprintf('H Internal conduction loss= %12.9f J\n',Qhlircyl);
fprintf('total Internal conduction loss= %12.9f J\n',Qlircyl);
```

```
fprintf('total External conduction loss= %12.9f J\n',Qrextcyl);
fprintf('total Qloss  = %12.9f J\n',Qlosstotal);
fprintf('heat balance  = %12.9f\n',Heatbalance);
fprintf('efficiency= %12.9f %\n',effi);
end

%*****************************************************************
*******
 %plot graphs

%*****************************************************************
*******
if graphworking==1
 fig1=figure(1);
 plot(Ddegree,DTe,'b',Ddegree,DTh,'-.',Ddegree,DTr10,'--
',Ddegree,DTr1,'--',Ddegree,DTk,'--
',Ddegree,DTc,'',Ddegree,DTm1,':k',Ddegree,DTm10,':k')
  title('The temperature distribution respect with the crank angle
')
  xlabel('Crank angle (degree)')
  ylabel('Temperature (K)')
  legend ('Te','Th','Tr10','Tr1','Tk','Tc','Tm1','Tm10');

save T-degree.xls Ddegree DTc DTk DTr1 DTr10 DTh DTe DTm1 DTm10 -
ascii;

 fig2=figure(2);
 plot(DVe,DPe,'k',DVc,DPc,'--')
 title('P-V diagram')

 xlabel('Volume (m3)')
  ylabel('Pressure (Pa)')
 legend ('Pe','Pc');
 save P-V.xls DVe DPe DVc DPc -ascii;

 fig3=figure(3);
 plot(Ddegree,DVe,'-',Ddegree,DVc,'--
',Ddegree,Vh,'b',Ddegree,Vr1,'m',Ddegree,Vr10,'g',Ddegree,Vk,'k',D
degree,DVt,'r')
 title('The volume distribution respect with the crank angle')
    xlabel('Crank angle (degree)')
  ylabel('Volume (m3)')
   legend ('Ve','Vc','Vh','Vr1','Vr10','Vk','Vt');
 save V-degree.xls Ddegree DVe DVc DVt -ascii;

 fig4=figure(4);
 plot(Ddegree,DdWe,'r',Ddegree,DdWc,'b',Ddegree,DdW,'y')
  title('Work')
   xlabel('degree')
  ylabel('Workdone (J)')
 legend ('We','Wc','W');
```

```
fig5=figure(5);
  plot(Ddegree,DPe,'k',Ddegree,DPh,'--',Ddegree,DPr1,'-
.',Ddegree,DPr10,'-.',Ddegree,DPk,'b',Ddegree,DPc,'m')
 title('The pressure distribution respect with the crank angle')
     xlabel('Crank angle (degree)')
  ylabel('Pressure (Pa)')
  legend ('Pe','Ph','Pr1','Pr10','Pk','Pc');
  save P-degree.xls Ddegree DPc DPk DPr1 DPr10 DPh DPe -ascii;

fig6=figure(6);
 plot(Ddegree,DdeltaP,'-',Ddegree,DdeltaPr1,'-
.',Ddegree,DdeltaPr,'--
',Ddegree,DdeltaPk,'b',Ddegree,DdeltaPh,'m')
%title('The pressure drop in the regenerator respect with the
crank angle')
 %axis([0 360 -200 200]);
   xlabel('Crank angle (degree)')
  ylabel('Pressure drop (Pa)')
   legend ('delP','delPr1','delPr','delPk','delPh');
  save Pdrop-degree.xls Ddegree DdeltaP DdeltaPk DdeltaPr DdeltaPh
-ascii;

 fig7=figure(7);
  plot(Ddegree,DRee,'k',Ddegree,DReh,'r',Ddegree,DRer1,'-
.',Ddegree,DRer2,'--',Ddegree,DRek,'b',Ddegree,DRec,'m')
 title('The pressure distribution respect with the crank angle')
     xlabel('Crank angle (degree)')
  ylabel('Reynolds Number')
    legend ('Re','Rh','Rr1','Rr2','Rk','Rc');

     fig8=figure(8);
  plot(Ddegree,Dhe,'k',Ddegree,Dhh,'r',Ddegree,Dhr1,'-
.',Ddegree,Dhr2,'--',Ddegree,Dhk,'b',Ddegree,Dhc,'m')
 title('The pressure distribution respect with the crank angle')

  xlabel('Crank angle (degree)')
  ylabel('Heat transfer coefficient (W/m2K)')
  legend ('he','hh','hr1','hr2','hk','hc');

     fig9=figure(9);
  plot(Ddegree,Dme,'k',Ddegree,Dmh,'r',Ddegree,Dmr1,'-
.',Ddegree,Dmr2,'-.',Ddegree,Dmk,'b',Ddegree,Dmc,'m')
 title('The pressure distribution respect with the crank angle')
  xlabel('Crank angle (degree)')
  ylabel('mass (kg)')
  legend ('me','mh','mr1','mr2','mk','mc');

  fig10=figure(10);
  plot(Ddegree,Dmck,'k',Ddegree,Dmkr1,'r',Ddegree,Dmr1r2,'--
',Ddegree,Dmr10h,'-.',Ddegree,Dmhe,'b')
 title('The pressure distribution respect with the crank angle')

  xlabel('Crank angle (degree)')
  ylabel('mass (kg/s)')
  legend ('mck','mkr1','mr1r2','mr10h','mhe');
```

```
fig11=figure(11);
 plot(Ddegree,DVe,'-',Ddegree,DVc,'--')
 title('The volume distribution respect with the crank angle')

  xlabel('Crank angle (degree)')
  ylabel('Volume (m3/s)')
  legend ('Ve','Vc');


 fig12=figure(12);

plot(Ddegree,DdQH,'r',Ddegree,DdQr1,'g',Ddegree,DdQr10,'k',Ddegree
,DdQC,'b')
  title('heat')
  save Q-degree.xls Ddegree DdQH DdQr DdQC DQlir DQdiss DQshtl
DdQrext -ascii;

   fig13=figure(13);
 plot(Ddegree,DXp,'k',Ddegree,DXd,'--')
 title('P-V diagram')

 xlabel('Crank angle (degree)')
  ylabel('XP,Xd')
 legend ('Xp','Xd');

    fig14=figure(14);
 plot(DVt,DP)
  title('P-V diagram')

 xlabel('Total volume')
  ylabel('DP')
 legend ('PV diagram');

    fig15=figure(15);
 plot(Ddegree,DVelp,'k',Ddegree,DVeld,'--')
  title('Velocity of piston and displacer')
  ylabel('VelP,Veld')
 legend ('Velp','Veld');


     fig16=figure(16);
 plot(Ddegree,DVt)
  title('TotalVolume')

 xlabel('degree')
  ylabel('Tvol')
 legend ('Volume');

 figure(17)
plot(DXd,DVeld)
xlabel('displacer displacement(m)')
ylabel('displacer velocity(m/s)')
title('displacer velocity-displacer displacement')
```

```
figure(18)
plot(DXp,DVelp);
xlabel('piston displacement(m)')
ylabel('piston velocity(m/s)')
title('piston velocity-piston displacement')

      fig19=figure(19);
 plot(Ddegree,effi)
  title('efficiency')
 %text(DVe(200),DPe(200),'Pe')
 %text(DVk(200),DPk(200),'Pk')
 xlabel('degree')
  ylabel('Tvol')
 legend ('Volume');
end
end
end
```

Define_y_parameter_FPSE

```
% define_y_parameter_MTD
Xd      =   1;    displacement of displacer [m]
Veld    =   2;    %velocity of displacer [m/s]
Xp      =   3;    %piston displacement [m]
Velp    =   4;     %velocity of piston [m/s]
P       =   5;      % pressure [Pa]
Tm1     =   6;      % temparature of matrix part 1 [K]
Tm2     =   7;      % temparature of matrix part 1 [K]
Tm3     =   8;      % temparature of matrix part 1 [K]
Tm4     =   9;      % temparature of matrix part 1 [K]
Tm5     =   10;      % temparature of matrix part 1 [K]
Tm6     =   11;      % temparature of matrix part 1 [K]
Tm7     =   12;      % temparature of matrix part 1 [K]
Tm8     =   13;      % temparature of matrix part 1 [K]
Tm9     =   14;     % temparature of matrix part 1 [K]
Tm10    =   15;      % temparature of matrix part 1 [K]
mc      =   16;      % mass of compression space [kg]
mk      =  17;      % mass of compression space [kg]
mr1     =  18;      % mass of regenerator space part 1 [kg]
mr2     =  19;      % mass of regenerator space part 2 [kg]
mr3     =  20;      % mass of regenerator space part 3 [kg]
mr4     =  21;      % mass of regenerator space part 4 [kg]
mr5     =  22;      % mass of regenerator space part 5 [kg]
mr6     =  23;      % mass of regenerator space part 6 [kg]
mr7     =  24;      % mass of regenerator space part 7 [kg]
mr8     =  25;      % mass of regenerator space part 8 [kg]
mr9     =  26;      % mass of regenerator space part 9 [kg]
mr10    =  27;      % mass of regenerator space part 10 [kg]
mh      =  28;      % mass of heater space [kg]
me      =  29;      % mass of cooler space [kg]
Pbounce =   30;     %bounce pressure[Pa]
QC      =  31;      % heat flow rate in cooler [W]
```

```
QH      =  32;      % heat flow rate in heater [W]
Qr1     =  33;      % heat flow rate in regenerator part 1 [W]
Qr2     =  34;      % heat flow rate in regenerator part 2 [W]
Qr3     =  35;      % heat flow rate in regenerator part 3 [W]
Qr4     =  36;      % heat flow rate in regenerator part 4 [W]
Qr5     =  37;      % heat flow rate in regenerator part 5 [W]
Qr6     =  38;      % heat flow rate in regenerator part 6 [W]
Qr7     =  39;      % heat flow rate in regenerator part 7 [W]
Qr8     =  40;      % heat flow rate in regenerator part 8 [W]
Qr9     =  41;      % heat flow rate in regenerator part 9 [W]
Qr10    =  42;      % heat flow rate in regenerator part 10[W]
Wc      =  43;      % indicated work by compression space [W]
We      =  44;      % indicated work by expansion space [W]
W       =  45;      % indicated work [W]
Qhdiss  =  46;      % heat dissipation loss in heater [W]
Qr1diss =  47;      % heat dissipation loss in regenerator part 1
[W]
Qr2diss =  48;      % heat dissipation loss in regenerator part 2
[W]
Qr3diss =  49;      % heat dissipation loss in regenerator part 3
[W]
Qr4diss =  50;      % heat dissipation loss in regenerator part 4
[W]
Qr5diss =  51;      % heat dissipation loss in regenerator part 5
[W]
Qr6diss =  52;      % heat dissipation loss in regenerator part 6
[W]
Qr7diss =  53;      % heat dissipation loss in regenerator part 7
[W]
Qr8diss =  54;      % heat dissipation loss in regenerator part 8
[W]
Qr9diss =  55;      % heat dissipation loss in regenerator part 9
[W]
Qr10diss=  56;      % heat dissipation loss in regenerator part 10
[W]
Qkdiss  =  57;      % heat dissipation loss in heater [W]
Qshtl   =  58;      % heat shuttle loss [W]
Qklir   =  59;      % internal heat conduction loss in cooler [W]
Qr1lir  =  60;      % internal heat conduction loss in regenerator
part 1 [W]
Qr2lir  =  61;      % internal heat conduction loss in regenerator
part 2 [W]
Qr3lir  =  62;      % internal heat conduction loss in regenerator
part 3 [W]
Qr4lir  =  63;      % internal heat conduction loss in regenerator
part 4 [W]
Qr5lir  =  64;      % internal heat conduction loss in regenerator
part 5 [W]
Qr6lir  =  65;      % internal heat conduction loss in regenerator
part 6 [W]
Qr7lir  =  66;      % internal heat conduction loss in regenerator
part 7 [W]
Qr8lir  =  67;      % internal heat conduction loss in regenerator
part 8 [W]
Qr9lir  =  68;      % internal heat conduction loss in regenerator
part 9 [W]
```

```
Qr10lir =  69;      % internal heat conduction loss in regenerator
part 10 [W]
Qhlir   =  70;      % internal heat conduction loss in heater [W]
Tc      =  71;      % gas temperature of compression space [K]
Tk      =  72;      % gas temperature of cooler space [K]
Tr1     =  73;      % gas temperature of regnerator part 1 [K]
Tr2     =  74;      % gas temperature of regnerator part 2 [K]
Tr3     =  75;      % gas temperature of regnerator part 3 [K]
Tr4     =  76;      % gas temperature of regnerator part 4 [K]
Tr5     =  77;      % gas temperature of regnerator part 5 [K]
Tr6     =  78;      % gas temperature of regnerator part 6 [K]
Tr7     =  79;      % gas temperature of regnerator part 7 [K]
Tr8     =  80;      % gas temperature of regnerator part 8 [K]
Tr9     =  81;      % gas temperature of regnerator part 9 [K]
Tr10    =  82;      % gas temperature of regnerator part 10 [K]
Th      =  83;      % gas temperature of heater space [K]
Te      =  84;      % gas temperature of expansion space [K]
Vc      =  85;      % gas volume of compression space [m3]
Vt      =  86;      % total gas volume [m3]
Ve      =  87;      % gas volume of expansion space [m3]
Pc      =  88;      % gas pressure of compression space [Pa]
Pk      =  89;      % gas pressure of cooler space [Pa]
Pr1     =  91;      % gas pressure of regenerator space part 1
[Pa]
Pr2     =  92;      % gas pressure of regenerator space part 1
[Pa]
Pr3     =  93;      % gas pressure of regenerator space part 1
[Pa]
Pr4     =  94;      % gas pressure of regenerator space part 1
[Pa]
Pr5     =  95;      % gas pressure of regenerator space part 1
[Pa]
Pr6     =  96;      % gas pressure of regenerator space part 1
[Pa]
Pr7     =  97;      % gas pressure of regenerator space part 1
[Pa]
Pr8     =  98;      % gas pressure of regenerator space part 1
[Pa]
Pr9     =  99;      % gas pressure of regenerator space part 1
[Pa]
Pr10    =  100;      % gas pressure of regenerator space part 1
[Pa]
Ph      =  101;      % gas pressure of heater space [Pa]
Pe      =  102;      % gas pressure of expansion space [Pa]
deltaP  =  103;      % total pressure drop [Pa]
deltaPk =  104;      % pressure drop of cooler [Pa]
deltaPr1    = 105;   % pressure drop of regenerator part 1 [Pa]
deltaPr2    = 106;  % pressure drop of regenerator part 2 [Pa]
deltaPr3    = 107;  % pressure drop of regenerator part 3 [Pa]
deltaPr4    = 108;  % pressure drop of regenerator part 4 [Pa]
deltaPr5    = 109;  % pressure drop of regenerator part 5 [Pa]
deltaPr6    = 110;  % pressure drop of regenerator part 6 [Pa]
deltaPr7    = 111;  % pressure drop of regenerator part 7 [Pa]
deltaPr8    = 112;  % pressure drop of regenerator part 8 [Pa]
deltaPr9    = 113;  % pressure drop of regenerator part 9 [Pa]
```

```
deltaPr10   = 114;  % pressure drop of regenerator part 10 [Pa]
deltaPr     = 115;  % pressure drop of regenerator [Pa]
deltaPh     = 116;  % pressure drop of heater [Pa]
he      =  117;   % heat tansfer coefficient of expansion wall
[W/m2K]
hh      =  118;     % heat tansfer coefficient of heater [W/m2K]
hr1     =  119;     % heat tansfer coefficient of regenerator part
1 [W/m2K]
hr2     =  120;     % heat tansfer coefficient of regenerator part
2 [W/m2K]
hr3     =  121;     % heat tansfer coefficient of regenerator part
3 [W/m2K]
hr4     =  122;     % heat tansfer coefficient of regenerator part
4 [W/m2K]
hr5     =  123;     % heat tansfer coefficient of regenerator part
5 [W/m2K]
hr6     =  124;     % heat tansfer coefficient of regenerator part
6 [W/m2K]
hr7     =  125;     % heat tansfer coefficient of regenerator part
7 [W/m2K]
hr8     =  126;     % heat tansfer coefficient of regenerator part
8 [W/m2K]
hr9     =  127;     % heat tansfer coefficient of regenerator part
9 [W/m2K]
hr10    =  128;     % heat tansfer coefficient of regenerator part
10 [W/m2K]
hk      =  129;     % heat tansfer coefficient of cooler [W/m2K]
hc      =  130;     % heat tansfer coefficient of compression wall
[W/m2K]
mck     =  131;     % mass flow from compression to cooler [kg/s]
mkr1    =  132;     % mass flow from cooler to regenerator part 1
[kg/s]
mr1r2   =  133;     % mass flow from regenerator part 1 to
regenerator part 2 [kg/s]
mr2r3   =  134;     % mass flow from regenerator part 2 to
regenerator part 3 [kg/s]
mr3r4   =  135;     % mass flow from regenerator part 3 to
regenerator part 4 [kg/s]
mr4r5   =  136;     % mass flow from regenerator part 4 to
regenerator part 5 [kg/s]
mr5r6   =  137;     % mass flow from regenerator part 5 to
regenerator part 6 [kg/s]
mr6r7   =  138;     % mass flow from regenerator part 6 to
regenerator part 7 [kg/s]
mr7r8   =  139;     % mass flow from regenerator part 7 to
regenerator part 8 [kg/s]
mr8r9   =  140;     % mass flow from regenerator part 8 to
regenerator part 9 [kg/s]
mr9r10  =  141;     % mass flow from regenerator part 9 to
regenerator part 10 [kg/s]
mr10h   =  142;     % mass flow from regenerator part 10 to heater
[kg/s]
mhe     =  143;     % mass flow from heater to expansion [kg/s]
epsilon =  144;     % effectiveness of regenerator
Wpirre  =  145;     % gas hysteresis loss of expansion space
```

```
Wpirrc  =  146;     % gas hysteresis loss of compression space
Ree     =  147;     % Reynolds number of expansion space
Reh     =  148;     % Reynolds number of heater space
Rer1    =  149;     % Reynolds number of regenerator part 1
Rer2    =  150;     % Reynolds number of regenerator part 2
Rer3    =  151;     % Reynolds number of regenerator part 3
Rer4    =  152;     % Reynolds number of regenerator part 4
Rer5    =  153;     % Reynolds number of regenerator part 5
Rer6    =  154;     % Reynolds number of regenerator part 6
Rer7    =  155;     % Reynolds number of regenerator part 7
Rer8    =  156;     % Reynolds number of regenerator part 8
Rer9    =  157;     % Reynolds number of regenerator part 9
Rer10   =  158;     % Reynolds number of regenerator part 10
Rer     =  159;     % Reynolds number of regenerator
Rek     =  160;     % Reynolds number of cooler space
Rec     =  161;     % Reynolds number of compression space
Tck     =  162;     % gas temperature of mass flow from cooler to
compression space [K]
Tkr1    =  163;     % gas temperature of mass flow from
compression space to regnerator part 1 [K]
Trk     =  164;     % gas temperature of mass flow at interface of
cooler and regnerator [K]
Trr1    =  165;     % gas temperature of mass flow of regnerator
part 1 [K]
Trr2    =  166;     % gas temperature of mass flow of regnerator
part 2 [K]
Trr3    =  167;     % gas temperature of mass flow of regnerator
part 3 [K]
Trr4    =  168;     % gas temperature of mass flow of regnerator
part 4 [K]
Trr5    =  169;    % gas temperature of mass flow of regnerator
part 5 [K]
Trr6    =  170;     % gas temperature of mass flow of regnerator
part 6 [K]
Trr7    =  171;     % gas temperature of mass flow of regnerator
part 7 [K]
Trr8    =  172;     % gas temperature of mass flow of regnerator
part 8 [K]
Trr9    =  173;     % gas temperature of mass flow of regnerator
part 9 [K]
Trh     =  174;     % gas temperature of mass flow at interface of
heater and regnerator [K]
Tr10h   =  175;     % gas temperature of mass flow from regnerator
part 10 to heater [K]
The     =  176;     % gas temperature of mass flow from heater to
expansion space [K]
Qr1ext  =  177;     % External conduction loss of regnerator part
1 [W]
Qr2ext  =  178;     % External conduction loss of regnerator part
2 [W]
Qr3ext  =  179;     % External conduction loss of regnerator part
3 [W]
Qr4ext  =  180;     % External conduction loss of regnerator part
4 [W]
Qr5ext  =  181;     % External conduction loss of regnerator part
5 [W]
```

```
Qr6ext  =  182;     % External conduction loss of regnerator part
6 [W]
Qr7ext  =  183;     % External conduction loss of regnerator part
7 [W]
Qr8ext  =  184;     % External conduction loss of regnerator part
8 [W]
Qr9ext  =  185;     % External conduction loss of regnerator part
9 [W]
Qr10ext =  186;     % External conduction loss of regnerator part
10 [W]
hh1     =  187;     % heat tansfer coefficient of heater area1
[W/m2K]
hh2     =  188;     % heat tansfer coefficient of heater area2
[W/m2K]
Pd      =  189;     %
Pp      =  190;     %
Pdbounce=  191;
```

Objective_function_FPSE

```
function ff=objective_function_FPSE_GA(x)

global_file_FPSE_GA

    for i=1:1:popsize
        Cpc=x(i,1);
        CHdc=x(i,2);
        lh=x(i,3);
        lr=x(i,4);
        lk=x(i,5);
        Dh=x(i,6);
        Dr=x(i,7);
        Deepk=x(i,8);
        Wk=x(i,9);
        poros=x(i,10);
        Dw=x(i,11);
        u=pi*De;
        Nhtube=fix(u/(2*x(i,6)));
        Nktube=fix(u/(2*x(i,9)));
       [Pmax, Pmin,Poweri,effi,deltaPsummax, Pmean]=
FPSE_modelling_quasi_GA;
        fprintf('i=%9.5f f=%9.5f De=%9.5f  Dr=%9.5f    Dc=%9.5f
lh=%9.5f  lr=%9.5f  lk=%9.5f  Wk=%9.5f Dh=%9.5f Deepk=%9.5f
Dw=%9.5f poros=%9.5f Nhtube=%9.5f Nktube=%9.5f  Poweri=%9.5f
eff=%9.5f Pmax=%9.5f Pmin=%9.5f Pmax/Pmin=%9.5f Pmean=%9.5f
deltaPsummax=%9.5f
\n\n',i,f,De,Dr,Dc,lh,lr,lk,Wk,Dh,Deepk,Dw,poros,Nhtube,Nktube,Pow
eri,effi,Pmax, Pmin,Pmax/Pmin,Pmean,deltaPsummax);
        Dpoweri(i,1)=Poweri;
        Deffi(i,1)=effi;
        DNhtube(i,1)=Nhtube;
        DNktube(i,1)=Nktube;
```

```
        DdeltaPsummax(i,1)=deltaPsummax;
    end

 ff = [Dpoweri,Deffi,DNhtube,DNktube,DdeltaPsummax];

end
```

Call_function_FPSE

```
function [y,dy]=cal_function_FPSE(t,y)

%*****************************************************************
*********
%Public parameter
global_file_FPSE
%*****************************************************************
*********
%define y-parameter
define_y_parameter_FPSE
%define_y_parameter_FPSEc
%*****************************************************************
*********
%calculate angles
theta=2*pi*f*t;
thetad= theta;
degree=thetad/pi*180;
%fprintf('theta= %12.9f\n',theta);
%fprintf('degree= %12.9f\n',degree);
%*****************************************************************
*********
if TypeOfheatcof_h ==5
    Dhh=4*(Wh*Deeph)/(2*Wh+2*Deeph)  ;
else
    Dhh=Dh;
end
if TypeOfheatcof_k ==4
    Dhk=4*(Wk*Deepk)/(2*Wk+2*Deepk)  ;
else
    Dhk=Dk;
end
%*****************************************************************
*********
%Calulate Volume
%fprintf('t= %12.9f  degree= %12.9f \n',t,degree);
if TypeOfEngine==2
   Ldead=0.00;
else
   Ldead=Vclc1;
end
DeadspaceE=Vcleh+Vclhr;
if TypeOfEngine==3
   DeadspaceC=Vclrk+Vclkc++Vclc2+Vclc1;
```

```
else
   DeadspaceC=Vclrk+Vclkc+Vclc2;
end

% calculate dispacement and volume type

switch(TypeOfEngine)
%Alfa
    case 1
            y(Ve)=0.5*VswD*(1+cos(theta))+DeadspaceE;
            y(Vc)=0.5*VswP*(1+cos(theta-alfa))+DeadspaceC;
        %    dy(Ve)=-0.5*VswD*(2*pi*f)*sin(theta);
        %    dy(Vc)=-0.5*VswP*(2*pi*f)*sin(theta-alfa);
%Beta
    case 2
            x0=Zc;
            yp0=Ze;
            y(xip)=x0/2*(1+cos(theta-pi/2)); % Displacement of a
power piston
            y(xid)=yp0/2*(1+cos(theta));  % Displacement of a
displacer
           % dy(xip)=-x0/2*sin(theta-pi/2);
            %dy(xid)=-yp0/2*sin(theta);
            kp=Zc/Ze;
            %Vno=VswD/2*((kp^2-2*kp*cos(alfa)+1)^0.5-(1+kp));
            y(Ve)=0.5*VswD*(1+cos(theta))+DeadspaceE;
            y(Vc)=pi*Dc^2/4*(Ze/2*(1-
cos(theta))+Zc/2*(1+cos(theta-alfa))+Ldead)+DeadspaceC;
         %   dy(Ve)=-0.5*VswD*(2*pi*f)*sin(theta);
          %  dy(Vc)=pi*Dc^2/4*(2*pi*f)*(Ze/2*sin(theta)-
Zc/2*sin(theta-alfa));
%Gamma
    case 3
        %Hamonic
            y(Ve)=0.5*VswD*(1+cos(theta))+DeadspaceE;
            y(Vc)=0.5*VswP*(1+cos(theta-alfa))+0.5*(VswD_c)*(1-
cos(theta))+DeadspaceC;
           % dy(Ve)=-0.5*VswD*(2*pi*f)*sin(theta);
           % dy(Vc)=-0.5*VswP*(2*pi*f)*sin(theta-
alfa)+0.5*(VswD_c)*(2*pi*f)*sin(theta);
%Free piston
    case 4
            %calculate displacement and velocity of pistons

            y(Pbounce)=Pmean*(1+((Cap/Cav)*(Ap/Vbo)*y(Xp)));

            y(Pdbounce)=Pmean*(1+((Cap/Cav)*(Adr/Vdo)*y(Xd)));

            CHpc = 0;

            dy(Xd)=y(Veld);

           dy(Veld)= -(CHdc)/Md*y(Veld)+(y(Pc)-
Pmean*(1+((Cap/Cav)*(Adr/Vdo)*y(Xd))))*(Adr/Md)+(y(deltaP)*(Ad/Md)
);
            dy(Xp)=y(Velp);
```

```
           dy(Velp)=-(Cpc+CHpc)/Mp*(y(Velp))+((y(Pc)-
Pmean*(1+((Cap/Cav)*(Ap/Vbo)*y(Xp))))*(Ap/Mp));
            y(Ve)=(EE+y(Xd))*Ad  ;            % expansion space
volume
            y(Vc)=(CC+y(Xp))*Ap-(Ad-Adr)*(y(Xd)); % compression
space volume
            dy(Ve)=(dy(Xd))*Ad;
            dy(Vc)=(dy(Xp)*Ap)-(dy(Xd)*(Ad-Adr));

           % fprintf('Vc= %12.9f\n',y(Vc));
           % fprintf('Ve= %12.9f\n',y(Ve));
            %fprintf('dVc= %12.9f\n',dy(Vc));
            %fprintf('dVe= %12.9f\n',dy(Ve));1
end
%total volume

y(Vt)=y(Vc)+Vk+Vr1+Vr2+Vr3+Vr4+Vr5+Vr6+Vr7+Vr8+Vr9++Vr10+Vh+y(Ve);
%fprintf('y(Vc)= %12.9f   y(Ve)= %12.9f  \n',y(Vc),y(Ve));
%fprintf('dy(Vc)= %12.9f   dy(Ve)= %12.9f  \n',dy(Vc),dy(Ve));
%*****************************************************************
*********
%*****************************************************************
*********
%area
%cross flow area
dhr = 4*poros*Dw/(fshp*(1-poros)); %Hydraulic diameter of matrix
Acc=pi*Dc^2/4;
%Ack=pi*Dhk^2*Nktube/4;
Ack=Deepk*Wk*Nktube;
Acr1=pi*(Dr^2-dr^2)*poros*Nr/4;
Acr2=pi*(Dr^2-dr^2)*poros*Nr/4;
Acr3=pi*(Dr^2-dr^2)*poros*Nr/4;
Acr4=pi*(Dr^2-dr^2)*poros*Nr/4;
Acr5=pi*(Dr^2-dr^2)*poros*Nr/4;
Acr6=pi*(Dr^2-dr^2)*poros*Nr/4;
Acr7=pi*(Dr^2-dr^2)*poros*Nr/4;
Acr8=pi*(Dr^2-dr^2)*poros*Nr/4;
Acr9=pi*(Dr^2-dr^2)*poros*Nr/4;
Acr10=pi*(Dr^2-dr^2)*poros*Nr/4;
if TypeOfheatcof_h==4;
    Ach=pi*(Dho^2-Dhi^2)*Nhtube/4;
else
    Ach=pi*(Dhh^2)*Nhtube/4 ;
    % Ach=Deeph*Wh*Nhtube;
end
Ace=pi*De^2/4;
%*****************************************************************
*********
%%Calculate Surface Area
Atepe=4*y(Ve)/De;
Ateph=pi*Dhh*lh*Nhtube;
%Ateph=(2*Deeph+Wh)*lh*Nhtube;
Atepr1=4*pi*(1-poros)*(Dr^2-dr^2)/4*lr1*Nr/Dw;
Atepr2=4*pi*(1-poros)*(Dr^2-dr^2)/4*lr2*Nr/Dw;
Atepr3=4*pi*(1-poros)*(Dr^2-dr^2)/4*lr3*Nr/Dw;
```

```
Atepr4=4*pi*(1-poros)*(Dr^2-dr^2)/4*lr4*Nr/Dw;
Atepr5=4*pi*(1-poros)*(Dr^2-dr^2)/4*lr5*Nr/Dw;
Atepr6=4*pi*(1-poros)*(Dr^2-dr^2)/4*lr6*Nr/Dw;
Atepr7=4*pi*(1-poros)*(Dr^2-dr^2)/4*lr7*Nr/Dw;
Atepr8=4*pi*(1-poros)*(Dr^2-dr^2)/4*lr8*Nr/Dw;
Atepr9=4*pi*(1-poros)*(Dr^2-dr^2)/4*lr9*Nr/Dw;
Atepr10=4*pi*(1-poros)*(Dr^2-dr^2)/4*lr10*Nr/Dw;
if TypeOfReg==2
    Atepr=0;
    for i=1:NumberOfLayers
        Atepr=Atepr+(dr+i*SpaceBLayers)*pi*lr;
        Atepr=Atepr+(dr+i*SpaceBLayers+Dw)*pi*lr;
    end
    Atepr=Atepr*1.05;
end
%Atepk=pi*Dhk*lk*Nktube;
  Atepk=(2*Deepk+Wk)*lk*Nktube;
Atepc=4*y(Vc)/Dc  ;
%*****************************************************************
*********
%*****************************************************************
*********
%define the temperature of the mass flow rate between the chamber
y(Trk)=(3*y(Tr1)-y(Tr2))/2;
y(Trr1)=(y(Tr1)+y(Tr2))/2;
y(Trr2)=(y(Tr2)+y(Tr3))/2;
y(Trr3)=(y(Tr3)+y(Tr4))/2;
y(Trr4)=(y(Tr4)+y(Tr5))/2;
y(Trr5)=(y(Tr5)+y(Tr6))/2;
y(Trr6)=(y(Tr6)+y(Tr7))/2;
y(Trr7)=(y(Tr7)+y(Tr8))/2;
y(Trr8)=(y(Tr8)+y(Tr9))/2;
y(Trr9)=(y(Tr9)+y(Tr10))/2;
y(Trh)=(3*y(Tr10)-y(Tr9))/2;
%*****************************************************************
*********
if y(mck)>0
   y(Tck)=y(Tc);
else
    y(Tck)=y(Tk);
end

if y(mkr1)>0
    y(Tkr1)=y(Tk);
else
    y(Tkr1)=y(Trk);
end

if y(mr10h)>0
    y(Tr10h)=y(Trh);
else
    y(Tr10h)=y(Th);
end
```

```
if y(mhe)>0
    y(The)=y(Th);
else
    y(The)=y(Te);
end
%*****************************************************************
*********
%*****************************************************************
*********
%*****************************************************************
*********
%main Equation for determining dP inside the engine
dy(P)=1/(Cav*y(Vt))*(R*(y(QH)+y(Qr1)+y(Qr2)+y(Qr3)+y(Qr4)+y(Qr5)+y
(Qr6)+y(Qr7)+y(Qr8)+y(Qr9)+y(Qr10)+y(QC)-y(Qhdiss)-y(Qr1diss)-
y(Qr2diss)-y(Qr3diss)-y(Qr4diss)-y(Qr5diss)-y(Qr6diss)-y(Qr7diss)-
y(Qr8diss)-y(Qr9diss)-y(Qr10diss)-y(Qkdiss)-y(Qshtl))-
Cap*((y(P))*dy(Ve)+(y(P))*dy(Vc)));
%y(Pbounce)=y(P)*(1+(gammaa*(Ap/Vbo)*y(Xp)));
%dy(Pbounce)=dy(P)*(1+(gammaa*(Ap/Vbo)*y(Xp)))+y(P)*((gammaa*(Ap/V
bo)*dy(Xp)));


%conservation of energy for matrix
dy(Tm1)=-(y(epsilon)*y(hr1)*Atepr1*(y(Tm1)-y(Tr1))-
y(Qr1lir))/(Capm*mm1);
dy(Tm2)=-(y(epsilon)*y(hr2)*Atepr2*(y(Tm2)-y(Tr2))-
y(Qr2lir))/(Capm*mm2);
dy(Tm3)=-(y(epsilon)*y(hr3)*Atepr3*(y(Tm3)-y(Tr3))-
y(Qr3lir))/(Capm*mm3);
dy(Tm4)=-(y(epsilon)*y(hr4)*Atepr4*(y(Tm4)-y(Tr4))-
y(Qr4lir))/(Capm*mm4);
dy(Tm5)=-(y(epsilon)*y(hr5)*Atepr5*(y(Tm5)-y(Tr5))-
y(Qr5lir))/(Capm*mm5);
dy(Tm6)=-(y(epsilon)*y(hr6)*Atepr6*(y(Tm6)-y(Tr6))-
y(Qr6lir))/(Capm*mm6);
dy(Tm7)=-(y(epsilon)*y(hr7)*Atepr7*(y(Tm7)-y(Tr7))-
y(Qr7lir))/(Capm*mm7);
dy(Tm8)=-(y(epsilon)*y(hr8)*Atepr8*(y(Tm8)-y(Tr8))-
y(Qr8lir))/(Capm*mm8);
dy(Tm9)=-(y(epsilon)*y(hr9)*Atepr9*(y(Tm9)-y(Tr9))-
y(Qr9lir))/(Capm*mm9);
dy(Tm10)=-(y(epsilon)*y(hr10)*Atepr10*(y(Tm10)-y(Tr10))-
y(Qr10lir))/(Capm*mm10);
%fprintf('dy(P)= %12.9f\n',dy(P));
%*****************************************************************
*********
%Conservation of mass
dy(mc)=-y(mck);
dy(mk)=y(mck)-y(mkr1);
dy(mr1)=y(mkr1)-y(mr1r2);
dy(mr2)=y(mr1r2)-y(mr2r3);
dy(mr3)=y(mr2r3)-y(mr3r4);
dy(mr4)=y(mr3r4)-y(mr4r5);
dy(mr5)=y(mr4r5)-y(mr5r6);
dy(mr6)=y(mr5r6)-y(mr6r7);
```

```
dy(mr7)=y(mr6r7)-y(mr7r8);
dy(mr8)=y(mr7r8)-y(mr8r9);
dy(mr9)=y(mr8r9)-y(mr9r10);
dy(mr10)=y(mr9r10)-y(mr10h);
dy(mh)=y(mr10h)-y(mhe);
dy(me)=y(mhe);
%fprintf('y(mr10h)= %12.9f\n',y(mr10h));
% Total mass
M=y(mc)+y(mk)+y(mr1)+y(mr2)+y(mr3)+y(mr4)+y(mr5)+y(mr6)+y(mr7)+y(m
r8)+y(mr9)+y(mr10)+y(mh)+y(me);
%*****************************************************************
*********
%Conservation of energy of the compression chamber
y(mck) = -1/(R*y(Tck))*(Cav/Cap*y(Vc)*dy(P)+y(P)*dy(Vc));
%Conservation of energy of the cooler
y(mkr1) = 1/(Cap*y(Tkr1))*(y(QC)-y(Qkdiss)-
Cav*Vk/R*dy(P)+y(mck)*Cap*y(Tck));
%fprintf('y(mkr)= %12.9f\n',y(mkr));
%Conservation of energy of the regenerator part 1
y(mr1r2) = 1/(Cap*y(Trr1))*(y(Qr1)-y(Qr1diss)-
Cav*Vr1/R*dy(P)+y(mkr1)*Cap*y(Tkr1));
%fprintf('y(mkr)= %12.9f\n',y(mkr));
%Conservation of energy of the regenerator part 2
y(mr2r3) = 1/(Cap*y(Trr2))*(y(Qr2)-y(Qr2diss)-
Cav*Vr2/R*dy(P)+y(mr1r2)*Cap*y(Trr1));
%Conservation of energy of the regenerator part 3
y(mr3r4) = 1/(Cap*y(Trr3))*(y(Qr3)-y(Qr3diss)-
Cav*Vr3/R*dy(P)+y(mr2r3)*Cap*y(Trr2));
%Conservation of energy of the regenerator part 4
y(mr4r5) = 1/(Cap*y(Trr4))*(y(Qr4)-y(Qr4diss)-
Cav*Vr4/R*dy(P)+y(mr3r4)*Cap*y(Trr3));
%Conservation of energy of the regenerator part 5
y(mr5r6) = 1/(Cap*y(Trr5))*(y(Qr5)-y(Qr5diss)-
Cav*Vr5/R*dy(P)+y(mr4r5)*Cap*y(Trr4));
%Conservation of energy of the regenerator part 6
y(mr6r7) = 1/(Cap*y(Trr6))*(y(Qr6)-y(Qr6diss)-
Cav*Vr6/R*dy(P)+y(mr5r6)*Cap*y(Trr5));
%Conservation of energy of the regenerator part 7
y(mr7r8) = 1/(Cap*y(Trr7))*(y(Qr7)-y(Qr7diss)-
Cav*Vr7/R*dy(P)+y(mr6r7)*Cap*y(Trr6));
%Conservation of energy of the regenerator part 8
y(mr8r9) = 1/(Cap*y(Trr8))*(y(Qr8)-y(Qr8diss)-
Cav*Vr8/R*dy(P)+y(mr7r8)*Cap*y(Trr7));
%Conservation of energy of the regenerator part 9
y(mr9r10) = 1/(Cap*y(Trr9))*(y(Qr9)-y(Qr9diss)-
Cav*Vr9/R*dy(P)+y(mr8r9)*Cap*y(Trr8));
%Conservation of energy of the regenerator part 10
%fprintf('y(Qr10)= %12.9f\n',y(Qr10));
y(mr10h) = 1/(Cap*y(Tr10h))*(y(Qr10)-y(Qr10diss)-
Cav*Vr10/R*dy(P)+y(mr9r10)*Cap*y(Trr9));
%fprintf('y(mkr)= %12.9f\n',y(mkr));
%Conservation of energy of the heater
y(mhe) = 1/(Cap*y(The))*(y(QH)-y(Qhdiss)-
Cav*Vh/R*dy(P)+y(mr10h)*Cap*y(Tr10h));
%fprintf('y(mck)= %12.9f          y(mkr1)= %12.9f   y(mr1r2)=
```

```
%12.9f   y(mr10h)= %12.9f         y(mhe)= %12.9f \n',
y(mck),y(mkr1),y(mr1r2),y(mr10h),y(mhe));
%*****************************************************************
*********
 Tg(1)=y(Tc);
 Tg(2)=y(Tk);
 Tg(3)=y(Tr1);
 Tg(4)=y(Tr2);
 Tg(5)=y(Tr3);
 Tg(6)=y(Tr4);
 Tg(7)=y(Tr5);
 Tg(8)=y(Tr6);
 Tg(9)=y(Tr7);
 Tg(10)=y(Tr8);
 Tg(11)=y(Tr9);
 Tg(12)=y(Tr10);
 Tg(13)=y(Th);
 Tg(14)=y(Te);
for i=1:14
     mu(i)=mu0*(300+Tmu)/(Tg(i)+Tmu)*((Tg(i))/300)^1.5;
     k(i)=k0*(300+Tku)/(Tg(i)+Tku)*((Tg(i))/300)^1.5;
     Prd(i)=Cap*mu(i)/k(i);
end
%Velocity*density
gk=(y(mkr1)+y(mck))/(2*Ack);
gr1=(y(mkr1)+y(mr1r2))/(2*Acr1);
gr2=(y(mr1r2)+y(mr2r3))/(2*Acr2);
gr3=(y(mr2r3)+y(mr3r4))/(2*Acr3);
gr4=(y(mr3r4)+y(mr4r5))/(2*Acr4);
gr5=(y(mr4r5)+y(mr5r6))/(2*Acr5);
gr6=(y(mr5r6)+y(mr6r7))/(2*Acr6);
gr7=(y(mr6r7)+y(mr7r8))/(2*Acr7);
gr8=(y(mr7r8)+y(mr8r9))/(2*Acr8);
gr9=(y(mr8r9)+y(mr9r10))/(2*Acr9);
gr10=(y(mr9r10)+y(mr10h))/(2*Acr10);
gh=(y(mr10h)+y(mhe))/(2*Ach);

%*****************************************************************
*********
%Friction factor of the heat exchanger in the heater chamber
%calculate Reynolds number for heater
y(Reh)=abs(2*(y(mr10h)+y(mhe))/(mu(13)*Nhtube*pi*Dhh));
if isnan(y(Reh))==1
    y(Reh)=inf;
end
if y(Reh)<1
    y(Reh)=1;
end
%fprintf('Reh= %12.9f  gh= %12.9f\n',y(Reh),gh);
switch(TypeOffriction_hk)
    case 1 % Kay&London -unidirectional flow
        if y(Reh)< 2000
                frh=16;
        elseif y(Reh)<= 4000 || y(Reh)>= 2000
                frh=7.3439e-4*y(Reh)^1.3142;
```

```
          elseif y(Reh)> 4000
                frh=0.0791*y(Reh)^0.75;



        end
    case 2 % Frank Incopera -unidirectional flow
        if y(Reh)< 2000
            fh=64/y(Reh);
        elseif y(Reh)<=20000 || y(Reh)>= 2000
            fh=0.316*y(Reh)^-0.25;
        elseif y(Reh)>20000
            fh=0.184*y(Reh)^-0.2;
        end
        frh=fh*y(Reh)/4; % Reynolds friction coefficient
    case 3 %Schulz&Schwendig -oscillation flow
        muheff=mu(13)/(64*100^0.25)*y(Reh)^0.75;
        Reheff=2*pi*f*Dhh^2*(y(Ph)/(R*y(Th)))/muheff;
        if y(Reh)<2000
            fh=64/Reheff;
        else
            fh=(1/(100*y(Reh)))^0.25;
        end
        frh=fh*y(Reh); % Reynolds friction coefficient
end
%*****************************************************************
*********
%Heat transfer coeficient of the heat exchanger in the heater
chamber
switch(TypeOfheatcof_h)
    case 1 %Dittus-Boelter -unidirectional flow
        y(hh)= 0.023*y(Reh)^0.8*Prd(13)^0.4*k(13)/Dhh;
    case 2 % Colburn correlation -unidirectional flow
        if y(Reh)< 3000
             Jh=exp(0.337-0.812*log(y(Reh)));
        elseif y(Reh)<= 4000 || y(Reh)>= 3000
               Jh=0.0021;
        elseif y(Reh)<= 7000 || y(Reh)>= 4000
            Jh=exp(13.31+0.861*log(y(Reh)));
        elseif y(Reh)<= 10000 || y(Reh)>= 7000
            Jh=0.0034;
        elseif  y(Reh)> 10000
            Jh=exp(-3.575-0.229*log(y(Reh)));
        end

y(hh)=Jh*Cap*abs((y(mr10h)+y(mhe))/2)/((Ach)*Prd(13)^(2/3));
    case 3 % Kays&London -unidirectional flow
        y(hh)=frh*mu(13)*Cap/(2*Dhh*Prd(13));
    case 4 % W. M. Kays and H. C. Perkins, in W. M. Rohsenow and
J. P. Hartnett, Eds.,
           %Handbook of Heat Transfer, Chap. 7, McGraw-Hill, New
York, 1972.cited in Incropera, Introduction heat transfer 6th-
concentric tube annulus
        y(hh1)=4.85*k(13)/Dhh;
        %y(hh2)=2.43*(2*Ze*N/60)^(1/3)*(y(Ph)/101325*y(Th))^0.5;
```

```
y(hh2)=0;
    case 5 %
           %Handbook of Heat Transfer, Chap. 7, McGraw-Hill, New
York, 1972.cited in Incropera,
           Nuh=(Deeph/Wh-4)/(8-4)*(5.6-4.44)+4.44;
          if y(Reh)< 2300
              y(hh)= Nuh*k(13)/Dhh;
          else
              y(hh)= 0.023*y(Reh)^0.8*Prd(13)^0.4*k(13)/Dhh;
          end
end
%*****************************************************************
*********
%Heat transfer coeficient of the metrix in the regenerator chamber
%*****************************************************************
*********
switch(TypeOfheatcof_reg)
    case 1  % Tanaka correlation
        y(Rer1)=
(VswD*N*1/(30*Acr1))*(y(P)/(R*y(Tr1)))/(y(P)/(R*y(Te)))*dhr/mu(3);
        y(Rer2)=
(VswD*N*1/(30*Acr2))*(y(P)/(R*y(Tr2)))/(y(P)/(R*y(Te)))*dhr/mu(4);
        y(Rer3)=
(VswD*N*1/(30*Acr3))*(y(P)/(R*y(Tr3)))/(y(P)/(R*y(Te)))*dhr/mu(5);
        y(Rer4)=
(VswD*N*1/(30*Acr4))*(y(P)/(R*y(Tr4)))/(y(P)/(R*y(Te)))*dhr/mu(6);
        y(Rer5)=
(VswD*N*1/(30*Acr5))*(y(P)/(R*y(Tr5)))/(y(P)/(R*y(Te)))*dhr/mu(7);
        y(Rer6)=
(VswD*N*1/(30*Acr6))*(y(P)/(R*y(Tr6)))/(y(P)/(R*y(Te)))*dhr/mu(8);
        y(Rer7)=
(VswD*N*1/(30*Acr7))*(y(P)/(R*y(Tr7)))/(y(P)/(R*y(Te)))*dhr/mu(9);
        y(Rer8)=
(VswD*N*1/(30*Acr8))*(y(P)/(R*y(Tr8)))/(y(P)/(R*y(Te)))*dhr/mu(10)
;
        y(Rer9)=
(VswD*N*1/(30*Acr9))*(y(P)/(R*y(Tr9)))/(y(P)/(R*y(Te)))*dhr/mu(11)
;
        y(Rer10)=
(VswD*N*1/(30*Acr10))*(y(P)/(R*y(Tr10)))/(y(P)/(R*y(Te)))*dhr/mu(1
2);

y(Rer)=(y(Rer1)+y(Rer2)+y(Rer3)+y(Rer4)+y(Rer5)+y(Rer6)+y(Rer7)+y(
Rer8)+y(Rer9)+y(Rer10))/10;
        Nu = 0.33*y(Rer)^0.67;

kaverage=(k(3)+k(4)+k(5)+k(6)+k(7)+k(8)+k(9)+k(10)+k(11)+k(12))/10
;
        y(hr1) = Nu*kaverage/dhr;
        y(hr2) = Nu*kaverage/dhr;
        y(hr3) = Nu*kaverage/dhr;
        y(hr4) = Nu*kaverage/dhr;
        y(hr5) = Nu*kaverage/dhr;
        y(hr6) = Nu*kaverage/dhr;
        y(hr7) = Nu*kaverage/dhr;
```

```
        y(hr8) = Nu*kaverage/dhr;
        y(hr9) = Nu*kaverage/dhr;
        y(hr10) = Nu*kaverage/dhr;

Prdaverage=(Prd(3)+Prd(4)+Prd(5)+Prd(6)+Prd(7)+Prd(8)+Prd(9)+Prd(1
0)+Prd(11)+Prd(12))/10;
        NTU=4*Nu*lr/(Prdaverage*y(Rer)*dhr);
        y(epsilon) = NTU/(NTU+2);

    case 2 %Gedeon&wood -oscillation flow
        y(Rer1)=abs(gr1*dhr/(mu(3)));
        y(Rer2)=abs(gr2*dhr/(mu(4)));
        y(Rer3)=abs(gr3*dhr/(mu(5)));
        y(Rer4)=abs(gr4*dhr/(mu(6)));
        y(Rer5)=abs(gr5*dhr/(mu(7)));
        y(Rer6)=abs(gr6*dhr/(mu(8)));
        y(Rer7)=abs(gr7*dhr/(mu(9)));
        y(Rer8)=abs(gr8*dhr/(mu(10)));
        y(Rer9)=abs(gr9*dhr/(mu(11)));
        y(Rer10)=abs(gr10*dhr/(mu(12)));
        Nur1=(1+0.99*(y(Rer1)*Prd(3))^0.66)*poros^1.79;
        Nur2=(1+0.99*(y(Rer2)*Prd(4))^0.66)*poros^1.79;
        Nur3=(1+0.99*(y(Rer3)*Prd(5))^0.66)*poros^1.79;
        Nur4=(1+0.99*(y(Rer4)*Prd(6))^0.66)*poros^1.79;
        Nur5=(1+0.99*(y(Rer5)*Prd(7))^0.66)*poros^1.79;
        Nur6=(1+0.99*(y(Rer6)*Prd(8))^0.66)*poros^1.79;
        Nur7=(1+0.99*(y(Rer7)*Prd(9))^0.66)*poros^1.79;
        Nur8=(1+0.99*(y(Rer8)*Prd(10))^0.66)*poros^1.79;
        Nur9=(1+0.99*(y(Rer9)*Prd(11))^0.66)*poros^1.79;
        Nur10=(1+0.99*(y(Rer10)*Prd(12))^0.66)*poros^1.79;
        y(hr1) = Nur1*k(3)/dhr;
        y(hr2) = Nur2*k(4)/dhr;
        y(hr3) = Nur3*k(5)/dhr;
        y(hr4) = Nur4*k(6)/dhr;
        y(hr5) = Nur5*k(7)/dhr;
        y(hr6) = Nur6*k(8)/dhr;
        y(hr7) = Nur7*k(9)/dhr;
        y(hr8) = Nur8*k(10)/dhr;
        y(hr9) = Nur9*k(11)/dhr;
        y(hr10) = Nur10*k(12)/dhr;

Nuaverage=(Nur1+Nur2+Nur3+Nur4+Nur5+Nur6+Nur7+Nur8+Nur9+Nur10)/10;

Prdaverage=(Prd(3)+Prd(4)+Prd(5)+Prd(6)+Prd(7)+Prd(8)+Prd(9)+Prd(1
0)+Prd(11)+Prd(12))/10;

y(Rer)=(y(Rer1)+y(Rer2)+y(Rer3)+y(Rer4)+y(Rer5)+y(Rer6)+y(Rer7)+y(
Rer8)+y(Rer9)+y(Rer10))/10;
        NTU=4*Nuaverage*lr/(Prdaverage*y(Rer)*dhr);
        y(epsilon) = NTU/(NTU+1);
end
%*****************************************************************
*********
%Friction factor of the heat exchanger in the cooler chamber
%*****************************************************************
*********
```

```
%calculate Reynolds number for cooler
y(Rek)=abs(2*(y(mkr1)+y(mck))/(mu(2)*Nktube*pi*Dhk));
if isnan(y(Rek))==1
    y(Rek)=inf;
end
if y(Rek)<1
   y(Rek)=1;
end

%fprintf('Rek= %12.9f  gk= %12.9f\n',y(Rek),gk);
switch(TypeOffriction_hk)
    case 1 % Kay&London -unidirectional flow
        if y(Rek)< 2000
            frk=16;
        elseif y(Rek)<= 4000 || y(Rek)>= 2000
            frk=7.3439e-4*y(Rek)^1.3142;
        elseif y(Rek)> 4000
            frk=0.0791*y(Rek)^0.75;
        end
    case 2 % Frank Incopera -unidirectional flow
        if y(Rek)< 2000
            fk=64/y(Rek);
        elseif y(Rek)<=20000 || y(Rek)>= 2000
            fk=0.316*y(Rek)^-0.25;
        elseif y(Rek)>20000
            fk=0.184*y(Rek)^-0.2;
        end
        frk=fk*y(Rek)/4;
     case 3 %Schulz&Schwendig -oscillation flow
        mukeff=mu(2)/(64*100^0.25)*y(Rek)^0.75;
        Rekeff=2*pi*f*Dhk^2*(y(Pk)/(R*y(Tk)))/mukeff;
        if y(Rek)<2000
            fk=64/Rekeff;
        else
            fk=(1/(100*y(Rek)))^0.25;
        end
        frk=fk*y(Rek); % Reynolds friction factor
end
%*****************************************************************
*********
%Heat transfer coeficient of the heat exchanger in the cooler
chamber
%*****************************************************************
*********
switch(TypeOfheatcof_k)
    case 1 %Dittus-Boelter -unidirectional flow
        y(hk)= 0.023*y(Rek)^0.8*Prd(2)^0.3*k(2)/Dhk;
    case 2 % Colburn correlation -unidirectional flow
        if y(Rek)< 3000
            Jk=exp(0.337-0.812*log(y(Rek)));
        elseif y(Rek)<= 4000 || y(Rek)>= 3000
            Jk=0.0021;
        elseif y(Rek)<= 7000 || y(Rek)>= 4000
            Jk=exp(13.31+0.861*log(y(Rek)));
        elseif y(Rek)<= 10000 || y(Rek)>= 7000
```

```
           Jk=0.0034;
        elseif  y(Rek)> 10000
            Jk=exp(-3.575-0.229*log(y(Rek)));
        end

y(hk)=Jk*Cap*abs((y(mkr1)+y(mck))/2)/((Ack)*Prd(2)^(2/3));
    case 3 % Kays&London -unidirectional flow
        y(hk)=frk*mu(2)*Cap/(2*Dhk*Prd(2));
    case 4 %
           %Handbook of Heat Transfer, Chap. 7, McGraw-Hill, New
York, 1972.cited in Incropera,
            Nuk=(Deepk/Wk-4)/(8-4)*(5.6-4.44)+4.44;
        if y(Rek)< 2300
              y(hk)= Nuk*k(2)/Dhk;
        else
              y(hk)= 0.023*y(Rek)^0.8*Prd(2)^0.3*k(2)/Dhk;
        end
end
%*****************************************************************
*********
%*****************************************************************
*********
% Pressure drop calculation
%*****************************************************************
*********
%*****************************************************************
*********
%calculation of Velocity*density
gk=(y(mkr1)+y(mck))/(2*Ack);
gr1=(y(mkr1)+y(mr1r2))/(2*Acr1);
gr2=(y(mr1r2)+y(mr2r3))/(2*Acr2);
gr3=(y(mr2r3)+y(mr3r4))/(2*Acr3);
gr4=(y(mr3r4)+y(mr4r5))/(2*Acr4);
gr5=(y(mr4r5)+y(mr5r6))/(2*Acr5);
gr6=(y(mr5r6)+y(mr6r7))/(2*Acr6);
gr7=(y(mr6r7)+y(mr7r8))/(2*Acr7);
gr8=(y(mr7r8)+y(mr8r9))/(2*Acr8);
gr9=(y(mr8r9)+y(mr9r10))/(2*Acr9);
gr10=(y(mr9r10)+y(mr10h))/(2*Acr10);
gh=(y(mr10h)+y(mhe))/(2*Ach);
%*****************************************************************
*********
%Calulation pressure drop in the regenerator
%*****************************************************************
*********
switch(TypeOffriction_reg)
    case 1
%Tanaka correlation -oscillation flow

Rermax1=(1.042*pi*VswD*N*1/(60*Acr1))*y(P)/(R*y(Tr1))*dhr/mu(3);

Rermax2=(1.042*pi*VswD*N*1/(60*Acr2))*y(P)/(R*y(Tr2))*dhr/mu(4);

Rermax3=(1.042*pi*VswD*N*1/(60*Acr3))*y(P)/(R*y(Tr3))*dhr/mu(5);

Rermax4=(1.042*pi*VswD*N*1/(60*Acr4))*y(P)/(R*y(Tr4))*dhr/mu(6);
```

```
Rermax5=(1.042*pi*VswD*N*1/(60*Acr5))*y(P)/(R*y(Tr5))*dhr/mu(7);

Rermax6=(1.042*pi*VswD*N*1/(60*Acr6))*y(P)/(R*y(Tr6))*dhr/mu(8);

Rermax7=(1.042*pi*VswD*N*1/(60*Acr7))*y(P)/(R*y(Tr7))*dhr/mu(9);

Rermax8=(1.042*pi*VswD*N*1/(60*Acr8))*y(P)/(R*y(Tr8))*dhr/mu(10);

Rermax9=(1.042*pi*VswD*N*1/(60*Acr9))*y(P)/(R*y(Tr9))*dhr/mu(11);


Rermax10=(1.042*pi*VswD*N*1/(60*Acr10))*y(P)/(R*y(Tr10))*dhr/mu(12
);
    fr1=(175/Rermax1+1.6);
    fr2=(175/Rermax2+1.6);
    fr3=(175/Rermax3+1.6);
    fr4=(175/Rermax4+1.6);
    fr5=(175/Rermax5+1.6);
    fr6=(175/Rermax6+1.6);
    fr7=(175/Rermax7+1.6);
    fr8=(175/Rermax8+1.6);
    fr9=(175/Rermax9+1.6);
    fr10=(175/Rermax10+1.6);


DPmax1=0.5*fr1*(1.042*pi*VswD*N*1/(60*Acr1))^2*lr1/dhr*(y(P)/(R*y(
Tr1)));

DPmax2=0.5*fr2*(1.042*pi*VswD*N*1/(60*Acr2))^2*lr2/dhr*(y(P)/(R*y(
Tr2)));

DPmax3=0.5*fr3*(1.042*pi*VswD*N*1/(60*Acr3))^2*lr3/dhr*(y(P)/(R*y(
Tr3)));

DPmax4=0.5*fr4*(1.042*pi*VswD*N*1/(60*Acr4))^2*lr4/dhr*(y(P)/(R*y(
Tr4)));

DPmax5=0.5*fr5*(1.042*pi*VswD*N*1/(60*Acr5))^2*lr5/dhr*(y(P)/(R*y(
Tr5)));

DPmax6=0.5*fr6*(1.042*pi*VswD*N*1/(60*Acr6))^2*lr6/dhr*(y(P)/(R*y(
Tr6)));

DPmax7=0.5*fr7*(1.042*pi*VswD*N*1/(60*Acr7))^2*lr7/dhr*(y(P)/(R*y(
Tr7)));

DPmax8=0.5*fr8*(1.042*pi*VswD*N*1/(60*Acr8))^2*lr8/dhr*(y(P)/(R*y(
Tr8)));

DPmax9=0.5*fr9*(1.042*pi*VswD*N*1/(60*Acr9))^2*lr9/dhr*(y(P)/(R*y(
Tr9)));

DPmax10=0.5*fr10*(1.042*pi*VswD*N*1/(60*Acr10))^2*lr10/dhr*(y(P)/(
R*y(Tr10)));
```

```
 y(deltaPr1) = DPmax1*sin(theta);
    y(deltaPr2) = DPmax2*sin(theta);
    y(deltaPr3) = DPmax3*sin(theta);
    y(deltaPr4) = DPmax4*sin(theta);
    y(deltaPr5) = DPmax5*sin(theta);
    y(deltaPr6) = DPmax6*sin(theta);
    y(deltaPr7) = DPmax7*sin(theta);
    y(deltaPr8) = DPmax8*sin(theta);
    y(deltaPr9) = DPmax9*sin(theta);
    y(deltaPr10) = DPmax10*sin(theta);


    case 2
%Kay&London correlation -unidirectional flow
    y(Rer1)=abs(gr1*dhr/(mu(3)));
    y(Rer2)=abs(gr2*dhr/(mu(4)));
    y(Rer3)=abs(gr3*dhr/(mu(5)));
    y(Rer4)=abs(gr4*dhr/(mu(6)));
    y(Rer5)=abs(gr5*dhr/(mu(7)));
    y(Rer6)=abs(gr6*dhr/(mu(8)));
    y(Rer7)=abs(gr7*dhr/(mu(9)));
    y(Rer8)=abs(gr8*dhr/(mu(10)));
    y(Rer9)=abs(gr9*dhr/(mu(11)));
    y(Rer10)=abs(gr10*dhr/(mu(12)));

    fr1=54+1.43*y(Rer1)^0.78;
    fr2=54+1.43*y(Rer2)^0.78;
    fr3=54+1.43*y(Rer3)^0.78;
    fr4=54+1.43*y(Rer4)^0.78;
    fr5=54+1.43*y(Rer5)^0.78;
    fr6=54+1.43*y(Rer6)^0.78;
    fr7=54+1.43*y(Rer7)^0.78;
    fr8=54+1.43*y(Rer8)^0.78;
    fr9=54+1.43*y(Rer9)^0.78;
    fr10=54+1.43*y(Rer10)^0.78;

    y(deltaPr1) = -((2*fr1*mu(3)*Vr1*gr1*lr1/(y(mr1)*(dhr)^2)));
    y(deltaPr2) = -((2*fr2*mu(4)*Vr2*gr2*lr2/(y(mr2)*(dhr)^2)));
    y(deltaPr3) = -((2*fr3*mu(5)*Vr3*gr3*lr3/(y(mr3)*(dhr)^2)));
    y(deltaPr4) = -((2*fr4*mu(6)*Vr4*gr4*lr4/(y(mr4)*(dhr)^2)));
    y(deltaPr5) = -((2*fr5*mu(7)*Vr5*gr5*lr5/(y(mr5)*(dhr)^2)));
    y(deltaPr6) = -((2*fr6*mu(8)*Vr6*gr6*lr6/(y(mr6)*(dhr)^2)));
    y(deltaPr7) = -((2*fr7*mu(9)*Vr7*gr7*lr7/(y(mr7)*(dhr)^2)));
    y(deltaPr8) = -((2*fr8*mu(10)*Vr8*gr8*lr8/(y(mr8)*(dhr)^2)));
    y(deltaPr9) = -((2*fr9*mu(11)*Vr9*gr9*lr9/(y(mr9)*(dhr)^2)));
    y(deltaPr10) = -
((2*fr10*mu(12)*Vr10*gr10*lr10/(y(mr10)*(dhr)^2)));
%*************************************************************
*********
    case 3 % Gedeon&Wood oscillation flow
        y(Rer1)=abs(gr1*dhr/(mu(3)));
        y(Rer2)=abs(gr2*dhr/(mu(4)));
        y(Rer3)=abs(gr3*dhr/(mu(5)));
        y(Rer4)=abs(gr4*dhr/(mu(6)));
        y(Rer5)=abs(gr5*dhr/(mu(7)));
```

```
        y(Rer6)=abs(gr6*dhr/(mu(8)));
        y(Rer7)=abs(gr7*dhr/(mu(9)));
        y(Rer8)=abs(gr8*dhr/(mu(10)));
        y(Rer9)=abs(gr9*dhr/(mu(11)));
        y(Rer10)=abs(gr10*dhr/(mu(12)));
        frf1=129/y(Rer1)+2.91/y(Rer1)^0.103;
        frf2=129/y(Rer2)+2.91/y(Rer2)^0.103;
        frf3=129/y(Rer3)+2.91/y(Rer3)^0.103;
        frf4=129/y(Rer4)+2.91/y(Rer4)^0.103;
        frf5=129/y(Rer5)+2.91/y(Rer5)^0.103;
        frf6=129/y(Rer6)+2.91/y(Rer6)^0.103;
        frf7=129/y(Rer7)+2.91/y(Rer7)^0.103;
        frf8=129/y(Rer8)+2.91/y(Rer8)^0.103;

        frf9=129/y(Rer9)+2.91/y(Rer9)^0.103;
        frf10=129/y(Rer10)+2.91/y(Rer10)^0.103;
        fr1=frf1*y(Rer1)/4;
        fr2=frf2*y(Rer2)/4;
        fr3=frf3*y(Rer3)/4;
        fr4=frf4*y(Rer4)/4;
        fr5=frf5*y(Rer5)/4;
        fr6=frf6*y(Rer6)/4;
        fr7=frf7*y(Rer7)/4;
        fr8=frf8*y(Rer8)/4;
        fr9=frf9*y(Rer9)/4;
        fr10=frf10*y(Rer10)/4;
    y(deltaPr1) = -((2*fr1*mu(3)*Vr1*gr1*lr1/(y(mr1)*(dhr)^2)));
    y(deltaPr2) = -((2*fr2*mu(4)*Vr2*gr2*lr2/(y(mr2)*(dhr)^2)));
    y(deltaPr3) = -((2*fr3*mu(5)*Vr3*gr3*lr3/(y(mr3)*(dhr)^2)));
    y(deltaPr4) = -((2*fr4*mu(6)*Vr4*gr4*lr4/(y(mr4)*(dhr)^2)));
    y(deltaPr5) = -((2*fr5*mu(7)*Vr5*gr5*lr5/(y(mr5)*(dhr)^2)));
    y(deltaPr6) = -((2*fr6*mu(8)*Vr6*gr6*lr6/(y(mr6)*(dhr)^2)));
    y(deltaPr7) = -((2*fr7*mu(9)*Vr7*gr7*lr7/(y(mr7)*(dhr)^2)));
    y(deltaPr8) = -((2*fr8*mu(10)*Vr8*gr8*lr8/(y(mr8)*(dhr)^2)));
    y(deltaPr9) = -((2*fr9*mu(11)*Vr9*gr9*lr9/(y(mr9)*(dhr)^2)));
    y(deltaPr10) = -
((2*fr10*mu(12)*Vr10*gr10*lr10/(y(mr10)*(dhr)^2)));
%*************************************************************
*********
end
y(deltaPr)=y(deltaPr1)+y(deltaPr2)+y(deltaPr3)+y(deltaPr4)+y(delta
Pr5)+y(deltaPr6)+y(deltaPr7)+y(deltaPr8)+y(deltaPr9)+y(deltaPr10);
%y(deltaPr)=0;
y(deltaPr1)=y(deltaPr)/10;
y(deltaPr2)=y(deltaPr)/10;
y(deltaPr3)=y(deltaPr)/10;
y(deltaPr4)=y(deltaPr)/10;
y(deltaPr5)=y(deltaPr)/10;
y(deltaPr6)=y(deltaPr)/10;
y(deltaPr7)=y(deltaPr)/10;
y(deltaPr8)=y(deltaPr)/10;
y(deltaPr9)=y(deltaPr)/10;
y(deltaPr10)=y(deltaPr)/10;
%*************************************************************
*********
```

```
%Calculate pressure drop in the heater
y(deltaPh) = -((2*frh*mu(13)*Vh*gh*lh/(y(mh)*(Dhh)^2)));
%y(deltaPh)=0;
%Calculate pressure drop in the cooler
y(deltaPk) = -((2*frk*mu(2)*Vk*gk*lk/(y(mk)*(Dhk)^2)));
%y(deltaPk)=0;
%Calculate total pressure drop
y(deltaP)=y(deltaPk)+ y(deltaPr)+y(deltaPh);
%y(deltaP)=0;
%fprintf('y(deltaPk)= %12.9f     y(deltaPr)= %12.9f
y(deltaPh)= %12.9f\n',y(deltaPk),y(deltaPr),y(deltaPh));
%*****************************************************************
*********
%calculating the pressure
%fprintf('y(Pc)= %12.9f          y(Pk)= %12.9f        y(Pr5)=
%12.9f         y(Ph)= %12.9f          y(Pc)= %12.9f  \n',
y(Pc),y(Pk),y(Pr5),y(Ph),y(Pe));
y(Pc)= y(P);
y(Pk)= y(Pc)+y(deltaPk)/2;
y(Pr1)=y(Pk)+y(deltaPk)/2+y(deltaPr1)/2;
y(Pr2)=y(Pr1)+y(deltaPr1)/2+y(deltaPr2)/2;
y(Pr3)=y(Pr2)+y(deltaPr2)/2+y(deltaPr3)/2;
y(Pr4)=y(Pr3)+y(deltaPr3)/2+y(deltaPr4)/2;
y(Pr5)=y(Pr4)+y(deltaPr4)/2+y(deltaPr5)/2;
y(Pr6)=y(Pr5)+y(deltaPr5)/2+y(deltaPr6)/2;
y(Pr7)=y(Pr6)+y(deltaPr6)/2+y(deltaPr7)/2;
y(Pr8)=y(Pr7)+y(deltaPr7)/2+y(deltaPr8)/2;
y(Pr9)=y(Pr8)+y(deltaPr8)/2-y(deltaPr9)/2;
y(Pr10)=y(Pr9)+y(deltaPr9)/2+y(deltaPr10)/2;
y(Ph)= y(Pr10)+y(deltaPr10)/2+y(deltaPh)/2;
y(Pe)= y(Ph)+y(deltaPh)/2;
%fprintf('y(Pc)= %12.9f          y(Pk)= %12.9f        y(Pr1)=
%12.9f   y(Pr2)= %12.9f    y(Pr3)= %12.9f   y(Pr4)= %12.9f
y(Pr5)= %12.9f   y(Pr6)= %12.9f    y(Pr7)= %12.9f   y(Pr8)= %12.9f
y(Pr9)= %12.9f   y(Pr10)= %12.9f        y(Ph)= %12.9f
y(Pe)= %12.9f  \n',
y(Pc),y(Pk),y(Pr1),y(Pr2),y(Pr3),y(Pr4),y(Pr5),y(Pr6),y(Pr7),y(Pr8
),y(Pr9),y(Pr10),y(Ph),y(Pe));
%*****************************************************************
*********
%calculating the temperature
%Ideal gas equation
y(Tc)=y(Pc)*y(Vc)/(R*y(mc));
y(Tk)=y(Pk)*Vk/(R*y(mk));
y(Tr1)=y(Pr1)*Vr1/(R*y(mr1));
y(Tr2)=y(Pr2)*Vr2/(R*y(mr2));
y(Tr3)=y(Pr3)*Vr3/(R*y(mr3));
y(Tr4)=y(Pr4)*Vr4/(R*y(mr4));
y(Tr5)=y(Pr5)*Vr5/(R*y(mr5));
y(Tr6)=y(Pr6)*Vr6/(R*y(mr6));
y(Tr7)=y(Pr7)*Vr7/(R*y(mr7));
y(Tr8)=y(Pr8)*Vr8/(R*y(mr8));
y(Tr9)=y(Pr9)*Vr9/(R*y(mr9));
y(Tr10)=y(Pr10)*Vr10/(R*y(mr10));
y(Th)=y(Ph)*Vh/(R*y(mh));
y(Te)=y(Pe)*y(Ve)/(R*y(me));
```

```
%fprintf('y(Tc)= %12.9f          y(Tk)= %12.9f        y(Tr10)=
%12.9f
%y(Tr2)= %12.9f        y(Th)= %12.9f          y(Te)= %12.9f  \n',
y(Tc),y(Tk),y(Tr10),y(Tr2),y(Th),y(Te));
%*****************************************************************
*********
%*****************************************************************
*********
%Internal losses
Ak=pi*Dhk*0.001*Nktube;
Ah=pi*Dhh*0.0015*Nhtube;
Ar=pi*(Dr^2-dr^2)/4*Nr;
Ins=1;


if Ins==1
y(Qklir)= kC*(Ak)/lk*(y(Tkr1)-y(Tck));
y(Qr1lir)= kr*(Ar*(1-poros))/lr1*(y(Trr1)-y(Tkr1));
y(Qr2lir)= kr*(Ar*(1-poros))/lr2*(y(Trr2)-y(Trr1));
y(Qr3lir)= kr*(Ar*(1-poros))/lr3*(y(Trr3)-y(Trr2));
y(Qr4lir)= kr*(Ar*(1-poros))/lr4*(y(Trr4)-y(Trr3));
y(Qr5lir)= kr*(Ar*(1-poros))/lr5*(y(Trr5)-y(Trr4));
y(Qr6lir)= kr*(Ar*(1-poros))/lr6*(y(Trr6)-y(Trr5));
y(Qr7lir)= kr*(Ar*(1-poros))/lr7*(y(Trr7)-y(Trr6));
y(Qr8lir)= kr*(Ar*(1-poros))/lr8*(y(Trr8)-y(Trr7));
y(Qr9lir)= kr*(Ar*(1-poros))/lr9*(y(Trr9)-y(Trr8));
y(Qr10lir)= kr*(Ar*(1-poros))/lr10*(y(Tr10h)-y(Trr9));
y(Qhlir)= kH*(Ah)/lh*(y(The)-y(Trh));
else
y(Qklir)= 0;
y(Qr1lir)= 0;
y(Qr2lir)= 0;
y(Qr3lir)= 0;
y(Qr4lir)= 0;
y(Qr5lir)= 0;
y(Qr6lir)= 0;
y(Qr7lir)= 0;
y(Qr8lir)= 0;
y(Qr9lir)= 0;
y(Qr10lir)= 0;
y(Qhlir)= 0;
end
%*****************************************************************
*********
%Shuttle losses
y(Qshtl)=0;
%Dissipation losses
y(Qkdiss) = -(y(deltaPk)*gk*Ack/(y(Pk)/(R*y(Tk))));
y(Qr1diss) = -(y(deltaPr1)*gr1*Acr1/(y(Pr1)/(R*y(Tr1))));
y(Qr2diss) = -(y(deltaPr2)*gr2*Acr2/(y(Pr2)/(R*y(Tr2))));
y(Qr3diss) = -(y(deltaPr3)*gr3*Acr3/(y(Pr3)/(R*y(Tr3))));
y(Qr4diss) = -(y(deltaPr4)*gr4*Acr4/(y(Pr4)/(R*y(Tr4))));
y(Qr5diss) = -(y(deltaPr5)*gr5*Acr5/(y(Pr5)/(R*y(Tr5))));
y(Qr6diss) = -(y(deltaPr6)*gr6*Acr6/(y(Pr6)/(R*y(Tr6))));
y(Qr7diss) = -(y(deltaPr7)*gr7*Acr7/(y(Pr7)/(R*y(Tr7))));
y(Qr8diss) = -(y(deltaPr8)*gr8*Acr8/(y(Pr8)/(R*y(Tr8))));
```

```
y(Qr9diss) = -(y(deltaPr9)*gr9*Acr9/(y(Pr9)/(R*y(Tr9))));
y(Qr10diss) = -(y(deltaPr10)*gr10*Acr10/(y(Pr10)/(R*y(Tr10))));
y(Qhdiss) = -(y(deltaPh)*gh*Ach/(y(Ph)/(R*y(Th))));
%*****************************************************************
*********
%*****************************************************************
*********
%Heat input
if TypeOfheatcof_h==4
    y(QH)=y(hh1)*Ateph1*(Twh-y(Th))+y(hh2)*Ateph2*(Twh-y(Th))-
y(Qhlir);
else
    y(QH)=y(hh)*Ateph*(Twh-y(Th))-y(Qhlir);
end


%Heat tranfer in the regenerator
y(Qr1)=y(epsilon)*y(hr1)*Atepr1*(y(Tm1)-y(Tr1))-y(Qr1lir);
y(Qr2)=y(epsilon)*y(hr2)*Atepr2*(y(Tm2)-y(Tr2))-y(Qr2lir);
y(Qr3)=y(epsilon)*y(hr3)*Atepr3*(y(Tm3)-y(Tr3))-y(Qr3lir);
y(Qr4)=y(epsilon)*y(hr4)*Atepr4*(y(Tm4)-y(Tr4))-y(Qr4lir);
y(Qr5)=y(epsilon)*y(hr5)*Atepr5*(y(Tm5)-y(Tr5))-y(Qr5lir);

y(Qr6)=y(epsilon)*y(hr6)*Atepr6*(y(Tm6)-y(Tr6))-y(Qr6lir);
y(Qr7)=y(epsilon)*y(hr7)*Atepr7*(y(Tm7)-y(Tr7))-y(Qr7lir);
y(Qr8)=y(epsilon)*y(hr8)*Atepr8*(y(Tm8)-y(Tr8))-y(Qr8lir);
y(Qr9)=y(epsilon)*y(hr9)*Atepr9*(y(Tm9)-y(Tr9))-y(Qr9lir);
y(Qr10)=y(epsilon)*y(hr10)*Atepr10*(y(Tm10)-y(Tr10))-y(Qr10lir);
%Heat output
y(QC)=y(hk)*Atepk*(Twk-y(Tk))-y(Qklir);
%*****************************************************************
********
% External heat loss at regenerator
y(Qr1ext)=(1-y(epsilon))*(y(hr1)*Atepr1*(y(Tm1)-y(Tr1)));
y(Qr2ext)=(1-y(epsilon))*(y(hr2)*Atepr2*(y(Tm2)-y(Tr2)));
y(Qr3ext)=(1-y(epsilon))*(y(hr3)*Atepr3*(y(Tm3)-y(Tr3)));
y(Qr4ext)=(1-y(epsilon))*(y(hr4)*Atepr4*(y(Tm4)-y(Tr4)));
y(Qr5ext)=(1-y(epsilon))*(y(hr5)*Atepr5*(y(Tm5)-y(Tr5)));
y(Qr6ext)=(1-y(epsilon))*(y(hr6)*Atepr6*(y(Tm6)-y(Tr6)));
y(Qr7ext)=(1-y(epsilon))*(y(hr7)*Atepr7*(y(Tm7)-y(Tr7)));
y(Qr8ext)=(1-y(epsilon))*(y(hr8)*Atepr8*(y(Tm8)-y(Tr8)));
y(Qr9ext)=(1-y(epsilon))*(y(hr9)*Atepr9*(y(Tm9)-y(Tr9)));
y(Qr10ext)=(1-y(epsilon))*(y(hr10)*Atepr10*(y(Tm10)-y(Tr10)));
%power from the compression space
y(Wc) = y(Pc)*dy(Vc);
%power from the expansion space
y(We) = y(Pe)*dy(Ve);
dy(Vt)=dy(Ve)+dy(Vc);
y(W)=y(P)*dy(Vt);
%*****************************************************************
*********
end
```

Rk4

```
function [x, y, dy] = rk4(deriv,n,x,dx,y)
%Classical fourth order Runge-Kutta method
%Integrates n first order differential equations
%dy(x,y) over interval x to x+dx
%Israel Urieli - Jan 21, 2002
x0 = x;
y0 = y;
[y,dy1] = feval(deriv,x0,y);
for i = 1:n
    y(i) = y0(i) + 0.5*dx*dy1(i);
end
xm = x0 + 0.5*dx;
[y,dy2] = feval(deriv,xm,y);
for i = 1:n
    y(i) = y0(i) + 0.5*dx*dy2(i);
end
[y,dy3] = feval(deriv,xm,y);
for i = 1:n
    y(i) = y0(i) + dx*dy3(i);
end
x = x0 + dx;
[y,dy] = feval(deriv,x,y);
for i = 1:n
    dy(i) = (dy1(i) + 2*(dy2(i) + dy3(i)) + dy(i))/6;
    y(i) = y0(i) + dx*dy(i);
end
```

Appendix A Continuation - MATLAB codes for the second order mathematical model of the adiabatic free piston Stirling engine

The developed model consists of different codes in each subprogram:

FPSE_modelling_adiabatic

```
% Second-order model of the Free piston Stirling engine based on
% Adiabatic model by Urieli [1984]and Timoumi et.al [2008]
% main file for analysis of working process and prediction of
power output
% Engine space is divided into five main spaces-one compression
space, one
% cooler space, one regenerator spaces, one heater space and one
expansion space
% edited by Ayodeji Sowale
% last modified 11.09.2015


%Public parameter
global_file_adiabatic
%*****************************************************************
*********
%define y-parameter
define_y_parameter_adiabatic
%*****************************************************************
*********
%inputdata
inputdata_adiabatic
%*****************************************************************
*********
%initial condition
t=0;y(P)=pO;
Pmean=pO;
y(Xd)=0.01233;
y(Veld)=0;
y(Xp)=0.01145;
y(Velp)=0;
theta=0;
y(Pbounce)=pb;

degree=theta*180/pi;
t=t+dt;
theta=2*pi*freq*t;

%calculate volume
y(Ve)=(0.025+y(Xd))*Ad;                % expansion space volume
y(Vc)=(0.05+y(Xp))*Ap-(Ad*(y(Xd)));    %comp
```

```
%y(Vt)=y(Ve)+Vh+Vr+Vk+y(Vc);
%mass
y(mc)=(y(P).*y(Vc))/(R*y(Tc));
y(mk)=(y(P).*Vk)/(R*Tk);
y(mr)=(y(P).*Vr)/(R*Tr);
y(mh)=(y(P).*Vh)/(R*Th);
y(me)=(y(P).*y(Ve))/(R*y(Te));

Minit=((y(P)*y(Ve))/(R*(y(Te)-
100)))+((y(P)*Vh)/(R*Th))+((y(P)*Vr)/(R*Tr))+((y(P)*Vk)/(R*Tk))+((
y(P)*y(Vc))/(R*(y(Tc)-100)));
Mass=y(mc)+y(mk)+y(mr)+y(me)+y(mh);

y(mck)= 0.0001;
y(mkr)=0.0001;
y(mhe)=0.0001;
y(mrh)=0.0001;
%calculating temperature
y(tempe)=(y(P).*y(Ve))/(R*y(me));
y(tempc)=(y(P).*y(Vc))/(R*y(mc));

%calculate workdone
%calculate workdone
y(We)=0;
y(Wc)=0;
dy(We)=0;
dy(Wc)=0;

conv(1)=1; conv(2)=1;
conv(3)=1000000;conv(4)=1;conv(5)=1;conv(6)=1000000;
Form3text21=0;
pOnew=pO;
Xpmax=y(Xp);
Xdmax=y(Xd);
it= 1;
t=0;

while (abs(conv(1))>=0.1 || abs(conv(2))>=0.1
||abs(conv(3))>=5000|| abs(conv(4))>=0.01 ||abs(conv(5))>=0.01)&&
it <=94
    fprintf('it = %6.3f\n',it)
    cycle_No = 1;
    for j=1:1:cycle
        fprintf('cycle = %6.3f\n',cycle_No)
        Te0=y(Te); Tc0=y(Tc); Xp0max=Xpmax; Xd0max=Xdmax;
        Pmean0=Pmean;
        for i=1:1:numberoftimestep
            [t,y,dy]=rk4('CONVCALL_FUNCTION',12,t,dt,y);
            %fprintf('numberoftimestep =  %12.9f  t= %12.9f   P=
%12.5f      Te= %6.3f    Tc= %6.3f      Xp= %6.3f      Velp= %8.8f
mk= %8.8f\n\n',i,t,y(P),y(Te),y(Tc),y(Xp),y(Velp),y(mk));
            %fprintf('Xd= %12.9f   Veld=
%12.5f\n\n',y(Xd),y(Velp));
            theta=2*pi*freq*t;degree=theta*180/pi;
            time(i)=t;
            DXd(i)=y(Xd);
            DXp(i)=y(Xp);
```

```
            DVeld(i)=y(Veld);
            DVelp(i)=y(Velp);
            DVc(i)=y(Vc);
            DVe(i)=y(Ve);
            DdVc(i)=dy(Vc);
            DdVe(i)=dy(Ve);
            DTc(i)=y(Tc);
            DTe(i)=y(Te);
            DdTc(i)=dy(Tc);
            DdTe(i)=dy(Te);
            DnTk(i)=y(nTk);
            DnTr(i)=y(nTr);
            DnTh(i)=y(nTh);
            DP(i)=y(P);
            DdP(i)=dy(P);
            DPbounce(i)=y(Pbounce);
            %DdPbounce(i)=dy(Pbounce);
            Ddegree(i)=degree;
            Dtheta(i)=theta;
            DVt(i)=y(Vt);
            Dtempe(i)=y(tempe);
            Dtempc(i)=y(tempc);
            DdWe(i)=y(We);
            DdWc(i)=y(Wc);
            DQk(i)=y(Qk);
            DQr(i)=y(Qr);
            DQh(i)=y(Qh);
            Dmc(i)=y(mc);
            Dmh(i)=y(mh);
            Dmr(i)=y(mr);
            Dmk(i)=y(mk);
            Dme(i)=y(me);

        end
        Pmean=sum(DP*timestep)/tT;
        Pmax=max(DP);
        Wexp=sum(DdWe)*timestep;
        Wcomp=sum(DdWc)*timestep;
        Twork=Wexp+Wcomp;
        IndicatedPower=Twork*freq;
        Xpmax = max(DXp);
        Xdmax = max(DXd);
        Tcmax= max(DTc);
        Temax= max(DTe);
        fprintf('t =   %12.9f Wexp = %12.9f Wcomp = %12.9f  Pi =
%12.9f Xpmax = %12.9f Xdmax = %12.9f Pmax = %12.9f Tcmax = %12.9f
Temax = %12.9f W\n',t
,Wexp,Wcomp,IndicatedPower,Xpmax,Xdmax,Pmax,Tcmax,Temax);
        conv(1)=(y(Te)-Te0)/Te0; conv(2)=(y(Tc)-Tc0)/Tc0;
conv(3)=(Pmean-Pmean0); conv(4)=(Xpmax-Xp0max)/Xp0max;
conv(5)=(Xdmax-Xd0max)/Xd0max; conv(6)=(Pmean-pO);
        fprintf('conv(1) =   %12.9f conv(2)= %12.9f conv(3) =
%12.9f  conv(4) =  %12.9f conv(5) =  %12.9f conv(6) =
%12.9f\n',conv(1),conv(2),conv(3),conv(4),conv(5),conv(6));
        cycle_No = cycle_No+1;
    end
```

```
    it=it+1;

disp('tttttttttttttttttttttttttttttttttttttttttttttttttttttttttttt
tttt')
end

    %fprintf('t =   %12.9f Wexp = %12.9f Wcomp = %12.9f  Pi =
%12.9f  W\n',t ,Wexp,Wcomp,IndicatedPower);


 %#######################################################
fprintf('Work in expansion= %12.9f J\n',Wexp);
fprintf('Work in compression= %12.9f J\n',Wcomp);
fprintf('Total Workdone= %12.9f J\n',Twork);
fprintf('Power from the P-V diagram= %12.9f W\n',IndicatedPower);


figure (1)
plot(time,DXd);
%axis([0 0.6 0 360])
%degree = 0:10:360;
%plot(degree,DXd)
xlabel('time')
ylabel('Xd(m)')
%axis([0 360 0 4.5E-2 ])
title('displacer position')

figure(2)
plot(time,DVeld);
xlabel('time')
ylabel('Veld(m/s)')
%axis([0 360 -4 4 ])
title('displacer velocity')

figure(3)
plot(time,DXp);
xlabel('time')
ylabel('Xp(m)')
%axis([0 360 0 7E-2 ])
title('piston position')

figure(4)
plot(time,DVelp);
xlabel('time')
ylabel('Velp(m/s)')
%axis([0 360 -6 8 ])
title('piston velocity')

figure(5)
plot(time,DVe);
xlabel('time')
ylabel('Ve')
%axis([0 360 0 1.2E-3 ])
title('expansion volume')
```

```
figure(6)
plot(time,DVc);
xlabel('time')
ylabel('Vc')
%axis([0 360 -9E-4 1E-4 ])
title('compression volume')

figure(7)
plot(time,DP);
xlabel('time')
ylabel('P')
%axis([0 360 6.8E6 7.8E6 ])
title('Pressure')

figure(8)
plot(Ddegree,DdP);
xlabel('time')
ylabel('dP')
%axis([0 360 -6E6 9E6 ])
title('Pressure')

figure(9)
plot(time,DXd,'r',time,DXp,'b');
xlabel('time')
ylabel('Xd,Xp')
%axis([0 360 0 7E-2 ])
title('displacer-piston position')

figure(10)
plot(Ddegree,DdVe);
xlabel('time')
ylabel('Ve')
%axis([0 360 -1E-1 15E-2 ])
title('dVe volume')

figure(11)
plot(Ddegree,DdVc);
xlabel('time')
ylabel('Vc')
%axis([0 360 -1.2E-1 8E-2 ])
title('dVc volume')

figure(12)
plot(DXd,DVeld);
xlabel('displacer displacement(m)')
ylabel('displacer velocity(m/s)')
title('displacer velocity-displacer displacement')

figure(13)
plot(DXp,DVelp);
xlabel('piston displacement(m)')
ylabel('piston velocity(m/s)')
title('piston velocity-piston displacement')
```

```
figure(14)
plot(Ddegree,DTe,'r',Ddegree,DTc,'b');
%axis([0 360 300 873]);
xlabel('time')
ylabel('Te,Tc')
%axis([0 360 1E2 10E2 ])
title('temperature')

figure(15)
plot(Ddegree,DdTe,'r',Ddegree,DdTc,'b');
xlabel('time')
ylabel('dTe,dTc')
%axis([0 360 -8E2 7E2 ])
title('The change of temperature')

figure(16)
plot(DVt,DP);
xlabel('volume(m^3)')
ylabel('Pressure')
title('Pressure-volume')

figure17=figure(17);
plot(Ddegree,DVe,'r',Ddegree,DVc,'b')
xlabel('time')
ylabel('Vexp & Vcomp(m^3)')
legend('Ve','Vc')
%axis([0 360 -9E-4 1.2E-3 ])

figure(18)
plot(DVe,DP, 'k',DVc,DP, '--');
xlabel('DVe-DVc')
ylabel('dP')

figure(19)
plot(Ddegree,Dtempe,'r',Ddegree,Dtempc,'b');
%axis([0 360 300 873]);
xlabel('time')
ylabel('Te,Tc')
%axis([0 360 2.8E2 9E2 ])
title('temperature')

figure(20)
plot(DdVe,DP, 'k',DdVc,DP, '--');
%axis([0 360 300 873]);
xlabel('dVe,dVc')
ylabel('Pressure')
%axis([0 360 2.8E2 9E2 ])
title('Pressure-Volume')
figure(21)
plot(Ddegree,DVt);
xlabel('degree')
ylabel('volume(m^3)')
title('Totalvolume')
figure(22)
plot(time,Dmc,'r',time,Dme,'b');
xlabel('time(s)')
```

```
ylabel('mass')
title('mass of compression and expansion')

figure(23)
plot(time,DPbounce);
xlabel('degree')
ylabel('Pb')
title('Bounce space pressure)

figure(24)
plot(time,DQk);
xlabel('degree')
ylabel('Qk')
title('Heat transfer in cooler')

figure(25)
plot(time,DQr);
xlabel('degree')
ylabel('Qr')
title('Heat transfer in regenerator')

figure(26)
plot(time,DQh);
xlabel('degree')
ylabel('Qh')
title('Heat transfer in heater')
```

Call_function_adiabatic

```
function [y,dy]= cal_function_adiabatic(t,y)
%*****************************************************************
*********
%Public parameter
global_file_adiabatic
%*****************************************************************
*********
%define y-parameter
define_y_parameter_adiabatic
%define_y_parameter_FPSEc
%*****************************************************************
*********


%calculate displacement and velocity of pistons

theta=2*pi*freq*t;
degree=theta*180/pi;

dy(Xd)=y(Veld);
dy(Veld)= -((Cd/Md)*y(Veld))-((Kd/Md)*y(Xd))+(y(P)*(0.15*Ad/Md));
dy(Xp)=y(Velp);
dy(Velp)=-((Cp/Mp)*y(Velp))-((Kp/Mp)*y(Xp))+Ap*((y(P)-
Pbounce)/Mp);
```

```
%fprintf('Xd= %12.9f\n',y(Xd));
%fprintf('Xp= %12.9f\n',y(Xp));

y(Vt)=y(Ve)+Vh+Vr+Vk+y(Vc);
%calculate volume
dy(Ve)=(dy(Xd))*Ad;
dy(Vc)=(dy(Xp)*Ap)-(dy(Xd)*Ad);
y(Ve)=(0.025+y(Xd))*Ad;                % expansion space volume
y(Vc)=(0.05+y(Xp))*Ap-(Ad*(y(Xd))); % compression space volume
%fprintf('Vc= %12.9f\n',y(Vc));
%fprintf('Ve= %12.9f\n',y(Ve));
%fprintf('dVc= %12.9f\n',dy(Vc));
%fprintf('dVe= %12.9f\n',dy(Ve));
%fprintf('Vt= %12.9f\n',y(Vt));

%calculate pressure
dy(P)=(-
(gamma*y(P)).*((dy(Vc)/y(Tck))+(dy(Ve)/y(The)))).//((y(Vc)/y(Tck))+
(gamma*((Vk/Tk)+(Vr/Tr)+(Vh/Th)))+(y(Ve)/y(The)));
dy(Pbounce)=dy(P)*(1+(gamma*(Ap/Vbo)*y(Xp)));
%fprintf('P= %12.9f\n',y(P));
%fprintf('dP= %12.9f\n',dy(P));


%Conditional Temperatures
if y(mck)>0
    y(Tck)=y(Tc);
else y(Tck)=Tk;
end
if y(mhe)>0
    y(The)=Th;
else y(The)=y(Te);
end


%mass rate
dy(mc) =((y(P).*dy(Vc))+((y(Vc).*dy(P))/gamma))/(R*y(Tck));
dy(me) =((y(P).*dy(Ve))+((y(Ve).*dy(P))/gamma))/(R*y(The));
dy(mk) =(y(mk).*dy(P))./y(P);
dy(mr) =(y(mr).*dy(P))./y(P);
dy(mh) =(y(mh).*dy(P))./y(P);

%fprintf('mc= %12.9f\n',y(mc));
%fprintf('me= %12.9f\n',y(me));
%fprintf('mk= %12.9f\n',y(mk));
%fprintf('mr= %12.9f\n',y(mr));
%fprintf('mh= %12.9f\n',y(mh));
%inital temperature conditions
y(tempe)=y(P).*y(Ve)/R*y(me);
y(tempc)=y(P).*y(Vc)/R*y(mc);
%Temperatures
dy(Te)=y(Te)*(((dy(P)/y(P))+(dy(Ve)/y(Ve)))-(dy(me)/y(me)));
dy(Tc)=y(Tc)*(((dy(P)/y(P))+(dy(Vc)/y(Vc)))-(dy(mc)/y(mc)));
%fprintf('dmc= %12.9f\n',dy(mc));
%fprintf('dme= %12.9f\n',dy(me));
```

```
%fprintf('Tc= %12.9f\n',y(Tc));
%fprintf('Te= %12.9f\n',y(Te));



%Mass flow
y(mck)=-dy(mc);
y(mkr)=y(mck)-dy(mk);
y(mhe)=dy(me);
y(mrh)=y(mhe)+dy(mh);

 %Calculating temperature in each compartment from the ideal gas
law
y(Tc)=y(P)*y(Vc)/(R*y(mc));
y(Te)=y(P)*y(Ve)/(R*y(me));

y(nTk)=(y(P)*Vk)/(R*y(mk));
y(nTr)=(y(P)*Vk)/(R*y(mr));
y(nTh)=(y(P)*Vk)/(R*y(mh));

%calculate workdone
y(We)=dy(Ve)*y(P);
y(Wc)=dy(Vc)*y(P);

%Heat transfer in each space
y(Qk)=((Vk*y(P)*cav)/R)-(cap*((Tck*mck)-((Tk)*mkr)));
y(Qr)=((Vr*y(P)*cav)/R)-(cap*(((Tr)*mkr)-((Th)*mrh)));
y(Qh)=((Vh*y(P)*cav)/R)-(cap*(((Th)*mrh)-(The*mhe)));



end
```

Global_file_adiabatic

```
global Ad  % surface area of disaplcer (m^2)
global Ap  % surface area of piston (m^2)
global Mp  %mass of piston (kg)
global Md  %mass of displacer (kg)
global Cp  %piston damping (Ns/m)
global Cd  %displacer damping (Ns/m)
global Kp  %piston spring stiffness
global Kd  % displacer spring stiffness
global Pb  % pounce space pressure
global Th  % temperature of heater
global Tk  % temperature of cooler
global Tr  % temperature of regenerator
global gamma
global M
global R    % universal gas constant
global Vk   % volume of cooler
```

```
global Vr   % volume of regenerator
global Vh   % volume of heater
global degree % angle
global theta
global dt   %timestep
global Dk   %diameter of cooler
global Nktube %number of cooler tubes
global Dr  % outer diameter of regenerator
global dr   %inner diameter of regenerator
global Dh   %diameter of heater
global lh   %length of heater
global lr  %length of regenerator
global lk  %length of cooler
global cap %specific heat capacity at constant pressure
global cav %specific heat capacity at constant volume
global Vbo  %bounce space volume
```

Inputdata_adiabatic

```
freq=30; %frequency
theta=2*pi*freq*t;
degree=theta/pi*180;

%new input
Vbo=0.0015; %bounce space volume
Dk=0.0012;  %diameter of cooler
Dr=0.08;    % outer diameter of regenerator
dr=0.064; %inner diameter or regenerator
Dh=0.003; % diameter of heater
lh=0.24; %length of heater
lr=0.04; %length of regenerator
lk=0.05; %length of cooler
Ap=0.0018; %surface area of piston
Ad=0.0018; %surface area of displacer
Md=0.426;  %mass of displacer
Mp=6.2;   %mass of piston
Cp=461.5; %piston damping
Cd=85.34; %displacer damping
Kp=296000; %piston spring stiffness
Kd=25000; %displacer spring stiffness
M=4; %mass of helium gas
R=2077;  %universal gas constant
Tk=350;   %temperature of cooler
y(Tc)=350; %temperature of compression space
Th=780; %temperature of heater
y(Te)=780; %temperature of expansion space
Tr=(Th-Tk)/log(Th/Tk); %temperature of regenerator
y(Tck)=y(Tc);
Pb=70E5; %bounce space pressure
y(The)=Th;
Vh=0.000016286; %volume of heater
Vr=0.000027143; %volume of regenerator
Vk=0.000010857; %volume of cooler
gamma=36;
```

```
freq=30; %frequency
numberoftimestep=1000;   % number of timestep
timestep=1/(freq*numberoftimestep);
cycle=5; % number of cycles
n=numberoftimestep*cycle;

num=1000;           %number of time step per cycle
tT=1/freq;
%maximum pressure [Pa]
%timestep =tT/num;
dt=timestep;
cap= 5190; %specific heat capacity at constant pressure
cav= 3110; %specific heat capacity at constant volume
pO=70E5;   %mean pressure
%initial condition
t=0;y(P)=pO;
Pmean=pO;
y(Xd)=0.01233; %initial position of displacer
y(Veld)=0; % initial velocity of displacer
y(Xp)=0.01145; %initial position of piston
y(Velp)=0; % initial velocity of piston
theta=0;
y(Pbounce)=pb;
```

Define_y_parameter_adiabatic

```
%define y parameter
Xd=1; % displacement of displacer
Veld=2; %velocity of displacer
Xp=3; %displacement of piston
Velp=4; % velocity of piston
P=5; % dynamic pressure (Pa)
Pbounce=6; %bounce space pressure
mc=7; mass of compression space(kg)
me=8; mass of expansion space(kg)
mk=9; mass of cooler (kg)
mr=10; %mass of regenerator space (kg)
mh=11; %mass pf heater space (kg)
Te=12; %temperature of expansion space (K)
Tc=13; %temperature of compression space (K)
nTk=14; %temperature of cooler (K)
nTr=15; %temperature of regenerator(K)
nTh=16; %temperature of heater(K)
Ve=17;  % gas volume of expansion space
Vc=18; % gas volume of compression space (m^3)
Tck=19; % gas temperature of mass flow at interface of compression
space and cooler [K]
The=20; % gas temperature of mass flow at interface of heater and
expansion space [K]
mck=21; % mass flow from compression to cooler [kg/s]
mkr=22; % mass flow from cooler to regenerator[kg/s]
mhe=23; % mass flow from heater to expansion space [kg/s]
mrh=24; % mass flow from regenerator to heater [kg/s]
```

```
Vt=25; % total gas volume
degree=26;
We=27; %workdone in expansion space
Wc=28; %workdone in compression space
Qk=29; %heat transfer in cooler

Qr=30; %heat transfer in regenerator
Qh=31; %heat transfer in heater
```

rk4

```
function [x, y, dy] = rk4(deriv,n,x,dx,y)
%Classical fourth order Runge-Kutta method
%Integrates n first order differential equations
%dy(x,y) over interval x to x+dx
%Israel Urieli - Jan 21, 2002
x0 = x;
y0 = y;
[y,dy1] = feval(deriv,x0,y);
for i = 1:n
    y(i) = y0(i) + 0.5*dx*dy1(i);
end
xm = x0 + 0.5*dx;
[y,dy2] = feval(deriv,xm,y);
for i = 1:n
    y(i) = y0(i) + 0.5*dx*dy2(i);
end
[y,dy3] = feval(deriv,xm,y);
for i = 1:n
    y(i) = y0(i) + dx*dy3(i);
end
x = x0 + dx;
[y,dy] = feval(deriv,x,y);
for i = 1:n
    dy(i) = (dy1(i) + 2*(dy2(i) + dy3(i)) + dy(i))/6;
    y(i) = y0(i) + dx*dy(i);
end
```

Appendix A Continuation - MATLAB codes for the mathematical model of the isothermal free piston Stirling engine

```
% Isothermal model of the Free piston Stirling engine based on
% Schmidt model by G.T Reader and C Hooper [1983].
% file for analysis and prediction of the masses, diameters of
piston and displacer and also to determine the amplitude of the
displacer
% edited by Ayodeji Sowale
% last modified 26.09.2015


function FPSE_optimize
global A1   %amplitude of displacer
global A2   %amplitude of piston
global freq  %frequency of operation
global beta  %phase angle
global D     %piston diameter
global d     %displacer diameter
global Ne    %power
global Pmax  %maximum pressure
global w
global gamma2
global gamma1
global Vs
global Th   %temperature of heater
global Tk   %temperature of cooler
global S

%Define Inputs
t=0;  %time
freq=30;
vsr=0.45; %volume of regenerator
vsx=0.35; %volume of cooler
vsc=0.2;  %volume of compression space
d=0.18;
D=0.2;
Pmax= 71E5;
Th=780;
Tk=320;
Ne=1600;
tao=Tk/Th;
w=2*pi*freq; %angular frequency
deltaPmax=0.07*Pmax;
miu=(d/D)^2;
gamma1=(80/(180*pi));
gamma2= (80/(180*pi));
A1=0.0025;  %displacer amplitude
A2=0.0015;  %piston amplitude
V1=pi*D^2/2*A1;
V2=pi*d^2/2*A2;
Vs=1.8;
taor=(2*Tk)/(Tk+Th);
```

```
Ts=(tao*vsx)+vsc+(taor*vsr);
S=Ts*Vs

%beta_d=beta;
%beta = ((2*pi*beta_d)/360);
it =0;
for beta_d = 0:10:80
    fprintf('Beta =  %12.9f degree\n',beta_d);
    beta = (beta_d/(180*pi));
    %theta=pi-gamma2+beta;
    conv(1)=0.01;
    if (abs (conv(1))<=0.05)
        it=it+1;
        if it > 1
            d = d_new;
            D = D_new;
        end
        miu=(d/D)^2

        tgteta=tan(180-80+beta);

        G=sin(beta)/tgteta

        H=cos(beta)-G

        Z= 0.49351/H

        phy = atan((Z*sin(beta))/((Z*cos(beta)-((d/D)^2))))

        K=((Z^2)+1+2*Z+cos(beta))

        W= miu*sqrt(K)

        Mo= (miu*Z)*(miu*Z)-2*miu*Z*(miu-tao)*cos(beta)+(miu-
tao)*(miu-tao)

        sigma = (sqrt(Mo)/(tao+W+S))

        Ly = Z*sqrt((1-sigma)/(1+sigma))*(sigma/(1+sqrt(1-
(sigma^2))));

        teta= atan(sin(beta)/(cos(beta)-((miu-tao)/Z)));

        Pressure= Pmax*((1-sigma)/1-sigma*cos(w*(t-teta)));

        P_dash = Pmax*sqrt((1-sigma)/(1+sigma));

        n2= (2*w)/tan(gamma2);

        n1= (2*w)/tan(gamma1);

        E = (P_dash*sigma*pi)/(2*(1+sqrt(1-
(sigma^2)))*A2*sqrt((n2^4)+(4*(n2^2)*(w^2))))

        J = (2*Ne)/(n2*(A2^2)*(w^2))
```

```
        Y = (2*E)-((1/8)*deltaPmax)*(pi/(A2*n2*w))*sin(gamma2)

        d_new = (sqrt(4*Y*J))/(2*Y)

        Yi = (1/2)*P_dash*((sigma*pi)/(1+sqrt(1-(sigma^2))))-
(1/8)*deltaPmax*pi*sin(gamma1)*(sqrt(1+(1/((tan(gamma1))^2))))

        Ji = ((1/2)*P_dash*((pi*sigma*(d^2))/(1+sqrt(1-
(sigma^2)))))+((1/8)*deltaPmax*pi*(d^2)*sin(gamma1))*(sqrt(1+(1/((
tan(gamma1))^2))))

        D_new = (sqrt(4*Yi*Ji))/(2*Yi)

        conv(1) = (d/D)^2-(d_new/D_new)^2

    end


C2=(1/8)*deltaPmax*((pi*(d^2))/(A2*w))*sin(gamma2)+((2*Ne)/((A2^2)
*(w^2)));

    M2_new= (C2/(2*n2));

    A1_new=A2*(miu/Z);

    C1=(1/8)*deltaPmax*((pi*((D^2)-
(d^2)))/(A1_new*w))*sin(gamma1);

    M1_new= (C1/(2*n1));

    fprintf('Z= %12.9f W\n',Z);
    fprintf('phy= %12.9f rad\n',phy);
    fprintf('W= %12.9f W\n',W);
    fprintf('sigma= %12.9f W\n',sigma);
    fprintf('workdone= %12.9f W\n',Ly);
    fprintf('average pressure= %12.9f \n',P_dash);
    fprintf('pressure= %12.9f \n',Pressure);
    fprintf('teta= %12.9f \n',teta);
    fprintf('E= %12.9f \n',E);
    fprintf('J= %12.9f \n',J);
    fprintf('Y= %12.9f \n',Y);
    fprintf('Ji= %12.9f \n',Ji);
    fprintf('Yi= %12.9f \n',Yi);
    fprintf('piston diameter= %12.9f m\n',d_new);
    fprintf('displacer diameter= %12.9f m\n',D_new);
    fprintf('mass of piston= %12.9f \n',M2_new);
    fprintf('mass of displacer= %12.9f \n',M1_new);
    fprintf('Amplitude of displacer= %12.9f \n',A1_new);
    fprintf('piston C2= %12.9f \n',C2);
    fprintf('displacer C1= %12.9f \n',C1);
    fprintf('n2 = %12.9f \n',n2);
    fprintf('n1= %12.9f \n',n1);

disp('**********************************************************
****')
end
end
```

Appendix B Publications: 'Numerical Modelling of Free Piston Stirling Cycle Machines'

Sowale, A. and Mahkamov, K. *Numerical Modelling of Free Piston Stirling Cycle Machines. Proceeding of 16th International Stirling Engine Conference*. 2014. Bilbao, Spain.

Numerical Modelling of Free Piston Stirling Cycle Machines

Ayodeji Sowale, Khamid Mahkamov

Northumbria University, Newcastle upon Tyne, NE1 8ST, UK

Keywords: *Free piston Stirling engine, Thermodynamic, Micro CHP*

Abstract

Due to their relative simplicity, higher specific power and efficiency together with a long life cycle free-piston Stirling Cycle machines have been successful in the progression towards commercial applications (MCHP and cooling). The work is under way at Northumbria University on feasibility study of application of CFD modelling for the above machines. Multi-dimensional CFD modelling requires significantly longer computational times. The number of variable design and operational parameters is increased in free-piston machines due to coupling of the working process and piston dynamics and therefore it is highly desirable to derive the initial set of these parameters as accurate as possible using thermodynamic models. This work describes activities in the first stage or research work, namely the development of first and second-order thermodynamic models of free piston machines using experience acquired by one of the authors in 1980s. The first-order model based on a combination of the Schmidt model and equations of forced harmonic oscillations of mass-spring systems. Such approach allows us to rapidly estimate the set of design and operational parameters which can then be further refined during modelling with the use of a second order technique. In the second order modelling stage differential equations of the working process and of piston dynamics solved simultaneously using Runge-Kutta 4th order method in MATLAB environment. A special attention is paid to analysis of each cycle where minimum and maximum values of such parameters as piston displacements, gas pressure and temperatures and frequency are traced in order to determine whether a stable operation of the machine was reached during simulations. Influence of heat transfer and pressure losses in the internal gas circuit of the machine are also taken into account. In future work, such second order model will be coupled with GA code for rapid optimisation of the machine.

Nomenclature

A_d	Cross sectional area of the piston (m^2)	A_p	Cross sectional area of the displacer (m^2)
m_d	Mass of the displacer (kg)	m_p	Mass of the piston (kg)
mck '	mass flow from compression space to cooler	*mhe* '	mass flow from heater to expansion space
k_p	Stiffness of piston spring(N/m)	k_d	Stiffness of displacer spring (N/m)
P_b	Bounce space pressure below the piston (Pa)	V_b	Bounce space volume(m^3)
V_r	Volume of the regenerator(m^3)	V_h	Volume of the heater(m^3)

V_k Volume of the cooler(m^3)

T_k Temperature of the cooler (K)

T_r Temperature of the regenerator (K)

T_h Temperature of the heater (K)

T_{ck} Temperature of compression space to cooler (K)

T_{he} Temperature of heater to expansion space (K)

T_{rh} Temperature of regenerator to heater (K)

T_{kr} Temperature of cooler to regenerator (K)

W_e Work done in expansion space (J/cycle)

W_c Work done in compression space (J/cycle)

Q_e Heat transfer in expansion space (W)

Q_c Heat transfer in compression space (W)

V_{clc} Compression space clearance volume(m^3)

V_{cle} Expansion space clearance volume(m^3)

x_p Displacement of piston (m)

$\dot{x}_p$ Velocity of piston (m/s)

$\ddot{x}_p$ Acceleration of piston (m/s^2)

x_d Displacement of displacer (m)

$\dot{x}_d$ Velocity of displacer (m/s)

$\ddot{x}_d$ Acceleration of displacer (m/s^2)

Introduction

A lot of ways and methods have been researched to create an alternative means of energy saving and benefit to the environment. The combination of heat and power generation in micro scale was introduced and examined. The energetic, financial and environmental benefits of the micro CHP has given it an advantage as an uprising source of energy for use in residence and medium scale commercial enviroment. The use of micro CHP will decrease the consumption of primary energy, emission of CO2 and the end user or individual bill. Based on research and investigations the Stirling engines have been considered for micro CHP generation due to the ability to use various fuel, low level of emission, good performance at partial load, high efficiency, low vibration and noise level [1]. In the energy market today, there has been an increase in demand for systems that are powerful with durable development policies which can produce and transform energy [2]. There has been a major interest in the use of cogeneration technologies due to the rapid increase in the request for energy forms that are less pollutant [2]Cogeneration systems have been used in micro scale applications. Amongst the different types of technologies and energy sources available, combined heat and power (CHP) has emerged. To reduce the effect of pollution from emissions on the change of climate and increase the efficiency of energy conversion, an effective decentralized energy system that can combine heat and power in its operation is highly recognized[3]. Stirling engines have been used for different applications and purposes since its invention by Robert Stirling in 1816[4]. Prototype Stirling engines have been designed and tested in automotive such as buses, trucks and boats[5]. It has also been used as a propulsion engine in passenger ships [6]. Stirling engines are suitable for Micro-CHP applications where high thermal efficiencies and the ability to use various fuels are needed. A lot of researchers have carried out investigations on the effect of irreversibility and heat losses on the FPSE performance. It was observed that in all the technological parameters of the Stirling engine non-ideal regeneration and dead volume have the greatest influence on the engine performance [19, 36]**.** According to Popescu et al. noted that the non-adiabatic regenerator has the most effect on the performance reduction of the engine[37]. A research was conducted by Kongtragool on the efficiency of regenerator and dead volumes on the total work done and engine efficiency without taking into consideration the heat transfer within the heat exchangers, heat source and sink[38]**.** A study was performed on the conventional Stirling engine cycle performance which took into account the effects of incomplete heat regeneration, heat transfers within the heat exchangers and the cycle irreversibility, friction between the displacer and piston with the walls of the engine and pressure losses by Costea et al [50]**.** The Schmidt analysis was conducted on the Stirling engine using the dead volume with assumptions for

isothermal conditions and ideal regeneration[22].. Realistic results of the FPSE can be developed with the use of dynamic-thermodynamic studies. Therefore, an accurate global method of approach using a thermodynamic isothermal model in agreement with the dynamic analysis is required to design a free piston Stirling engine.

Thermodynamic cycle of the Stirling engine

The free piston Stirling engine has four phases in its working cycle

(I) Isothermal compression: This is the first stage of the cycle, the working gas in between the displacer and the piston is compressed by their oscillatory movements and the gas pressure rises.

(II) Isochoric heating: This is the stage where the working gas is transferred through the heat exchangers and absorbs the heat from the regenerator to increase its temperature.

(III) Isothermal expansion: At this stage the pressure of the gas is reduced during the expansion in the hot space when the displacer is in a downward motion.

(IV) Isochoric cooling: This is the final stage or the cycle where the gas flows back through the heat exchanger, the heat from the gas is absorbed by the regenerator and the gas achieves minimum temperature at this stage due to heat transfer in the cooler

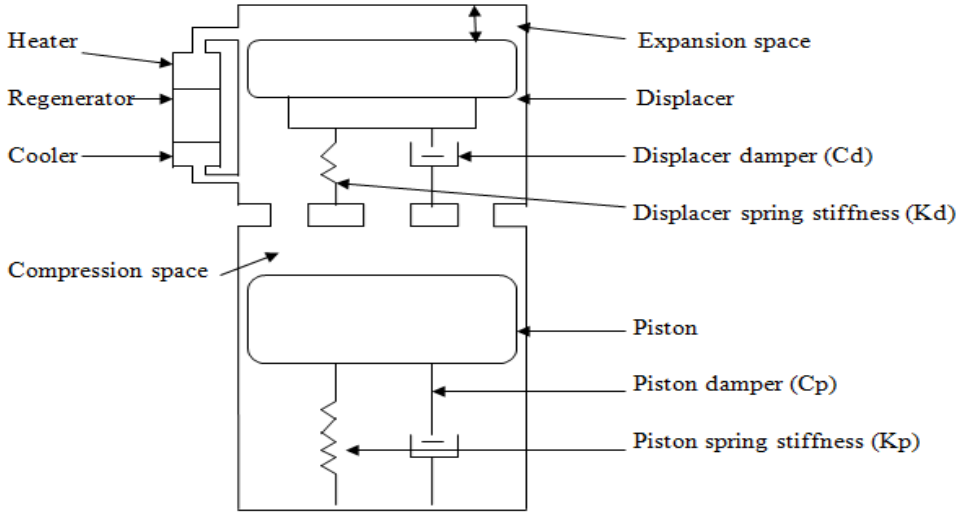

Figure 1. The layout diagram of the gamma type free piston Stirling engine.

Mechanism

The figure above depicts the layout diagram of the gamma type free piston Stirling engine used in this study. The engine consist of a piston and displacer, the heat exchangers (heater, regenerator and cooler), mechanical springs and dampers. There is no linkage between the displacer and piston, they are both connected to the engine casing via the springs. The displacer is lighter in weight than the piston this is to maintain the required phase angle and for effective results. The pressure acting on the piston and displacer is triggered by the working gas, which is a reversible process of the transfer of the working gas from the compression space to the expansion space and vice versa. The volume of the engine is made up of the working volume and the block volume. The working volume is made up of the cold and hot regenerative volume supplied by the heat exchangers. The regenerative volume is the volume of the working fluid that is displaced between the hot and cold volumes. The working cycle of the engine is achieved when an external source of heat is employed to increase the temperature of the working gas in the expansion space which increases the pressure and pushes the displacer in a downward motion from its equilibrium position, on its return the displacer pushes the working gas to the heater which increases the temperature and flows through the regenerator which absorbs

the heat from the gas before it moves to the cooler and to the expansion space. The displacer is lighter than the piston so it achieves a faster velocity and transfers the working gas through the heat exchangers to the compression space so as to push piston downwards. While the piston is in the downward motion, the pressure of the working gas is reduced and the displacer which has a higher velocity is in an upward motion so as to push the heated gas through the heat exchanger again. The pressure pushes the displacer downwards while the piston is in an upward motion due to the bounce pressure in the piston compartment which is equal to the mean pressure at the beginning of the cycle, thereby compressing the gas volume in between them, increases the gas pressure and pushes the gas volume back through the cooler to the regenerator which gives the gas the heat it absorbed from it and to the heater and back to the expansion space. The compression continues until the displacer reaches the upward stroke and the cycle ends when the displacer is in the downward stroke. The cycle is a reversible process

Assumptions for the mathematical model.

Certain assumptions were in order to obtain the mathematical model of the free piston Stirling engine.

1. The engine block is stationary.
2. The pressure losses are taken into consideration in the calculation.
3. The working volume pressure and block pressure is equal when the engine is in static equilibrium.
4. The temperatures of the working gas in the heat exchangers are in thermal equilibrium in the surrounding walls.
5. The temperatures of the surrounding walls of the working gas volume changes with time.
6. The masses of the piston and displacer springs are not considered.
7. The springs are positioned in a linear order.
8. No leakage is expected to occur between the mechanical components of the engine.
9. The effect of gravitation is not considered in this analysis.
10. The working fluid is a perfect gas.
11. To maintain the necessary phase angle between the displacements of the moving elements the mass of the displacer is lighter than the piston.
12. The regenerator temperature is required to be equal to the average of the cooler and heater temperature.

Equations used in the mathematical model

An Ideal adiabatic model was considered for the free piston Stirling engine. Therefore from the Newton's second law which is applied to describe the motion of the piston and the displacer states:

$$\sum F = m\ddot{x} \quad (1)$$

$$F + F_{damping} + F_{spring} = M\ddot{x} \quad (2)$$

The motion of the displacer is a result of the spring force, damping force, area of the displacer and the pressure of the working fluid.

$$m_d\ddot{x} + K_d x_d + C_d\dot{x} = P(A_d) \quad (3)$$

Where m_d is the mass of the displacer. K_d displacer spring constant. C_d displacer damping constant. A_d cross sectional area of the displacer. The motion of the piston is a result of the damping force, spring force, area of piston, the bounce space pressure and the pressure of the working fluid.

$$m_p\ddot{x} + K_p x_p + C_p\dot{x} = A_p(P - P_b) \quad (4)$$

Where m_p is the mass of the piston. K_p piston spring constant C_p piston damping constant. A_p cross sectional area of the piston. P_b bounce space pressure. The equation for pressure in the engine for a closed cycle operation [117]

$$P = \frac{MR}{\left(\frac{Vc}{Tck}+\frac{Vk}{Tk}+\frac{Vr}{Tr}+\frac{Vh}{Th}+\frac{Ve}{The}\right)} \quad (5)$$

Boundary conditions for the conditional temperatures

If *mck' > 0 then Tck = Tc else Tck = Tk If mhe' > 0 then The = Th else The = Te* (6)

From the engine's geometry the positions of the piston and displacer x_p and x_d with the expansion and compression volumes Ve and Vc can be derived from the following equations:

$$Ve = (V_{cle} + x_d)A_d \quad (7)$$

$$Vc = \left(V_{clc} + x_p\right)A_p - (x_d + V_{cle})A_d \quad (8)$$

Where V_{cle} and V_{clc} are the expansion and compression space clearance volumes. By differentiating Ve and Vc above the new equations resulted to

$$dVe = \dot{x}\ (A_d) \quad (9)$$

$$dVc = \dot{x}\left(A_p\right) - \dot{x}(A_d) \quad (10)$$

The momentum equation for the displacer from the equation (32) above is

$$m_d\ddot{x}_d + K_d x_d + C_d\dot{x}_d = P(A_d) \quad (11)$$

The momentum equation for the piston from the equation (33) above is

$$m_p\ddot{x}_p + K_p x_p + C_p\dot{x}_p = A_p(P - P_b) \quad (12)$$

Bounce pressure

Pb= P (1+ gamma (Ap/Vbo) Xp)) (13)

The values used in the case study

Engine Data	Value		Value
General		**General**	
Mean pressure	70 bar	Displacer frontal Area	0.018m^2
Temperature of the heater	780 K	Expansion space clearance volume	0.02m^3
Temperature of the cooler	350 K	Compression space clearance volume	0.016m^3
Phase angle	120 degree	**Masses**	
Oscillating frequency	30Hz	Mass of the piston	6.2kg
Geometric		Mass of the displacer	0.426kg
Dead Volume	0.054mm^3	**Dynamic**	
Volume of the heater	0.016mm^3	Piston spring stiffness	296000 N/m
Volume of the regenerator	0.027mm^3	Displacer spring stiffness	25000 N/m
Volume of the cooler	0.011mm^3	Piston damping load	461.5 Nsm^-1
Piston frontal Area	0.018m^2	Displacer damping load	35.34Nsm^-1

Methodology

The figure below depicts the flow chart of the simulation carried out with the aid of rk4 in MATLAB to achieve the second order modelling of the free piston Stirling engine.

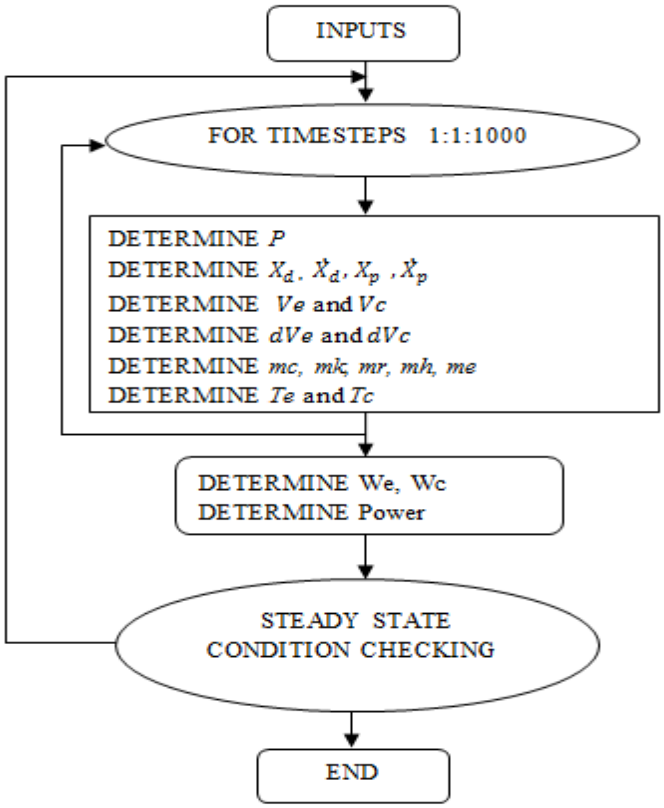

Figure 2-. Flow chart of the second order modelling of the free piston Stirling engine.

Simulation Results and Discussion

MATLAB was employed to write the codes for the numerical simulation using the mathematical equations above. The initial input parameters for the engine are determined at the beginning of the program, some which are variable and constant. The variable parameters are: The damping load and the spring stiffness of the piston and displacer, temperature of the heater, cooler and regenerator. The constant parameters are: The working fluid (gas) constant, oscillating frequency, area of the piston and displacer, masses of the piston and displacer, volume of the heater, cooler and regenerator. The set of differential equations were expressed as dY/dt=F(t,Y) and the unknown function Y(t) that satisfies the initial conditions and the differential equations was the objective which was performed for each of the output parameters. The simulation was carried out using the fourth order Runge Kutta method that solves ordinary differential equations. The calculation was carried out with 1000 time steps in 5 cycles. The equations in operating system were integrated through complete cycles in order to determine the pressure, the displacement and velocity of the piston and displacer, the volume of the expansion and compression spaces until the steady state operation of the engine is achieved. The consecutive process of the computation for the numerical procedure is listed in the flow chart. The figures 4.8 to 4.21 illustrate the behaviour of the free piston Stirling engine at steady state operation. The mean pressure, the temperature of the hot source, the frequency and the strokes of the piston and displacer determines the output power produced by the engine. There is a correlation between the pressure, the phase and the stroke amplitude of the displacer and piston because it was noticed that when there is an increase or decrease in the mean pressure it affects the amplitude and the phase of both the piston and displacer respectively.

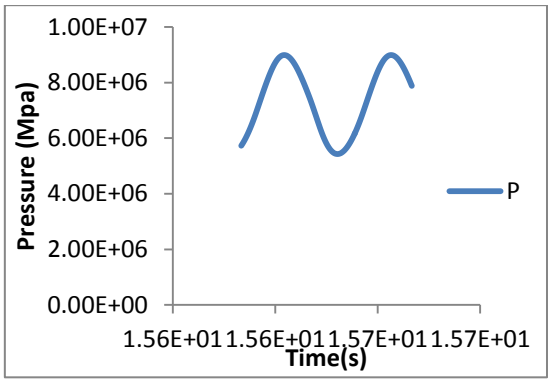

Fig. 3. Pressure variation at a frequency of 30Hz

.

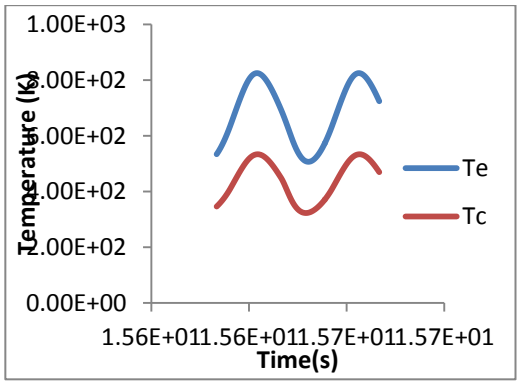

Fig. 4. Temperature variation in the expansion and compression space

The figure 4.13 above shows the pressure variation in the engine at steady state, the bounce space pressure was 70 bar which was the same as the mean pressure at the beginning of the operation. There is a variation between 5Mpa and 9Mpa which on the average results to the bounce pressure at the initial stage of the engine. This shows a good performance at an output power of 1.5Kw. The figure 4.13 above shows the variation in temperature in the expansion and compression space. The expansion space temperature range between 520K to 820K and the compression space temperature range between 320K to 560K. The large variation in the cyclic temperature in the expansion space gives a mean value of 670K which is less than the heater temperature of 780K, also the mean temperature value in the compression space of 440K is higher than the cooler temperature of 380K. This shows that major loss in engine performance is not from the adiabatic work spaces.

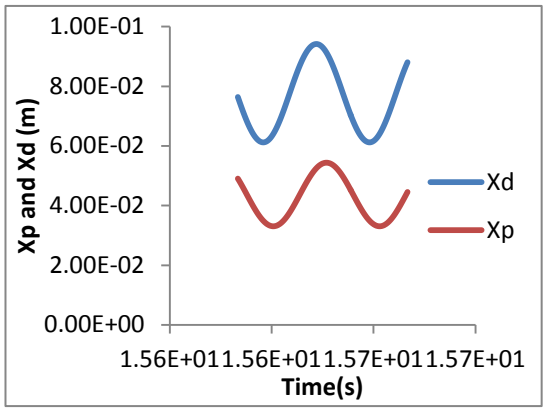

Fig. 5. Displacement of piston and displacer

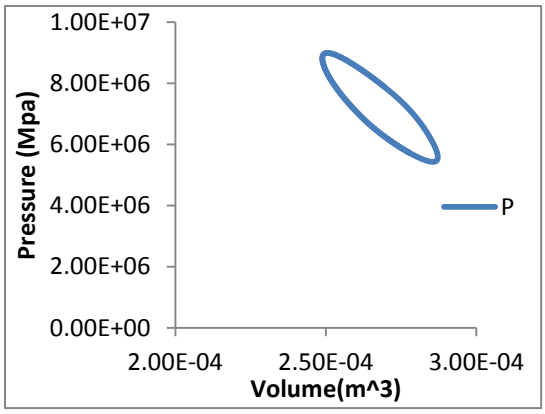

Fig. 6. Pressure-volume diagram

The figure 4.13 above shows the relationship between the piston and displacer at 100 degree phase angle. The stroke of the piston is 0.04 m while that of the displacer is 0.11m. Figure 4.12- The P-V diagram of the engine at an output power of 1.5kw. The figure 4.12 above shows the pressure to volume diagram of the free piston engine at steady state with a heater temperature of 780k and cooler temperature of a frequency of 30Hz and a mean pressure of 70bar was able to generate a power of 1.5kW. The working gas volume is an essential parameter in determining the pressure.

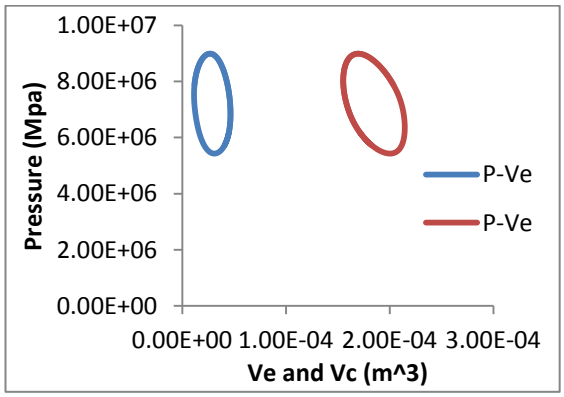

Fig. 7. Pressure-volume diagram in expansion and compression compression space

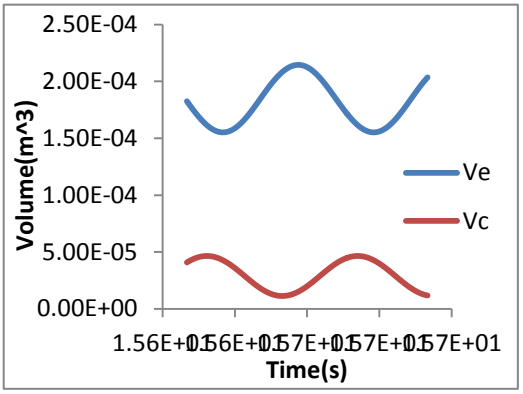

Fig. 8. Volume variation of expansion and space

The figure 4.13 above shows the pressure to volume diagram in the expansion and compression space**.** The figure 4.13 above shows the relationship between the volume of the expansion space and compression space with phase angle in the cycle.

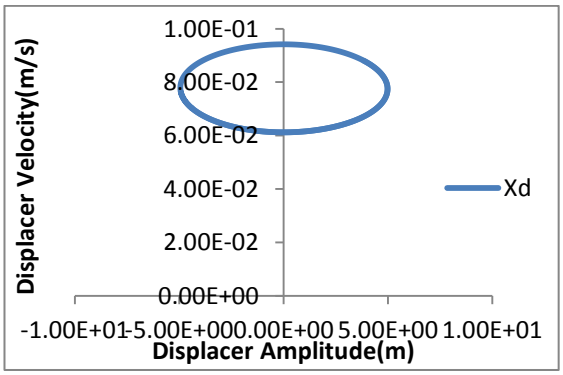

Fig.9**.** Displacer velocity against displacer. amplitude steady state.

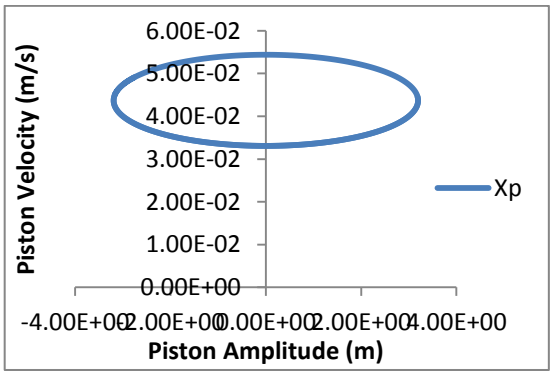

Fig. 10 Piston velocity against Piston amplitude at at steady state.

Validation

To validate the model developed in this present study, a documented model of the Sun power inc. RE-1000 model which was developed to investigate the applications of free piston Stirling engine [124]. The results obtained from the validation of the Sunpower Re-1000 FPSE model with the model in this present study is tabulated below:

SUNPOWER RE-1000	EXPERIMENT	SIMULATION
Frequency	30Hz	30Hz
Output power	1.00kW	1.67kW

Table 4.7- Comparison of the Sunpower RE-1000 FPSE with the developed model.

The geometric data and the operating conditions of the Sunpower RE-1000 FPSE listed in the table 4.6 above were used on the developed model in this present study with an oscillating frequency of 30Hz and the results between the theoretical results generated from the simulation by the model were compared with the experimental results of the Sunpower RE-1000 engine. The agreement is good enough due to the output power generated as it is shown in the table 4.7 above. This shows that the developed model analysis can return realistic results.

Conclusion

The second order numerical model of the free piston Stirling engine is developed and the outputs generated are realistic in performance of the engine. The validation carried out with the RE-1000 experimental data proves a good agreement in comparison with the output results. Further work will be carried out on the free piston Stirling engine model by developing a second order quasi-steady-flow system also considering the losses that occur during the operation of the engine such as heat losses, dissipation losses, pressure drop and the mass flow rates in the working fluid in relation to the dynamic motion of the system and it will be coupled with GA code for rapid optimisation of the machine, in order to achieve the best technical output of the steady state operation and to produce realistic results.

References

1. d'Accadia, M.D., et al., Micro-combined heat and power in residential and light commercial applications. Applied Thermal Engineering, 2003. 23(10): p. 1247-1259.

2. Boucher, J., F. Lanzetta, and P. Nika, Optimization of a dual free piston Stirling engine. Applied Thermal Engineering, 2007. 27(4): p. 802-811.

3. Jackson, J., Ensuring emergency power for critical municipal services with natural gas-fired combined heat and power (CHP) systems: A cost-benefit analysis of a preemptive strategy. Energy Policy, 2007. 35(11): p. 5931-5937.

4. Stirling Cycle Engine Analysis - Urieli,I, Berchowitz,D. Alternative Sources of Energy, 1984(68): p. 71-71.

5. Brandhorst Jr., H.W., Free-Piston Stirling Convertor Technology for Military and Space Applications.2007.

6. Chicco, G., Mancarella, P, Performance evaluation of cogeneration systems:an Approach Based on Incremental Indicators. Proceedings of the 6th WSEAS International Conference on Power Systems,, (2006): p. pp 34 - 39.

7. Wu, F., et al., Optimum performance of irreversible stirling engine with imperfect regeneration. Energy Conversion and Management, 1998. 39(8): p. 727-732.

8. Popescu, G., et al., Optimisation thermodynamique en temps fini du moteur de Stirling endo- et exo-irréversible. Revue Générale de Thermique, 1996. 35(418–419): p. 656-661.

9. Kongtragool, B. and S. Wongwises, Thermodynamic analysis of a Stirling engine including dead volumes of hot space, cold space and regenerator. Renewable Energy, 2006. 31(3): p. 345-359.

10. Costea, M., S. Petrescu, and C. Harman, The effect of irreversibilities on solar Stirling engine cycle performance. Energy Conversion and Management, 1999. 40(15–16): p. 1723-1731.

11. G., S., The theory of lehmans calorimetric machine. 1871. 15(1).

12. Urieli, I., Stirling cycle machine analysis. (2001).

13. Beale, W.T., 'Free piston Stirling- some model tests and simulation' International Automotive Engineering Congress, Society of Automotive Engineers Inc. , 1969.